ZEOLITE INCORPORATED MATERIALS FOR TARGETED BIOMASS RETENTION AND POLLUTANT REMOVAL

A DISSERTATION
SUBMITTED TO THE FACULTY OF THE UNIVERISTY OF MINNESOTA
BY

ANNDEE LEE HUFF CHESTER

IN PARTIAL FULFILLMENT OF THE REQUIREMENTS
FOR THE DEGREE OF
DOCTOR OF PHILOSOPHY

Dr. Paige J. Novak, Advisor

April 2022

Acknowledgements

There are many people whom I need to thank, for without them, completing this journey and this research would not have been possible.

First, I would like to thank my advisor, Dr. Paige Novak, for the academic guidance and mentorship over the years. Pushing me to approach ideas from new and scholarly perspectives. I would also like to thank the Novak Lab team, specifically Hanna, Kuang, Rachel, and Bailey for the advice, spontaneous troubleshooting, moral support, and friendship that made the hours in lab more enjoyable. A special thank you to Sara and Adel for their advice and guidance on membrane development. Most of the data in this dissertation were analyzed by the team of undergraduate researchers who helped me over the years. A big thank you to Kalie, Nikhil, Doug, Justin, and Karen. I also want to acknowledge the many meaningful conversations I have had with faculty, staff, and other graduate students in this department and at the University.

There was also a huge team of supporters behind the scenes making it possible for me to finish this journey. I am forever grateful for the love and support from my husband, Tony, for always being there for me, for picking up the slack, and keeping me fed. My parents, for their unconditional love from day one and instilling in me the stubbornness to never give up. My loving sisters, the team of ladies I am lucky to call friends, and the rest of my family that have stood behind me, providing encouragement and emotional support. Finally, I would like to thank my dog, Hazel, for frequently sharing my desk chair, listening to all my zoom meetings, and keeping me company many late nights.

Dedication

I dedicate this work to my grandpa, Donald “Buck” Burkhartzmeyer for being one of my biggest advocates. You might not have understood the intricacies of my research, but you would still brag to anyone who would listen. Thank you for the unconditional love and support. May you rest in love and peace.

Abstract

This dissertation describes the assessment and treatment of pollutants, namely nutrients, in waste streams. Nutrients such as nitrogen, are of major and growing concern because nitrogen removal from waste streams is energy and cost intensive; yet, without treatment cause eutrophication in aquatic systems.

The aquatic health of the Volta River in Ghana was assessed by monitoring pollutants including water quality parameters, contaminants of emerging concern, antibiotic resistance, and the microbial community. While Ghana is a low- to middle- income country, inadequate sanitation infrastructure and environmental regulations contribute to environmental and human health issues. In this highly collaborative work, common (*e.g.,* nitrogen) and emerging contaminants (*e.g.,* DEET, PFAS) were detected and the microbial community was analyzed from samples collected along the length of the lower Volta River. Spikes in microbial detection (16S rRNA gene) and antibiotic resistant genes were associated with anthropogenic activities indicating adverse effects of human activities on the health of the river.

Additionally, novel biofilm technologies were explored to enhance nitrogen removal from waste streams. Specifically, zeolite-coated hollow fiber membranes and zeolite-coated biofilm carriers were designed to facilitate the partial nitritation-anammox (PNA) processes in mainstream wastewater, where significant cost savings and improved treatment could be realized. Zeolite particles and zeolite coated membranes in batch systems fed with mainstream-like synthetic wastewater demonstrated that anammox bacteria could be enriched and total nitrogen removal enhanced when compared to control systems without zeolite. By varying the mass of zeolite in the system it was discovered that a minimum amount of zeolite, or ammonium sorption capacity, was needed to achieve anammox retention.

Zeolite-coated materials were further tested in flow-through systems to determine under what wastewater-relevant conditions nitrogen treatment enhanced. Zeolite-coated carriers in reactors under anaerobic conditions significantly retained anaerobic ammonia oxidizing

(anammox) bacteria over systems with uncoated carriers; however, identical reactors operated under aerobic conditions did not retain aerobic oxidizing bacteria (AOB) on the carriers themselves. In both anaerobic and aerobic conditions, AOB were preferentially retained in the liquid of the reactors containing zeolite-coated carriers. Unexpectedly, denitrifying genes (specifically *nirS*, *nirK,* and *nosZ*) were also retained in systems with zeolite-coated carriers, indicating the nitrite-shunt process maybe another application. Zeolite-coated membranes were configured in flow-through membrane-aerated reactors and subject to varying operating lengths, inter-lumen oxygen concentrations, and influent nitrite with mixed results. Anammox bacteria were only detected in high quantities on zeolite membranes when operated for two weeks with 100% oxygen with and without nitrite in the influent. AOB were not enriched under any conditions at a 95% confident interval. Further exploration is needed to better understand the lack of AOB retention on both zeolite-carriers and membranes.

Finally, zeolite-coated carriers were tested in stormwater-like systems both in the field and in laboratory reactors for retention of anammox, AOB, and feammox bacteria. Anammox bacteria and AOB were detected in increased quantities on zeolite-coated carriers over uncoated carriers when deployed in a raingarden, but not when deployed in a stormwater pond outlet structure. Carriers were also pre-seeded with anammox biofilm prior to field deployment in order to monitor biomass retention, and at the 2.5-month time scale tested, both control and zeolite carriers in both stormwater systems demonstrated excellent retention of biomass. Biomass was also well retained when both carrier types were pre-seeded and tested in laboratory reactors with simulated storm events. When pre-seeded, both reactors also demonstrated high rate of ammonium removal. Systems containing zeolite carriers inoculated with pond-water, however, had much higher rates of ammonium removal over control carriers indicating that under some conditions, zeolite coating did improve reactor performance. Finally, zeolite particles and zeolite-coated carriers were explored to determine if they also would preferentially retain feammox bacteria, the only known microorganism to defluorinate per- and polyfluorinated alkylated

compounds. Reactors with zeolite particles and zeolite-coated carriers, had increased feammox bacteria and higher rates of ammonium removal.

Overall, this research has demonstrated that zeolite-incorporated technologies are promising solutions to retaining anammox, AOB, and feammox bacteria and enhancing nitrogen removal in waste streams if applied under the right conditions. Treating waste streams to reduce the impacts of excess nutrients and other pollutants from human sources is important to protecting the health of aquatic systems.

Table of contents

List of Tables

List of Figures

Chapter 1: Introduction and Literature Review

Wastewater- and runoff-derived surface water pollution

Nutrients, microbial contaminants, and so-called contaminants of emerging concern (CECs), including pharmaceuticals, personal care products, agricultural pesticides, and industrial chemicals, are ubiquitous in aquatic environments across all populated continents.[1–3] Some of these pollutants are a result of our collection and centralized treatment of wastewater,[3] with other pollutants coming from a range of activities, including agriculture, aquaculture, and urban stormwater runoff.[3–9] Progress has been made in understanding the sources, transport, and biological effects of contaminants through detailed studies performed mostly in high income countries (HICs).[2,3,10–12] Nevertheless, the sources, concentrations, and treatment options for environmental pollutants may differ substantially in low- and medium-income countries (LMICs).[1,13–15] For example, pharmaceuticals that do not require prescriptions, such as many antibiotics and anti-inflammatory drugs, are commonly found in wastewater and surface water in both HICs and LMICs.[1] Deficiencies in wastewater treatment technology in many LMICs result in insufficient removal of these compounds, as well as insufficient removal of nutrients prior to discharge into aquatic environments, resulting in surface water pollution.[1,13,14,16,17] Furthermore, per- and polyfluorinated compounds (PFAS) are ubiquitous in consumer products used globally[18,19] and are likely to be present in surface waters in both HICs and LMICs,[20,21] though perhaps from different sources: wastewater,[22–24] runoff through urban-derived rubbish,[25] and runoff from more diffuse stormwater sources.[26] If the concentrations and sources of common pollutants in LMICs can be better established, existing treatment plants or stormwater treatment systems might be able to be retrofitted for more effective treatment.

Nitrogen in wastewater

If properly operated, wastewater treatment is one important line of defense that removes pollutants from human-generated waste streams.[27,28] Domestic and industrial activities in both HICs and LMICs produce waste streams concentrated with nutrients such as nitrogen, largely in the form of ammonium.[29] If untreated, these wastewater streams could cause eutrophication in receiving waters, especially in populated coastal areas where nitrogen has become the largest pollution problem globally.[30–33] Although excess nitrogen is effectively targeted by wastewater treatment, particularly in HICs,[34] effluent nutrient limits are becoming increasingly stringent, requiring the application of more costly and energy-intensive treatment technologies.[35–37]

Conventional mainstream nitrogen removal in wastewater treatment is a two-step process: 1) nitrification and 2) denitrification (Figure 1.1). Most nitrogen enters the front of the wastewater facility in the form of ammonium or is quickly converted to ammonium from organic nitrogen, with typical influent concentrations in municipal wastewater of 37±17 mg-N/L.[30] Nitrification is the oxidation of ammonium to nitrite and subsequently, nitrite to nitrate. This is often performed by two groups of organisms (Figure 1.1). Ammonia oxidation is carried out by aerobic ammonia oxidizing bacteria (AOB) and archaea. Nitrite oxidizing bacteria (NOB) carry out the conversion of nitrite to nitrate. Nitrification is an autotrophic process and requires oxygen. Denitrification is an anaerobic process during which nitrate and nitrite are reduced to nitrous oxide (N_2O) and ultimately to dinitrogen gas (N_2) (Figure 1.1). An electron donor, typically an organic compound is required to drive nitrate reduction during denitrification. Influent carbon concentrations to the wastewater treatment plan are approximately 100±46 mg/L as soluble chemical oxygen demand (COD), which can be used to drive denitrification if a portion of the nitrified effluent is recycled to the front of the treatment plant for denitrification.[30] There are a large number of microorganisms that perform denitrification and most are heterotrophic facultative aerobes.

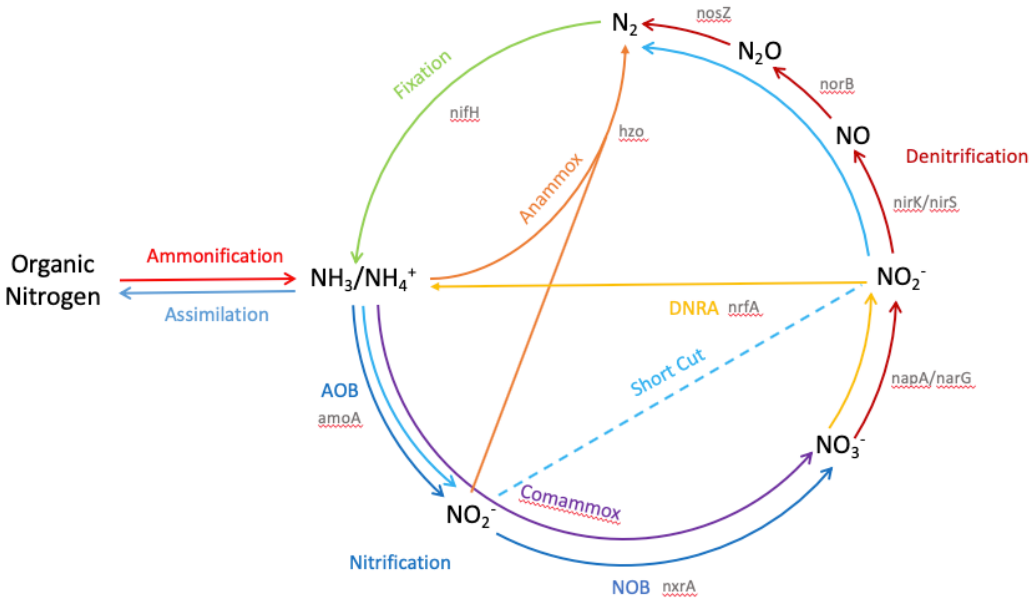

Figure 1.1 Nitrogen Cycle

Energy Efficient Nitrogen Removal

While conventional nitrogen removal wastewater processes (nitrification/denitrification) are reliable, these processes are also the most energy intensive components of a wastewater treatment facility.[38] In fact, aeration, which drives nitrification, consumes 40-75% of a treatment facility's energy.[39,40] This equates to approximately 3% of the total US electricity use and costs an annual $2.8 billion.[39] The high energy demand contributes to a large carbon footprint and therefore has a substantial impact on climate change. The annual emission of wastewater treatment plants is more than 45 million tons of greenhouse gases globally.[41] Enhancing nutrient removal processes in mainstream wastewater treatment to use less aeration and therefore less energy, would provide substantial savings to treatment facilities, reductions in GHG emissions, and move wastewater treatment from being energy consuming to resource producing.

Anaerobic ammonium oxidizing (anammox) bacteria offer a promising alternative to the conventional nitrogen removal process. Anammox bacteria convert nearly equimolar ratios of

ammonium and nitrite to N_2 using nitrite as the electron acceptor (Eq. 1), by-passing many of the steps required for conventional treatment.[42,43]

$$\text{(Eq. 1)} \qquad NH_4^+ + NO_2^- \rightarrow N_2 + 2H_2O$$

Anammox bacteria are chemolithoautotrophs and therefore do not require the addition of a carbon source. Today, there are five known genera of anammox, including: Brocadia, Kuenenia, Scalindua, Anammoxoglobus, and Jettenia,[44,45] of which Brocadia and Kuenenia are the most common genera in wastewater.[46] Anammox bacteria have a very slow growth rate with doubling time ranging from 7 days to 3 weeks.[42] In addition to their slow growth rates, anammox bacteria are sensitive to oxygen and inhibited at even low dissolved oxygen (DO) levels (less than 1 μM), which can result in other taxa, such as ammonium oxidizing bacteria, dominating in many wastewater-like environments.[42] Interestingly, since anammox bacteria are reliant on a nitrite source, they are frequently found in clusters with AOB.[42,47] Heterotrophic denitrifiers are a large, diverse group of bacteria that can also be a source of nitrite for anammox via their reduction of nitrate, and are commonly found with anammox bacteria as well. As chemolithoautotrophs, anammox bacteria can respond negatively to the presence of organic carbon, which denitrifiers typically require.[48] Denitrifiers can also consume nitrite, competing with anammox, especially in carbon rich environments, such as mainstream wastewater.[36] The conditions and environments where anammox bacteria are found and can thrive are still not well understood, which has inhibited widespread application of anammox mainstream wastewater treatment.[40,45,49–51]

Anammox bacteria have been used for ammonium removal in wastewater treatment via a process known as partial nitrification-anammox (PNA).[36,52–54] In this process the only oxygen requirement is for the transformation of half of the incoming ammonium to nitrite by AOB, utilizing three moles of oxygen to convert two moles of ammonium to nitrite. Anammox bacteria can then utilize the remaining ammonium with the AOB-produced nitrite to anaerobically generate N_2. The combination of partial nitritation of half of the ammonium to nitrite with subsequent anammox-driven generation of N_2 reduces the oxygen demand by approximately 60%

compared to conventional nitrification systems.[54,55] Additionally, since the anammox process performs complete nitrogen removal, the denitrification process can be eliminated. Anammox bacteria and AOB also produce very little sludge, reducing yet another cost in terms of biosolids stabilization and disposal (Table 1.1).[55] Complete nitrogen removal via PNA can occur in one bioreactor as well; potentially simplifying complex conventional reactor configurations (i.e., nitrification-denitrification).[56,57] If the PNA process could be used for mainstream nitrogen treatment, estimated cost savings are approximately 60% of the operating costs of a wastewater treatment facility, with some estimates of even higher cost savings, at 90%.[42]

Table 1.1 Operational parameters for biological n-removal systems. [55,58]

	Energy Consumption (kWh/kg N)	Carbon to Nitrogen Ratio	Sludge Production (kg dry weight./kg N)	Number of reactors
Conventional Process	2.3	3 - 6	1 – 1.2	2
Anammox Process	0.9	0	<0.1	1 - 2
Nitrite Shunt Process	1.7	2 - 4	0.8 – 0.9	1 - 2

Another cost- and energy-reducing nitrogen removal process is the nitrite shunt (NS) process, or nitritation/denitritation. The NS process combines nitrification of ammonium to nitrite with the anaerobic conversion of nitrite to N_2 by nitrite-consuming denitrifiers. Benefits of the NS process are similar to, though not as extensive as, the anammox process and are also described in Table 1.1. The NS process reduces oxygen demand by 25%, which reduces energy input.[30] Unlike the anammox process, however, this process requires conversion of all of the ammonium present to nitrite. Carbon addition can be reduced by approximately 40% by avoiding nitrate production, but it cannot be eliminated because denitrifiers require an electron donor and are typically heterotrophic.[58] Other benefits of the NS process include faster overall conversion rates to N_2, 20% lower greenhouse gas emissions, 33-35% lower sludge production during nitrification, and 55% lower sludge production during denitrification.[58] While the cost savings are not as extensive

as PNA, the NS process may be easier to achieve in mainstream treatment, especially in the presence of influent COD. Even in autotrophic biofilms, however, carbon will be present as a result of decay and the formation of soluble microbial products, making heterotrophic growth unavoidable;[59] therefore, PNA and NS processes are not exclusive of each other, and under the correct conditions should occur simultaneously.[60,61]

The anammox process, coupled with PN and potentially NS, has been successful for total nitrogen removal when implemented to treat so called "side-streams," which are typically the nutrient-rich anaerobic supernatants from digester sludge or dewatering liquor.[30] Side-stream treatment is a separate treatment train that treats a different waste stream from mainstream wastewater treatment and has been installed at over 100 full-scale facilities world-wide as of 2014.[62,58,63,64] What makes side-stream ideal for the anammox process is the high ammonium concentrations (500 to 1500 mg-N/L), low C:N ratios, and warm wastewater temperatures that characterize anaerobic supernatants from digester sludge or dewatering liquor.[63,65] These conditions allow anammox to replicate fast enough to not wash out from the reactor,[66] particularly when coupled with methods of anammox retention, such as fixed film growth on biofilm carriers, gel entrapment, and granular anammox growth.[65,67–69] Examples of successful anammox treatment systems include the deammonification over nitrite (DEMON), completely autotrophic nitrogen removal of nitrite (CANON), oxygen limited autotrophic nitrification-denitrification (OLAND), and stable high-rate ammonium removal over nitrite (SHARON) with anammox processes.[57,70,71] These systems have careful control of oxygen delivery to balance the growth of the aerobic nitrifiers, producing nitrite from half of the influent ammonium, and facilitate the growth and retention of anammox, again, primarily through fixed film or granular anammox growth.[72–74]

Challenges of anammox and NS processes

Despite the potential for energy and cost saving, the anammox and NS processes have not been widely implemented for mainstream wastewater nitrogen removal. As mentioned, anammox

bacteria are slow growing and require long solid residence times to be retained, they also appear to prefer temperatures above 30°C.[30,75] In fact, at low temperatures (12.5 ºC) their doubling time can increase to 79 days.[52] High influent carbon concentrations can lead to competition with heterotrophic bacteria, and possibly, anammox bacteria performing different metabolic processes other than ammonium oxidation.[48] DO concentrations as low as 1% have been reported to reversibly inhibit anammox activity, which could slow anaerobic ammonium oxidation even further.[76] Some oxygen delivery is required, however, for production of nitrite by AOB. Competition between anammox bacteria and NOB for nitrite is also problematic, with NOB suppression essential in PNA and NS systems, but practically challenging to achieve at cooler mainstream wastewater temperatures and low ammonium concentrations.[73,74,77] Successful NOB suppression has been achieved using low DO concentrations (0.17 and 0.60 mg O_2/L) and intermittent aeration in low strength wastewater, and does provide a path forward with respect to achieving PNA and/or NS in mainstream wastewater treatment, but only if successfully coupled with anammox or nitrite reduction via denitrifiers.[52,72,73,77,78]

To overcome the challenges associated with the application of PNA in particular for mainstream treatment, we can look to side-stream nitrogen removal and consider ways to mimic those conditions in mainstream wastewater treatment. Indeed, if the typical conditions of side-stream treatment (low and spatially controlled DO, high ammonium concentrations, and specific retention of anammox bacteria, as mentioned previously) could be simulated in the mainstream, low-energy enhanced nitrogen removal via PNA might be able to occur.

Beyond wastewater: other environmental nitrogen removal needs

Improving and facilitating low energy complete nitrogen removal from wastewater is a critical need to reduce treatment costs; nevertheless, there are other systems that could also benefit from the enhancement of the activity and retention of anammox bacteria, such as stormwater treatment. Stormwater runoff is a major contributor to pollution in receiving aquatic

systems, especially in urban areas.[79] Stormwater has notably different characteristics from wastewater, such as flow patterns, pollutant concentrations, and temperatures, and are summarized in Table 1.2.[79,80]

Table 1.2 Comparison of typical wastewater and stormwater conditions

	Flow patterns	TSS, mg/L	COD, mg/L	TKN, mg/L	Ammonia, mg/L	Temperature, ºC
Mainstream municipal wastewater	Diurnal and seasonal[81]	120-400[82]	260-900[82]	20-705[82]	45-12[82]	7-35[82]
Urban stormwater runoff	Storm events and seasonal	67-458[79,82]	5-113[82]	0.2-5.8[79,83]	0-2.6[83]	0-35+[84]

Average ammonium concentrations are lower than wastewater, typically 0.44±1.4 mg/L, but concentrations vary with region, land use, storm event size, season, and more.[83,85] Nationally, freeways were found to have the highest runoff ammonia concentrations according to the National Stormwater Quality Database, with a median concentration of 1.07 mg/L, but peak concentrations of 12 mg/L.[83,86] Other forms of nitrogen reported in stormwater include TN, Total Kjeldahl Nitrogen (TKN), nitrite, and nitrate, with average national concentrations of 1.4±1.2 mg/L for TKN and 0.60±0.97 mg/L for nitrite and nitrate combined.[83] In Minnesota, peak TN runoff concentrations occur in the winter and spring, with average highest concentrations of 3.4 mg/L for TN in the winter and 2.4 mg/L for TKN in the spring.[85] Although nitrogen species and pollutants are typically present in oxidized forms in stormwater, retention ponds can be anaerobic and can also contain decaying organic matter, leading to the generation and release of ammonium.[87,88] It is clear that nitrogen cycling microbes, including anammox bacteria, are present in a wide range of environments, including lakes, natural and engineered wetlands, and soil.[50,89] If they could be specifically enriched and retained in stormwater treatment systems, such as raingardens, detention systems, or in the outlet structures of stormwater retention ponds, it is possible that enhanced TN removal via a PNA-type process could occur.[90]

Benefits of fixed growth systems

Encouraging fixed growth in the form of biofilms is an important way to retain bacteria, while also providing protection for those bacteria from sudden changes in environmental conditions, such as high or low nutrient loading, DO changes, or the introduction of pollutants or toxins.[1] Generally, biofilms consist of active biomass, dead biomass, extracellular polymeric substances (EPS), and void spaces.[92] Materials have been used for years to encourage biofilm attachment and retention in treatment systems,[93–95] with newer materials often utilizing polyethylene as a support in a sponge-like, chip-shaped, coin-shaped, or tube-shaped carrier.[96] The overall biofilm structure and thickness on such carriers are dependent on factors such as the microbial community composition, the shear velocity, and nutrient concentrations in the bulk surrounding the biofilm.[97–103] The thickness of the biofilm itself impacts the diffusion of substrates into the biofilm, and in turn, the location and distribution of specific taxa within the biofilm.[98,104–106] Oxygen diffusion into the outer layers of a biofilm allows for aerobic growth of AOB and production of nitrite and potentially, the growth of NOB and production of nitrate.[107] Once thick enough for oxygen to be consumed in the outer biofilm layer, an anoxic zone can develop within the biofilm, allowing for the co-existence of AOB in the bulk liquid or in the outer regions of a biofilm and anaerobic bacteria, such as anammox, deeper within the biofilm.[68] Because anammox bacteria tend to form granules and biofilms in wastewater environments,[108–110] biofilm carriers can facilitate their retention and prevent the washout of anammox bacteria from particular systems,[53] such as a stormwater pond, raingarden, or mainstream wastewater treatment system. Alternative biofilm supports that are able to supply oxygen through the biofilm substratum via porous membranes have also been studied for their ability to facilitate total nitrogen removal[103,105,106,111] and partial nitritation[72] and could also be a way to encourage anammox retention and PNA in a mainstream wastewater environment.

Controlled Membrane-Based Oxygen Delivery

The delivery of oxygen using membranes has been widely studied[112–114] and has resulted in the development of full-scale treatment processes, such as membrane aerated bioreactors (MABR), also referred to as membrane biofilm reactors.[115,116] Here, membranes, typically polymer-based, serve as a surface upon which biofilm can grow and through which gas is transferred. Rapid oxygen consumption within the membrane-supported biofilm creates anaerobic zones on the outer layers of the biofilm, resulting in a unique stratification of environmental conditions and taxa compared to conventional biofilms (Figure 1.2).[117] Controlled oxygen delivery through such a membrane system has also been shown to successfully suppress the growth of NOB, which could be utilized to support a PNA process.[58,59,118–120] Oxygen delivery through membranes has additional advantages of high gas transfer efficiency and fine control of oxygen delivery, as a result of bubbleless operation and the ability to optimize both the membrane surface area and the membrane lumen gas pressure.[30,105,121,122]

Zeolites to stabilize anammox growth

While careful control of DO to facilitate PN and NS is possible using membranes, the creation of localized micro-environments in which ammonium is concentrated may also be needed to stimulate growth and retain AOB and anammox bacteria under low-nitrogen conditions. Currently, of the few systems operating pilot or full-scale mainstream wastewater anammox systems, nearly all continuously bioaugmenting anammox biomass from side-stream reactors.[36] If a material could be created in which ammonium could be concentrated on a surface, it could enhance anammox activity and growth while providing a surface upon which to grow. Such materials could better retain slow-growing anammox bacteria in a low-nitrogen, high-flow environments.

Fortunately, localized increases in ammonium concentration can be accomplished with zeolite. Zeolite is both a naturally occurring and synthetically made aluminosilica mineral that

can exchange cations (referred to as "sorption"), including ammonium, and in so doing, concentrate them at the zeolite surface. Previous studies have shown that zeolite can enhance nitrogen removal[123–126] and that zeolite can be bio-regenerated, indicating that sorbed ammonium is available for microbial use.[127] Zeolite has also been shown to retain anammox bacteria, not only in wastewater environments, but also in environments such as wetlands.[128–130] A study by Pei et al. of a constructed wetland demonstrated the presence of anammox bacteria, via with denaturing gradient gel electrophoresis, in a layer of zeolite.[130] The conditions of the wetland were anoxic and therefore ideal for anaerobic ammonium oxidation. Their research also suggested that the anammox process was coupled with denitrification, which contributed to high rates of nitrogen removal in the zeolite zone, but the presence of denitrifying organisms was not verified. Other studies have also found anammox bacteria in wetlands containing zeolite where they have been credited with efficient rates of nitrogen removal.[129]

Zeolite incorporated into wastewater treatment processes has also been previously studied. Yapsakli et al. reported the first continuous flow fixed bed bioreactor system with zeolite media as a carrier to enhance anammox.[131] Their work found that zeolite helped sustain the anammox process, even when the influent stoichiometric ratios of nitrite and ammonium were not one to one. Zeolite particles have also been found to improve the performance of moving bed biofilm reactors (MBBR), enhancing microbial activity.[132] Fernández et al. also saw that the specific activity of anammox bacteria and biomass retention increased with the addition of zeolite particles.[109] The overall performance of reactors was improved with respect to systems lacking zeolite.[109] Reduced start up times were also reported with the incorporation of zeolite into anammox reactors.[109] Zeolite has also been incorporated into engineered carrier materials for more controlled deployment and addition of zeolite in wastewater systems. Chen et al. used high density polyethylene carriers with embedded zeolite particles in an aerobic-anaerobic MBBR system for COD and ammonium removal from leachate, though the presence of anammox bacteria were not specifically investigated.[133] Another study conducted with zeolite particles

inside spherical polymer cages serving as biofilm carriers (Lv et al., 2019) demonstrated that using a zeolite for biofilm attachment enhanced the PNA process in low strength, carbon-free wastewater, enriched anammox bacteria, retained AOB, and stimulated microbial metabolism.[134]

Although zeolite can sorb ammonium and encourage the growth of anammox, its use for extended wastewater or stormwater treatment is limited because zeolite is friable and as it breaks apart, it, and the biofilm growing on it, will be washed out of the system.[135] If zeolite could be immobilized on a surface to prevent washout, then it could provide a realistic solution for enhancing nitrogen removal and/or anammox retention in a flow-through treatment system, such as a wastewater treatment plant or a stormwater retention pond outlet structure. Not only would the zeolite be retained in the system, but slow-growing anammox bacteria would also be retained on its surface. Although one previous study has attempted to embed zeolite particles in high density polyethylene, the research was not performed in a manner to determine how successful this zeolite was in enriching ammonium on the carrier surface and in retaining and enriching anammox bacteria.[133] In addition, if a zeolite-coated surface could be further modified to transfer oxygen, as described above for gas transfer membranes, a single technology could be utilized to stimulate PN and enrich and retain anammox under the conditions found in mainstream wastewater or in stormwater retention systems.

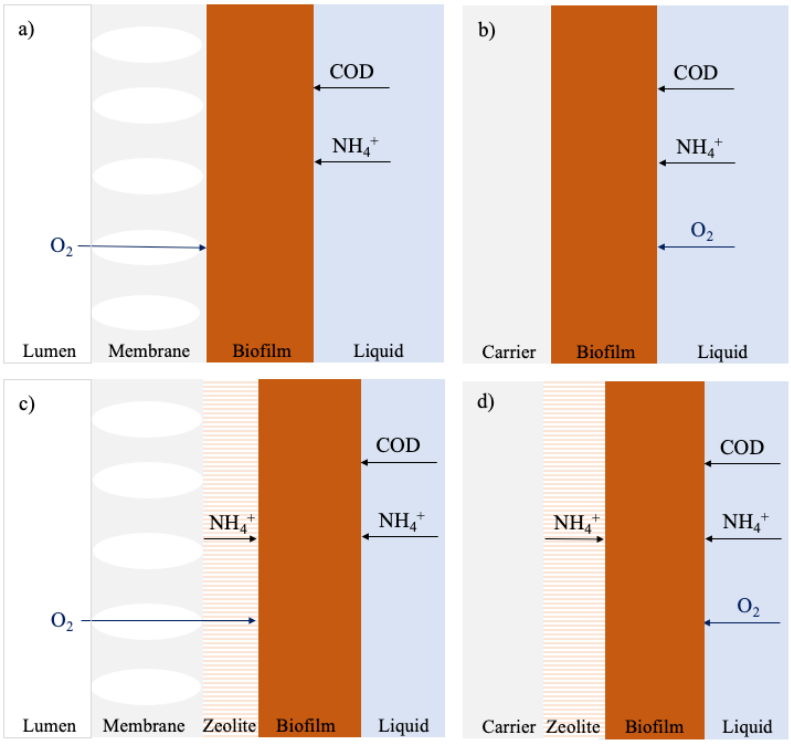

Figure 1.2 Membrane and carrier cross sections with biofilm growth. a) alumina, control hollow fiber membranes, b) PE control carriers, c) zeolite-coated alumina hollow fibers membranes and d) zeolite-coated PE carriers.

Objectives and organization of the dissertation

In this dissertation I describe a brief assessment of the sources and identity of pollutants in an LMIC, Ghana (Chapter 2), as well as a new approach to TN removal in wastewater or stormwater through the development of new technologies for biofilm support that also encourage ammonium sorption, and as a result, anammox growth and retention; these include zeolite-coated hollow fiber membranes (Chapters 3 and 4) and zeolite-coated biofilm carriers (Chapters 4 and 5 and Appendix A) (Figure 1.2).

The objectives for this research were:

1. Assess potential sources of pollutants along the Volta River in Ghana by examining water quality parameters, the concentrations of several contaminants of emerging concern, and

the microbial community along a transect of the river; this work was highly collaborative and my portion of it focused on the measurement of antibiotic resistance genes and analysis of the microbial community present.

2. Assist in developing and test a gas-permeable support that incorporates zeolite, creating a surface-localized microenvironment of increased ammonium concentration to retain anammox bacteria in mainstream-like synthetic wastewater.

3. Deploy zeolite-coated carriers and membranes in several wastewater environments to determine under what conditions anammox bacteria and ammonium oxidizing bacteria are retained and nitrogen removal enhanced.

4. Test zeolite-coated carriers in very low strength waste streams with high flow rates, namely stormwater, to access their performance and the retention of anammox bacteria, AOB, and feammox bacteria.

Ghana is a country of approximately 31 million people with one-quarter of the population residing in the two largest cities, Accra and Kumasi. As a stable democracy with a well-educated population and sustainable birth rates, Ghana has made it its mission to address environmental and human health issues (Ghana Vision, 2020). Nevertheless, insufficient and failing infrastructure, including sanitation infrastructure, remains a major obstacle to achieving this goal, a problem shared by many other LMICs (Egbi et al 2020; Gwenzi and Chaukura 2018, Asem-Hiablie et al. 2013). In this research, described in Chapter 2, I worked with a team to assess the presence of common (*e.g.*, nitrogen) and emerging (*e.g.*, PFAS, antibiotic resistance genes) contaminants along a transect of the Volta River, Ghana, with the goal of providing a baseline assessment to guide future efforts focused on understanding and mitigating pollution along the Volta River. **I hypothesize that given the lack of clear waste management infrastructure in Ghana and lack of regulation of pollutant-generating activities, a variety of pollutant**

sources will exist, releasing low concentrations of contaminants into the Volta River along its length.

With respect to the novel biofilm supports, both the carrier and the membrane sorb ammonium from solution, concentrating it at their surface, with the carrier delivering ammonium to a biofilm growing on the carrier and the membrane delivering both oxygen and ammonium to a biofilm growing on the membrane. **By delivering substrate from the support layer, I hypothesize that microenvironments are created that encourage the preferential proliferation and retention of anammox bacteria on these novel carriers.** The increased localized ammonium concentrations in turn should stabilize anammox and NS processes in the presence of low ammonium bulk concentrations, such as those found in mainstream wastewater and in stormwater treatment systems.[36,83,136] Potential applications for these novel membranes and carriers include their addition to an integrated fixed-film activated sludge (IFAS)-type system, improving conventional MABR systems with zeolite-coated membranes, or incorporation of the carriers into stormwater treatment systems such as raingardens or the outlet structures of retention ponds (see Figure 1.3).

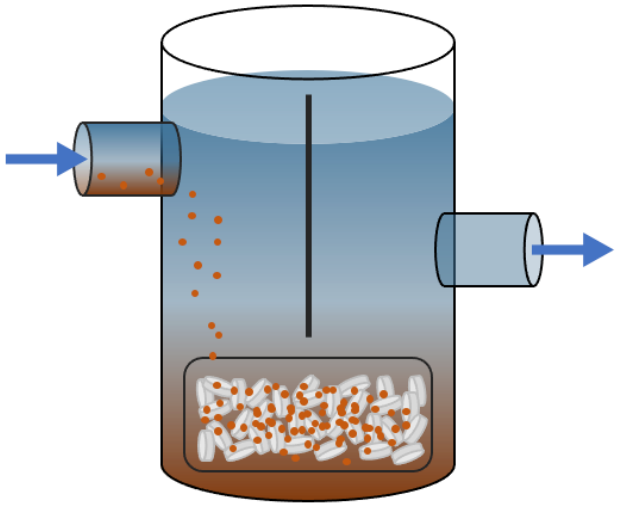

Figure 1.3 Potential deployment for carriers in stormwater outlet structure. Carriers (white) retained in stormwater structure could facilitate nitrogen removal and

retain target microbes (anammox bacteria) in the system. Naturally occurring nitrogen cycling microbes (red dots) would be enriched on the carriers while the nutrients (brown color) flowing into the system would be treated through sorption and microbial processes.

In this research I collaborated with colleagues in the Department of Chemistry and the Department of Chemical Engineering and Material Science to create zeolite-coated membranes and study their ability to enrich and retain target nitrogen-cycling bacteria in a mainstream wastewater environment (Chapters 3,[137] 4). I also collaborated with colleagues in the Department of Chemistry to investigate the material properties of zeolite-coated porous polyethylene carriers (Appendix A) and studied the performance and the ability of these carriers to enrich and retain target nitrogen-cycling bacteria in a mainstream wastewater environment (Chapter 4) and in a stormwater environment (Chapter 5). I also studied the ability of the zeolite-coated polyethylene carriers to retain PFAS-degrading feammox bacteria, which also utilize ammonium as their electron donor (Chapter 5).

References

(1) Fekadu, S.; Alemayehu, E.; Dewil, R.; Van der Bruggen, B. Pharmaceuticals in Freshwater Aquatic Environments: A Comparison of the African and European Challenge. *Sci. Total Environ.* **2019**, *654*, 324–337. https://doi.org/10.1016/j.scitotenv.2018.11.072.

(2) Bradley, P. M.; Journey, C. A.; Romanok, K. M.; Barber, L. B.; Buxton, H. T.; Foreman, W. T.; Furlong, E. T.; Glassmeyer, S. T.; Hladik, M. L.; Iwanowicz, L. R.; Jones, D. K.; Kolpin, D. W.; Kuivila, K. M.; Loftin, K. A.; Mills, M. A.; Meyer, M. T.; Orlando, J. L.; Reilly, T. J.; Smalling, K. L.; Villeneuve, D. L. Expanded Target-Chemical Analysis Reveals Extensive Mixed-Organic-Contaminant Exposure in U.S. Streams. *Environ. Sci. Technol.* **2017**, *51* (9), 4792–4802. https://doi.org/10.1021/acs.est.7b00012.

(3) Kolpin, D. W.; Furlong, E. T.; Meyer, M. T.; Thurman, E. M.; Zaugg, S. D.; Barber, L. B.; Buxton, H. T. Pharmaceuticals, Hormones, and Other Organic Wastewater Contaminants in U.S. Streams, 1999−2000: A National Reconnaissance. *Environ. Sci. Technol.* **2002**, *36* (6), 1202–1211. https://doi.org/10.1021/es011055j.

(4) Ongley, E. D.; Xiaolan, Z.; Tao, Y. Current Status of Agricultural and Rural Non-Point Source Pollution Assessment in China. *Environ. Pollut.* **2010**, *158* (5), 1159–1168. https://doi.org/10.1016/j.envpol.2009.10.047.

(5) Hua, L.; Li, W.; Zhai, L.; Yen, H.; Lei, Q.; Liu, H.; Ren, T.; Xia, Y.; Zhang, F.; Fan, X. An Innovative Approach to Identifying Agricultural Pollution Sources and Loads by Using Nutrient Export Coefficients in Watershed Modeling. *J. Hydrol.* **2019**, *571*, 322–331. https://doi.org/10.1016/j.jhydrol.2019.01.043.
(6) US EPA. National Management Measures to Control Nonpoint Source Pollution from Agriculture, 2003.
(7) Scavia, D.; Kalcic, M.; Muenich, R. L.; Read, J.; Aloysius, N.; Bertani, I.; Boles, C.; Confesor, R.; DePinto, J.; Gildow, M.; Martin, J.; Redder, T.; Robertson, D.; Sowa, S.; Wang, Y.; Yen, H. Multiple Models Guide Strategies for Agricultural Nutrient Reductions. *Front. Ecol. Environ.* **2017**, *15* (3), 126–132. https://doi.org/10.1002/fee.1472.
(8) Petrucci, G.; Gromaire, M.-C.; Shorshani, M. F.; Chebbo, G. Nonpoint Source Pollution of Urban Stormwater Runoff: A Methodology for Source Analysis. *Environ. Sci. Pollut. Res.* **2014**, *21* (17), 10225–10242. https://doi.org/10.1007/s11356-014-2845-4.
(9) Janke, B. D.; Finlay, J. C.; Hobbie, S. E. Trees and Streets as Drivers of Urban Stormwater Nutrient Pollution. *Environ. Sci. Technol.* **2017**, *51* (17), 9569–9579. https://doi.org/10.1021/acs.est.7b02225.
(10) Nilsen, E.; Smalling, K. L.; Ahrens, L.; Gros, M.; Miglioranza, K. S. B.; Picó, Y.; Schoenfuss, H. L. Critical Review: Grand Challenges in Assessing the Adverse Effects of Contaminants of Emerging Concern on Aquatic Food Webs. *Environ. Toxicol. Chem.* **2019**, *38* (1), 46–60. https://doi.org/10.1002/etc.4290.
(11) Arnold, K. E.; Brown, A. R.; Ankley, G. T.; Sumpter, J. P. Medicating the Environment: Assessing Risks of Pharmaceuticals to Wildlife and Ecosystems. *Philos. Trans. R. Soc. B Biol. Sci.* **2014**, *369* (1656), 20130569. https://doi.org/10.1098/rstb.2013.0569.
(12) Corcoran, J.; Winter, M. J.; Tyler, C. R. Pharmaceuticals in the Aquatic Environment: A Critical Review of the Evidence for Health Effects in Fish. *Crit. Rev. Toxicol.* **2010**, *40* (4), 287–304. https://doi.org/10.3109/10408440903373590.
(13) Gwenzi, W.; Chaukura, N. Organic Contaminants in African Aquatic Systems: Current Knowledge, Health Risks, and Future Research Directions. *Sci. Total Environ.* **2018**, *619–620*, 1493–1514. https://doi.org/10.1016/j.scitotenv.2017.11.121.
(14) Asem-Hiablie, S.; Church, C. D.; Elliott, H. A.; Shappell, N. W.; Schoenfuss, H. L.; Drechsel, P.; Williams, C. F.; Knopf, A. L.; Dabie, M. Y. Serum Estrogenicity and Biological Responses in African Catfish Raised in Wastewater Ponds in Ghana. *Sci. Total Environ.* **2013**, *463–464*, 1182–1191. https://doi.org/10.1016/j.scitotenv.2013.06.032.
(15) Parkinson, J.; Tayler, K. Decentralized Wastewater Management in Peri-Urban Areas in Low-Income Countries. *Environ. Urban.* **2003**, *15* (1), 75–90. https://doi.org/10.1177/095624780301500119.
(16) Bouwman, A. F.; Van Drecht, G.; Knoop, J. M.; Beusen, A. H. W.; Meinardi, C. R. Exploring Changes in River Nitrogen Export to the World's Oceans. *Glob. Biogeochem. Cycles* **2005**, *19* (1). https://doi.org/10.1029/2004GB002314.
(17) Van Drecht, G.; Bouwman, A. F.; Harrison, J.; Knoop, J. M. Global Nitrogen and Phosphate in Urban Wastewater for the Period 1970 to 2050: N AND P IN URBAN WASTE WATER. *Glob. Biogeochem. Cycles* **2009**, *23* (4), n/a-n/a. https://doi.org/10.1029/2009GB003458.
(18) Glüge, J.; Scheringer, M.; Cousins, I. T.; DeWitt, J. C.; Goldenman, G.; Herzke, D.; Lohmann, R.; Ng, C. A.; Trier, X.; Wang, Z. An Overview of the Uses of Per- and Polyfluoroalkyl Substances (PFAS). *Environ. Sci. Process. Impacts* **2020**, *22* (12), 2345–2373. https://doi.org/10.1039/D0EM00291G.
(19) Podder, A.; Sadmani, A. H. M. A.; Reinhart, D.; Chang, N.-B.; Goel, R. Per and Poly-Fluoroalkyl Substances (PFAS) as a Contaminant of Emerging Concern in Surface Water: A Transboundary Review of Their Occurrences and Toxicity Effects. *J. Hazard. Mater.* **2021**, *419*, 126361. https://doi.org/10.1016/j.jhazmat.2021.126361.

(20) Crone, B. C.; Speth, T. F.; Wahman, D. G.; Smith, S. J.; Abulikemu, G.; Kleiner, E. J.; Pressman, J. G. Occurrence of Per- and Polyfluoroalkyl Substances (PFAS) in Source Water and Their Treatment in Drinking Water. *Crit. Rev. Environ. Sci. Technol.* **2019**, *49* (24), 2359–2396. https://doi.org/10.1080/10643389.2019.1614848.
(21) Baabish, A.; Sobhanei, S.; Fiedler, H. Priority Perfluoroalkyl Substances in Surface Waters - A Snapshot Survey from 22 Developing Countries. *Chemosphere* **2021**, *273*, 129612. https://doi.org/10.1016/j.chemosphere.2021.129612.
(22) Lenka, S. P.; Kah, M.; Padhye, L. P. A Review of the Occurrence, Transformation, and Removal of Poly- and Perfluoroalkyl Substances (PFAS) in Wastewater Treatment Plants. *Water Res.* **2021**, *199*, 117–187. https://doi.org/10.1016/j.watres.2021.117187.
(23) Phong Vo, H. N.; Ngo, H. H.; Guo, W.; Hong Nguyen, T. M.; Li, J.; Liang, H.; Deng, L.; Chen, Z.; Hang Nguyen, T. A. Poly-and Perfluoroalkyl Substances in Water and Wastewater: A Comprehensive Review from Sources to Remediation. *J. Water Process Eng.* **2020**, *36*, 101393. https://doi.org/10.1016/j.jwpe.2020.101393.
(24) Castiglioni, S.; Valsecchi, S.; Polesello, S.; Rusconi, M.; Melis, M.; Palmiotto, M.; Manenti, A.; Davoli, E.; Zuccato, E. Sources and Fate of Perfluorinated Compounds in the Aqueous Environment and in Drinking Water of a Highly Urbanized and Industrialized Area in Italy. *J. Hazard. Mater.* **2015**, *282*, 51–60. https://doi.org/10.1016/j.jhazmat.2014.06.007.
(25) Sharma, B. M.; Bharat, G. K.; Tayal, S.; Larssen, T.; Bečanová, J.; Karásková, P.; Whitehead, P. G.; Futter, M. N.; Butterfield, D.; Nizzetto, L. Perfluoroalkyl Substances (PFAS) in River and Ground/Drinking Water of the Ganges River Basin: Emissions and Implications for Human Exposure. *Environ. Pollut.* **2016**, *208*, 704–713. https://doi.org/10.1016/j.envpol.2015.10.050.
(26) Pramanik, B. K.; Roychand, R.; Monira, S.; Bhuiyan, M.; Jegatheesan, V. Fate of Road-Dust Associated Microplastics and per- and Polyfluorinated Substances in Stormwater. *Process Saf. Environ. Prot.* **2020**, *144*, 236–241. https://doi.org/10.1016/j.psep.2020.07.020.
(27) Jiménez, B.; Mara, D.; Carr, R.; Brissaud, F. Wastewater Treatment for Pathogen Removal and Nutrient Conservation: Suitable Systems for Use in Developing Countries. *Wastewater Irrig. Health Assess. Mitigating Risk Low-Income Ctries.* **2010**, 149–169.
(28) Rahman, S. M.; Eckelman, M. J.; Onnis-Hayden, A.; Gu, A. Z. Comparative Life Cycle Assessment of Advanced Wastewater Treatment Processes for Removal of Chemicals of Emerging Concern. *Environ. Sci. Technol.* **2018**, *52* (19), 11346–11358. https://doi.org/10.1021/acs.est.8b00036.
(29) Li, Y.; Li, H.; Xu, X.; Xiao, S.; Wang, S.; Xu, S. Fate of Nitrogen in Subsurface Infiltration System for Treating Secondary Effluent. *Water Sci. Eng.* **2017**, *10* (3), 217–224. https://doi.org/10.1016/j.wse.2017.10.002.
(30) Delgado Vela, J.; Stadler, L. B.; Martin, K. J.; Raskin, L.; Bott, C. B.; Love, N. G. Prospects for Biological Nitrogen Removal from Anaerobic Effluents during Mainstream Wastewater Treatment. *Environ. Sci. Technol. Lett.* **2015**, *2* (9), 234–244. https://doi.org/10.1021/acs.estlett.5b00191.
(31) Howarth, R. W. Coastal Nitrogen Pollution: A Review of Sources and Trends Globally and Regionally. *Harmful Algae* **2008**, *8* (1), 14–20. https://doi.org/10.1016/j.hal.2008.08.015.
(32) Smetacek, V.; Zingone, A. Green and Golden Seaweed Tides on the Rise. *Nature* **2013**, *504* (7478), 84–88. https://doi.org/10.1038/nature12860.
(33) Ansa-Asare, O.; Mensah, E.; Entsua-Mensah, M.; Biney, C. Impact of Human Activities on Nutrient and Trophic Status of Some Selected Lagoons in Ghana. *West Afr. J. Appl. Ecol.* **2009**, *12* (1). https://doi.org/10.4314/wajae.v12i1.45761.

(34) Mojiri, A.; Bashir, M. J. K. Wastewater Treatment: Current and Future Techniques. *Water* **2022**, *14* (3), 448. https://doi.org/10.3390/w14030448.
(35) Water Quality: Two Year Milestones, 2015.
(36) Li, X.; Klaus, S.; Bott, C.; He, Z. Status, Challenges, and Perspectives of Mainstream Nitritation-Anammox for Wastewater Treatment. *Water Environ. Res.* **2018**, *90* (7), 634–649. https://doi.org/10.2175/106143017x15131012153112.
(37) Hu, Z.; Houweling, D.; Dold, P. Biological Nutrient Removal in Municipal Wastewater Treatment: New Directions in Sustainability. *J. Environ. Eng.* **2012**, *138* (3), 307–317. https://doi.org/10.1061/(ASCE)EE.1943-7870.0000462.
(38) Mamais, D.; Noutsopoulos, C.; Dimopoulou, A.; Stasinakis, A.; Lekkas, T. D. Wastewater Treatment Process Impact on Energy Savings and Greenhouse Gas Emissions. *Water Sci. Technol.* **2015**, *71* (2), 303–308. https://doi.org/10.2166/wst.2014.521.
(39) Crawford, G.; Sandino, J. *Energy Efficiency in Wastewater Treatment in North America: A Compendium of Best Practices and Case Studies of Novel Approaches*; 2010.
(40) Gu, J.; Zhang, M.; Liu, Y. A Review on Mainstream Deammonification of Municipal Wastewater: Novel Dual Step Process. *Bioresour. Technol.* **2020**, *299*, 122674. https://doi.org/10.1016/j.biortech.2019.122674.
(41) Tarallo, S. *A Guide to Net-Zero Energy Solutions for Water Resource Recovery Facilities*; 2015; Vol. 14. https://doi.org/10.2166/9781780407685.
(42) Jetten, M. S. M.; Cirpus, I.; Kartal, B.; van Niftrik, L.; van de Pas-Schoonen, K. T.; Sliekers, O.; Haaijer, S.; van der Star, W.; Schmid, M.; van de Vossenberg, J.; Schmidt, I.; Harhangi, H.; van Loosdrecht, M.; Gijs Kuenen, J.; Op den Camp, H.; Strous, M. 1994–2004: 10 Years of Research on the Anaerobic Oxidation of Ammonium. *Biochem. Soc. Trans.* **2005**, *33* (1), 119–123. https://doi.org/10.1042/BST0330119.
(43) Mulder, A.; van de Graaf, A. A.; Robertson, L. A.; Kuenen, J. G. Anaerobic Ammonium Oxidation Discovered in a Denitrifying Fluidized Bed Reactor. *FEMS Microbiol. Ecol.* **1995**, *16* (3).
(44) Zhang, L.; Narita, Y.; Gao, L.; Ali, M.; Oshiki, M.; Ishii, S.; Okabe, S. Microbial Competition among Anammox Bacteria in Nitrite-Limited Bioreactors. *Water Res.* **2017**, *125*, 249–258. https://doi.org/10.1016/J.WATRES.2017.08.052.
(45) Wang, S.; Peng, Y.; Ma, B.; Wang, S.; Zhu, G. Anaerobic Ammonium Oxidation in Traditional Municipal Wastewater Treatment Plants with Low-Strength Ammonium Loading: Widespread but Overlooked. *Water Res.* **2015**, *84*, 66–75. https://doi.org/10.1016/j.watres.2015.07.005.
(46) Qiao, L.; Ning, X.; Li, Y.; Zhang, Y. A Kinetics Study on Anammox Bacteria with a Disproportionate Substrate Concentration. *J. Chem. Technol. Biotechnol.* **2017**. https://doi.org/10.1002/jctb.5229.
(47) Schmidt, I.; Sliekers, O.; Schmid, M.; Cirpus, I.; Strous, M.; Bock, E.; Kuenen, J. G.; Jetten, M. S. M. Aerobic and Anaerobic Ammonia Oxidizing Bacteria – Competitors or Natural Partners? *FEMS Microbiol. Ecol.* **2002**, *39* (3), 175–181. https://doi.org/10.1016/S0168-6496(01)00208-2.
(48) Jin, R.-C.; Yang, G.-F.; Yu, J.-J.; Zheng, P. The Inhibition of the Anammox Process: A Review. *Chem. Eng. J.* **2012**, *197*, 67–79. https://doi.org/10.1016/J.CEJ.2012.05.014.
(49) Laureni, M.; Weissbrodt, D. G.; Szivák, I.; Robin, O.; Nielsen, J. L.; Morgenroth, E.; Joss, A. Activity and Growth of Anammox Biomass on Aerobically Pre-Treated Municipal Wastewater. *Water Res.* **2015**, *80*, 325–336. https://doi.org/10.1016/j.watres.2015.04.026.
(50) Wang, Y.; Xu, L.; Wang, S.; Ye, F.; Zhu, G. Global Distribution of Anaerobic Ammonia Oxidation (Anammox) Bacteria – Field Surveys in Wetland, Dryland, Groundwater Aquifer and Snow. *Front. Microbiol.* **2019**, *10*, 2583. https://doi.org/10.3389/fmicb.2019.02583.

(51) Zhang, J.; Zhang, Y.; Li, Y.; Zhang, L.; Qiao, S.; Yang, F.; Quan, X. Enhancement of Nitrogen Removal in a Novel Anammox Reactor Packed with Fe Electrode. *Bioresour. Technol.* **2012**, *114*, 102–108. https://doi.org/10.1016/j.biortech.2012.03.018.
(52) Akaboci, T. R. V.; Gich, F.; Ruscalleda, M.; Balaguer, M. D.; Colprim, J. Assessment of Operational Conditions towards Mainstream Partial Nitritation-Anammox Stability at Moderate to Low Temperature: Reactor Performance and Bacterial Community. *Chem. Eng. J.* **2018**, *350* (May), 192–200. https://doi.org/10.1016/j.cej.2018.05.115.
(53) Wells, G. F.; Shi, Y.; Laureni, M.; Rosenthal, A.; Sziva, I.; Weissbrodt, D. G.; Joss, A.; Buergmann, H.; Johnson, D. R.; Morgenroth, E. Comparing the Resistance, Resilience, and Stability of Replicate Moving Bed Biofilm and Suspended Growth Combined Nitritation− Anammox Reactors. *Environ. Sci. Technol.* **2017**, *51*, 5108–5117. https://doi.org/10.1021/acs.est.6b05878.
(54) Wagner, B. M.; Daigger, G. T.; Love, N. G. Assessing Membrane Aerated Biofilm Reactor Configurations in Mainstream Anammox Applications. *Water Sci. Technol.* **2022**, wst2022013. https://doi.org/10.2166/wst.2022.013.
(55) Mulder, A. The Quest for Sustainable Nitrogen Removal Technologies. *Water Sci. Technol.* **2003**, *48* (1), 67–75.
(56) The Development of Simultaneous Partial Nitrification, ANAMMOX and Denitrification (SNAD) Process in a Single Reactor for Nitrogen Removal. *Bioresour. Technol.* **2009**, *100* (4), 1548–1554. https://doi.org/10.1016/J.BIORTECH.2008.09.003.
(57) Bagchi, S.; Biswas, R.; Nandy, T. Alkalinity and Dissolved Oxygen as Controlling Parameters for Ammonia Removal through Partial Nitritation and ANAMMOX in a Single-Stage Bioreactor. *J. Ind. Microbiol. Biotechnol.* **2010**, *37* (8), 871–876. https://doi.org/10.1007/s10295-010-0744-3.
(58) Zhu, G.; Peng, Y. Biological Nitrogen Removal with Nitrification and Denitrification via Nitrite Pathway. *Harbin Gongye Daxue XuebaoJournal Harbin Inst. Technol.* **2008**, *40* (10), 1552–1557. https://doi.org/10.1007/s00253-006-0534-z.
(59) Ni, B.-J.; Ruscalleda, M.; Smets, B. F. Evaluation on the Microbial Interactions of Anaerobic Ammonium Oxidizers and Heterotrophs in Anammox Biofilm. *Water Res.* **2012**, *46* (15), 4645–4652. https://doi.org/10.1016/J.WATRES.2012.06.016.
(60) Li, X.; Peng, Y.; Zhang, J.; Du, R. Highly Efficient and Synchronous Nitrogen Removal from Ammonia-Rich Wastewater and Domestic Wastewater via a Novel Anammox Coupled with Double-Nitrite-Shunt Process at Low Temperature. *Chem. Eng. J.* **2021**, *425*, 131449. https://doi.org/10.1016/j.cej.2021.131449.
(61) Singh, V.; Ormeci, B.; Mishra, S.; Hussain, A. Simultaneous Partial Nitrification, ANAMMOX and Denitrification (SNAD) – A Review of Critical Operating Parameters and Reactor Configurations. *Chem. Eng. J.* **2022**, *433*, 133677. https://doi.org/10.1016/j.cej.2021.133677.
(62) Wang, X.; Gao, D. The Transformation from Anammox Granules to Deammonification Granules in Micro-Aerobic System by Facilitating Indigenous Ammonia Oxidizing Bacteria. *Bioresour. Technol.* **2018**, *250* (November 2017), 439–448. https://doi.org/10.1016/j.biortech.2017.11.046.
(63) Lackner, S.; Gilbert, E. M.; Vlaeminck, S. E.; Joss, A.; Horn, H.; van Loosdrecht, M. C. M. Full-Scale Partial Nitritation/Anammox Experiences - An Application Survey. *Water Res.* **2014**, *55* (2014), 292–303. https://doi.org/10.1016/j.watres.2014.02.032.
(64) Mulder, J. W.; Van Loosdrecht, M. C. M.; Hellinga, C.; Van Kempen, R. Full-Scale Application of the SHARON Process for Treatment of Rejection Water of Digested Sludge Dewatering. *Water Sci. Technol.* **2001**, *43* (11), 127–134. https://doi.org/10.2166/wst.2001.0675.
(65) Kosgey, K.; Chandran, K.; Gokal, J.; Kiambi, S. L.; Bux, F.; Kumari, S. Critical Analysis of Biomass Retention Strategies in Mainstream and Sidestream ANAMMOX-Mediated

Nitrogen Removal Systems. *Environ. Sci. Technol.* **2021**, *55* (1), 9–24. https://doi.org/10.1021/acs.est.0c00276.
(66) Environmental Protection Agency EPA. Wastewater Management Fact Sheet: Energy Conservation. **2006**.
(67) Hubaux, N.; Wells, G.; Morgenroth, E. Impact of Coexistence of Flocs and Biofilm on Performance of Combined Nitritation-Anammox Granular Sludge Reactors. *Water Res.* **2015**, *68*, 127–139. https://doi.org/10.1016/j.watres.2014.09.036.
(68) Winkler, M. K. H.; Kleerebezem, R.; Van Loosdrecht, M. C. M. Integration of Anammox into the Aerobic Granular Sludge Process for Main Stream Wastewater Treatment at Ambient Temperatures. *Water Res.* **2012**, *46* (1), 136–144. https://doi.org/10.1016/j.watres.2011.10.034.
(69) Magrí, A.; Vanotti, M. B.; Szögi, A. A. Anammox Sludge Immobilized in Polyvinyl Alcohol (PVA) Cryogel Carriers. *Bioresour. Technol.* **2012**, *114*, 231–240. https://doi.org/10.1016/j.biortech.2012.03.077.
(70) Vlaeminck, S. E.; Terada, A.; Smets, B. F.; De Clippeleir, H.; Schaubroeck, T.; Bolca, S.; Demeestere, L.; Mast, J.; Boon, N.; Carballa, M.; Verstraete, W. Aggregate Size and Architecture Determine Microbial Activity Balance for One-Stage Partial Nitritation and Anammox. *Appl. Environ. Microbiol.* **2010**, *76* (3), 900–909. https://doi.org/10.1128/AEM.02337-09.
(71) van Dongen, U.; Jetten, M. S. M.; van Loosdrecht, M. C. M. The SHARON®-Anammox® Process for Treatment of Ammonium Rich Wastewater. *Water Sci. Technol.* **2001**, *44* (1), 153–160.
(72) Ma, Y.; Domingo-Félez, C.; Plósz, B. Gy.; Smets, B. F. Intermittent Aeration Suppresses Nitrite-Oxidizing Bacteria in Membrane-Aerated Biofilms: A Model-Based Explanation. *Environ. Sci. Technol.* **2017**, *51* (11), 6146–6155. https://doi.org/10.1021/acs.est.7b00463.
(73) Ma, B.; Bao, P.; Wei, Y.; Zhu, G.; Yuan, Z.; Peng, Y. Suppressing Nitrite-Oxidizing Bacteria Growth to Achieve Nitrogen Removal from Domestic Wastewater via Anammox Using Intermittent Aeration with Low Dissolved Oxygen. *Nat. Publ. Group* **2015**. https://doi.org/10.1038/srep13048.
(74) Isanta, E.; Reino, C.; An Carrera, J.; Erez, J. P. Stable Partial Nitritation for Low-Strength Wastewater at Low Temperature in an Aerobic Granular Reactor. **2015**. https://doi.org/10.1016/j.watres.2015.04.028.
(75) Kuenen, J. G. Anammox Bacteria: From Discovery to Application. *Nat. Rev. Microbiol.* **2008**, *6* (4), 320. https://doi.org/10.1038/nrmicro1857.
(76) Egli, K.; Fanger, U.; Alvarez, P. J. J.; Siegrist, H.; van der Meer, J. R.; Zehnder, A. J. B. Enrichment and Characterization of an Anammox Bacterium from a Rotating Biological Contactor Treating Ammonium-Rich Leachate. *Arch. Microbiol.* **2001**, *175* (3), 198–207. https://doi.org/10.1007/s002030100255.
(77) Joss, A.; Derlon, N.; Cyprien, C.; Burger, S.; Szivak, I.; Traber, J.; Siegrist, H.; Morgenroth, E. Combined Nitritation-Anammox: Advances in Understanding Process Stability. *Environ. Sci. Technol.* **2011**, *45* (22), 9735–9742. https://doi.org/10.1021/es202181v.
(78) Mehrabi, S.; Houweling, D.; Dagnew, M. Establishing Mainstream Nitrite Shunt Process in Membrane Aerated Biofilm Reactors: Impact of Organic Carbon and Biofilm Scouring Intensity. *J. Water Process Eng.* **2020**, *37*, 101460. https://doi.org/10.1016/j.jwpe.2020.101460.
(79) Langeveld, J. G.; Liefting, H. J.; Boogaard, F. C. Uncertainties of Stormwater Characteristics and Removal Rates of Stormwater Treatment Facilities: Implications for Stormwater Handling. *Water Res.* **2012**, *46* (20), 6868–6880. https://doi.org/10.1016/j.watres.2012.06.001.

(80) Lee, H.; Swamikannu, X.; Radulescu, D.; Kim, S.; Stenstrom, M. K. Design of Stormwater Monitoring Programs. *Water Res.* **2007**, *41* (18), 4186–4196. https://doi.org/10.1016/j.watres.2007.05.016.
(81) US EPA. Hourly Diurnal Flow Variation in Publically-Owned Wasetwater Treatment Facilities, 1981.
(82) Metcalf and Eddy. *Wastewater Engineering Treatment and Reuse*; 1991.
(83) Pitt, R.; Maestre, A.; Morquecho, R. National Stormwater Quality Database. Version 1.1. **2004**.
(84) Zeiger, S.; Hubbart, J. Urban Stormwater Temperature Surges: A Central US Watershed Study. *Hydrology* **2015**, *2* (4), 193–209. https://doi.org/10.3390/hydrology2040193.
(85) Brezonik, P. L.; Stadelmann, T. H. Analysis and Predictive Models of Stormwater Runoff Volumes, Loads, and Pollutant Concentrations from Watersheds in the Twin Cities Metropolitan Area, Minnesota, USA. *Water Res.* **2002**, *36* (7), 1743–1757. https://doi.org/10.1016/S0043-1354(01)00375-X.
(86) Kayhanian, M.; Fruchtman, B. D.; Gulliver, J. S.; Montanaro, C.; Ranieri, E.; Wuertz, S. Review of Highway Runoff Characteristics: Comparative Analysis and Universal Implications. *Water Res.* **2012**, *46* (20), 6609–6624. https://doi.org/10.1016/j.watres.2012.07.026.
(87) Koch, B. J.; Febria, C. M.; Gevrey, M.; Wainger, L. A.; Palmer, M. A. Nitrogen Removal by Stormwater Management Structures: A Data Synthesis. *JAWRA J. Am. Water Resour. Assoc.* **2014**, *50* (6), 1594–1607. https://doi.org/10.1111/jawr.12223.
(88) Gold, A. C.; Thompson, S. P.; Piehler, M. F. Nitrogen Cycling Processes within Stormwater Control Measures: A Review and Call for Research. *Water Res.* **2019**, *149*, 578–587. https://doi.org/10.1016/j.watres.2018.10.036.
(89) Burgin, A. J.; Hamilton, S. K. Have We Overemphasized the Role of Denitrification in Aquatic Ecosystems? A Review of Nitrate Removal Pathways. *Front. Ecol. Environ.* **2007**, *5* (2), 89–96. https://doi.org/10.1890/1540-9295(2007)5[89:HWOTRO]2.0.CO;2.
(90) Sun, Y.; Zhang, D.; Wang, Z.-W. The Potential of Using Biological Nitrogen Removal Technique for Stormwater Treatment. *Ecol. Eng.* **2017**, *106*, 482–495. https://doi.org/10.1016/j.ecoleng.2017.05.045.
(91) Carvajal-Arroyo, J. M.; Sun, W.; Sierra-Alvarez, R.; Field, J. A. Inhibition of Anaerobic Ammonium Oxidizing (Anammox) Enrichment Cultures by Substrates, Metabolites and Common Wastewater Constituents. *Chemosphere* **2013**, *91* (1), 22–27. https://doi.org/10.1016/j.chemosphere.2012.11.025.
(92) Trigo, C.; Campos, J. L.; Garrido, J. M.; Méndez, R. Start-up of the Anammox Process in a Membrane Bioreactor. *J. Biotechnol.* **2006**, *126*, 475–487. https://doi.org/10.1016/j.jbiotec.2006.05.008.
(93) Siegrist, H.; Gujer, W. Demonstration of Mass Transfer and PH Effects in a Nitrifying Biofilm. *Water Res.* **1987**, *21* (12), 1481–1487. https://doi.org/10.1016/0043-1354(87)90131-X.
(94) Kuenen, J. G.; Jorgi~nsen, B.; Revsnech, N. P. OXYGEN MICROPROFILES OF TRICKLING FILTER BIOFILMS. *Wat Res* **1986**, *20* (12), 1589–1598.
(95) Zhang, L.; Liu, M.; Zhang, S.; Yang, Y.; Peng, Y. Integrated Fixed-Biofilm Activated Sludge Reactor as a Powerful Tool to Enrich Anammox Biofilm and Granular Sludge. **2015**. https://doi.org/10.1016/j.chemosphere.2015.02.001.
(96) Frankel, T. How to Select the Right MBBR Media, 2020.
(97) Picioreanu, C.; Kreft, J.-U.; Mark C. M. van Loosdrecht. Particle Based Multidimensional Multispecies Biofilm Model. *Appl. Environ. Microbiol.* **2004**, *70* (5), 3024–3040. https://doi.org/10.1128/AEM.70.5.3024.
(98) Xavier, B.; Picioreanu, C.; M van Loosdrecht, M. C.; Xavier, J. B.; Picioreanu, C.; M van Loosdrecht, M. C. A Framework for Multidimensional Modelling of Activity and

Structure of Multispecies Biofilms. *Environ. Microbiol.* **2005**, *7* (8), 1085–1103. https://doi.org/10.1111/j.1462-2920.2005.00787.x.
(99) Wanner, O.; Gujer, W. A Multispecies Biofilm Model. *Biotechnol. Bioeng.* **1986**, *28* (3), 314–328. https://doi.org/10.1002/bit.260280304.
(100) Horn, H.; Lackner, S. Modeling of Biofilm Systems: A Review; Springer International Publishing, 2014; pp 53–76. https://doi.org/10.1007/10_2014_275.
(101) Horn, H.; Reiff, H.; Morgenroth, E. Simulation of Growth and Detachment in Biofilm Systems under Defined Hydrodynamic Conditions. *Biotechnol. Bioeng.* **2003**, *81* (5), 607–617. https://doi.org/10.1002/bit.10503.
(102) Casey, E.; Glennon, B.; Hamer, G. Biofilm Development in a Membrane-Aerated Biofilm Reactor: Effect of Flow Velocity on Performance. *Biotechnol. Bioeng.* **2000**, *67* (4), 476–486. https://doi.org/10.1002/(SICI)1097-0290(20000220)67:4<476::AID-BIT11>3.0.CO;2-2.
(103) Cole, A. C.; Semmens, M. J.; LaPara, T. M. Stratification of Activity and Bacterial Community Structure in Biofilms Grown on Membranes Transferring Oxygen. *Appl. Environ. Microbiol.* **2004**, *70* (4), 1982–1989. https://doi.org/10.1128/AEM.70.4.1982-1989.2004.
(104) Rittmann, B. E.; Manem, J. A. Development and Experimental Evaluation of a Steady-state, Multispecies Biofilm Model. *Biotechnol. Bioeng.* **1992**, *39* (9), 914–922. https://doi.org/10.1002/bit.260390906.
(105) LaPara, T. M.; Cole, A. C.; Shanahan, J. W.; Semmens, M. J. The Effects of Organic Carbon, Ammoniacal-Nitrogen, and Oxygen Partial Pressure on the Stratification of Membrane-Aerated Biofilms. *J. Ind. Microbiol. Biotechnol.* **2006**, *33* (4), 315–323. https://doi.org/10.1007/s10295-005-0052-5.
(106) Shanahan, J. W.; Semmens, M. J. Multipopulation Model of Membrane-Aerated Biofilms. *Environ. Sci. Technol.* **2004**, *38* (11), 3176–3183. https://doi.org/10.1021/es034809y.
(107) Kindaichi, T.; Tsushima, I.; Ogasawara, Y.; Shimokawa, M.; Ozaki, N.; Satoh, H.; Okabe, S. In Situ Activity and Spatial Organization of Anaerobic Ammonium-Oxidizing (Anammox) Bacteria in Biofilms. *Appl. Environ. Microbiol.* **2007**, *73* (15), 4931–4939. https://doi.org/10.1128/AEM.00156-07.
(108) van der Star, W. R. L.; Miclea, A. I.; van Dongen, U. G. J. M.; Muyzer, G.; Picioreanu, C.; van Loosdrecht, M. C. M. The Membrane Bioreactor: A Novel Tool to Grow Anammox Bacteria as Free Cells. *Biotechnol. Bioeng.* **2008**, *101* (2), 286–294. https://doi.org/10.1002/bit.21891.
(109) Fernández, I.; Vázquez-Padín, J. R.; Mosquera-Corral, A.; Campos, J. L.; Méndez, R. Biofilm and Granular Systems to Improve Anammox Biomass Retention. *Biochem. Eng. J.* **2008**, *42*, 308–313. https://doi.org/10.1016/j.bej.2008.07.011.
(110) Bagchi, S.; Lamendella, R.; Strutt, S.; Van Loosdrecht, M. C. M.; Saikaly, P. E. Metatranscriptomics Reveals the Molecular Mechanism of Large Granule Formation in Granular Anammox Reactor. *Sci. Rep.* **2016**, *6* (1), 28327. https://doi.org/10.1038/srep28327.
(111) Brindle, K.; Stephenson, T.; Semmens, M. J. Nitrification and Oxygen Utilisation in a Membrane Aeration Bioreactor. *J. Membr. Sci.* **1998**, *144* (1–2), 197–209. https://doi.org/10.1016/S0376-7388(98)00047-7.
(112) Pellicer-Nàcher, C.; Franck, S.; Gülay, A.; Ruscalleda, M.; Terada, A.; Al-Soud, W. A.; Hansen, M. A.; Sørensen, S. J.; Smets, B. F. Sequentially Aerated Membrane Biofilm Reactors for Autotrophic Nitrogen Removal: Microbial Community Composition and Dynamics. *Microb. Biotechnol.* **2014**, *7* (1), 32–43. https://doi.org/10.1111/1751-7915.12079.

(113) Semmens, M. J.; Dahm, K.; Shanahan, J.; Christianson, A. COD and Nitrogen Removal by Biofilms Growing on Gas Permeable Membranes. *Water Res.* **2003**, *37* (18), 4343–4350. https://doi.org/10.1016/S0043-1354(03)00416-0.
(114) Ahmadi Motlagh, A. R.; LaPara, T. M.; Semmens, M. J. Ammonium Removal in Advective-Flow Membrane-Aerated Biofilm Reactors (AF-MABRs). *J. Membr. Sci.* **2008**, *319* (1–2), 76–81. https://doi.org/10.1016/j.memsci.2008.03.020.
(115) Uri-Carreño, N.; Nielsen, P. H.; Gernaey, K. V.; Flores-Alsina, X. Long-Term Operation Assessment of a Full-Scale Membrane-Aerated Biofilm Reactor under Nordic Conditions. *Sci. Total Environ.* **2021**, *779*, 146366. https://doi.org/10.1016/j.scitotenv.2021.146366.
(116) He, H.; Wagner, B. M.; Carlson, A. L.; Yang, C.; Daigger, G. T. Recent Progress Using Membrane Aerated Biofilm Reactors for Wastewater Treatment. *Water Sci. Technol.* **2021**, *84* (9), 2131–2157. https://doi.org/10.2166/wst.2021.443.
(117) LaPara, T. M.; Cole, A. C.; Shanahan, J. W.; Semmens, M. J. The Effects of Organic Carbon, Ammoniacal-Nitrogen, and Oxygen Partial Pressure on the Stratification of Membrane-Aerated Biofilms. *J. Ind. Microbiol. Biotechnol.* **2006**, *33* (4), 315–323. https://doi.org/10.1007/s10295-005-0052-5.
(118) Soliman, M.; Eldyasti, A. Development of Partial Nitrification as a First Step of Nitrite Shunt Process in a Sequential Batch Reactor (SBR) Using Ammonium Oxidizing Bacteria (AOB) Controlled by Mixing Regime. *Bioresour. Technol.* **2016**, *221*, 85–95. https://doi.org/10.1016/j.biortech.2016.09.023.
(119) Pollice, A.; Tandoi, V.; Lestingi, C. Influence of Aeration and Sludge Retention Time on Ammonium Oxidation to Nitrite and Nitrate. *Water Res.* **2002**, *36* (10), 2541–2546. https://doi.org/10.1016/S0043-1354(01)00468-7.
(120) Winkler, M. K. H.; Kleerebezem, R.; Kuenen, J. G.; Yang, J.; Van Loosdrecht, M. C. M. Segregation of Biomass in Cyclic Anaerobic/Aerobic Granular Sludge Allows the Enrichment of Anaerobic Ammonium Oxidizing Bacteria at Low Temperatures. *Env. Sci Technol* **2011**, *45*, 7330–7337. https://doi.org/10.1021/es201388t.
(121) Li, J.; Zhu, L. P.; Xu, Y. Y.; Zhu, B. K. Oxygen Transfer Characteristics of Hydrophilic Treated Polypropylene Hollow Fiber Membranes for Bubbleless Aeration. *J. Membr. Sci.* **2010**, *362* (1–2), 47–57. https://doi.org/10.1016/j.memsci.2010.06.013.
(122) Ahmed, T.; Semmens, M. J. Use of Sealed End Hollow Fibers for Bubbleless Membrane Aeration: Experimental Studies. *J. Membr. Sci.* **1992**, *69* (1–2), 1–10. https://doi.org/10.1016/0376-7388(92)80162-D.
(123) Mery, C.; Guerrero, L.; Alonso-Gutiérrez, J.; Figueroa, M.; Lema, J. M.; Montalvo, S.; Borja, R. Evaluation of Natural Zeolite as Microorganism Support Medium in Nitrifying Batch Reactors: Influence of Zeolite Particle Size. *J. Environ. Sci. Health Part A* **2012**, *47* (3), 420–427. https://doi.org/10.1080/10934529.2012.646129.
(124) Huang, X.; Liu, C.; Gao, C.; Wang, Z.; Zhu, G.; Liu, L.; Lin, G. Comparison of Nutrient Removal and Bacterial Communities between Natural Zeolite-Based and Volcanic Rock-Based Vertical Flow Constructed Wetlands Treating Piggery Wastewater. **2013**. https://doi.org/10.1080/19443994.2012.747422.
(125) Zhu, X.; Tian, J.; Liu, C.; Chen, L. Composition and Dynamics of Microbial Community in a Zeolite Biofilter-Membrane Bioreactor Treating Coking Wastewater. *Appl. Microbiol. Biotechnol.* **2013**, *97* (19), 8767–8775. https://doi.org/10.1007/s00253-012-4558-2.
(126) Miazga-Rodriguez, M.; Han, S.; Yakiwchuk, B.; Wei, K.; English, C.; Bourn, S.; Bohnert, S.; Stein, L. Y. Enhancing Nitrification at Low Temperature with Zeolite in a Mining Operations Retention Pond. *Front. Microbiol.* **2012**, *3* (JUL), 1–9. https://doi.org/10.3389/fmicb.2012.00271.
(127) Semmens, M. J.; Goodrich, R. R. Biological Regeneration of Ammonium-Saturated Clinoptilolite. I. Initial Observations. *Environ. Sci. Technol.* **1977**, *11* (3), 255–259. https://doi.org/10.1021/es60126a010.

(128) Yapsakli, K.; Aktan, C. K.; Mertoglu, B. Anammox-Zeolite System Acting as Buffer to Achieve Stable Effluent Nitrogen Values. *Biodegradation* **2017**, *28* (1), 69–79. https://doi.org/10.1007/s10532-016-9778-1.
(129) Grismer, M. E.; Collison, R. S. The Zeolite-Anammox Treatment Process for Nitrogen Removal from Wastewater-A Review. *Water Switz.* **2017**, *9* (11). https://doi.org/10.3390/w9110901.
(130) Pei, Y.; Wang, J.; Wang, Z.; Tian, B. Anammox Bacteria Community and Nitrogen Removal in a Strip-like Wetland in the Riparian Zone. *J. Environ. Sci. Health Part A* **2011**, *46* (7), 715–722. https://doi.org/10.1080/10934529.2011.571582.
(131) Yapsakli, K.; Aktan, C. K.; Mertoglu, B. Anammox-Zeolite System Acting as Buffer to Achieve Stable Effluent Nitrogen Values. *Biodegradation* **2017**, *28* (1), 69–79. https://doi.org/10.1007/s10532-016-9778-1.
(132) Montalvo, S.; Guerrero, L.; Borja, R.; Sánchez, E.; Milán, Z.; Cortés, I.; Angeles de la la Rubia, M. Application of Natural Zeolites in Anaerobic Digestion Processes: A Review. *Appl. Clay Sci.* **2012**, *58*, 125–133. https://doi.org/10.1016/j.clay.2012.01.013.
(133) Chen, S.; Sun, D.; Chung, J.-S. Simultaneous Removal of COD and Ammonium from Landfill Leachate Using an Anaerobic–Aerobic Moving-Bed Biofilm Reactor System. *Waste Manag.* **2008**, *28* (2), 339–346. https://doi.org/10.1016/j.wasman.2007.01.004.
(134) Lv, P.; Luo, J.; Zhuang, X.; Zhang, D.; Huang, Z.; Bai, Z. Diversity of Culturable Aerobic Denitrifying Bacteria in the Sediment, Water and Biofilms in Liangshui River of Beijing, China. *Sci. Rep.* **2017**, *7* (1), 10032. https://doi.org/10.1038/s41598-017-09556-9.
(135) Klieve, J. R.; Semmens, M. J. An Evaluation of Pretreated Natural Zeolites for Ammonium Removal. *Water Res.* **1980**, *14* (2), 161–168. https://doi.org/10.1016/0043-1354(80)90232-8.
(136) Martin, K. J.; Nerenberg, R. The Membrane Biofilm Reactor (MBfR) for Water and Wastewater Treatment: Principles, Applications, and Recent Developments. *Bioresour. Technol.* **2012**, *122*, 83–94. https://doi.org/10.1016/j.biortech.2012.02.110.
(137) Huff Chester, A. L.; Eum, K.; Tsapatsis, M.; Hillmyer, M. A.; Novak, P. J. Enhanced Nitrogen Removal and Anammox Bacteria Retention with Zeolite-Coated Membrane in Simulated Mainstream Wastewater. *Environ. Sci. Technol. Lett.* **2021**, *8* (6), 468–473. https://doi.org/10.1021/acs.estlett.1c00154.

Chapter 2: Contaminants of Emerging Concern in the Lower Volta River, Ghana, West Africa: The Agriculture, Aquaculture, and Urban Development Nexus

This Chapter has been published in the journal *Environmental toxicology and chemistry* and is cited as:

Huff Chester, A., Gordon, C., Hartmann, H. A., Bartell, S. E., Ansah, E., Yan, T., ... & Schoenfuss, H. L. (2022). Contaminants of Emerging Concern in the Lower Volta River, Ghana, West Africa: The Agriculture, Aquaculture, and Urban Development Nexus. *Environmental toxicology and chemistry*, *41*(2), 369-381.

Abstract

Contaminants of emerging concern (CECs) are ubiquitous in aquatic environments across all continents and are relatively well known in the developed world. However, few studies have investigated their presence and biological effects in low- and middle-income countries. Here, we provide a first survey of CEC presence in the Volta River, Ghana and examine microbial consequences of anthropogenic activities along this economically and ecologically important African river. Water and sediment samples were taken by boat or from shore at 14 sites spanning 118 km of river course from the Volta estuary to the Akosombo dam. Sample extracts were prepared for targeted analysis of antimicrobial CECs, N,N-diethyl-meta-toluamide (DEET), and perfluorochemicals (PFAS, water only). Concurrent samples were extracted to characterize the microbial community and antibiotic resistant genes (ARGs). Antibiotics and PFAS (ΣPFAS: 2-20 ng/L) were found in all water samples, however, their concentration were usually in the low ng/L range and lower than reported for other African, European, and North American studies. DEET was present in all samples. The number of different genes detected (between one and ten) and total ARG concentrations varied in both water (9.1×10^{-6} to 8.2×10^{-3}) and sediment (2.2×10^{-4} to 5.3×10^{-2}), with increases in gene variety at sites linked to urban development, sand mining, agriculture, and shellfish processing. Total ARG concentration spikes in sediment samples were associated with agriculture. No correlations between water quality parameters, CEC presence, and /or ARGs were noted. The presence of CECs in the Lower Volta River highlights their global reach. The overall low concentrations of CECs detected is encouraging and coupled with mitigation measures, can stymy future CEC pollution in the Volta River.

INTRODUCTION

Contaminants of emerging concern (CECs), including pharmaceuticals, personal care products, agricultural pesticides, and industrial chemicals are ubiquitous in aquatic environments (Fekadu et al. 2019; Bradley et al. 2017; Borchardt et al. 2016; Kolpin et al. 2002). Progress has been made in understanding their sources, transport, and biological effects through detailed studies carried out mostly in high income countries (HIC) (Bradley et al 2017; Nilsen et al., 2017; Arnold et al. 2014; Corcoran et al., 2010; Kolpin et al., 2002). However, use, disposal, and treatment of CECs may differ substantially in low- and medium-income countries (LMICs) (Fekadu et al. 2019; Gwenzi and Chaukura 2018; Asem-Hiablie et al. 2013). For example, pharmaceuticals are often supplied without prescriptions, resulting in many antibiotics and anti-inflammatory drugs being commonly found in wastewater and surface water in both HICs and LMICs (Fekadu et al. 2019). Deficiencies in wastewater treatment technology in many LMICs result in insufficient removal of these compounds prior to discharge into aquatic environments (Gwenzi and Chaukura 2018, Asem-Hiablie et al. 2013) and subsequent high concentrations in receiving aquatic ecosystems (Fekadu et al. 2019). Consumption rates of other pharmaceuticals are greater in LMICs located in tropical regions due to the prevalence of infectious diseases (i.e., malaria), or region-specific health challenges. For example, anti-retroviral drugs are more commonly found in African waterways due to the prevalence of HIV/AIDS on this continent (Gwenzi and Chaukura 2018, Asem-Hiablie et

al. 2013). In contrast, opioids are found in higher concentrations in aquatic ecosystems of HIC in Europe and North America (DeJongh et al. 2012; Kostich et al. 2014).

Ghana is a country of approximately 31 million people with one-quarter of the population residing in the two largest cities, Accra and Kumasi. As a stable democracy with a well-educated population and sustainable birth rates, Ghana has made it its mission to address environmental and human health issues (Ghana Vision 2020, accessed at www.ircwash.org, July 2021) and meet the United Nations Sustainable Development Goals (SGDs; United Nations 2017), especially Goal Six on Water and Sanitation. Nevertheless, insufficient and failing infrastructure, including sanitation infrastructure, remains a major obstacle to achieving this goal, a problem shared by many other LMICs (Egbi et al 2020; Gwenzi and Chaukura 2018, Asem-Hiablie et al. 2013). Rural communities in Ghana rely on a patchwork of latrines, household septic systems, and under-performing sewage treatment facilities for the treatment of human waste (Egbi et al. 2020), all serving as potential sources of antibiotic resistant microorganisms and antibiotic resistance genes (ARGs) (Thongsamer et al., 2021; Ho et al., 2021; Agramont et al., 2019; Vikesland et al., 2019). Hormones (Aneck-Hahn et al., 2008) and pharmaceuticals (see review by Fekadu et al., 2019) also end up in surface water. Data collected from HICs suggests that with the increased availability and use of pharmaceuticals and personal care products, including those that incorporate perfluoroalkyl substances (PFASs), by the Ghanaian population, many CECs may pass untreated into surface water (Larsson et al., 2014; Vikesland et al., 2019). Indeed, PFASs have been detected in oceanic waters [1–3], numerous rivers [4,5], and polar regions [6–9] because of their transport properties and widespread use, suggesting that they could be

ubiquitous in many LMICs as well, including Ghana. Finally, in the peri-urban areas of Kumasi and Accra (Ghana), the potent estrogen 17β-estradiol was detected at concentrations of 6.6 ng/L, 4.9 ng/L, and 3.4 ng/L in wastewater stabilizing, wastewater polishing, and reference ponds, respectively, with total estrogenicity expressed in 17β-estradiol equivalency (EEQ) of 10.7 ng/L, 6.4 ng/L, and 3.8 ng/L EEQ, respectively (Asem-Hiablie et al., 2013).

The Volta River bisects Ghana from north to south and forms Lake Volta, one of the largest reservoirs in the world. The lower Volta River extends from the Akosombo Dam in the north, to the Volta estuary at the Gulf of Guinea in the south. With a growing population in the lower Volta River basin, aquaculture and agricultural activities are also expanding, requiring greater water resources and potentially polluting the river directly or producing greater runoff (UNEP-GEF 2016; Codjoe et al. 2020, 2017; Gordon et al. 2016; Mensah and Gordon, 2016). Lake Volta and the Volta River account for 88% of Ghana's cage/pen aquaculture production (Karikari 2016), 85% of Ghana's inland fish production, and 15% of Ghana's total domestic fish production (CSIR WRI 2016). Unfortunately, cage and pen-based aquaculture can result in inputs of pollutants, including pathogens and ARGs, to the sediment and water column from fish feces and unconsumed fish food, which has also been shown to contain ARGs (Karikari 2016; Konadu 2015; Clottey et al., 2016; Xiong et al., 2015; Han et al., 2017). Intensive pen-based aquaculture also frequently uses biocides and antimicrobials, creating a load of low concentration chemicals to the fish pens and, therefore, the surrounding environment (Karikari 2016; Liyanage and Manage, 2019; Gao et al., 2018; Xiong et al., 2015). Agriculture in the lower Volta River watershed includes livestock rearing, row cropping

of maize (corn) and rice, as well as cultivation of various vegetables (Andah et al. 2004). The river also serves several other purposes. It is a major source of drinking water for the city of Accra, with an urban population of two million (populationreview.com/countries/Ghana-population; accessed 7.4.2021). In addition, sand mining operations along the Volta River vacuum sand from the river bottom with large gasoline powered pumps operated on floats anchored in the river (Egbi et al. 2018). These operations resuspend sediments (Ashraf et al. 2011) and may pollute by the accidental release of petroleum products as well as the aerial deposition of combustion byproducts.

Given the need for continued supply of clean drinking water, domestic food production, and the increasing need for building materials, including sand, surveying CEC presence in the Volta Rivers is a key component to managing this natural resource. The current study was designed to provide a first longitudinal assessment of CEC presence in the Volta River, Ghana. The current study had three distinct objectives: (i) to carry out a limited survey of CECs across a river continuum in Sub-Saharan Africa; (ii) to correlate the presence of CECs with alterations to the river microbiome; and (iii) to identify key commonalities and differences in CEC occurrence to guide future efforts to measure their presence, sources, and impact along the Volta River, and more generally, in LMICs. To accomplish these objectives, we used a three-pronged approach. First, targeted analysis of seven antibiotics (sulfonamide, macrolide, diaminopyrimidine, and fluoroquinolone compounds) and 12 ARGs was performed using isotopic dilution and real-time polymerase chain reaction (qPCR), respectively, on water and sediment samples taken at sampling sites along the lower Volta River. Second, targeted analysis of PFAS

was performed to survey the concentration of these analytes and to gain a fuller understanding of the global occurrence and distribution of PFAS. Thirdly, untargeted analysis was performed to gain a broader picture of the possible anthropogenic pollutants present in the lower Volta River, with a focus on compounds uniquely detected at sites immediately downstream of substantial aquaculture activity as compared to a site upstream of aquaculture. In addition, the potential for CECs or land use changes to alter the microbiome of the river was explored.

MATERIALS AND METHODS

Study Sites and Sampling

Several logistical considerations factored into study site selection. These included accessibility by vehicle or boat, vicinity to pen-based aquaculture, settlements (upstream/downstream), or sand mining operations, and representation of a river segment. Sites were reconnoitered during the dry season in December 2018 and sampled in December 2019. At each site, duplicate water samples were collected at 50% of depth to river bottom using a Kemmerer water sampler. This approach was chosen to avoid surface contamination (oil) from boat motors and sand mining equipment as well as avoiding the inclusion of sediment in the sample. Samples were transferred into triple-rinsed 1L Nalgene bottles cleaned with ethanol prior to sampling. No head space was permitted, and samples were placed immediately on ice and maintained in this condition until return to the laboratory (within 24 hours).

Sediment samples were collected using an Ekman Dredge, transferred into baked amber glass vials, and stored on ice until return to the laboratory (within 24 hours).

General water quality parameters (temperature, pH, specific conductivity, dissolved oxygen, and total nitrate) were measured concurrently at each site at 50% river depth with sample collection using a multi-parameter water quality meter (YSI Pro Plus multimeter).

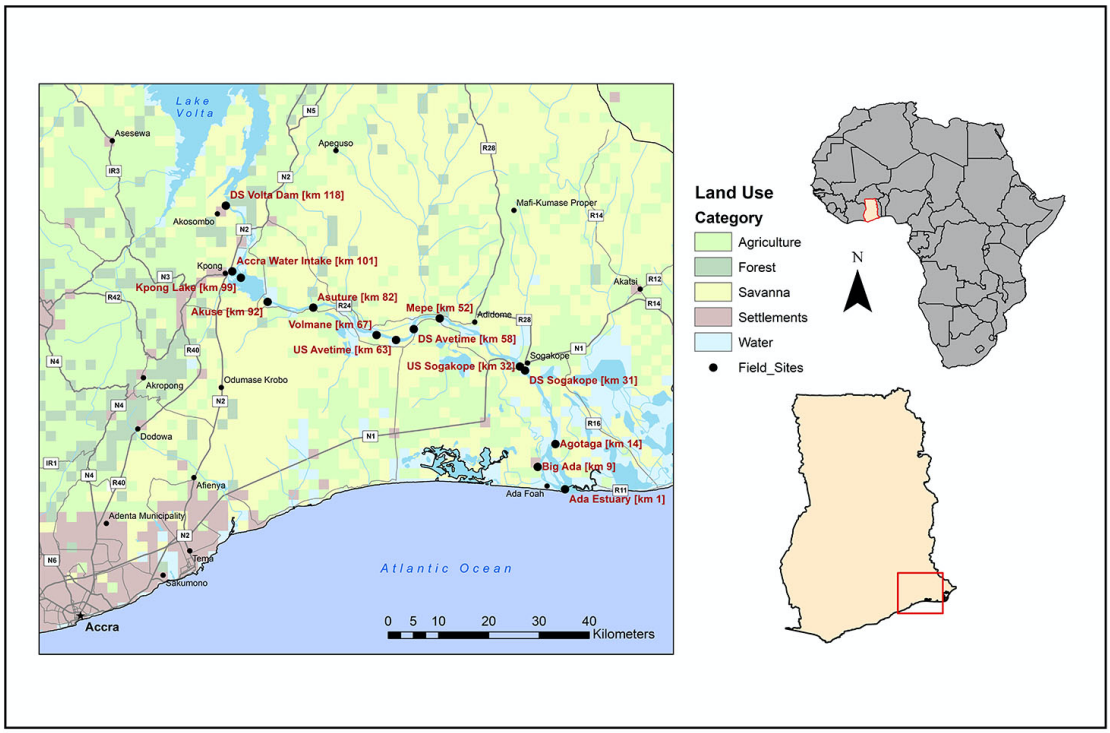

Figure 2.1 Sampling sites on the lower Volta River.

Table 2.1 Study site characteristics

river km	Name	Description	Lat	Long	Water Characteristics				
					Temp [°C]	pH	Spec Cond [uS/cm]	DO [mg/L]	NO3-N [mg/L]
118	Downstream (DS) Volta Dam	below small aquaculture facility, river-side resorts	N06°14'44.1"	E00°05'31.6"	28.2	6.72	56.7	2.23	0.20
101	Accra Water Intake	Kpong Lake, large man-made lake	N06°09'57.5"	E00°04'17.8"	29.6	7.12	57.4	2.08	0.31
99	Kpong Lake	downstream of Kpongwater intake, near town	N06°09'24.4"	E00°04'47.3"	29.7	6.86	56.9	1.97	0.15
92	Akuse	urban influence from small town	N06°06'44.5"	E00°07'52.5"	29.8	6.92	57.8	3.65	0.14
82	Asuture	downstream of large pen aquaculture	N06°06'03.6"	E00°12'55.7"	30.0	6.88	57.3	3.73	0.12
67	Volmane	downstream of aquaculture	N06°03'07.5"	E00°19'43.5"	30.6	7.34	58.4	4.38	0.39
63	Upstream (US) Avetime	upstream of town, near sand mining	N06°02'25.0"	E00°22'52.8"	30.4	7.17	58.8	3.66	0.35
58	Downstream Avetime	downstream of town, near sand mining	N06°03'13.7"	E00°23'41.1"	30.3	6.93	58.8	3.83	0.21
52	Mepe	rural market and sand mining	N06°04'56.2"	E00°25'41.5"	30.2	6.74	57.9	4.26	0.11
32	Upstream Sogakope	fishing pier, agricultural land use	N05°59'56.1"	E00°35'08.0"	30.5	6.89	58.9	3.10	0.19
31	Downstream Sogakope	downstream of resort town and aquaculture	N05°59'24.5"	E00°35'36.8"	30.6	7.24	60.1	4.31	0.26
14	Agotaga	downstream of aquaculture and sand mining	N05°51'27.2"	E00°38'54.5"	30.2	7.26	57.3	4.46	0.20

9	Big Ada	fishing village with rural market and shellfish processing, resorts, vacation homes along river	N05°49’14.8”	E00°37’05.3”	30.4	7.65	237.1	4.58	1.46
1	Ada estuary	near river mouth, fishing village along river	N05°46’33.2”	E00°39’53.4”	30.3	7.39	5956	4.68	22.9

Chemical Analysis

Upon arrival at the Ecological Laboratories of the Institute for Environment and Sanitation Studies, University of Ghana, Legon, water samples (1L) for targeted analysis by liquid chromatography-mass spectrometry (LC-MS) were spiked with 50 ng of isotopically labeled surrogates (all CECs listed in Table 2, S1). The procedure for water and sediment targeted analysis of antibiotics followed previous procedures (Kim & Carlson, 2007). Samples were extracted using Oasis HLB (3 mL, 200 mg) solid phase extraction (SPE) cartridges. Cartridges were conditioned with 5 mL of methanol followed by 5 mL of distilled H_2O. After sample application 1L at < 5mL/min followed by a 5 mL rinse with H_2O, cartridges were eluted with 5 mL of methanol, evaporated under N_2, and reconstituted in 1.0 mL of 75:25 H_2O: methanol with 1 % formic acid. LC-MS analytes were measured using Agilent 1200 Series HPLC coupled to an Agilent 6410 QqQ MS/MS, operated in positive ion mode using selective reaction monitoring. Analytes were separated on an Infinity Poroshell 120 C18 column (2.7 μm, 2.1 x 100 mm) at 60° C with gradient elution, using 0.1 % formic acid in H_2O and 0.1 % formic acid in methanol. The injection volume was 10 μL. The gradient profile, transition, and fragmentation parameters for targeted analysis are provided in Appendix C (Tables C.S1, C.S2).

Perfluoroalkyl substances (PFASs) were in surface water and sediment as reported previously (Zhou et al.2013). Analytes were measured by MRM using a negative ion mode using 5 mM ammonium acetate in water B: 95% methanol + 5 mM ammonium acetate with a flow rate of 0.250 mL/min at temperature of 35°C (see Table C.S2 for gradient parameters, and Table C.S3 for analyte list and MRM transitions). The injection volume for PFAS analysis was 5 μL. Calibration curves were run for each

analyte from 0.2-1,000 μg/mL. Two types of blanks were also tested. The first was a field blank of 1L DI water. The second was water in contact with a gloved hand since water samples were hand collected from surface water, Tap water from the laboratory in Ghana where samples were prepared was also tested.

Sediment was dried (approximately 50°C for 90 minutes) and sieved using a 60-mesh screen. Aliquots of sediment (200 mg) were extracted with 1.1 mL of methanol containing 50 ng of surrogates. After shaking for 1 hour on a platform shaker the sediment was removed by centrifugation. The methanol was decanted, evaporated, and the sample reconstituted in 100 uL 75:25 H_2O: methanol. Targeted analysis of antibiotics was performed in the same manner as water extracts. Recovery of surrogates from both water and sediment samples is reported in Appendix C, Table C.S4.

Untargeted analysis was performed using an Agilent 1260/6545 HPLC-Q/ToF instrument. Compounds were separated using a ZORBAX Eclipse+ C18 column (1.8 μm, 2.1 mmx 100 mm) using 1% formic acid in water and methanol as the mobile phase. Injection volumes were 5 μL and gradient was performed (Table C.S2). Positive ion mode with a mass window of 100-1100 m/z with a capillary voltage of +4000V at 320°C. Both high mass resolution data and autoMS/MS data were collected in separate chromatographic runs. Data was processed using ProFinder 10.0 with 0.2 min retention time matching. After chromatographic alignment Mass Profiler 10.0 was used to find compounds unique to duplicate samples upstream vs. downstream of aquaculture. Features were identified from the high-resolution mass data using a NIST MS/MS library and an Agilent water library containing common environmental analytes. Identifications were made with the following criteria: >70% score, <0.2 min retention time deviation,

and a peak height >15,000 counts. Using these criteria, <20% of the features could be presumptively identified. Additional feature identification of some samples was done using Agilent Qualitative Analysis under the same criteria noted above to tentatively identify compounds downstream of aquaculture sites. The identifications are all reported at a Schymanski level = 4 (Schymanski et al. 2014), corresponding to data that allows determination of a molecular formula via isotopic profile, providing the ability to propose structures.

Microbial Analysis

DNA extractions

Sediment samples were split into replicates for immediate DNA extraction. Approximately 0.5 g of each sample was weighed and placed into the DNA extraction tube for subsequent extraction. The exact mass of each sediment sample was recorded for normalization. DNA extractions from sediment samples were performed using the FastDNA Spin Kit for Soil. (MP Bio, Irvine, CA).

Water samples were split into replicates for immediate DNA extraction. Approximately 50 mL of each sample was filtered through a 0.22 μm filter, rinsed with a small quantity of deionized water, and the entire filter was placed into a microcentrifuge tube for DNA extraction. The exact volume of water filtered for each sample was recorded for normalization. DNA extractions from filtered water samples were performed using the FastDNA Spin Kit (MP Bio, Irvine, CA). Again, DNA extracts were stored in the freezer or on ice during transport until further analysis.

qPCR

DNA extracts were used for quantification of 12 antibiotic resistant genes (ARGs) (Table C.S5) by qPCR. qPCR quantification of 16S rRNA gene was also performed to estimate total bacterial biomass. Primers and cycling conditions for qPCR assays are provided in supporting material (Table C.S5).

The qPCR reactions were run in duplicate on a CFX Connect Optics Thermocycler (Bio-Rad, Hercules, CA). Briefly, the qPCR reaction mixtures (15 ml) contained 7.5x EvaGreen Supermix (Bio-Rad, Hercules, CA), 100 nM of each primer, 1x of bovine serum albumin (BSA), and 1 mL of DNA template. The general qPCR cycle was 95 °C initial denaturation for 10 min followed by 40 cycles of 95 °C denaturation for 15 s and 1 min anneal/extension at the specific annealing temperature for each primer set (Table C.S5). A melting curve was completed at the end of each run for quality control.

Synthesized DNA from IDT (IDT, Coralville, IA) containing the targeted gene fragments were used as DNA standards for qPCR. Calibration curves for ARGs and 16S rRNA gene were constructed from 10-fold dilutions ranging from 10^6 to 10^9 gene copies per reaction. The amplification efficiency of qPCR assays in this study generally ranged from 91% to 104%, with the efficiency for *sul1* and *tetE* worse, at 120% and 86%, respectively. Negative controls for the qPCR reaction (blank) were included in each qPCR run. Cycle threshold (Ct) value of each sample was calculated using arithmetic mean of duplicates. The concentration of target gene was calculated from the standard curve and reported as gene copies per mL or g. Samples were checked for PCR inhibition with a ten-fold serial dilution of template. No obvious inhibitions were observed in samples at these dilution levels.

Sequencing

Sequencing of 16S rRNA gene was completed on DNA extracted from sediment and water samples. First, the DNA was amplified using the V5V6 region with primers (V5F-RGGATTAGATACCC and V6R-CGACRRCCATGCANCACCT). The DNA was then purified, quantified and pooled as previously described (LaPara et al. 2015). Amplicon sequencing was performed on the purified 16 rRNA gene fragments on the Illumina MiSeq platform with paired ends (2x300) by the University of Minnesota Genomics Center (UMGC). DNA sequences are available on NCBI under BioProject PRJNA745167.

The data was analyzed using the Minnesota Supercomputing Institute (MSI). Paired-end sequence reads were demultiplexed, trimmed, and filtered with QIIME2 (version 2018.2). Amplicon sequence variants were determined using "DADA2" (Callahan et al., 2016, 2017), and then assigned consensus taxonomy using the SILVA rRNA database (release 128) (Quast et al. 2013).

Statistical analysis

Shannon alpha diversity, Faith's phylogenetic diversity, and Pielou's evenness indices were calculated by QIIME2. Microbial community analysis was performed using the 'vegan' package in R and PCoA plots were generated based on Bray-Curtis distance matrix. Non-metric multi-dimensional scaling (NMDS) plot was also generated using the 'vegan' package in R. An outlier was removed from the plot provided in this manuscript for clarity (Figure 2.4; the outlier is included in Fig S5). A figure with the outlier included is available in Appendix C. Both Mantel tests and ANOSIM tests were performed in R using the 'vegan' package to determine if the environmental factors and

the targeted antibiotic concentrations had impacts on the microbial community composition. Student's t-test was used to compare the diversity indices of the sediment vs. water samples and ANOVA was used to compare the diversity indices between the sample locations. Correlations between water quality parameters (temp, pH, conductivity, DO) and ARG were explored using nonparametric Spearman analyses (Graphpad Prism 9.1).

RESULTS AND DISCUSSION

Targeted chemical and microbial analytes

Targeted antibiotics and DEET. Concentrations of antibiotics in Volta River water samples were generally <1 ng/L in water samples across all sampling sites (Table 2.2). An exception was trimethoprim, detected at 7 ng/L at river km 14, the same location in which an increase in the total PFAS concentrations (see below) were observed. For comparison, trimethoprim has been found at 1-100 ng/L in UK river systems (Kasprzyk-Hordern et al., 2008) and 0-2 ng/L in Kenyan river systems (Kairigo et al., 2020). Use of antibiotics in aquaculture has been reported [10] and amounts have been found in nearby surface waters (Zou et al. 2011, Muziasari et al. 2014). Trimethoprim is commonly used in aquaculture (Chen et al., 2018; Dawood et al., 2018; Defoirdt et al., 2011) and has been shown to remain at a constant concentration through the course of a river (80% downstream vs. upstream) in an UK watershed (Kasprzyk-Hordern et al., 2008). There was intensive pen-aquaculture activity upstream (river km 31 and further upstream), which could perhaps have served as a source of trimethoprim to the Volta River; nevertheless, previous measurements of trimethoprim in aquaculture could not detect the

drug in nearby sediment (Muziasari et al., 2014), suggesting that there may have been another source nearer to river km 14. The scope of the current study and the information available did not allow for further investigation of an alternative source for trimethoprim. Concentrations of ciprofloxacin and sulfamerazine in river water samples were above that of blanks at all sampling sites; nevertheless, they were only in the low ng/L range and far below concentrations reported elsewhere in Africa, Europe, and North America (Fekadu et al. 2019; Elliott et al. 2017). Indeed, ciprofloxacin, together with sulfamethoxazole, was among the ten most detected antibiotics in African surface waters at concentrations reaching as high as 53828 ng/L (Mozambique) and 14331 ng/L (South Africa), respectively (as reviewed by Fekadu et al. 2019). Erythromycin was not detected in the lower Volta River, which is consistent with the data reviewed by Fekadu et al. (2019), in which erythromycin was seldom detected in Africa, with more frequent detection in European surface waters. For the current study, DEET was detected above the concentrations of blanks in all water samples. In comparison, DEET was detected in two-thirds of 291 samples taken from tributaries to the North American Great Lakes, at median concentrations of 21 ng/L and maximum concentrations of 5070 ng/L (Elliott et al. 2017). It is noteworthy that in the current study, water samples along the lower Volta River were collected during the dry season when mosquito densities were low, while Elliott et al. (2017) collected samples during the mosquito-rich summer months. In the current study, except for the detection of higher concentrations of trimethoprim at river km 14, no obvious correlation between DEET and the antibiotics analyzed (correlation coefficient DEET:TRI = -0.024) , and land use was observed, suggesting multiple diffuse CEC sources along the lower Volta River. Antibiotics in Volta River sediment samples

were below the detection limit (< 1 ng/g) in all samples, while DEET was detected in all sediment samples (see Appendix C, Table C.S10).

Table 2.2 Targeted analysis of Volta River water samples.

river km [site #]	**concentration (ng/L)**							
	CIP	ERY	SMA	SMX	SMZ	TBD	TRI	DEET
118	0.3±0.1*	<0.2	0.24±0.02	<0.02	0.24±0.02	<0.1	1.7±0.1	110±10
101	0.51	<0.2	0.18	<0.02	0.2	<0.1	1.4	120±40
99	0.4±0.2	<0.2	0.4±0.3	<0.02	0.4±0.4	<0.1	1.9±0.4	130
92	0.32±0.05	<0.2	0.30±0.01	<0.02	0.3±0.1	<0.1	1.4±0.1	170±40
82	0.46	<0.2	0.22	<0.02	0.2	<0.1	1.2	200
67	0.6±0.1	<0.2	0.12±0.05	<0.02	0.08±0.02	<0.1	1.4±0.2	140±100
63	0.60±0.08	<0.2	0.12±0.06	<0.02	0.13±0.06	<0.1	1.3±0.1	80±10
58	0.47±0.06	<0.2	0.16±0.04	<0.02	0.20±0.04	<0.1	1.3±0.3	120±80
52	0.4±0.1	<0.2	0.14±0.02	<0.02	0.12±0.03	<0.1	1.4±0.1	150±40
32	0.4±0.1	<0.2	0.18±0.08	<0.02	0.12±0.07	<0.1	1.6±0.2	120±20
31	0.49±0.08	<0.2	0.14±0.04	<0.02	0.20±0.04	<0.1	1.4±0.2	200±70
14	0.38±0.07	<0.2	0.10±0.04	<0.02	0.17±0.04	<0.1	6.6±7	130±60
9	1.4±0.5	<0.2	0.2±0.1	<0.02	0.19±0.04	<0.1	1.6±0.3	160±70
1	0.3±0.2	<0.2	0.10±0.04	<0.02	0.17±0.04	<0.1	1.3±0.3	280±40
DI water	0.05±0.1	<0.2	0.03±0.04	<0.02	0.2±0.3	<0.1	1.3±0.1	60±50
Tap	<0.02	<0.2	<0.01	<0.02	0.34±0.05	<0.1	1.4±0.2	35±4

Glove	0.2±0.1	<0.2	0.16±0.05	<0.02	0.2±0.2	<0.1	1.3±0.1	60±30

* Error is standard deviation of replicate samples (n=2).

ciprofloxacin	CIP
erythromycin	ERY
sulfamerazine	SMA
sulfamethoxazole	SMX
sulfamethazine	SMZ
thiabendazole	TBD
trimethoprim	TRI

Targeted PFAS. Concentrations of individual PFAS analytes in river water were generally in the 0.2-1.0 ng/L range across the sampling sites (Table 2.3, see Appendix C, Table C.S10 for sediment data). Total PFAS concentrations (ΣPFAS) were 2-20 ng/L, with PFPeA, PFOA, and PFOS being the most predominant. Widespread detection of PFAS in the lower Volta River matches studies from other river systems, indicating that these compounds have become ubiquitous in the hydrosphere. For comparison, PFAS levels have been measured in Asia and in Europe at higher concentrations, with ΣPFAS levels around 5-250 ng/L (Yellow River ΣPFAS of 50-250 ng/L [11]; Korean rivers ΣPFAS of 5-30 ng/L [12]; Rhine River ΣPFAS of 10-250 ng/L [13]. PFAS concentrations have also been measured in a limited number of African river systems (for a recent review see Sebugere et al. 2020) where ΣPFAS typically range 10-60 ng/L, similar to the concentrations detected in the lower Volta River. As observed with trimethoprim, the concentration of PFAS in the Volta River samples was highest at river km 14 (ΣPFAS = 114 ng/L). Concentrations exceeding 100 ng/L have also been measured in some South

African rivers. Interestingly, the concentration of PFASs progressively decreased downstream of km 14, presumably due to dilution or losses to adsorption. The spike in ΣPFAS suggests a point source for PFAS between river km 31 and 14. Concentrations of PFAS in the Accra tap water sample were low (<1 ng/L) or near levels in the blank. It should be noted that measurements where not performed using isotopic dilution, resulting in the potential for some PFAS concentrations to be under-reported. In addition, recovery of short-chain PFAS compounds by Oasis HLB have been found to be low (van Leeuwen and de Boer 2007), again highlighting the potential for some of the PFAS measured to be under-reported. These data indicate that future work would be helpful in monitoring water quality and identifying potential point sources in the Volta River watershed. Routine monitoring of PFAS in African river systems has also been recommended by other researchers.

Table 2.3 PFAS Presence and Concentrations

river km	concentration (ng/L)										
	PBFA	**PFPeA**	**PFHxA**	**PFHpA**	**PFOA**	**PFNA**	**PFDA**	**PFBS**	**PFHxS**	**PFOS**	**ΣPFAS**
118	0.9±1.1*	2±2	1.9±1.6	0.0±0.2	0.7±0.1	0.4±0.2	0.2±0.1	1.2±0.6	0.7±1	0.7±0.4	**9.1**
101	0.3	1.0	0.4	0.7	0.7	0.3	0.1	0.3	<0.2	<0.2	**3.8**
99	0.4±0.2	0.9±0.7	0.4±0.3	0.3±0.4	0.5±0.4	0.3±0.1	0.1±0.07	0.2±0.2	0.2±0.06	0.5±0.3	**3.9**
92	0.3±0.1	1.2±0.3	0.2±0.2	0.812	0.7±0.2	0.20±0.1	0.1±0.01	0.3±0.04	0.1±0.1	0.5±0.2	**4.3**
82	0.7±0.2	1.0±0.1	0.8±0.3	0.7±0.3	1.6±1.1	1.5±1.8	0.9±0.9	0.3±0.40	0.2±0.40	1.5±1.2	**9.4**
67	0.4±0.3	1.4±0.3	0.7±0.5	1.1±0.3	0.8±0.4	0.3±0.01	0.1±0.1	0.3±0.04	<0.2	1.5±1.5	**6.8**
63	2.6±3.4	2.9±1.7	1.2±1.7	1.1±0.3	1.2±0.8	1.0±0.7	0.6±0.5	0.6±0.5	0.5±0.8	1.8±1.8	**14**
58	0.5±0.2	1.4±0.1	1.1±0.01	1.2±0.1	2.0±0.3	0.7±0.6	0.3±0.2	0.7±0.02	0.9±0.6	1.1±0.6	**9.8**
52	0.8±0.1	1.6±0.7	2.9±3.1	1.7±1.2	2.8±1.6	3.0±0.4	1.2±0.4	1.5±1.8	2.0±2.9	2.4±2.9	**20**
32	0.6±0.4	1.9±0.3	0.9±0.2	1.2±0.1	1.1±0.1	0.8±0.2	0.6±0.3	0.3±0.1	0.1±0.1	0.6±0.1	**8.3**
31	1.0±0.3	1.7±0.1	2.1±0.5	1.6±0.3	3.4±1.6	0.7±0.2	0.21±0.1	5.1±6.7	1.8±2.5	1.2±0.8	**19**
14	6.1±3.5	9.7±3.2	22±17	5.2±1.4	8.9±1.3	11±3	7.5±1.2	13±11	8.7±1.9	21.5±0.5	**114**
9	5.2±6.4	3.8±3.6	1.6±0.4	1.4±0.01	13±17	0.5±0.04	0.2±0.1	0.5±0.22	0.2±0.1	0.6±0.1	**27**

1	1.2±1.2	1.7±1.4	4.2±5.3	1.8±1.4	8 ±10	1.2±1.5	0.7±0.8	0.4±0.2	0.1±0.2	0.4± 0.5	**19**
DI water	0.5±0.01	0.1±0.2	0.3±0.4	0.09±0.01	0.4±0.1	0.2±0.2	0.06±0.02	0.1±0.1	0.1±0.1	0.2±0.3	**2.1**
Tap	0.6±0.5	0.5±0.3	0.4±0.4	0.4±0.1	0.9±0.3	0.9±1.1	0.6±1.0	0.5±0.1	0.2±0.1	0.5± 0.2	**5.6**
Glove	0.4	0.2	0.3	0.1	0.5	0.4	0.4	0	0	0	**2.2**

*Errors are reported as standard deviation (n=2)

Targeted ARG genes. Gene copy numbers in river water samples and in river sediment samples for 12 different ARGs are summarized in Figure 2.2. Total ARG concentrations normalized by the 16S rRNA gene copy numbers ranged from approximately 9.1×10^{-6} to 8.2×10^{-3} in the water samples and 2.2×10^{-4} to 5.3×10^{-2} in the sediment samples (Figure 2.2A), increasing around the location of one of the aquaculture facilities on the Volta River (river km 82), as well as upstream at a small aquaculture facility where the overall bacterial numbers were low (river km 118). The number of different genes detected along the length of the Volta River varied in both the water and sediment samples (Figure 2.2B). Between one and ten different ARG genes were detected in each sample and increases in the variety of genes detected in the water samples occurring at sites linked to urban development (river km 92 and 1), agriculture (river km 32), and shellfish processing (river km 1) and no clear patterns observed with the sediment samples. Total ARG concentrations also varied along the length of the Volta River, with spikes observed in the water samples associated with urban development (river km 92 and 1), sand mining (river km 63), agriculture (river km 32), and shellfish processing (river km 1). In contrast, spikes observed in the sediment samples were primarily associated with agriculture (river km 32) (Figure 2.2C). Interestingly, there were no ARG concentration increases associated with river km 14, where increases in the concentration of trimethoprim and total PFAS (see below) were observed (Tables 2.2 and 2.3), again suggesting multiple diffuse CEC sources along the lower Volta River. Finally, none of the water quality parameters measured correlated statistically with the total quantity of genes present, nor the number of different ARG detected in a sample ($p>0.05$, nonparametric Spearman correlation, data not shown).

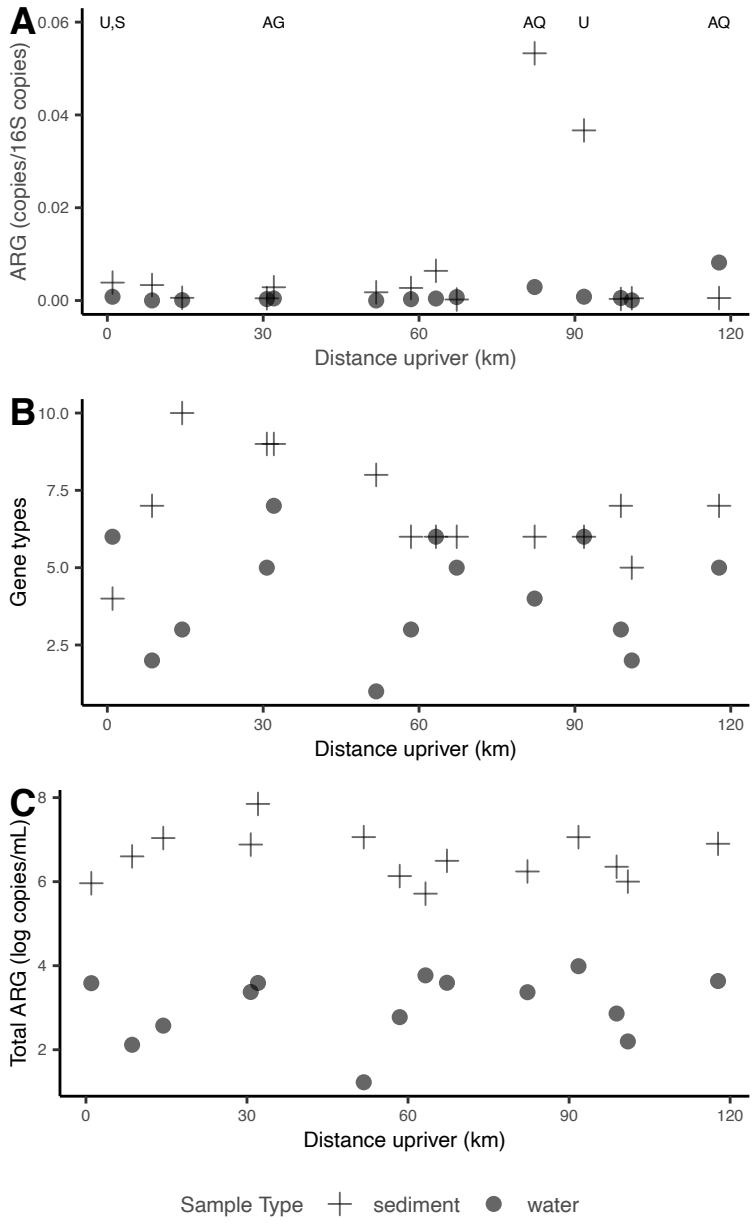

Figure 2.2. Antibiotic resistance genes in water and sediment samples along the length of the lower Volta River. "+" indicate sediment samples and circles indicate water samples.

Globally, there has been widespread detection of ARGs (e.g., Han et al., 2019; Almakki et al., 2019; Nnadozie and Odume 2019; Vikesland et al. 2019). Therefore, not surprisingly, our research also found ARGs throughout the samples taken along the Volta River, indicating multiple sources of ARGs, possibly including aquaculture (river km 118, 82 and 67), urban development (Akuse, river km 92), small poorly developed villages (Mepe, river km 52), agriculture (upstream of Sogakope, river km 32), and shellfish processing (Ada estuary, river km 1). Most of the genes analyzed were detected in at least one sampling location. Nevertheless, and perhaps not surprising given the size of the Volta River, the diffuse inputs, and the fact that it was the dry season with limited runoff, when normalized by total 16S gene copy numbers, overall ARG concentrations were relatively low (Figure 2.2B), with other researchers often observing much higher normalized ARG concentrations in rivers in Thailand, Bolivia, India, China, and Finland impacted by wastewater (e.g., Thongsamer et al., 2021; Agramont et al., 2020; Devarajan et al. 2016) or aquaculture facilities (e.g., Gao et al., 2018; Xiong et al., 2015; Muziasari et al., 2014). Given the number of small and large villages/towns along the Volta River, it is possible that fecal contamination is a source of ARGs, which is thought to be a primary driver of ARG contamination in fresh water globally (Thongsamer et al., 2021; Ho et al., 2021; Agramont et al., 2020; Almakki et al., 2019; Vikesland et al. 2019;1 Devarajan et al. 2016). Because it was the dry season, however, it is also possible that over-land fecal contamination was limited. Aquaculture may have also impacted the number and types of ARGs detected in the lower Volta River, as tetracycline resistance genes and *sul1* and *sul2* have been found to be associated with aquaculture facilities globally (Liyanage and Manage 2020; Fang et al., 2019; Xiong et al., 2015; Gao et al.

2012; Gao et al. 2018; Muziasari et al., 2014), as well as the fishmeal used in aquaculture (Han et al., 2017), and were also commonly detected in our study (Figures C.S7 and C.S8, Appendix C).

Untargeted chemical analysis

Non-target analysis was performed on the river water samples using untargeted HPLC-Q/ToF data collected in tandem with targeted analysis. A wide variety of anthropogenic compounds were putatively identified by library matching (Tables C.S6, C.S7, Appendix C), including pharmaceuticals (ibuprofen, trimethoprim); pesticides (paraquat, mexacarbate); and industrial chemicals (tris(2-butoxyethyl) phosphate, texanol). Compounds listed were from level 4 features of relatively high abundance and MS data quality matched using a NIST library with common pharmaceutical compounds. Overall, antibiotics beyond those targeted were not identified in the untargeted suspect screening process. The lack of antibiotic detections uniquely downstream of aquaculture supports the ARG data and shows, for this sampling event, relatively low impact with respect to antibiotic and ARG release from pen-based aquaculture in the lower Volta River. Nevertheless, many other CECs [14] were detected. Since these data only examine two sampling sites, it would be speculative to attach a compound to a specific source, especially without further MS^2 analysis across the whole series of sites. The initial results reported herein provide a first glimpse into contaminants present in the Volta River system and can help guide future work involving targeted analysis or suspect screening driven by hypothesis testing regarding the impact of aquaculture, fecal contamination, sand mining, shellfish processing, or other activities. In general, the data suggest that surface waters can be impacted by activities in a region with limited amounts of industrial

manufacturing activity. Further analysis of MS^2 data is planned in the future to provide greater certainty in identifications and track individual compounds through the river system,

Microbial community analysis

Diversity of the microbial community

There were no significance differences between the Shannon, PD, or evenness indices (P= 0.550, 0.071, and 0.71) when comparing water vs. sediment samples (Figure C.S1, Table C.S8 in Appendix C). In addition, these values did not vary significantly by location, as determined via ANOVA, with P values for the Shannon, PD, and evenness indices of 0.0805, 0.161, and 0.225, respectively (Figure C.S2, Table C.S8 in Appendix C). These results indicate that within our data set, neither sample type nor location statistically influenced the diversity or evenness of the microbial community (Figures C.S1 and C.S2 in Appendix C).

Microbial community composition and correlation to environmental factors

A total of 136 genera were identified in these samples with the Silva classifier database. The top 15 genera were identified, and their relative abundance is shown in Figures C.S3 and C.S4 (Appendix C). *Acinetobacter*, a potential pathogen (Klobučar et al. 2018), was the most abundant genus in the water samples (accounting for 15.8% of the total number of sequences). Of possible interest was the dominance of unknown *Betaproteobacteria*, consisting of 62.0% of the sequences in one replicate water sample, at river km 9, the location of a rural market, shellfish processing, and housing. In sediment, an unknown *Archaea*, *Bathyarchaeota* (20.0% of sequences) was the most

abundant genus detected in all samples and dominated (93.2%) both sediment samples taken at river km 118. An unknown *Bacteria* was also widely abundant in sediment samples (8.0% of sequences) and was detected in most samples. Notably, *Methanolinea* dominated one of the replicate sediment samples taken at river km 118, the location of a large aquaculture facility, accounting for 84.8% of the sequences in that sample. Other major genera detected in the both the water and sediment samples included *Procholococcus, Candidatus methylacidihpilum*, uncultured *Armatimonadales, Methanolinea,* and *Methanoregula*.

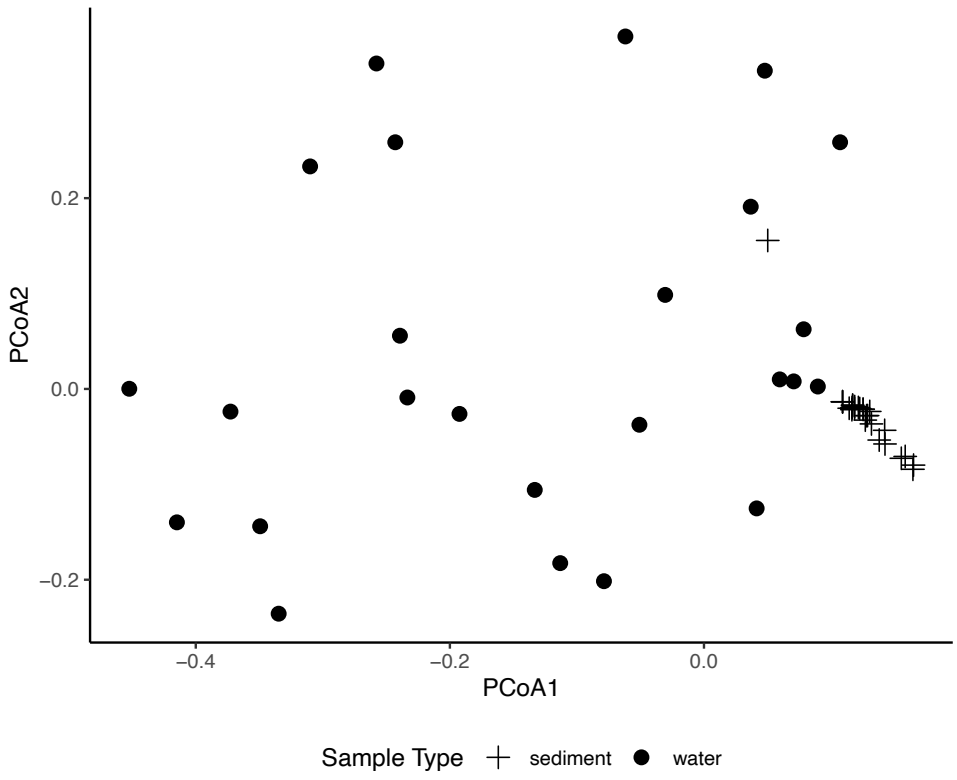

Figure 2.3 Principal coordinates analysis of the bacterial communities of all samples. PCoA 1 and PCoA2 account for 72.5% and 46.4% of the variance. "+" indicate sediment samples and circles indicate water samples.

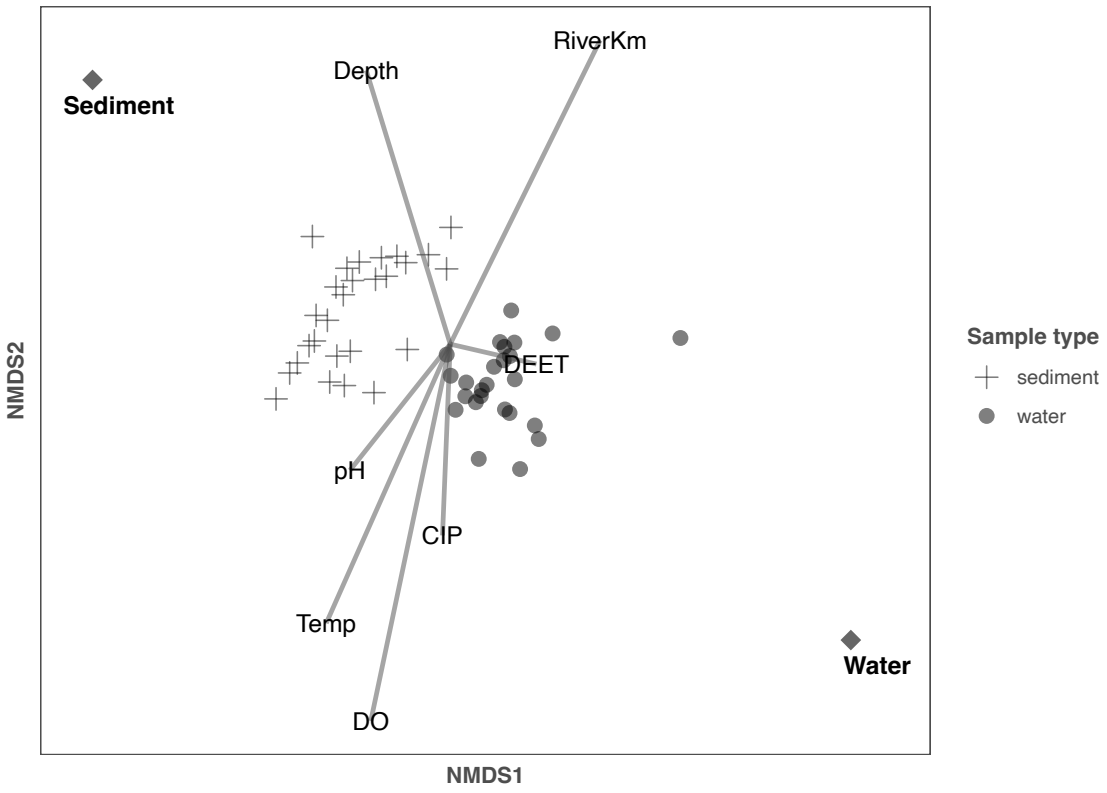

Figure 2.4 Non-metric multidimensional scaling (NMDS) plot using the Bray-Curtis dissimilarity to visualize the microbial communities and the impact of environmental factors and the targeted antibiotics. "+" indicate sediment samples and circles indicate water samples.

The similarity of the microbial community composition in all samples is presented in a PCoA plot calculated based on the Bray-Curtis distance matrix (Figure 2.3). The water and sediment samples clearly separate, indicating differences between the community structures as a function of sample type. This was demonstrated further with ANOSIM analysis (Table C.S9). The microbial communities in the different sample types (water and sediment) and those at different locations along the Volta River were significantly different ($P<0.0001$ and $P<0.0001$, respectively). Community divergence

between sediment and water samples was also observed in a similar study that analyzed the microbial communities of the Maozhou River in China using PCoA plots (Ouyang et al., 2020). Samples from impacted sites (notably sites with aquaculture and sand mining) were not significantly different from sites without these activities present (P=0.70) and again point to the fact that there were likely impacts from multiple types of land use along the Volta River, and even at each sampling site, that could have influenced the microbial community. This also highlights the lack of available, documented information on pollution sources and land use along the Volta River, unlike HICs, where land use and environmental impacts are closely monitored and regulated.

Statistical correlations between environmental factors and the microbial community structure were also investigated using a Mantel test. The Mantel test found that river distance from the estuary (e.g., location), DO, pH, and sampling depth all had a statistically significant influence on the community structure. The community structure was also correlated to the concentration of one of the 7 antibiotics analyzed, CIP (P=0.011), as well as with DEET (P=0.0046) (Table C.S9). Of the environmental factors identified in this study, pH, DO and antibiotics were found to also impact the community composition in studies of other impacted rivers indicating that these environmental factors commonly drive microbial community structures (Ouyang et al., 2020; Ott et al., 2021). A study in Malaysia (Ott et al., 2021), found that DO levels also correlated with the presence of ARGs, largely driven by the impact of fecal/wastewater inputs. A similar correlation was not observed on the lower Volta River, which is not surprising given the number of non-point sources along the river, the fact that it was the dry season and run off events were largely absent, and the size of the river. The significant environmental

factors and antibiotics were plotted with the microbial community on a non-metric multi-dimensional scaling (NMDS) plot (Figure 2.4).

Lessons for future research and water management on the Volta River

The objective of the current study was to identify key commonalities and differences in CEC occurrence to guide future research efforts. Regarding this, we identified several sampling sites that may warrant further investigation. Samples taken at km 118, 92, 63, 31, and 14 appear to be impacted by upstream anthropogenic activity that will require detailed investigation. Close pairing of upstream/downstream sites should be expanded in future sampling campaigns to better bracket specific activities such as aquaculture, sand mining, or urban settlements to shed light on specific CEC sources. At the same time, several diffuse sources, such as agriculture (particularly rice farming and its water use) were not fully assessed in the current study and could be studied with a sampling design to assess these sites, as well as assess these sites during wet seasons. Untargeted analysis has provided preliminary data showing a diverse set of anthropogenic compounds in Volta River water that may be linked to agricultural and other practices in the region. Indeed, the strong seasonal precipitation cycle in Ghana requires attention, as sources of CECs, use patterns of CECs, and fate of CECs are likely to differ dramatically between wet and dry seasons (Fairbairn et al. 2016). While the latter is easier to sample, the wet season, while logistically challenging, may offer a wealth of insights into CEC fate and transport in the lower Volta River. Expanding sampling regimes to capture weekly, monthly, or seasonal samples in the same set of locations could dramatically expand our understanding of CEC pollution in this system and guide additional mitigation measures.

The current study provides a first survey of CEC presence in the lower Volta River. The results of targeted chemical and microbiological analytes are consistent with those from studies in other regions, confirming the ubiquitous nature of these compounds in aquatic ecosystems (Fekadu et al. 2019). Interestingly, CEC concentrations were on average lower than reported in other studies for both HICs and LMICs, providing a positive counterpoint to the environmental degradation observed in aquatic ecosystems globally. Concurrently, the presence of these CECs in the river water and sediment provides perhaps an early warning, given the anticipated rapid development and population growth in the lower Volta Basin. Implementing mitigation measures, such as reducing agricultural runoff, better managing antibiotic application in pen-based aquaculture systems, improving sanitation, use of nature based solutions such as riverine buffer zones, and changing consumer habits, can stymy future CEC pollution in the Volta River.

References

Agramont J, Gutierrez-Cortez S, Joffre E, Sjoling A, Toledo CC. 2020. Fecal pollution drives antibiotic resistance and class 1 integron abundance in aquatic environments of the Bolivian Andes impacted by mining and wastewater. *Microorganisms* 8:1122.

Ahrens L, Xie Z, Ebinghaus R. 2010. Distribution of perfluoroalkyl compounds in seawater from Northern Europe, Atlantic Ocean, and Southern Ocean. *Chemosphere*. 78(8):1011–1016. doi:10.1016/j.chemosphere.2009.11.038.

Almakki A, Jumas-Bilak E, Marchandin H, Licznar-Fajardo P. 2019. Antibiotic resistance in urban runoff. *Sci Tot Environ* 667:64-76. https://doi.org/10.1016/j.scitotenv.2019.02.183.

Alves DD, Riegel RP, de Quevedo DM, Osório DMM, da Costa GM, do Nascimento CA, Telöken F. 2018. Seasonal assessment and apportionment of surface water pollution using multivariate statistical methods: Sinos River, southern Brazil. *Environ Monitoring Assess* 190:384. doi:10.1007/s10661-018-6759-3.

Andah WEI, Van de Giesen N, Biney CA. 2004. Water, climate, food, and environment in the Volta Basin. Report to project ADAPT. Accessed 7.4.2021 http://weap21.org/downloads/AdaptVolta.pdf.

Aneck-Hahn NH, Bornman MS, Jager C. 2009. Oestrogenic activity in drinking water from a rural area in the Waterberg District, Limpopo Province, South Africa. *Water SA* 35:245-252.

Arnold KE, Brown AR, Anklet GT, Sumpter JP. 2014 Medicating the environment: assessing risk of pharmaceuticals to wildlife and ecosystems. Phil Trans Royal Soc B 369:20130569.

Asem-Hiablie S, Church CD, Elliott HA, Shappell NW, Schoenfuss HL, Drechsler P, Williams CF, Knopf A, Dabie MY. 2013. Serum estrogenicity and biological responses in African catfish raised in wastewater ponds in Ghana. *Sci Tot Environ* 463-464:1182-1191.

Ashraf MA, Maah MJ, Yusoff I, Wajid A, Mahmood K. 2011. Sand mining effects, causes and cocnerns: a case study from Bestari Jaya, Selangor, Peninsular Malaysia. *Sci Res Essays* 6:1216-1231.

Bradley PM, Journey CA, Romanok KM, Barber LB, Buxton HT, Foreman WT, Furlong ET, Glassmeyer ST, Hladik ML, Iwanowicz LR, Jones DK, Kolpin DW, Kuivila KM, Loftin KA, Mills MA, Meyer MT, Orlando JL, Reilly TJ, Smalling KL, Villeneuve DL. 2017. Expanded target-chemical analysis reveals extensive mixed-organic-contaminant exposure in U.S. streams. *Environ Sci Technol* 51:4792-4802.

Borchardt D, Gordon C, Alcamo J, Dannis e JG, Müller RA, Mensah, A. 2016. Solutions to the water quality challenge: a preliminary review. *In*: UNEP, A Snapshot of the World's Water Quality: Towards a Global Assessment (pp. 81-93), United Nations Environment Programme: Nairobi. 162p.

Butt CM, Berger U, Bossi R, Tomy GT. 2010. Levels and trends of poly- and perfluorinated compounds in the arctic environment. *Sci Total Environ* 408:2936–2965. doi:10.1016/j.scitotenv.2010.03.015.

Cabello FC, Godfrey HP, Tomova A, Ivanova L, Dölz H, Millanao A, Buschmann AH. 2013. Antimicrobial use in aquaculture re-examined: its relevance to antimicrobial resistance and to animal and human health. *Environ Microbiol* 15:1917-1942.

Callahan BJ, McMurdie PJ, Holmes SP. 2017.Exact Sequence Variants Should Replace Operational Taxonomic Units in Marker-Gene Data Analysis. *ISME J* 11: 2639–2643. https://doi.org/10.1038/ismej.2017.119.

Callahan BJ, McMurdie PJ, Rosen MJ, Han A W, Johnson AJA, Holmes SP. 2016. DADA2: High-Resolution Sample Inference from Illumina Amplicon Data. *Nat. Methods* 13:581–583. https://doi.org/10.1038/nmeth.3869.

Campo J, Lorenzo M, Pérez F, Picó Y, Farré Marinel la, Barceló D. 2016. Analysis of the presence of perfluoroalkyl substances in water, sediment and biota of the Jucar River (E Spain). Sources, partitioning and relationships with water physical characteristics. Environ Res 147:503–512. doi:10.1016/j.envres.2016.03.010.

Chee-Sanford JC, Mackie RI, Koike S, Krapac IG, Lin YF, Yannarell AC, Maxwell S, Aminov RI. 2009. Fate and transport of antibiotic residues and antibiotic resistance genes following land application of manure waste. *J Environ Qual* 38:1086–1108.

Chen B, Lan Lin, Fang L, Yang Y, Chen E, Yuan K, Zou S, Wang X, Luan T. 2018. Complex pollution of antibiotic resistance genes due to beta-lactam and aminoglycoside use in aquaculture farming. *Water Res* 134:200-208. https://doi.org/10.1016/j.watres.2018.02.003.

Chen H, Liu S, Xu X-R, Diao Z-H, Sun K-F, Hao Q-W, Liu S-S, Ying G-G. 2018. Tissue Distribution, Bioaccumulation Characteristics and Health Risk of Antibiotics in Cultured

Fish from a Typical Aquaculture Area. *J Haz Mat* 343, 140–148. https://doi.org/10.1016/j.jhazmat.2017.09.017.

Clottey MNK, Asmah R, Ofori-Danson PK, Ameworwor MY, Karikari AY. 2016. Impacts of cage culture on physico-chemical and bacteriological water quality in Lake Volta, Ghana. *African J Aquat Sci* 41:473–480.

Codjoe SNA, Addo KA, Tagoe CA, Nyarko K, Martey F, Nelson WA, Jayson-Quashigah P-N, Atiglo DY, Adjei Po-W, Anderson K, Mensah A, Ofori-Danson PK, Amisigo BA, Ayamga J, Asmah EE, Asenso JK, Owusu G, Quaye RM, Abu M. 2020. The Volta Delta: challenges in an African Setting. Chapter 4 in: *Deltas in the Anthropocene* (Nichols RJ, ed).

Codjoe SNA, Nyamedor FH, Sward J, Dovie DB. 2017. Environmental hazard and migration intentions in a coastal area in Ghana: A case of sea flooding. *Popul Environ* 39:128–146.

Corcoran J, Winter MJ, Tyler CR. 2010 Pharmaceuticals in the aquatic environment: a critical review of the evidence for health effects in fish. *Crit Rev Toxicol* 2010:1-18.

CSIR WRI. 2016. Annual Report 2016. Retrieved from: http://www.ifc.org/wps/wcm/connect/corp_ext_content/ifc_external_corporate_site/annual+report/2016+online+report/printed+version.

Dawood MAO, Koshio S, Esteban MÁ. 2018. Beneficial roles of feed additives as immunostimulants in aquaculture: a review. *Rev Aquacult* 10:950–974. https://doi.org/10.1111/raq.12209.

Defoirdt T, Sorgeloos P, Bossier P. 2011. Alternatives to antibiotics for the control of bacterial disease in aquaculture. *Curr Opinion Microbiol* 14:251–258. https://doi.org/10.1016/j.mib.2011.03.004.

De Jongh CM, Kooji PJF, de Voogt P, ter Laak TL. 2012. Screening and human health risk assessment of pharmaceuticals and their transformation products in Dutch surface and drinking water. *Sci Total Environ* 427–428:70–77.

Dekić S, Klobučar G, Ivanković T, Zanella D, Vucić M, Bourdineaud JP, Hrenović J. 2018. Emerging human pathogen Acinetobacter baumannii in the natural aquatic environment: a public health risk?. *Internat J Environ Health Res* 28:315-322.

Devarajan N, Laffite A, Mulaji CK, Otamonga J-P, Mpiana PT, Mubedi JI, Prabakar K, Ibelings BW, Poté J. 2016. Occurrence of antibiotic resistance genes and bacterial markers in a tropical river receiving hospital and urban wastewaters. *PLoS ONE* 11(2): e0149211. doi:10.1371/journal.pone.0149211.

Egbi CD, Anornu GK, Ganyaglo SY, Appiah-Adjei EK, Li S-L, Dampare SB. 2020. Nitrate contamination of groundwater in the Lower Volta River Basin of Ghana: sources and related human health risks. *Ecotoxicol Environ Safety* 191:110227.

Egbi CD, Anurnu G, Appiah-Adjei EK, Ganyaglo SY, Dampare SB. 2018 Evaluation of water quality using hydrochemistry, stable isotopes, and water quality indices in the Lower Volta River Basin of Ghana. *Environ Dev Sustain* https://doi.org/10.1007/s10668-018-0180-5.

Elliott SM, Brigham ME, Lee KE, Banda JA, Choy SJ, Gefell DJ, Minarik TA, Moore JN, Jorgenson ZG. 2017. Contaminants of emerging concern in the Laurentian Great Lakes: I. patterns of occurrence. *PLoS One* 12(9): e0182868.

Fairbairn DJ, Karpuzcu ME, Arnold WA, Barber BL, Kaufenberg EF, Koskinen WC, Novak PJ, Rice PJ, Swackhamer DL. 2016. Sources and transport of contaminants of emerging concern: A two-year study of occurrence and spatiotemporal variation in a mixed land use watershed. *Sci Total Environ* 551–552:605-613.

Fang H, Huang K, Yu J, Ding C, Wang Z, Zhao C, Yuan H, Wang Z, Wang S, Hu J, Cui Y. 2019. Metagenomic analysis of bacterial communities and antibiotic resistance genes in the Eriocheir Sinensis freshwater aquaculture environment. *Chemosphere* 224:202-211. https://doi.org/10.1016/j.chemosphere.2019.02.068.

Fekadu S, Alemayehu E, Dewil R, Van der Bruggen B. 2019. Pharmaceuticals in freshwater aquatic environments: A comparison of the African and European challenge. *Sci Total Environ* 654:324-337.

Gao P, Mao D, Luo Y, Wang L, Xu B, Xu L. 2012. Occurrence of sulfonamide and tetracycline-resistant bacteria and resistance genes in aquaculture environment. *Water Res* 46:2355-2364.

Gao Q, Li Y, Qi Z, Yue Y, Min M, Peng S, Shi Z, Gao Y. 2018. Diverse and abundant antibiotic resistance genes from mariculture sites of China's coastline. *Sci Total Environ* 630:117-125. https://doi.org/10.1016/j.scitotenv.2018.02.122.

González-Gaya B, Casal P, Jurado E, Dachs J, Jiménez B. 2019. Vertical transport and sinks of perfluoroalkyl substances in the global open ocean. *Environ Sci: Process Impacts* 21:1957–1969. doi:10.1039/C9EM00266A.

González-Gaya B, Dachs J, Roscales JL, Caballero G, Jiménez B. 2014. Perfluoroalkylated Substances in the Global Tropical and Subtropical Surface Oceans. *Environ Sci Technol* 48:13076–13084. doi:10.1021/es503490z.

Gordon C, Mensah AM, Nikiema J. 2016 Water Quality and Public Health. *In:* Volta River Basin: Water for Food, Economic Growth and Environment (pp. 214-227), Routledge: London. 281p Williams, TO, Mul ML, Biney CA, Smakhtin, V. (Eds.)

Gwenzi W, Chaukura N. 2018. Organic contaminants in African aquatic systems: current knowledge, health risks, and future research directions. *Sci Total Environ* 619-620:1493-1514.

Han Y, Wang J, Zhao Z, Chen J, Lu H, Liu G. 2017. Fishmeal Application Induces Antibiotic Resistance Gene Propagation in Mariculture Sediment. *Environ Sci Technol* 51:10850–10860. https://doi.org/10.1021/acs.est.7b02875

Han Y, Zhou Z-C, Zhu L, Wei Y-Y, Feng W-Q, Xu L, Liu Y, Lin Z-J, Shuai X-Y, Zhang Z-J, Chen H. 2019. The impact and mechanism of quaternary ammonium compounds on the transmission of antibiotic resistance genes. *Environ Sci Poll Res Internat* 26:28352-28360.

Heuer H, Schmitt H, Smalla K. 2011. Antibiotic resistance gene spread due to manure application on agricultural fields. *Curr Opin Microbiol* 14:236–243.

Ho JY, Jong M-C, Acharya K, Liew SSX, Smith DR, Noor ZZ, Goodson ML, Werner D, Graham DW, Eswaran J. 2021. Multidrug-resistant bacteria and microbial communities in a river estuary with fragmented suburban waste management. *J Haz Mat* 405:124687. https://doi.org/10.1016/j.jhazmat.2020.124687.

Kairigo P, Ngumba E, Sundberg L-R, Gachanja A, Tuhkanen T. 2020. Occurrence of antibiotics and risk of antibiotic resistance evolution in selected Kenyan wastewaters, surface waters

and sediments. *Sci Total Environ* 720:1375-1380. https://doi.org/10.1016/j.scitotenv.2020.137580.

Karikari AY. 2016. Assessment of environmental impacts of cage aquaculture on Lake Volta of Ghana. Ph.D. Dissertation, Kwame Nkrumah University of Science and Technology, Ghana.

Kasprzyk-Hordern B, Dinsdale RM, Guwy AJ. 2008. The occurrence of pharmaceuticals, personal care products, endocrine disruptors and illicit drugs in surface water in South Wales, UK. *Water Res* 42:3498–3518. https://doi.org/10.1016/j.watres.2008.04.026.

Kemper N. 2008. Veterinary antibiotics in the aquatic and terrestrial environment. *Ecol Indic* 8:1–13. doi:10.1016/j.ecolind.2007.06.002.

Kim SC, Carlson, K .2007. Quantification of human and veterinary antibiotics in water and sediment using SPE/LC/MS/MS. Anal. Bioanal. Chem., 387: 1301-1315. doi: 10.1007/s00216-006-0613-0

Kolpin DW, Furlong ET, Meyer MT, Thurman EM, Zaugg SD, Barber LB, Buxton HT. 2002. Pharmaceuticals, hormones, and other organic wastewater contaminants in U.S. streams, 1999–2000: A national reconnaissance. *Environ Sci Technol* 36:1202–1211.

Konadu L.O. 2015. Effects of fish cage culture on sediment and water quality in the Gorge Area of the Volta Lake. Thesis, Kwame Nkrumah University of Science and Technology, Ghana.

Kostich MS, Batt AL, Lazorchk JM. 2014. Concentrations of prioritized pharmaceuticals in effluents from 50 large wastewater treatment plants in the US and implications for risk estimation. *Environ Pollut* 184:354–359.

Lam N-H, Cho C-R, Lee J-S, Soh H-Y, Lee B-C, Lee J-A, Tatarozako N, Sasaki K, Saito N, Iwabuchi K, et al. 2014. Perfluorinated alkyl substances in water, sediment, plankton and fish from Korean rivers and lakes: A nationwide survey. *Sci Total Environ* 491–492:154–162. doi:10.1016/j.scitotenv.2014.01.045.

LaPara TM, Wilkinson KH, Strait JM, Hozalski RM, Sadowksy MJ, Hamilton MJ. 2015. The Bacterial Communities of Full-Scale Biologically Active, Granular Activated Carbon Filters Are Stable and Diverse and Potentially Contain Novel Ammonia-Oxidizing Microorganisms. *Appl Environ Microbiol* 81:6864–6872. https://doi.org/10.1128/AEM.01692-15.

Larsson DGJ. 2014. Pollution from drug manufacturing: Review and perspectives. *Philos Trans R Soc B* 369:20130571.

Liyanage GY, Manage PM. 2020. Occurrence and distribution of tetracycline resistance determinants and their pollution profile in the aquaculture environment in Sri Lanka. *J Nat Sci Found Sri Lanka* 47:455–465. DOI: http://doi.org/10.4038/jnsfsr.v47i4.8703

MacInnis JJ, French K, Muir DCG, Spencer C, Criscitiello A, De Silva AO, Young CJ. 2017. Emerging investigator series: a 14-year depositional ice record of perfluoroalkyl substances in the High Arctic. *Environ Sci: Processes Impacts* 19:22–30. doi:10.1039/C6EM00593D.

Mensah A, Gordon C. 2016. Water pollution in River Basins: River Basin 3-Volta, In UNEP, A Snapshot of the World's Water Quality: Towards a Global Assessment (pp. 59-62), United Nations Environment Programme: Nairobi. 162p

Möller A, Ahrens L, Surm R, Westerveld J, van der Wielen F, Ebinghaus R, de Voogt P. 2010. Distribution and sources of polyfluoroalkyl substances (PFAS) in the River Rhine watershed. *Environ Poll* 158:3243–3250. doi:10.1016/j.envpol.2010.07.019.

Muir D, Bossi R, Carlsson P, Evans M, De Silva A, Halsall C, Rauert C, Herzke D, Hung H, Letcher R, et al. 2019. Levels and trends of poly- and perfluoroalkyl substances in the Arctic environment – An update. *Emerg Contam* 5:240–271. doi:10.1016/j.emcon.2019.06.002.

Muziasari WI, Managaki S, Pa¨rna¨nen K, Karkman A, Lyra C, Tamminen M, Suzuki S, Virta M. 2014. Sulphonamide and trimethoprim resistance genes persist in sediments at Baltic Sea aquaculture farms but are not detected in the surrounding environment. *PLoS ONE* 9(3): e92702. doi:10.1371/journal.pone.0092702

Muziasari WI, Managaki S, Pärnänen K, Karkman A, Lyra C, Tamminen M, Suzuki S, Virta M. 2014. Sulphonamide and Trimethoprim Resistance Genes Persist in Sediments at Baltic Sea Aq*uaculture Farms but Are Not Detected in the Surrounding Environment.* LOS ONE. 9(3):e92702. doi:10.1371/journal.pone.0092702.

Nilsen E, Smalling KL, Ahrens L, Gros M, Miglioranza KSB, Pico Y, Schoenfuss HL. 2019. Critical Review: grand challenges in assessing the adverse effects of contaminants of emerging concern on aquatic food webs. *Environ Toxicol Chem* 38:46-60

Nnadozie CF, Odume ON. 2019. Freshwater environments as reservoirs of antibiotic resistant bacteria and their role in the dissemination of antibiotic resistance genes. *Environ Poll* 254:113067. https://doi.org/10.1016/j.envpol.2019.113067.

Ott, A.; O'Donnell, G.; Tran, N. H.; Mohd Haniffah, M. R.; Su, J.-Q.; Zealand, A. M.; Gin, K. Y.-H.; Goodson, M. L.; Zhu, Y.-G.; Graham, D. W. 2021. Developing surrogate markers for predicting antibiotic resistance "hot spots" in rivers where limited data are available. *Environ Sci Technol* 55:7466–7478. https://doi.org/10.1021/acs.est.1c00939.

Ouyang L, Chen H, Liu X, Wong MH, Xu F, Yang X, Xu W, Zeng Q, Wang W, Li S. 2020. Characteristics of spatial and seasonal bacterial community structures in a river under anthropogenic disturbances. *Environ Pollut* 264, 114818. https://doi.org/10.1016/j.envpol.2020.114818.

Quast C, Pruesse E, Yilmaz P, Gerken J, Schweer T, Yarza P, Peplies J, Glöckner FO. 2013. The SILVA ribosomal rna gene database project: improved data processing and web-based tools. *Nucleic Acids Res* 41 (D1), D590–D596. https://doi.org/10.1093/nar/gks1219

Sauvé S, Desrosiers M. 2014. A review of what is an emerging contaminant. *Chem Central J* 8:15. doi:10.1186/1752-153X-8-15.

Schymanski EL, Jeon J, Gulde R, Fenner K, Ruff M, Singer HP, Hollender J. 2014. Identifying Small Molecules via High Resolution Mass Spectrometry: Communicating Confidence. *Environ Sci Technol* 48:2097–2098. doi:10.1021/es5002105.

Seki M, Yokota H, Maeda M, Kobayashi K. 2005. Fish full life-cycle testing for 17β-estradiol on medaka (*Oryzias latipes*). *Environ Tox Chem* 24:1259-1266.

Ssebugere P, Sillanpää M, Matovu H, Wang Z, Schramm K-W, Omwoma S, Wanasolo W, Ngeno EC, Odongo S. 2020. Environmental levels and human body burdens of per- and poly-fluoroalkyl substances in Africa: a critical review. *Sci Total Environ* 739:139913.

Thongsamer T, Neamchan R, Blackburn A, Acharya K, Sutheeworapong S, Tirachulee B, Pattanachan P, Vinitnantharat S, Zhou X-Y, Su J-Q, Zhu Y-G, Graham D, Werner D. 2021. Environmental antimicrobial resistance is associated with faecal pollution in

Central Thailand's coastal aquaculture region. *J HazMat* 416:125718. https://doi.org/10.1016/j.jhazmat.2021.125718.

United Nations Environment Programme. 2016. Addressing transboundary concerns in the Volta River Basin and its downstream coastal areas. GFL/2328-2731-4957.

United Nations. 2017. Resolution adopted by the General Assembly on 6 July 2017, Work of the Statistical Commission pertaining to the 2030 Agenda for Sustainable Development (A/RES/71/313 Archived 28 November 2020 at the Wayback Machine).

van Leeuwen SPJ, de Boer J. 2007. Extraction and clean-up strategies for the analysis of poly- and perfluoroalkyl substances in environmental and human matrices. *J Chromato A* 1153:172–185. doi:10.1016/j.chroma.2007.02.069.

Vento SD, Halsall C, Gioia R, Jones K, Dachs J. 2012. Volatile per- and polyfluoroalkyl compounds in the remote atmosphere of the western Antarctic Peninsula: an indirect source of perfluoroalkyl acids to Antarctic waters? *Atmos Poll Res* 3:450–455. doi:10.5094/APR.2012.051.

Vikesland P, Garner E, Gupta S, Kang S, Maile-Moskowitz A, Zhu N. 2019. Differential drivers of antimicrobial resistance across the world. *Acc Chem Res* 52:916–924.

Xiong W, Sun Y, Zhang T, Ding X, Li Y, Wang M, Zeng Z. 2015. Antibiotics, antibiotic resistance genes, and bacterial community composition in fresh water aquaculture environment in China. *Microb Ecol* 70:425–432. https://doi.org/10.1007/s00248-015-0583-x

Zhao P, Xia X, Dong J, Xia N, Jiang X, Li Y, Zhu Y. 2016. Short- and long-chain perfluoroalkyl substances in the water, suspended particulate matter, and surface sediment of a turbid river. *Sci Total Environ* 568:57–65. doi:10.1016/j.scitotenv.2016.05.221.

Zhou Z, Liang Y, Shi Y, Xu L, Cai Y. 2013. Occurrence and transport of perfluoroalkyl acids (PFAAs), including short-chain PFAAs in Tangxun Lake, China. *Environ Sci & Tech.* 2013 47:9249-57. https://doi.org/10.1021/es402120y

Zou S, Xu W, Zhang R, Tang J, Chen Y, Zhang G. 2011. Occurrence and distribution of antibiotics in coastal water of the Bohai Bay, China: Impacts of river discharge and aquaculture activities. *Environ Poll* 159(10):2913–2920. doi:10.1016/j.envpol.2011.04.037.

Chapter 3: Enhanced nitrogen removal and anammox bacteria retention with zeolite-coated membrane in simulated mainstream wastewater

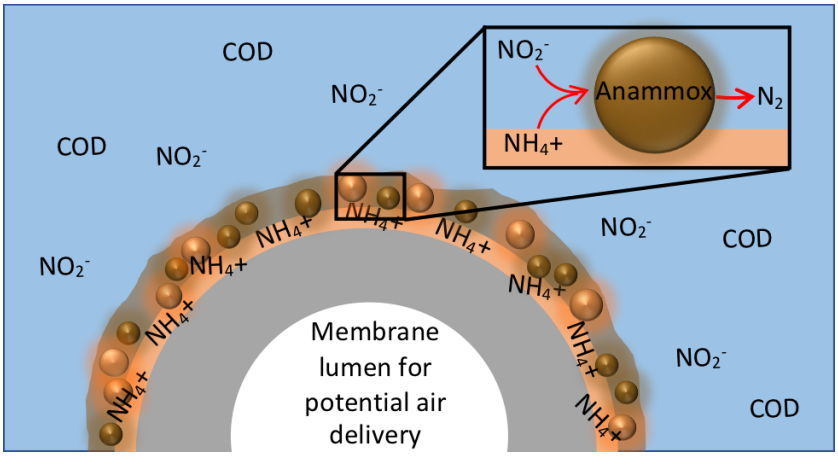

This chapter has been published in the journal *Environmental Science & Technologies Letters* and is cited as:

Huff Chester, A. L., Eum, K., Tsapatsis, M., Hillmyer, M. A., & Novak, P. J. (2021). Enhanced Nitrogen Removal and Anammox Bacteria Retention with Zeolite-Coated Membrane in Simulated Mainstream Wastewater. *Environmental Science & Technology Letters*, 8(6), 468-473.

Abstract

The anammox process has been used for side-stream nitrogen removal. Mainstream anammox is challenging, however, as a result of low ammonium concentrations and retention times that wash out slow growing anammox bacteria. To overcome these challenges, hollow fiber membranes with zeolite-coated surfaces were prepared to create near-surface microenvironments that mimic attributes of side-stream treatment systems. Results showed that in mainstream-type media, zeolite-coated membranes enhanced the growth of anammox bacteria on the membranes and in the bulk liquid of the reactor compared to reactors containing uncoated control membranes. The zeolite-coated membranes also improved the average total nitrogen (TN) removal to 73±10% compared to 1±49% in the control reactors. Additional experiments containing zeolite particles demonstrated that increasing zeolite mass increased the number of anammox gene copies present and improved TN removal, with effluent TN concentrations decreasing from 51.8±5.9 to 7.78±2.6 mg-N/L (P=0.00085) as zeolite increased from 0.05 to 1.0 g/reactor, respectively. These results suggest that membranes/surfaces containing a greater quantity of zeolite should further improve retention of anammox bacteria and TN removal. Application of such membranes in an IFAS-type system or membrane aerated biofilm reactor (MABR) with intermittent aeration and low bulk DO concentrations should facilitate mainstream anammox.

Introduction

Anaerobic ammonia oxidation (anammox) is the autotrophic bioconversion of ammonium (electron donor) and nitrite (electron acceptor) to dinitrogen (N_2). Since the

discovery of the process, anammox has received attention for its potential to reduce oxygen requirements at wastewater treatment plants (WWTPs), resulting in substantial cost savings.[1] Concomitant with the anammox process, partial nitrification (PN) supplies nitrite, by converting half of the influent ammonium to nitrite *via* aerobic ammonia oxidizing bacteria (AOB).[2,3] The PN-anammox process has been successfully implemented in side-stream treatment, where a single constituent, ammonium, is targeted. In side-streams the ammonium concentrations are high and the biodegradable carbon concentrations are low, preventing the proliferation of heterotrophs and providing a niche for anammox.[4,5] In addition, side-stream flows are not subject to discharge regulations, facilitating anammox-focused control of dissolved oxygen (DO) and solids residence time (SRT).[4] Unfortunately, the conditions that make side-stream successful create challenges for mainstream PN-anammox.[3,6] First, ammonium concentrations in mainstream wastewater are too low for high rates of anammox activity; this, with abundant biodegradable carbon, results in heterotrophs outcompeting anammox bacteria.[7] Second, the need to balance effluent standards with energy use typically leads to SRTs that wash out slow-growing anammox bacteria,[6,8] with the few mainstream anammox applications in operation requiring continuous biomass augmentation.[9,10] Third, PN requires careful control to avoid proliferation of nitrite oxidizing bacteria (NOB).[11,12] If side-stream conditions were established as microenvironments in mainstream wastewater treatment, then implementation of mainstream anammox could be successful.[13]

Membrane aerated biofilm reactor (MABR) technology allows for precise control of oxygen transfer rates by manipulating the inter-membrane pressure, membrane surface

area, and water velocity across the membrane surface[13–15] and has been successfully used to stimulate PN in side-stream conditions with bulk anaerobic conditions.[16] Additionally, cyclic aeration patterns have proven successful for regulating NOB activity.[17,18] These prior studies suggest that such systems could be applied where ammonium concentrations are high enough to allow anammox bacteria to compete.[11,18] Therefore, if ammonium concentrations could be increased locally and coupled with existing MABR technology to provide limited oxygen for localized ammonia oxidation, the anammox process could be stimulated in a largely anaerobic mainstream environment.

Zeolites, which contain charged nanocages that exchange or absorb cations, create high localized concentrations of charged species in otherwise dilute media.[20,21] Zeolite surfaces with localized elevated ammonium can enrich anammox bacteria in otherwise ammonium-dilute environments, as demonstrated in wetlands[22] and other engineered systems.[23] Studies have also shown that zeolite can be bio-regenerated,[24,25] demonstrating that absorbed ammonium is bioavailable. Zeolite also provides the benefit of additional surface area for biofilm formation, thereby minimizing wash out and increasing the retention time of biomass.[26] Therefore, the incorporation of zeolite into mainstream wastewater treatment could retain anammox bacteria, particularly if zeolite could also be retained.[20]

In this research we describe novel gas transfer membranes that incorporate zeolite onto the membrane surface, facilitating ammonium sorption/ion exchange and enhancing anammox retention in the presence of relatively low ammonium and moderate/typical

organic carbon concentrations in the bulk solution. The results described below suggest that zeolite-coated membranes could help overcome current challenges associated with mainstream anammox.

Materials and Methods

Materials and membrane preparation. Faujasite-type (FAU) zeolite particles were purchased from Sigma Aldrich and used as received. Bare alumina hollow fibers and zeolite-coated alumina hollow fibers were prepared as described previously (Appendix D).[27,28] To grow the zeolite layer, dried alumina fibers were immersed in a solution of 7.7 M NaOH, colloidal silica (Ludox TM-40, Sigma Aldrich), and 0.15 g aluminum for 24 h at 75°C. An additional fiber was immersed for 48 h to grow a thicker layer of zeolite, which was used to test permeance (Appendix D). Fibers were sonicated and rinsed with deionized water. Scanning Electron Microscopy (SEM) and Dispersive X-ray Spectroscopy (EDS) verified the zeolite layer thickness and type (Figures D.S1 and D.S2, Table D.S2). Membranes were tested for porosity *via* a dead-end single-gas permeance test at 25°C (Appendix D).[29]

Biomass Seed and Synthetic Wastewater. Activated sludge and anammox sludge for inoculation are described in the Appendix D. The synthetic wastewater (SWW) used for all experiments was modified from a previous study (Table D.S4)[30] with addition of nitrite to remove the need for aeration control and PN. The SWW was autoclaved and stored in sealed containers until used.

Experimental set-up

Sorption experiments. Zeolite particles and zeolite-coated membranes were tested for ammonium sorption/ion exchange in synthetic wastewater with initial [ammonium] of 33.3±4.8 mg-N/L (see Appendix D for details). An ammonium removal isotherm was also developed for the membranes in ammonium chloride solution (see Appendix D for details). Sorption was also measured after the batch experiments described below were completed (Appendix D).

Zeolite particle batch experiment. Experiments were performed to determine whether zeolite particles could enhance TN removal and retain anammox bacteria under conditions of low ammonium and moderate/typical COD. Triplicate reactors contained either zeolite particles (0.05 g-1.0 g) or bare alumina particles (control) and were incubated on a shaker table in an anaerobic glovebag at room temperature (21±2°C). All reactors were started with a common well-mixed solution of 500 mL SWW (Table D.S4), 7.5 mL activated sludge, and 2.5 mL anammox sludge.

Liquid was removed from the reactors and exchanged with fresh, sterile SWW every three days for an SRT of 9 days. This exchange allowed for (1) continuous ammonium addition, thereby challenging the sorption capacity of the zeolite, and (2) the washout of slow-growing anammox bacteria, which were expected to be removed from the system at this SRT and temperature if no favorable niche was established. This SRT was also selected to be conservative (*i.e.*, on the long side of typical to not artificially wash out the

anammox), but still within values normally used for wastewater treatment. The removed liquid was analyzed for ammonium, TN, nitrate, and nitrite. Liquid biomass samples were collected at the end of the experiment (Day 33) and stored at –20°C until DNA was extracted. Details are provided in Appendix D.

Membrane batch experiments. Another experiment was performed to determine if the novel zeolite-coated hollow fiber membranes could also enhance nitrogen removal and increase anammox bacterial numbers in simulated mainstream conditions. Three treatments were established: zeolite-coated membranes in the presence of bacteria, zeolite-coated membranes in abiotic SWW (abiotic control), and uncoated alumina membranes in the presence of bacteria (no-zeolite control). All treatments were set up in triplicate, had a liquid volume of 9 mL, and contained 260 membranes, 75±2 mm in length, cut into thirds, with 41 mL of headspace (98% N_2, 2% H_2). Although the quantity of membrane was high, this was selected for proof-of-concept to achieve high rates of nitrogen removal and provide an ammonium removal capacity equivalent to 0.75 g zeolite particles. Inoculation and operation were identical to that described for the zeolite particle experiment, except only 3 mL of the liquid was exchanged every 3 days and abiotic reactors received only sterile SWW. Lower TN levels were present in the SWW used in this experiment to account for the smaller sorption capacity of the membranes; organic carbon was added at 200 mg/L COD (Table D.S4). Liquid biomass samples (0.5 mL) were collected throughout the experiment (36 days). Biofilm samples were also collected throughout the experiment by carefully removing membrane pieces with tweezers and preserving them in lysis buffer at –20°C until DNA was extracted.

This experiment was repeated with the addition of 10 mM sodium azide in the abiotic zeolite-coated membrane reactors to confirm abiotic transformation of amended nitrite. The same reactors and membranes were used in this experiment after rinsing thoroughly with DI water and autoclaving. Halfway through this repeated experiment (Day 15), the influent ammonium chloride and sodium nitrite concentrations were both increased (20 mg-N/L) to enable quantification of possible (abiotic) degradation products. Other than these changes, the operation of the experiment was identical to the first experiment.

Analytical methods. Methods are described in Appendix D.

Molecular methods. DNA extraction is described in the Appendix D. qPCR was performed on 16S rRNA genes and several genes associated with nitrogen cycling (Anammox-specific 16S rRNA gene (Amx), *amoA*, *nxrA*, *nosZ*, *nirK*, and *nirS*), as described in the Appendix D.

Data Analysis. Statistical tests were performed with R software. Concentrations of nitrogen species in various treatments were compared first using a non-parametric Kruskal-Wallis test. If the null hypothesis was rejected ($P<0.05$), then the Wilcoxon Rank Sum test was used to compare individual treatments. qPCR results were also analyzed using the Wilcoxon Rank Sum test. For the particle experiment, samples collected at the end of the experiment were compared. For the membrane experiment, samples collected

throughout the experiment were compared. Significance was set at $P<0.05$. An FDR correction was performed for multiple comparisons.

Results & Discussion

Characterization of zeolite-coated gas transfer membranes. Fabrication of zeolite-coated hollow fiber membranes was verified with SEM-EDS (Appendix D, Figure D.S1), with a zeolite layer 2.6±0.4 μm thick, based on 15 measurements, and aluminum:silicon consistent with the formation of FAU (Table D.S2). Assuming the density of the zeolite coating and the alumina hollow fiber base were similar to expected pure materials (~1.93 g/cm^3 for FAU, ~3.7 g/cm^3 for alumina) and the two phases had a similar porosity (35%), the zeolite was approximately 1-2% of the total fiber mass. The gas transfer ability of the zeolite-coated membranes was tested, with lower gas permeance values measured for the zeolite-coated membranes compared to uncoated alumina membranes (Table D.S3); this suggests that the ability to deliver oxygen, and therefore support production of nitrite and ultimately PN, may be controlled by the thickness of the zeolite layer. Ammonium removal tests in ammonium chloride solution indicated that the zeolite-coated membranes fit both Langmuir and Freundlich isotherms and that the uncoated membranes did not remove ammonium (Appendix D, Figure D.S3). The ammonium sorption capacity was retained after the biological experiments (3.68±0.74 mg-N/L per membrane for the used zeolite-coated membranes, compared to 3.96±0.13 for new zeolite-coated membranes, $P=0.7$) (Appendix D, Figure D.S5), suggesting that minimal zeolite leaching occurred over this time period. When tested in SWW, the average ammonium sorption of the coated membranes and zeolite particles in SWW were 0.35±0.17 mg-N/g membrane

(19.3±9.5 mg-N/g zeolite on membrane) and 5.0±2.4 mg-N/g FAU particle (Appendix D, Figure D.S4).

Enhancement of biological nitrogen removal and anammox retention by zeolite particles. The mass of zeolite had a significant effect on the concentrations of ammonium, nitrite, and TN present, with significantly lower concentrations in the reactors containing 1.0 g (P=0.0005, 0.013, and 0.0004 for ammonium, nitrite, and TN, respectively) and 0.5 g zeolite (P= 0.0005, 0.0035, and 0.0004 for ammonium, nitrite, and TN, respectively), as compared to the no-zeolite control (Figure 3.1). The TN concentrations in the reactors containing 0.05 g (P=0.0006) and 0.10 g (P=0.0017) zeolite were also significantly different than the control, as were the ammonium concentrations in the reactors containing 0.10 g zeolite (P=0.021).

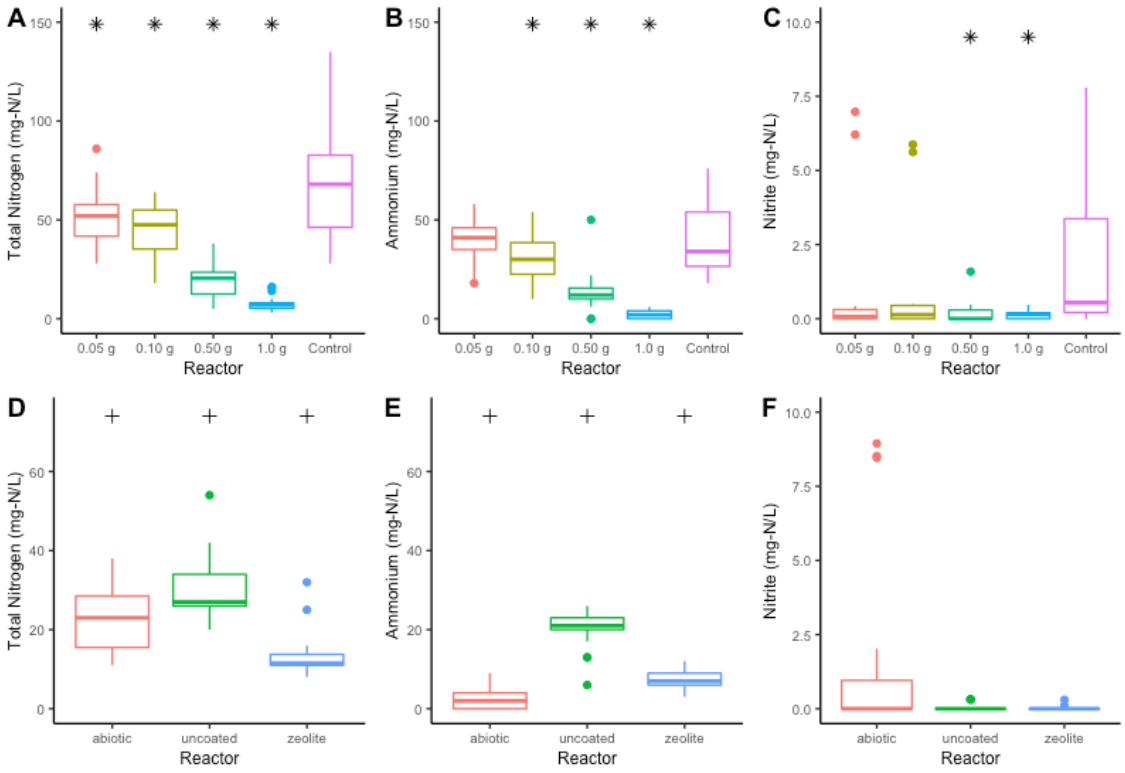

Figure 3.1 Box plot of effluent concentrations in zeolite particle reactors. A) TN, B) ammonium, and C) nitrite; and membrane reactors D) TN, E) ammonium, and F) nitrite. + indicates treatments were significantly different from all of the other treatments. The y-axis is different for panels C and F.

Because the reactors were anaerobic, biologically active, and contained COD, ammonification of organic nitrogen and denitrification of added nitrite was expected. In the presence of zeolite particles, ammonium sorption was also expected. Therefore, the quantities of nitrogen-cycling genes were also determined as an indicator of the active biological processes in the system. Indeed, supporting the observation of enhanced biological anaerobic ammonium degradation, Amx gene copies were higher (at the 90% confidence level) in all reactors containing zeolite compared to the biological control

reactors with no zeolite present (Figure 3.2; P=0.1). Perhaps more telling was the fact that the average Amx gene copy numbers increased with zeolite mass (Figure 3.2A), reaching a relatively stable level in the 0.5 g and 1.0 g zeolite reactors ($7.7x10^7$ and $5.6x10^7$ copies/mL reactor bulk for the 0.5 g and 1.0 g reactors, respectively). Similar patterns were observed when Amx gene copy numbers were normalized to 16S rRNA gene copy numbers (Appendix D, Figure D.S8), with all zeolite reactors being statistically significant at the 90% confidence level. Given the SRT of 9 days and the operating temperature of approximately 21°C, anammox biomass was expected to wash out of the reactors if a favorable niche was not established; the zeolite particles appeared to provide this niche.

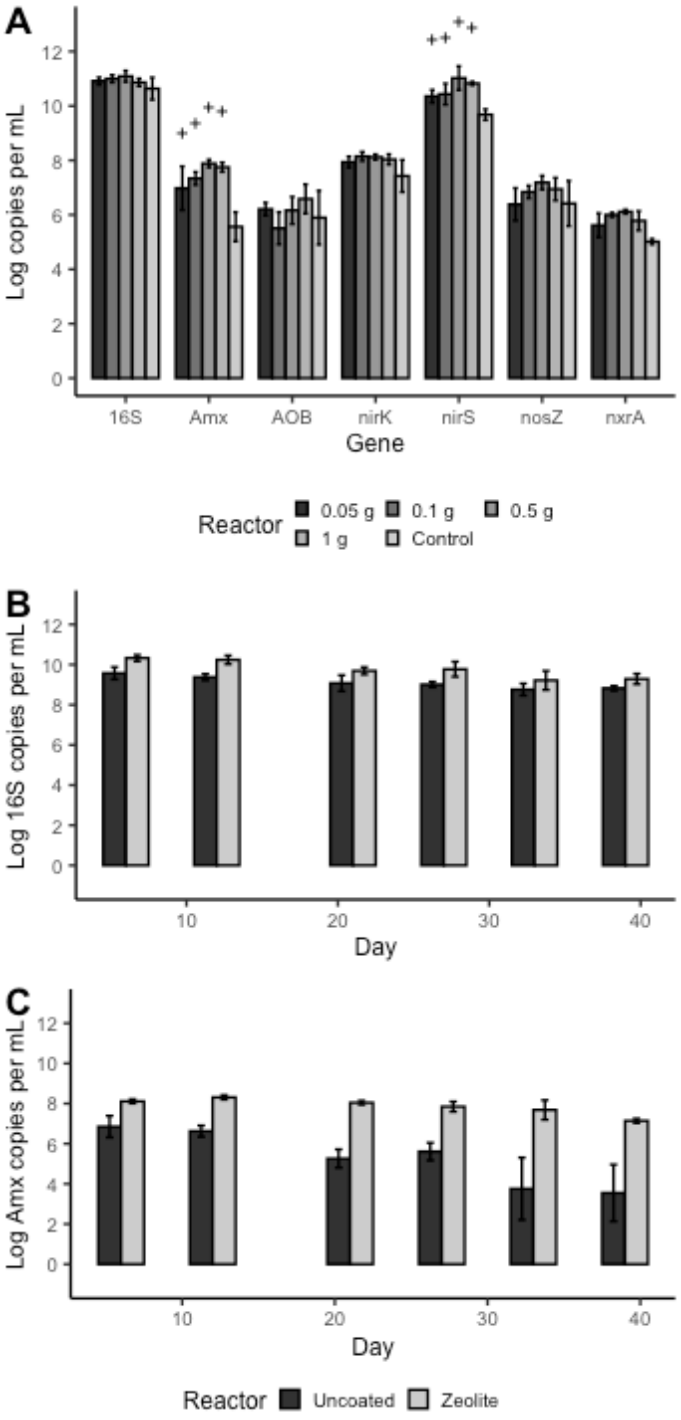

Figure 3.2. qPCR results of nitrogen cycling and 16S rRNA genes. Panel A shows qPCR results from the zeolite particle experiment on Day 33. + indicates samples with more gene copies/mL reactor bulk than control samples, with a $P<0.1$. The bars go in spatial order of darkest grey (0.05 g zeolite) to lightest grey

(control), with zeolite quantities increasing to 0.1, 0.5, and 1.0 g zeolite as the bar color lightens. Panels B and C show the log 16S rRNA gene copies and log Amx gene copies, respectively, from the membrane experiment. The zeolite-coated membrane reactors had significantly ($P<0.05$) more gene copies/mL than uncoated membrane reactors when data was pooled for all of the time points.

Additionally, *nirS* gene copies appeared to be enriched in the reactors containing zeolite, also increasing with zeolite mass until reaching a steady level in the 0.5 and 1.0 g zeolite reactors at 1.05×10^{11} and 6.7×10^{10} copies/mL reactor bulk, respectively. All reactors containing zeolite had higher *nirS* gene copy numbers compared to the no-zeolite controls at the 90% confidence level. Both heterotrophic denitrifying bacteria and anammox bacteria possess the *nirS* gene;[31] therefore, it is unclear whether the increase in Amx and *nirS* copies represent enrichment of only anammox bacteria or anammox plus denitrifying bacteria, in which case the presence of zeolite may enrich additional nitrogen cycling activities.

Stimulation of biological ammonium degradation and anammox retention in the presence of zeolite-coated membranes. In the biologically active membranes reactors, the presence of zeolite-coated membranes enhanced removal of ammonium ($P<0.0001$ and $P=0.021$ in membrane experiments 1 and 2, respectively) and TN ($P=0.0003$ and $P=0.046$ in membrane experiments 1 and 2, respectively) compared to the uncoated membranes (Figures 3.1D and 3.1E). Interestingly, in experiment 1, the abiotic reactors with zeolite-coated membranes (3.0 mg-N/L) had lower ammonium concentrations

compared to the biologically active reactors (7.3 mg-N/L) (P=0.00031); this was attributed to the absence of ammonification of organic nitrogen in the abiotic reactors. There was enhanced TN removal in the biologically active zeolite-coated membrane reactors compared to the abiotic reactors in the first experiment (P=0.0003) and enhanced TIN removal compared to the abiotic reactors in the second experiment (P=0.031) (Figures 3.1D and D.S6), with near complete nitrogen removal observed. These results are consistent with (1) ammonium sorption/ion exchange occurring in the abiotic reactors containing zeolite-coated membranes, while (2) ammonification of organic nitrogen to ammonium with subsequent ammonium sorption and biotransformation via anammox occurred in the biologically active reactors containing zeolite-coated membranes.

Nitrite concentrations were similar in the biologically active zeolite-coated and uncoated membrane reactors (P=0.36), likely a result of denitrifying activity in both (Figure 3.1F). In experiment 1, nitrite concentrations were surprisingly only slightly lower in the biologically active zeolite-coated membrane reactors (0.025±0.039 mg-N/L) compared to the abiotic reactors (2.1±3.8 mg-N/L; P=0.03); degradation of nitrite was not expected in the abiotic reactors. The experiment was repeated (membrane experiment 2) with sodium azide in the abiotic reactors to ensure that any loss of nitrite that was observed was abiotic.

Influent TN was monitored and compared to the effluent TIN species, defined as the sum of ammonium, nitrite, and nitrate (Appendix D, Figure D.S9). After the influent ammonium and nitrite were increased, results showed that ammonium sorption from the

bulk and apparent nitrite oxidization to nitrate occurred in the abiotic treatments, with no TIN removal (P=0.25) (Appendix D, Figure D.S9). Again, excellent TN removal was observed in the biologically active zeolite-coated membrane reactors, with no build-up of abiotic transformation products. The average effluent TIN for the abiotic zeolite-coated membrane reactors was 71.5±7.8 mg-N/L verses 11.3±6.7 mg-N/L for the biologically active zeolite reactors (P=0.0022). Several studies have documented abiotic zeolite-catalyzed oxidation of nitrite[32,33] and zeolite catalysis in general,[34,35] which are possible explanations for the oxidation of nitrite in these experiments. More research is needed to understand this apparent abiotic oxidation.

Similar to biological treatments containing zeolite particles, the zeolite-coated membranes appeared to provide a niche for anammox bacteria (Figure 3.2C). The Amx gene copies were more abundant in biologically active zeolite-coated membrane reactors than in the uncoated membrane reactors. This was true for the bulk liquid ($7.2x10^7$ versus $1.9x10^5$ copies/mL, zeolite-coated versus uncoated membranes, P<0.0001) and the membranes ($4.4x10^3$ copies/mL versus no detected gene copies, zeolite-coated versus uncoated membranes, P=0.04). Other nitrogen cycling genes, specifically *nirK*, *nirS*, and *nosZ*, were present in both reactor types and in both liquid and biofilm samples (Figures D.S4 and D.S5). All of these gene copies were significantly higher in the bulk liquid of the reactors with zeolite-coated membranes compared to those containing uncoated membranes (P<0.0001 for *nirK*, *nirS*, and *nosZ*). These gene quantities were not significantly different on the membranes themselves (zeolite-coated versus uncoated) (P=0.20, 0.20, and 0.13 for *nirK*, *nirS*, and *nosZ,* respectively). Nitrification genes, *amoA*

and *nxrA*, were also detected in the bulk liquid of both reactors, but only at low quantities, if at all, on the membranes. All comparisons were made by pooling the data from all time points. Again, these results are consistent with the nitrogen removal and qPCR results obtained from the zeolite particle experiment and point to the potential utility of zeolite-coated membranes to enhance mainstream anammox.

Environmental Significance

While MABR technologies are relatively new, there are a number of manufacturers and full-scale applications of these systems, including Suez Technologies & Solutions ZeeLung®, Fluence Corporation, and OxyMem Limited.[36] Studies have shown that PN can be maintained and NOB growth suppressed with cyclic aeration strategies in mainstream wastewater; nevertheless, anammox enrichment and persistence is still a challenge.[37] Further enhancement of existing membrane technologies by concentrating ammonium on a membrane surface, as demonstrated here for the first time, provides an advantage to anammox bacteria, promoting their growth and stability in mainstream wastewater treatment systems. With further improved ammonium sorption/ion exchange capacity, such membranes could play a role in enabling mainstream anammox.

Acknowledgments

We would like to thank the undergraduate research assistants who worked on this project including Justin Garrison, Doug Shields, Nikhil Khurana, and Kalie Manke. We would also like to acknowledge the UMN Characterization Facility and Dr. Michael Manno with the Valspar Material Science and Engineering Lab for use of equipment. The work

was supported by the Environment and Natural Resources Trust Fund as recommended by the Legislative Citizen Commission on Minnesota Resources.

Summary of additional information in Appendix D.

Additional information for Materials and Methods in detail. Membrane SEM images, EDS mapping information, and permeance data. Ammonium isotherms for membranes and sorption data for membranes, particles, and post-experiment membranes. qPCR results for additional genes and relative abundance of Amx gene copies. Nitrogen concentrations for final zeolite-coated membrane experiment with sodium azide.

References

(1) Mulder, A. The Quest for Sustainable Nitrogen Removal Technologies. *Water Sci. Technol.* 2003, *48* (1), 67–75.

(2) Li, X.; Klaus, S.; Bott, C.; He, Z. Status, Challenges, and Perspectives of Mainstream Nitritation-Anammox for Wastewater Treatment. *Water Environ. Res.* 2018, *90* (7), 634–649. https://doi.org/10.2175/106143017x15131012153112.

(3) Xu, G.; Zhou, Y.; Yang, Q.; Lee, Z. M.-P.; Gu, J.; Lay, W.; Cao, Y.; Liu, Y. The Challenges of Mainstream Deammonification Process for Municipal Used Water Treatment. *Appl. Microbiol. Biotechnol.* 2015, *99* (6), 2485–2490. https://doi.org/10.1007/s00253-015-6423-6.

(4) Lackner, S.; Gilbert, E. M.; Vlaeminck, S. E.; Joss, A.; Horn, H.; van Loosdrecht, M. C. M. Full-Scale Partial Nitritation/Anammox Experiences - An Application Survey. *Water Res.* 2014, *55* (2014), 292–303. https://doi.org/10.1016/j.watres.2014.02.032.

(5) Winkler, M. K.; Straka, L. New Directions in Biological Nitrogen Removal and Recovery from Wastewater. *Curr. Opin. Biotechnol.* 2019, *57*, 50–55. https://doi.org/10.1016/j.copbio.2018.12.007.

(6) Jin, R.-C.; Yang, G.-F.; Yu, J.-J.; Zheng, P. The Inhibition of the Anammox Process: A Review. *Chem. Eng. J.* 2012, *197*, 67–79. https://doi.org/10.1016/J.CEJ.2012.05.014.

(7) Wells, G. F.; Shi, Y.; Laureni, M.; Rosenthal, A.; Sziva, I.; Weissbrodt, D. G.; Joss, A.; Buergmann, H.; Johnson, D. R.; Morgenroth, E. Comparing the Resistance, Resilience, and Stability of Replicate Moving Bed Biofilm and Suspended Growth Combined Nitritation− Anammox Reactors. *Environ. Sci. Technol.* 2017, *51*, 5108–5117. https://doi.org/10.1021/acs.est.6b05878.

(8) Van Der Star, W. R. L.; Miclea, A. I.; Van Dongen, U. G. J. M.; Muyzer, G.; Picioreanu, C.; Van Loosdrecht, M. C. M. The Membrane Bioreactor: A Novel Tool to Grow Anammox Bacteria as Free Cells. *Biotechnol. Bioeng.* 2008, *101* (2), 286–294. https://doi.org/10.1002/bit.21891.

(9) Abbassi, R.; Yadav, A. K.; Huang, S.; Jaffé, P. R. Laboratory Study of Nitrification,

Denitrification and Anammox Processes in Membrane Bioreactors Considering Periodic Aeration. *J. Environ. Manage.* 2014, *142*, 53–59. https://doi.org/10.1016/j.jenvman.2014.03.013.

(10) Wett, B.; Omari, A.; Podmirseg, S. M.; Han, M.; Akintayo, O.; Gómez Brandón, M.; Murthy, S.; Bott, C.; Hell, M.; Takács, I.; Nyhuis, G.; O'Shaughnessy, M. Going for Mainstream Deammonification from Bench to Full Scale for Maximized Resource Efficiency. *Water Sci. Technol.* 2013, *68* (2), 283–289. https://doi.org/10.2166/wst.2013.150.

(11) van Dongen, U.; Jetten, M. S. M.; van Loosdrecht, M. C. M. The SHARON®-Anammox® Process for Treatment of Ammonium Rich Wastewater. *Water Sci. Technol.* 2001, *44* (1), 153–160.

(12) Ma, Y.; Domingo-Félez, C.; Plósz, B. G.; Smets, B. F. Intermittent Aeration Suppresses Nitrite-Oxidizing Bacteria in Membrane-Aerated Biofilms: A Model-Based Explanation. *Environ. Sci. Technol.* 2017, *51* (11), 6146–6155. https://doi.org/10.1021/acs.est.7b00463.

(13) Johnson, D. W.; Semmens, M. J.; Gulliver, J. S. A Rotating Membrane Contactor: Application to Biologically Active Systems. *Water Environ. Res.* 1999, *71* (2), 163–168. https://doi.org/10.2175/106143099x121382.

(14) Li, J.; Zhu, L. P.; Xu, Y. Y.; Zhu, B. K. Oxygen Transfer Characteristics of Hydrophilic Treated Polypropylene Hollow Fiber Membranes for Bubbleless Aeration. *J. Memb. Sci.* 2010, *362* (1–2), 47–57. https://doi.org/10.1016/j.memsci.2010.06.013.

(15) Li, T.; Liu, J.; Bai, R. Membrane Aerated Biofilm Reactors: A Brief Current Review. *Recent Pat. Biotechnol.* 2008, *2* (2), 88–93. https://doi.org/10.2174/187220808784619739.

(16) Lackner, S.; Terada, A.; Horn, H.; Henze, M.; Smets, B. F. Nitritation Performance in Membrane-Aerated Biofilm Reactors Differs from Conventional Biofilm Systems. *Water Res.* 2010, *44* (20), 6073–6084. https://doi.org/10.1016/J.WATRES.2010.07.074.

(17) Pellicer-Nàcher, C.; Sun, S.; Lackner, S.; Terada, A.; Schreiber, F.; Zhou, Q.; Smets, B. F. Sequential Aeration of Membrane-Aerated Biofilm Reactors for High-Rate Autotrophic Nitrogen Removal: Experimental Demonstration. *Environ. Sci. Technol.* 2010, *44* (19), 7628–7634. https://doi.org/10.1021/es1013467.

(18) Pellicer-Nàcher, C.; Franck, S.; Gülay, A.; Ruscalleda, M.; Terada, A.; Al-Soud, W. A.; Hansen, M. A.; Sørensen, S. J.; Smets, B. F. Sequentially Aerated Membrane Biofilm Reactors for Autotrophic Nitrogen Removal: Microbial Community Composition and Dynamics. *Microb. Biotechnol.* 2014, *7* (1), 32–43. https://doi.org/10.1111/1751-7915.12079.

(19) Ahmadi Motlagh, A. R.; LaPara, T. M.; Semmens, M. J. Ammonium Removal in Advective-Flow Membrane-Aerated Biofilm Reactors (AF-MABRs). *J. Memb. Sci.* 2008, *319* (1–2), 76–81. https://doi.org/10.1016/j.memsci.2008.03.020.

(20) Klieve, J. R.; Semmens, M. J. An Evaluation of Pretreated Natural Zeolites for Ammonium Removal. *Water Res.* 1980, *14* (2), 161–168. https://doi.org/10.1016/0043-1354(80)90232-8.

(21) Margeta, K.; Zabukovec, N.; Siljeg, M.; Farkas, A. Natural Zeolites in Water Treatment – How Effective Is Their Use. In *Water Treatment*; InTech, 2013. https://doi.org/10.5772/50738.

(22) Pei, Y.; Wang, J.; Wang, Z.; Tian, B. Anammox Bacteria Community and Nitrogen Removal in a Strip-like Wetland in the Riparian Zone. *J. Environ. Sci. Heal. Part A* 2011, *46* (7), 715–722. https://doi.org/10.1080/10934529.2011.571582.

(23) Mery, C.; Guerrero, L.; Alonso-Gutiérrez, J.; Figueroa, M.; Lema, J. M.; Montalvo, S.; Borja, R. Evaluation of Natural Zeolite as Microorganism Support Medium in Nitrifying Batch Reactors: Influence of Zeolite Particle Size. *J. Environ. Sci. Heal. Part A* 2012, *47* (3), 420–427. https://doi.org/10.1080/10934529.2012.646129.

(24) Martins, T. H.; Souza, T. S. O.; Foresti, E. Ammonium Removal from Landfill Leachate

by Clinoptilolite Adsorption Followed by Bioregeneration. *J. Environ. Chem. Eng.* 2017, *5* (1), 63–68. https://doi.org/10.1016/j.jece.2016.11.024.
(25) Lahav, O.; Green, M. Ammonium Removal from Primary and Secondary Effluents Using a Bioregenerated Ion-Exchange Process. In *Water Science & Technology*; Int Water Assoc, 2000; Vol. 42, pp 179–185. https://doi.org/10.2166/wst.2000.0311.
(26) Fernández, I.; Vázquez-Padín, J. R.; Mosquera-Corral, A.; Campos, J. L.; Méndez, R. Biofilm and Granular Systems to Improve Anammox Biomass Retention. *Biochem. Eng. J.* 2008, *42*, 308–313. https://doi.org/10.1016/j.bej.2008.07.011.
(27) Novak, P.; Romero-Vargas Castrillón, S.; Huff, A.; Hillmyer, M.; Tsapatsis, M. SYSTEMS AND METHODS FOR TREATING WASTEWATER. 16/433,915, 2019.
(28) Shao, J.; Zhan, Z.; Li, J.; Wang, Z.; Li, K.; Yan, Y. Zeolite NaA Membranes Supported on Alumina Hollow Fibers: Effect of Support Resistances on Pervaporation Performance. *J. Membr. Sci. J.* 2013, *451* (2014), 10–17. https://doi.org/10.1016/j.memsci.2013.09.049.
(29) Eum, K.; Hayashi, M.; De Mello, M. D.; Xue, F.; Kwon, H. T.; Tsapatsis, M. ZIF-8 Membrane Separation Performance Tuning by Vapor Phase Ligand Treatment. *Angew. Chemie* 2019, *131* (46), 16542–16546. https://doi.org/10.1002/ange.201909490.
(30) Peterson, K. N.; Tan, D. T.; Bezares-Cruz, J. C.; Novak, P. J. Estrone Biodegradation in Laboratory-Scale Systems Designed for Total Nitrogen Removal from Wastewater. *Environ. Sci. Water Res. Technol.* 2017, *3* (6), 1051–1060. https://doi.org/10.1039/C7EW00164A.
(31) Han, P.; Gu, J.-D. More Refined Diversity of Anammox Bacteria Recovered and Distribution in Different Ecosystems. *Appl. Microbiol. Biotechnol.* 2013, *97* (8), 3653–3663. https://doi.org/10.1007/s00253-013-4756-6.
(32) Karolewski, J. S.; Sutherland, K. M.; Hansel, C. M.; Wankel, S. D. An Isotopic Study of Abiotic Nitrite Oxidation by Ligand-Bound Manganese (III). *Geochim. Cosmochim. Acta* 2021, *293*, 365–378. https://doi.org/10.1016/j.gca.2020.11.004.
(33) Lim, N. Y. N.; Frostegård, Å.; Bakken, L. R. Nitrite Kinetics during Anoxia: The Role of Abiotic Reactions versus Microbial Reduction. *Soil Biol. Biochem.* 2018, *119* (January), 203–209. https://doi.org/10.1016/j.soilbio.2018.01.006.
(34) Choi, E. Y.; Nam, I. S.; Kim, Y. G. TPD Study of Mordenite-Type Zeolites for Selective Catalytic Reduction of NO by NH3. *J. Catal.* 1996, *161* (2), 597–604. https://doi.org/10.1006/jcat.1996.0222.
(35) Centi, G.; Perathoner, S.; Biglino, D.; Giamello, E. Adsorption and Reactivity of NO on Copper-on-Alumina Catalysts: I. Formation of Nitrate Species and Their Influence on Reactivity in NO and NH3 Conversion. *J. Catal.* 1995, *152* (1), 75–92. https://doi.org/10.1006/jcat.1995.1062.
(36) Lu, D.; Bai, H.; Kong, F.; Liss, S. N.; Liao, B. Recent Advances in Membrane Aerated Biofilm Reactors. *Crit. Rev. Environ. Sci. Technol.* 2020. https://doi.org/10.1080/10643389.2020.1734432.
(37) Augusto, M. R.; Camiloti, P. R.; Souza, T. S. O. de. Fast Start-up of the Single-Stage Nitrogen Removal Using Anammox and Partial Nitritation (SNAP) from Conventional Activated Sludge in a Membrane-Aerated Biofilm Reactor. *Bioresour. Technol.* 2018, *266*, 151–157. https://doi.org/10.1016/j.biortech.2018.06.068.

Chapter 4: Advancements in biofilm carriers and gas-permeable membranes: assessment of zeolite technologies for shortcut nitrogen removal applications in low nitrogen wastewater

Abstract

The partial nitrification-anammox (PNA) process and other shortcut nitrogen removal processes have been widely studied because of their potential to offer cost savings during wastewater treatment; nevertheless, sustainable examples of full-scale mainstream shortcut nitrogen removal is lacking. The recent development of novel biofilms supports, specifically, zeolite-coated hollow fiber membranes and zeolite-coated biofilm carriers, that locally concentrate ammonium are promising for enhancing mainstream PNA. The ideal application of these technologies is yet to be determined, however. In this study, the zeolite-coated carriers were tested in flow-through reactors under both anaerobic and aerobic conditions and zeolite-coated hollow fiber membranes were tested in a membrane-aerated flow-through configuration with varying operating times, lumen oxygen concentrations, and with the presence and absence of amended nitrite. Under anaerobic conditions, reactors containing zeolite-coated carriers had significantly greater ammonium and total nitrogen removal (84.0±16.2% and 89.4±17.1%, respectively) compared to reactors containing control carriers (P=0.005). Anammox-specific 16S rRNA (Amx) genes and two genes associated with denitrifiers (*nirS* and *nosZ*) were preferentially retained in the bulk liquid and in the carrier biofilms in zeolite-coated carrier reactors at a statistically significant level. Genes specific to aerobic ammonium oxidizers (*amoA* genes) were preferentially retained in the bulk liquid of the zeolite-coated carrier reactors. The aerated zeolite-coated carrier reactors

also had higher ammonium and total nitrogen removal rates (83.8±10.9%) compared to the aerated control reactors (30.8±23.4%) (P=0.002). Again, despite aeration, *amoA* genes were only preferentially retained in the liquid of the reactors containing zeolite-coated carriers. Experiments with zeolite-coated membranes provided more mixed results, with Amx genes preferentially retained at significantly higher quantities under only two of the experimental conditions: two-week operation with 100% oxygen delivered in the membrane lumen and two-week operation with nitrite supplemented in the influent. Overall, the zeolite-coated carriers present promising potential for deployment in both anaerobic and aerated environments to enhance nitrogen removal and in particular, the retention of anammox bacteria, with the zeolite-coated membranes requiring more study before their optimal deployment strategy is developed.

Introduction

Nitrogen removal is an important part of wastewater treatment and protects the environment from excess nutrients. Wastewater technologies have been designed to remove both ammonium and nitrite/nitrate, forming harmless nitrogen gas, typically through the application of combined nitrification and denitrification processes. Although effective, these processes are energy and resource intensive, resulting in an industry shift towards implementing lower cost "shortcut" nitrogen removal processes.[1,2]

Shortcut nitrogen removal can make use of a variety of microbial metabolic processes, with the ultimate goal of streamlining microbiological oxidation and reduction for lower oxygen, carbon, and/or alkalinity requirements.[3–5] In general, shortcut nitrogen removal combines nitrification, anammox, and denitrification processes. Partial nitrification is the process of converting half of the influent ammonium to nitrite via the activity of aerobic ammonia oxidizing bacteria (AOB) (Eq. 1).[6] Subsequently, ammonium and nitrite are converted to nitrogen gas by anaerobic ammonium oxidizing (anammox) bacteria (Eq. 2).[7] Combined, this process is referred to as

partial nitrification-anammox (PNA). Alternatively, the nitrite produced by AOB can be converted to nitrogen gas by nitrite-consuming denitrifiers (Eq. 3).[6] These processes are summarized in Figure 4.1.

(Eq. 1) $2NH_4^+ + 3O_2 \rightarrow 2NO_2^- + 4H^+ + 2H_2O$

(Eq. 2) $NH_4^+ + NO_2^- \rightarrow N_2 + 2H_2O$

(Eq. 3) $0.33NO_2^- + 1.33H^+ + e^- \rightarrow 0.17N_2 + 0.67H_2O$

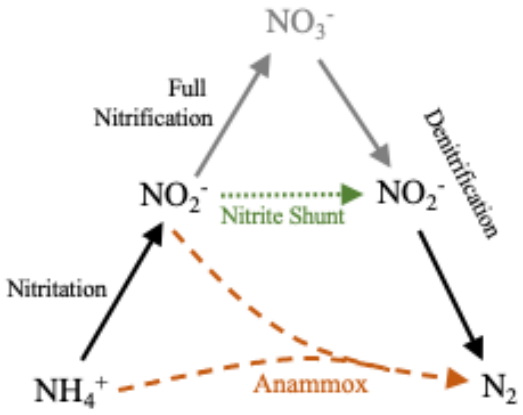

Figure 4.1. Diagram of shortcut nitrogen processes

Implementing shortcut nitrogen removal processes substantially reduces operating costs compared to conventional nitrification and denitrification. The anammox process reduces oxygen demand by approximately 60% with overall operating cost savings estimated at 60 to 90% if implemented for mainstream treatment.[3,5,8] Nitrite shunt, or nitritation/denitritation, can reduce oxygen demand by 25% and reduce overall energy costs by 60%.[4] Additional benefits associated with shortcut nitrogen removal are the elimination or reduction of carbon or alkalinity addition, a reduction in sludge production, and the potential decrease in reactor footprint.[1,4,8] Nevertheless, the implementation of such processes for mainstream treatment have presented challenges

because typical mainstream conditions do not allow for the retention of certain microorganisms, such as anammox.[1]

One way to improve shortcut nitrogen removal for mainstream wastewater treatment is the use of biofilm. Biofilm growth decouples the solids retention time and the hydraulic retention time (HRT) to retain slow growing, autotrophic microorganisms.[9] In some cases, specific biofilm carriers are used to further improve performance.[10] As biofilms develop and aerobic and anaerobic zones are created, complete nitrogen removal can occur in a single biofilm.[10–12] Technologies that take advantage of these benefits include integrated fixed film active sludge (IFAS) and moving bed biofilm reactors (MBBR).[13] Membrane aerated biofilm reactors (MABR) supply oxygen at the membrane base of the biofilm, creating a unique substrate profile that may enhance total nitrogen removal within a single biofilm.[14] Many studies have shown that biofilm technologies work well for shortcut nitrogen removal processes, but that there is still room for improvement, particularly with respect to enhancing the colonization and retention of anammox biomass.[10,13,15–17]

Because of their ability to sorb and therefore concentrate ammonium, zeolite-coated membranes and biofilm carriers could improve current biofilm technologies for shortcut nitrogen removal by improving the rate at which anammox bacteria colonize solid supports as well as their retention, and potentially retaining AOB as well.[16,18,19] In previous work (Chapter 3), we showed that zeolite technologies can attract and retain anammox bacteria in mainstream conditions.[18] With enough zeolite in the system, anammox bacteria were retained and outperformed systems without zeolite amendment with respect to both ammonium and total nitrogen (TN) removal. The wastewater conditions under which zeolite-coated carriers or membrane technologies can be applied for enhanced performance has yet to be explored, however. Aerated zeolite-coated membranes with anaerobic bulk conditions might encourage simultaneous AOB and anammox growth if biofilm

growth enables anaerobic zones on the outer biofilm layers. Under aerated conditions, it is possible that AOB and anammox could coexist on carriers colonized with thick biofilms. Regardless of the bulk conditions, both zeolite-coated carrier and membrane technologies should concentrate ammonium at the base of the biofilm and therefore retain and enrich anammox bacteria, if oxygen concentrations are not too high. The overall AOB and anammox bacteria retention will likely depend on bulk conditions, how much zeolite can be incorporated into these biofilm supports, and the oxygen permeance of the zeolite-coated membranes.

In this study, we explored how operating conditions impact the performance of novel zeolite-coated biofilm support technologies with respect to nitrogen removal and microbial enrichment/retention. We hypothesized that anammox bacteria will be preferentially retained in the presence of zeolite coatings and low oxygen concentrations, whereas AOB will be preferentially retained on zeolite-coated membranes that are able to supply oxygen and sorb ammonium. This research should indicate how best to implement these novel zeolite-coated biofilm supports for enhanced wastewater nitrogen removal and may also indicate other applications for these supports.

Materials and Methods

Biofilm attachment materials. Several methods of coating/attaching zeolite onto a support were tested in this research to create a material that maximized ammonium removal per support surface area. Detailed methods describing these processes are provided below or in previous publications.[18–21] Briefly, for development of zeolite-coated membranes, attachment onto a polymer surface was tested with four different methods of surface functionalization,[2-5] one method of embedding the zeolite into the polymer membrane, and one method of growing zeolite on alumina hollow fibers, which we have tested previously and is described in Chapter 3.[18] For development of porous zeolite-coated carriers, deposition into a porous polyethylene (PE) matrix

was tested, also described previously (Appendix A).[19] Control materials without zeolite were generated for some of these zeolite-coated supports as previously described.[18,19] Scanning electron microscope (SEM) images were taken using methods described in Chapter 3.[18]

Synthetic wastewater and seed. Three types of synthetic wastewater with ammonium concentrations of 35 mg-N/L were used, depending on the experimental objectives. One wastewater contained carbon at 200 mg/L and nitrite at 21 mg-N/L, modified from Huff Chester et al.,[18] and was intended to mimic mainstream wastewater in which PN was active. The second synthetic wastewater was identical to this but did not contain nitrite, mimicking mainstream wastewater influent.[18] A third synthetic wastewater was prepared without carbon and was modified from Peterson et al.[22] to limit the potential for heterotrophic activity. Tables E.S1 and E.S2 (Appendix E) detail the synthetic wastewater contents. Wastewater was autoclaved and sealed until used. The activated sludge and anammox sludge inoculum and their storage conditions are described in Chapter 3.

Experimental set-up and operation

Sorption measurements and isotherm tests. Sorption tests were carried out on membranes and carriers as described in Chapter 3.[18] Areas of membranes were measured using a calipers to determine ammonium removal per area of membrane. Carrier surface area was calculated as the apparent surface area, and not the surface area of the internal porous network. Sorption tests were also conducted for isotherm fitting, also described in Chapter 3.[18] Briefly, carriers were added to 10 mL of autoclaved synthetic wastewater amended with varying ammonium concentrations for 48 hours and mixed on a rotator. Ammonium measurements were taken with an ammonium probe. Isotherms were calculated and fit to Langmuir (Eq. 4), Freundlich (Eq. 5), and linear curves (Figure 4.4) using the R nonlinear least squares function (nls).

$$(Eq.4) \quad q_e = \frac{q_{max} \cdot K \cdot C_f}{1 + K \cdot C_f} = \frac{41.56 \cdot 0.000946 \cdot C_f}{1 + 0.000946 \cdot C_f} \text{ (Langmuir)}$$

$$(Eq.5) \quad q_e = k_f \cdot C_f^{\frac{1}{n}} = 0.0465 C_f^{\frac{1}{1.0588}} \text{ (Freundlich)}$$

Testing of carriers for ammonium sorption through a developed biofilm. In addition to testing fresh membranes and carriers for ammonium sorption, carriers upon which a biofilm layer had developed were also tested for ammonium sorption to ensure that 1) the zeolite deposited into the PE remained intact and 2) ammonium could still exchange into the zeolite with biofilm present. Two sets of zeolite-coated and control carriers were tested for ammonium sorption post-biofilm growth: one set that was harvested at the end of an aerated flow-through experiment (described below) and a second set that was harvested after being submerged in a DEMON reactor (described previously by Peterson et al.[22]) for 14 days. Once harvested, carriers were subjected to 925 Gy of gamma irradiation (GI) on a Cs-137 irradiator (JL Shepherd & Associates), after which they were tested for ammonium sorption in an ammonium chloride solution (29.5+/-0.4 mg-N/L), as previously described.

Carrier bioavailability test. Carriers were formed such that the zeolite particles were entrapped in a porous structure of polyethylene. Carriers were tested to ensure that the ammonium sorbed to the zeolite particles within the porous network was accessible for microbial use, specifically for anaerobic ammonium oxidation. First, ammonium was exchanged into the zeolite in the carriers by adding 387 carriers to 2 L of 100 mg-N/L ammonium chloride solution for 72 hours, after which the carriers were transferred to batch reactors. Carriers were then divided into three different reactor types: 1) zeolite-coated carriers to which an anammox enrichment culture was added, 2) zeolite-coated carriers amended with sodium azide (10 mM), as an abiotic control, and 3) control carriers to which an anammox enrichment culture was added. Serum bottles were used as reactors and contained 50 mL of headspace (97% N_2:3% H_2). Each reactor contained 43

carriers and 50 mL of synthetic carbon-free wastewater containing nitrite and was seeded with 2 mL of settled anammox biomass. This experiment was operated on a shake table (60 rpm) in a glove bag under anaerobic conditions at room temperature (21±2°C). The only ammonium added to the systems was the ammonium sorbed to the carriers. Control carriers were not pre-sorbed with ammonium. Ammonium and nitrite were sampled every 4 hours to monitor ammonium and nitrite degradation.

Permeance testing of hollow fiber membranes. Permeance testing of membranes was conducted for both zeolite-coated and uncoated alumina hollow fiber membranes using the methods described by Ahmed and Semmens.[23] To summarize, 10 membranes were potted in a long reactor, sealed on one end (dead-end configuration) (Figure 4.2).

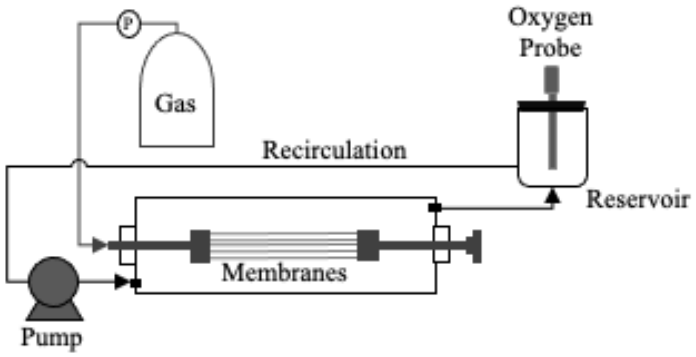

Figure 4.2. Schematic of membrane permeance test step-up

Oxygen was fed to the membranes at 5 PSI and oxygen transfer occurred from the membrane into bulk reactor water as the water flowed across the membrane surface. The water velocity used was that of the membrane flow-through reactor experiments (described below): 0.01 cm/min. Prior to testing, the water was deoxygenated via an N_2 gas purge and recirculated in the reactor system until oxygen probe (Unisense, Opto-3000) inserted in a reservoir at the end of the reactor measured <0.5 mg DO/L. Leakage tests with no oxygen fed through the membranes were also performed to enable the subtraction of oxygen leaking into the system from the oxygen permeating through the membranes. Once the mass transfer coefficient (k) was determined, the

mass flux of oxygen (J) into the zeolite and control membrane reactors was calculated using Eq. 6. Here A is the area of the membrane, C^* is average equilibrium dissolved oxygen concentration in the membrane, and C_L is the oxygen concentration in the bulk liquid.

$$(Eq. 6) \qquad J = kA(C^* - C_L)$$

Carrier flow-through reactors - anaerobic and aerobic. Flow-through reactors were designed to test the nitrogen-removal performance of zeolite-coated and control carriers under mainstream wastewater treatment conditions, as well as their ability to attract and retain anammox bacteria and AOB. Triplicate reactors were packed with 100 zeolite-coated carriers to obtain a "high ammonium zone" of 10 mL. Triplicate control reactors were set up similarly but contained control carriers. The reactor set-up is shown in Figure 4.3 below. Synthetic wastewater containing carbon flowed through the reactors continuously, with an HRT of 17 hours. The experiment was operated twice, once without aeration and with synthetic wastewater amended with nitrite (CFTR), and once with aeration provided by a stone diffuser and synthetic wastewater with no nitrite added (ACFTR). Oxygen measurements were taken at the reactor exit periodically throughout the ACFTR experiment with an oxygen probe (Unisense, Opto-3000). Carrier and liquid biomass samples were harvested from a side port in the reactor for microbial analysis throughout the experiment. Effluent was collected in a vial to which phosphoric acid was added (<pH 4) to ensure that no biological reactions occurred as the effluent was collected prior to analysis. Samples were immediately filtered (0.45 μm) and stored sealed at 4°C until analyzed for COD, ammonium, total nitrogen, nitrate, and nitrite as described below.

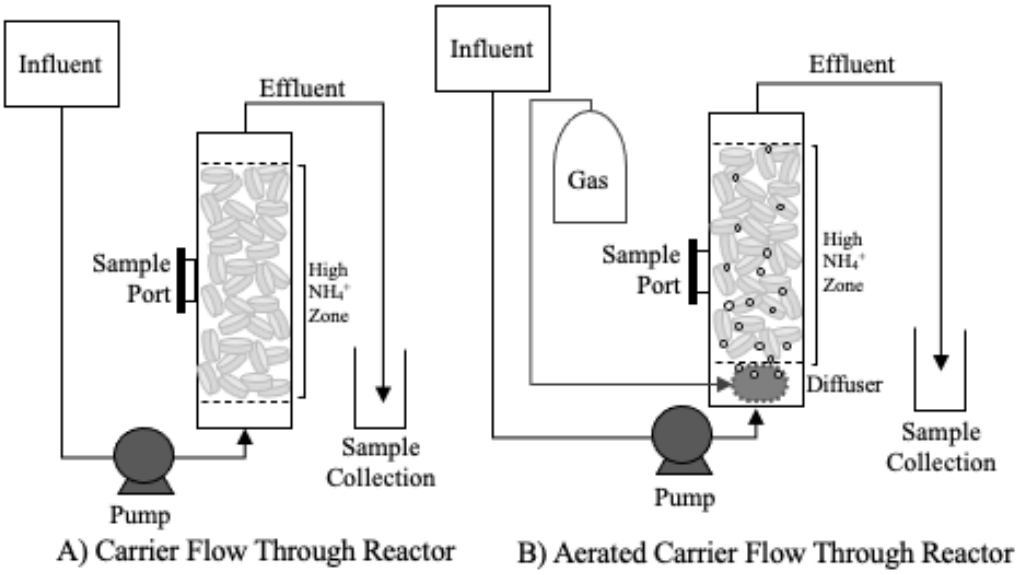

Figure 4.3. Schematic of CFTR and ACFTR reactor set-up

Membrane aerated flow-through reactor. Zeolite-coated and alumina control membranes were also tested in a flow-through configuration to access the growth and retention of anammox bacteria and AOB on the membranes. Synthetic wastewater to which no carbon and no nitrite was added was fed continuously into the reactors. Triplicate reactors were set up for both the zeolite-coated membranes and the alumina control membranes. They were 70 mL in volume and contained a single potted membrane, as shown in Figure 4.4. Oxygen was introduced into the membrane lumen from a compressed tank at 5 PSI in dead-end mode. Experiments were performed for 1, 7, 14, and 24 days to monitor colonization of the membranes; at the end of the experiment the membrane was harvested and biomass was extracted from the membrane surface (see below). Additional experiments were performed for 14 days in which N_2 or air were fed through the membrane. A final experiment was performed for 14 days in which nitrite was added to the synthetic wastewater fed to the system. For all experiments, 0.5 mL of activated sludge and 0.2 mL of settled anammox sludge were added to the reactors at the start of the experiment. Reactor liquid was recirculated for 24 hours at 1.0 mL/min to encourage biofilm attachment.

After 24 hours, settled sludge was drained and the flow-through experiment was started with a wastewater HRT of 23 hours. At the end of each experiment membranes were carefully harvested and cut into equal sample lengths of 52+/-3.4 mm for DNA extraction. Oxygen was monitored with an oxygen probe throughout the experiment; the bulk liquid of the reactors quickly became and stayed anaerobic during all experiments.

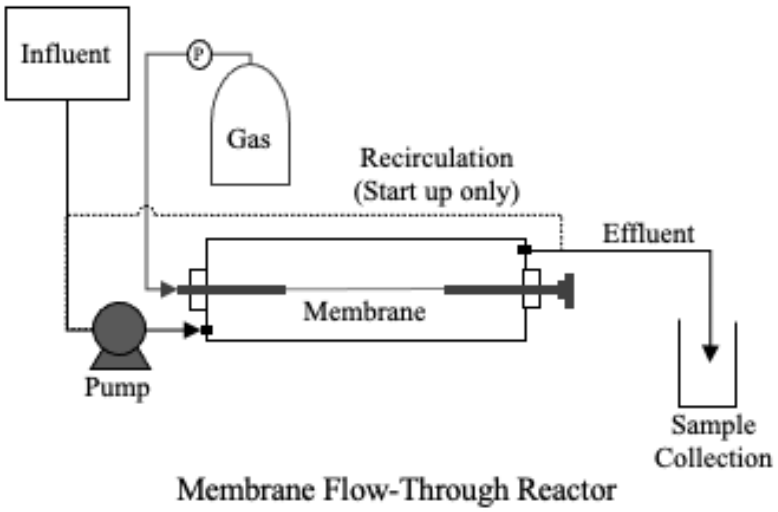

Figure 4.4. Schematic of MFTR reactor set-up

Analytical methods. Analytical methods, specifically nitrogen measurement methods, are described previously in Chapter 3. Briefly, ammonium concentrations for the sorption experiments were measured with an ammonium probe (Orion, Thermo Scientific). Ammonium and TN concentrations in reactor effluent samples were measured colorimetrically (Hach). Nitrite and nitrate concentrations in reactor effluent samples were measured with ion chromatography (930 Compact IC Flex, Metrohm). Dissolved organic carbon (DOC) measurements in reactor samples were analyzed using a TOC-L total organic carbon analyzer (Shimadzu) after first filtering samples through a 0.22 μm syringe filter. A 5-point calibration curve was generated from 500 mg/L stock solution ranging from 10 to 500 mg/L. Typical limits of detection were 2 mg/L.

Molecular methods. DNA extractions and qPCR were performed as previously described in Chapter 3.

Data and statistical analysis. Ammonium removal was calculated for the ammonium sorption experiments using the equation (Eq. 7) below.

$$(Eq. 7) \qquad Removal = \frac{C_{initial} - C_{final}}{C_{initial}}$$

Non-parametric Wilcoxon rank sum tests were used to compare data from the CFTR and ACFTR experiments, namely the nitrogen concentrations, DOC concentrations, and the qPCR data for the zeolite-coated and control carrier reactors. Comparisons of the ammonium concentrations from the carrier-biofilm sorption tests were also performed using the non-parametric Wilcoxon rank sum test. Parametric paired Student t tests were used to compare the qPCR data in the reactors containing zeolite-coated versus control membranes in the MFTR experiments after first checking for normality using the Shapiro-Wilk test. Typically, p-values less than 0.05 were considered significant, but p-values less than 0.1 were also reported and statistical significance with 90% confidence was clearly indicated. Statistical tests were performed with R software.

Results and Discussion

Characterization of membranes and carriers for bioreactor deployment. Materials prepared using different methods of zeolite attachment/coating were tested for ammonium sorption. SEM images of the developed materials are show in Figure 4.5.

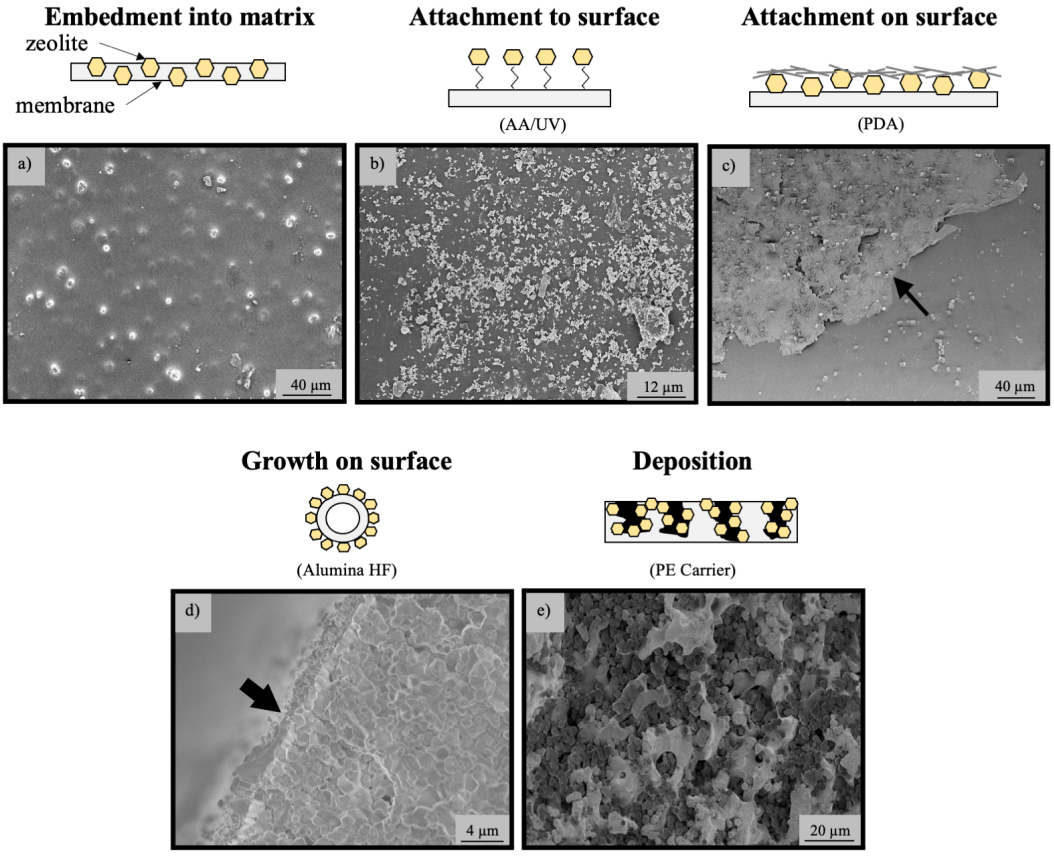

Figure 4.5. SEM images of membrane and carrier surfaces. a) Embedment into polymer membrane matrix, b) attachment to membrane surface using UV/AA method, c) attachment to membrane using PDA method, d) growth of zeolite on alumina HF membrane, and e) deposition into porous PE carrier.[24]

Ammonium sorption from synthetic wastewater as a function of carrier surface area is shown for each membrane and carrier type in Figure 4.6. Most of the zeolite coating methods were successful in attaching zeolite and facilitating at least some ammonium sorption from synthetic wastewater, except for the embedment method, which did not result in substantial ammonium removal (1.9×10-5±4.1×10-6 mg-N/L/mm2) (Figure 4.6). Membranes developed from the attachment methods all obtained some level of ammonium sorption (0.013±0.002, 0.012±0.003, 0.0019±0.0006, and 0.00029±0.0004 mg-N/L/mm2 for ultraviolet (UV), acrylic acid/UV, 1-

Ethyl-3-(3-dimethylaminopropyl)carbodiimide/N-Hydroxysuccinimide, and polydopamine, respectively). The zeolite-coated alumina hollow fiber membranes had the highest ammonium sorption per mm^2 of membrane, removing 0.029±0.004 mg-N/L/mm^2; they were therefore selected for further testing, both with respect to their sorption capacity and their ability to transfer oxygen and support anammox and/or AOB growth and retention. Likewise, the zeolite-coated porous biofilm carriers also showed excellent ammonium sorption capability (0.065±0.03 mg-N/L/mm^2) (Figure 4.4) and were also studied further.

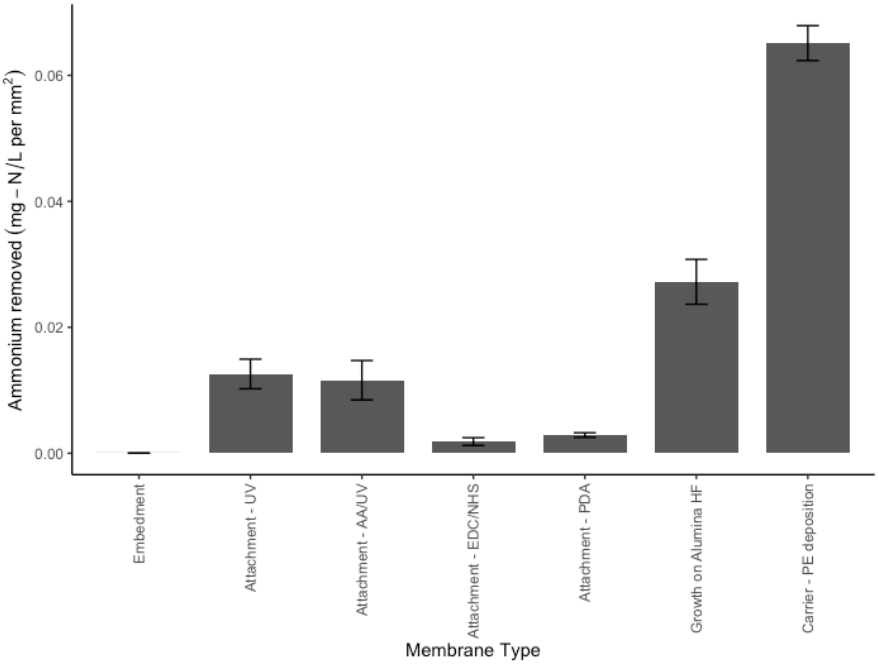

Figure 4.6. Ammonium removal from synthetic wastewater via sorption to zeolite-functionalized materials using zeolite attachment or coating methods. Error bars indicate the standard deviation of triplicate experiments. Note: For the porous carrier within which the zeolite was deposited, the apparent surface area, excluding the internal pore structure, was used for sorption calculations.

Isotherms for ammonium sorption of the zeolite-coated membranes and carriers were also developed and were fit to linear, Langmuir, and Freundlich isotherm models (Figure 4.7, note:

Figure 4.7A also appears in Appendix D and was published in Huff Chester et al.[18]). Both zeolite-coated membranes and carriers sorbed ammonium when submersed in synthetic wastewater while the control membranes and carriers did not. Zeolite-coated membranes were tested in the linear region and the linear isotherm had the highest R^2 (0.9981).[18] Both Langmuir and Freundlich isotherms also fit well, Langmuir with an R^2 of 0.9910 and Freundlich with an R^2 of 0.9914.[18] Zeolite carriers were tested beyond the linear region. As a result, the Langmuir isotherm model provided the best fit, with an R^2 of 0.992; the Freundlich isotherm model also provided a good fit to the data, with an R^2 of 0.981. The linear isotherm had the worst fit, with an R^2 of 0.85.

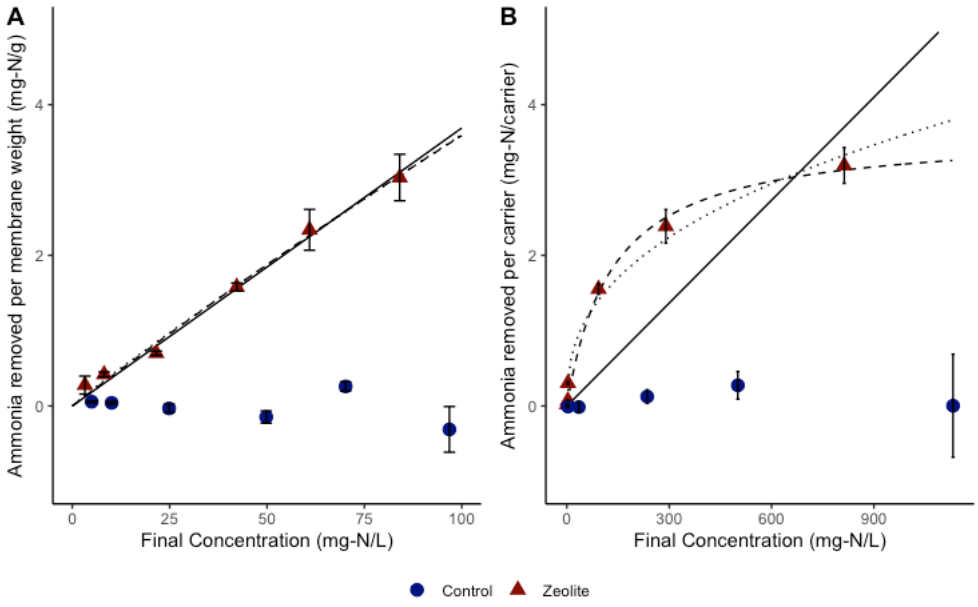

Figure 4.7. Ammonium sorption isotherms for zeolite-coated and control membranes (Panel A) and carriers (Panel B) in synthetic wastewater. Note, Figure 4.5A is also shown in Chapter 3 and has been published in Huff Chester et al. (Figure S3).[18] Lines indicate model fits, with the solid line showing the linear isotherm fit, the dashed line showing the Langmuir isotherm fit, and the dotted line showing the Freundlich isotherm fit. Control membranes and carriers were not fit to isotherm curves,

as they failed to sorb ammonium. Error bars indicate the standard deviation of triplicate experiments.

Carriers coated with biofilm were also tested for ammonium sorption to determine if biofilm growth created substantial blockage of ion exchange sites on the zeolite, as has been reported in other studies.[25] Zeolite-coated carriers, first gamma irradiated to inactive the biofilm, showed considerable ammonium removal (Figure 4.8) indicating that biofilm growth did not prevent ammonium sorption on zeolite-coated carriers. In fact, all zeolite-coated carriers showed ammonium sorption, removing significantly more ammonium compared to the control carriers ($P=0.0035$). The GI-ACFTR zeolite-coated carriers removed more ammonium compared to the GI-Amx zeolite-coated carriers (84.6±2% vs. 49.8±1%, respectively, $P<0.0001$), which is likely an indication that the GI-Amx biofilm was thicker than the GI-ACFTR biofilm and some blockage of the exchange sites did occur upon growth of a thick enough biofilm.

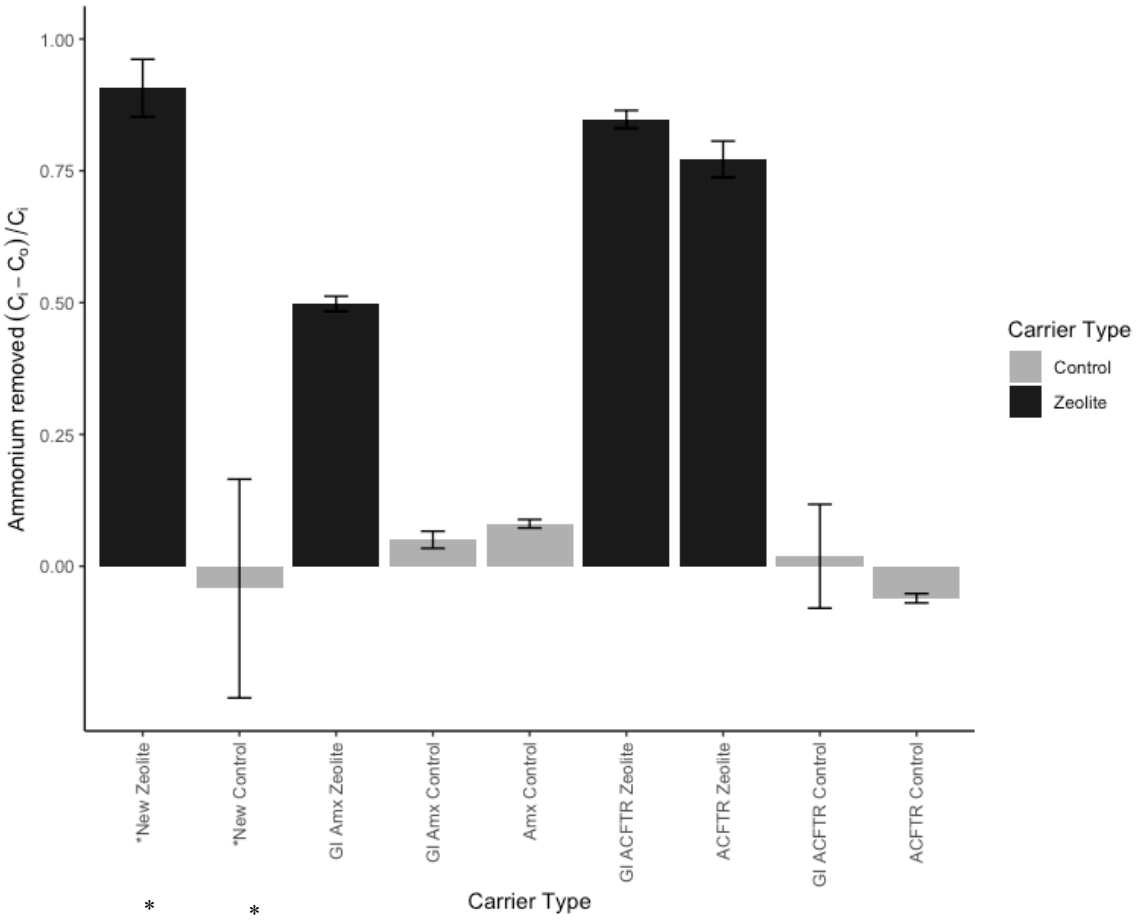

Figure 4.8. Ammonium removal [$(C_i-C_f)/C_i$] via sorption to biofilm covered zeolite-coated and control carriers subjected to gamma irradiation; these were compared to pristine (no biofilm present) zeolite-coated and control carriers. Amx indicates carriers submerged in an anammox enrichment reactor for biofilm growth, ACFTR indicates carriers sampled from the aerated CFTR experiment and also covered in biofilm growth; GI indicates gamma-irradiated carrier samples. Error bars indicate standard deviation of triplicate experiments. Data indicated by (*) is taken from previously published data by Feinberg et al., (Appendix B, Figure B.S57),[6] in which synthetic wastewater was used as the ammonium source rather than an ammonium chloride solution, which was used for the other samples shown in Figure 4.6.

Permeance tests with zeolite-coated alumina hollow fibers showed that the fibers were capable of transferring oxygen to water, with mass transfer coefficients calculated to be 6.3×10^{-6} cm/sec for the zeolite-coated membranes and 2.8×10^{-6} cm/sec for the control membranes. It is unclear why the zeolite-coated membranes were capable of greater oxygen transfer, but it could have been a result of their different surface chemistry and the low velocity of synthetic wastewater flowing past the membrane surface, and therefore the large liquid boundary layer. Measurements of the zeta potential and hydrophobicity of the zeolite-coated and control membranes were attempted, the curvature of the hollow fiber surfaces, however, made these parameters impossible to measure. The reasons for the greater oxygen transfer rates with the zeolite-coated membranes, therefore, could not be confirmed. The mass flux of oxygen into the system was calculated from the mass transfer coefficients to be $2.4\text{x}10^{-7}$ mg/sec for pure oxygen and $5.04\text{x}10^{-8}$ mg/sec for air fed to the lumen of the zeolite-coated membranes. For the control membranes, the mass flux was $1.0\text{x}10^{-7}$ mg/sec for pure oxygen and $2.2\text{x}10^{-8}$ mg/sec for air.

Our previous work on the zeolite-coated alumina hollow fibers (Chapter 3),[18] as well as work by others,[26,27] has suggested that ammonium sorbed to zeolite is accessible to microorganisms; nevertheless, given the sponge-like porous structure of the zeolite-coated carriers and the fact that materials like this have not been previously tested, the bioavailability of the sorbed ammonium with the zeolite-coated carriers was verified. As described in the methods, if the ammonium that was sorbed to the carriers was bioavailable, the nitrite in the bottles containing zeolite-coated carriers and anammox bacteria should degrade. As indicated in Figure 4.9, this is exactly what occurred, with the nitrite concentrations in the zeolite-coated carrier treatments decreasing from 19.16±0.5 to 0±0 mg-N/L within 25 hours and no appreciable nitrite decrease in the control carrier treatments. Indeed, the rate of nitrite degradation in the zeolite-coated carrier treatments

was significantly greater (0.97±0.04 mg/L per hour) than that in the control carrier treatments (0.052±0.005 mg/L per hour) (P=0.027). Additionally, negative control reactors containing zeolite-coated carriers amended with sodium azide showed an increase in ammonium to an average of 56.6±3.7 mg-N/L, as the ammonium desorbed into solution from the carriers and was not consumed biologically. These results clearly demonstrated the ability of the anammox culture to access sorbed ammonium from the zeolite-coated carriers.

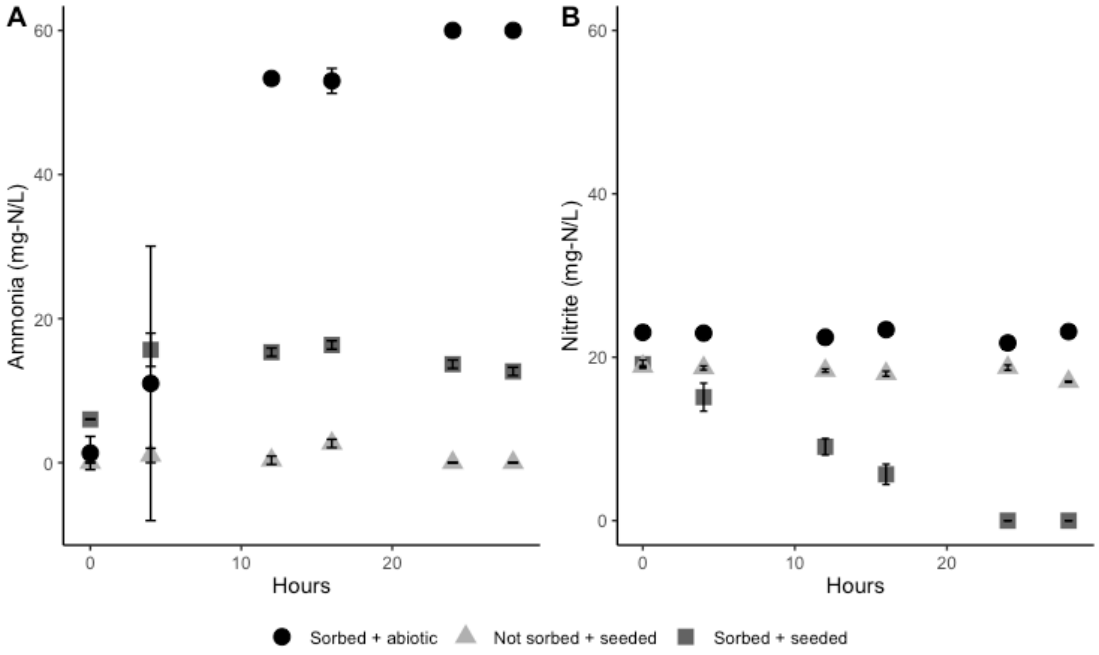

Figure 4.9. Measured ammonium and nitrite concentrations over time from the bioavailability tests, indicating that the ammonium sorbed to the carriers was bioavailable. Error bars show standard deviations of triplicate experimental replicates.

Overall, material testing was able to show that a variety of methods could be used to attach zeolite to supports and additional experiments with two of the most promising materials showed that ammonium sorption followed both a Langmuir and Freundlich sorption model, it could occur through a layer of biofilm, and ammonium exchanged into the zeolite-coated carriers was

biologically accessible. Taken together, this suggests that both the zeolite-coated alumina hollow fiber membranes and PE carriers should be excellent candidates for deployment into mainstream wastewater systems for enhanced shortcut nitrogen removal.

Carrier flow-through bioreactors. Zeolite-coated and control carriers were tested in a flow-through system fed synthetic wastewater containing ammonium and nitrite at concentrations of 15.7±2.33 mg-N/L and 17.4±4.0 mg-N/L, respectively, for a TN concentration of 37.2±6.9 mg-N/L. The influent also contained DOC at a concentration of 167.7±66.2 mg/L. Influent and effluent concentrations of ammonium, TN, nitrite, and nitrate are shown in Figure 4.9. DOC influent and effluent concentrations are shown in Figure 4.11. As a result of an error, no nitrite was added to the influent on Day 25, which is evident in the results shown in Figure 4.10.

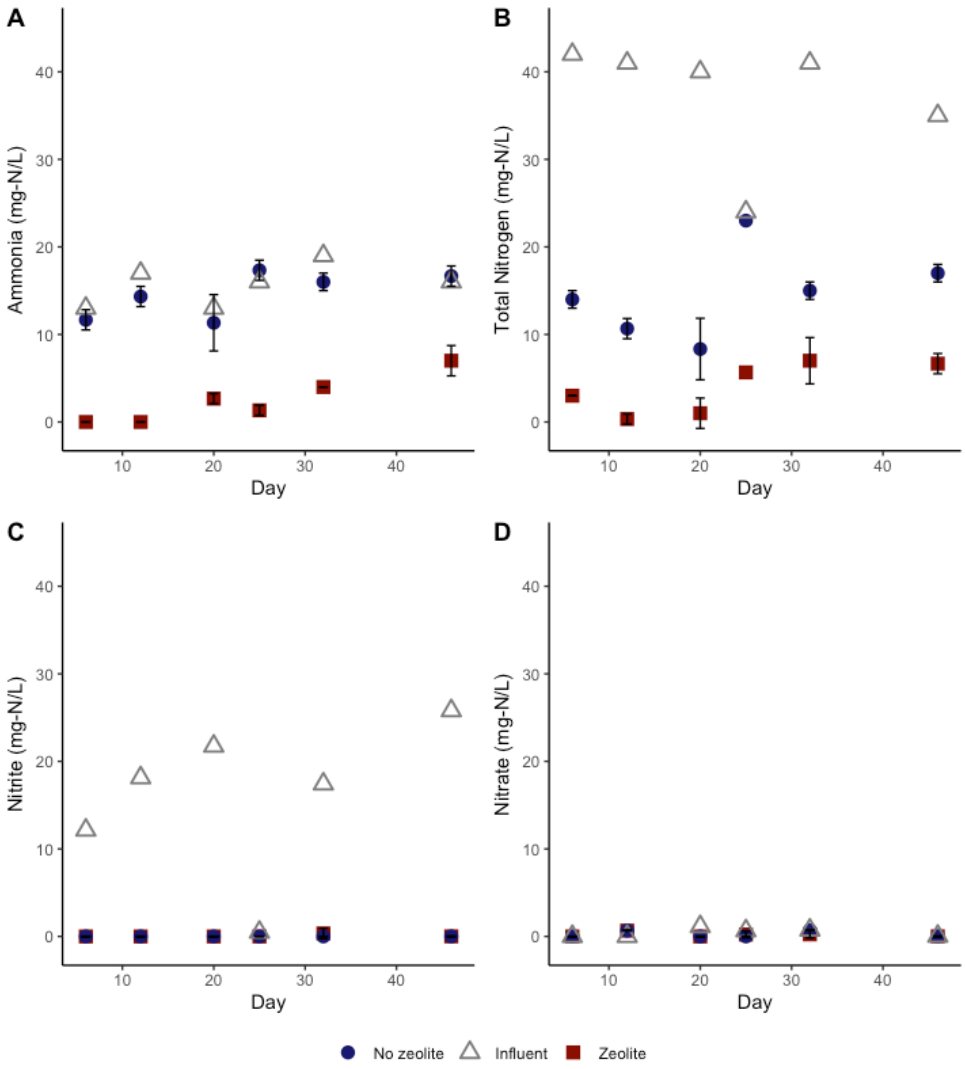

Figure 4.10. Influent and effluent concentrations of A) Ammonium, B) TN, C) Nitrite, and D) Nitrate in the CFTR experiment. Error bars indicate the standard deviation of triplicate reactors.

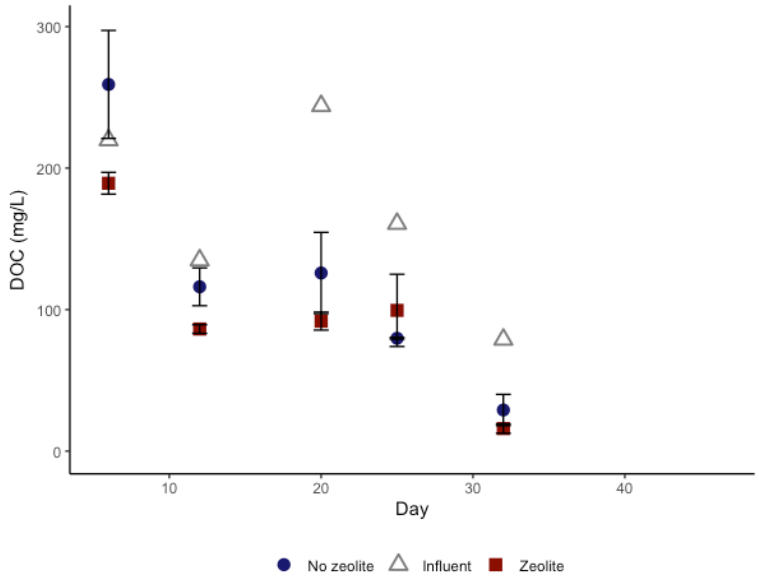

Figure 4.11. Influent and effluent DOC concentrations in the CFTR experiment. Error bars indicate standard deviation of triplicate reactors.

Over the course of the 46-day experiment, the reactors containing zeolite-coated carriers removed significantly more ammonium (84.0±16.2%) and TN (89.4±17.1%), and therefore had much lower effluent ammonium (2.50±2.62 mg-N/L) and TN (3.94±2.98 mg-N/L) concentrations compared to control reactors (14.56±2.79 and 14.7±5.37 mg-N/L for ammonium and TN, respectively) ($P<0.0001$ for both ammonium and TN) (Figure 4.10). It cannot be determined from the chemical data alone whether this was a result of the retention/enrichment of anammox bacteria on the zeolite-coated carriers and enhanced anammox activity, or a result of abiotic ammonium sorption coupled with the denitrification of amended nitrite. As seen in Figure 4.12, however, retention of anammox bacteria on the zeolite-coated carriers does appear to be at least one reason for the enhanced nitrogen removal in the reactors containing zeolite-coated carriers.

The log of the anammox gene copies per carrier or per mL was statistically greater in both the carrier biofilm samples and in the bulk liquid samples from the reactors containing zeolite-coated

carriers, compared to the same samples taken from the reactors containing control carriers (P=0.002 for the carrier biofilm samples and P=0.01 for the bulk liquid samples). The average log 16S rRNA copies per mL or per carrier for anammox (Amx) in the zeolite-coated carrier reactor liquid and carrier biofilm samples were 6.85±0.38/mL and 5.53±0.38 per carrier, respectively, compared to 6.13±0.69/mL and 4.84±0.54 per carrier for the control reactor liquid and carrier biofilm samples, respectively. This equated to a statistically greater percent of Amx genes in the liquid of the zeolite-coated (10.02±9.91%) versus control carrier (4.64±5.90%) reactors (P=0.01557). There was also a greater percent of Amx genes in the carrier biofilm in the zeolite-coated (1.6±0.49%) versus control carrier (0.33±0.31%) reactors, but only at the 90% confidence level (P=0.07359). When coupled with the chemical data, these results suggest that the zeolite-coated carriers were able to enhance the retention, and likely the activity, of the anammox bacteria in the system. Amx gene copies per mL decreased on Day 25 in the liquid of the zeolite-coated reactors, but not in the carrier biofilm samples. This was thought to be a result of the lack of nitrite in the feed on Day 25. The control reactors appeared to be less affected by the lack of nitrite, with no clear decline of Amx gene copies per mL occurring with the lack of nitrite addition.

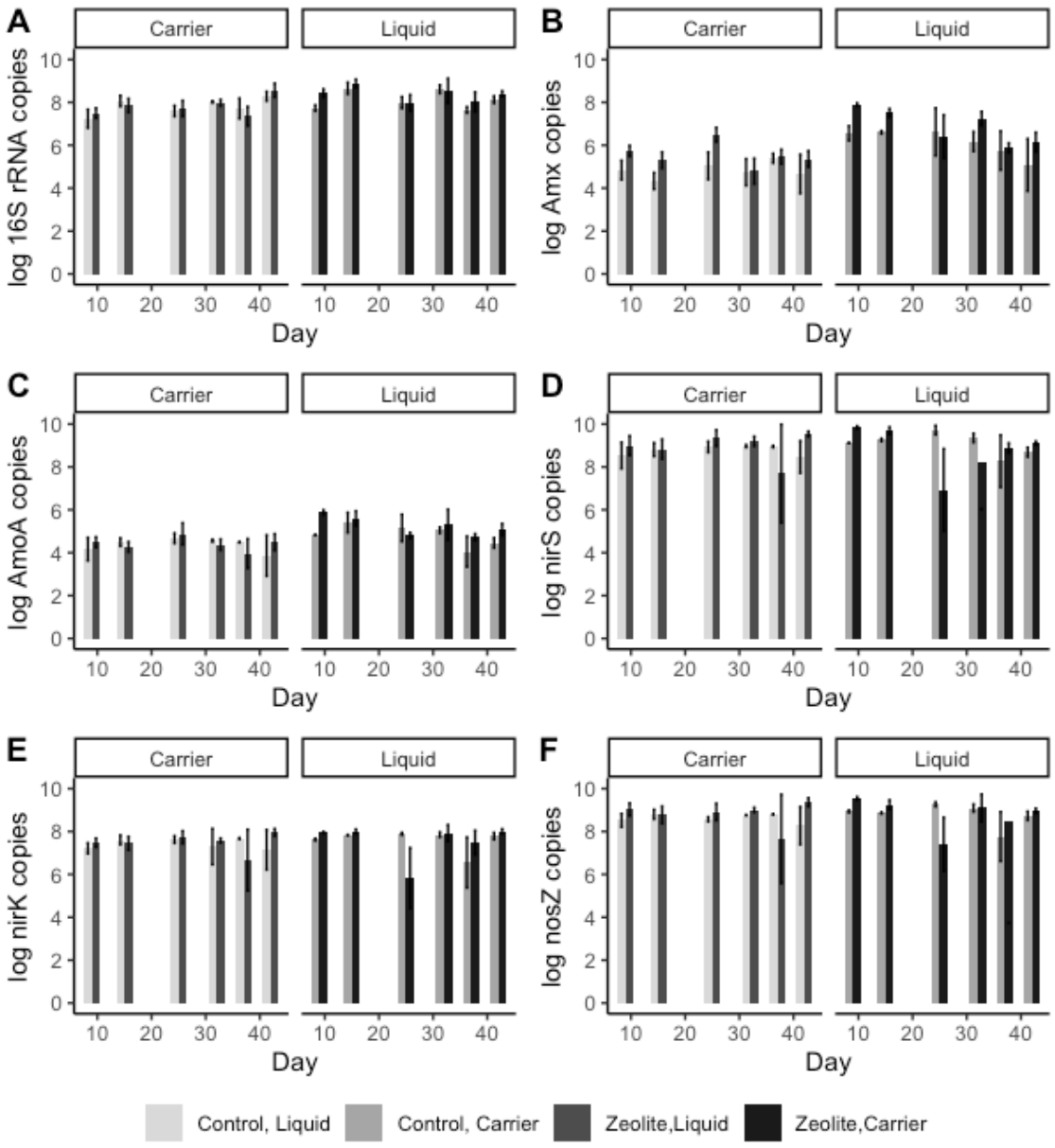

Figure 4.12. qPCR results from the CFTR experiment for the A) 16S rRNA, B) Amx, C) *amoA*, D) *nirS,* E) *nirK, and* F) *nosZ* genes, showing the log number copies per carrier for the carrier biofilm samples and the log number copies per mL for the reactor liquid from CFTR. Light grey indicates samples from control carrier rectors and dark grey indicates samples collected from zeolite-coated carrier reactors. Error bars show the standard deviation of the reactors run in triplicate.

Both reactors also showed excellent nitrite removal and little nitrate production, with effluent nitrite concentrations of 0.069±0.27 mg-N/L and 0 mg-N/L for the zeolite-coated and control carrier reactors, respectively, and effluent nitrate concentrations of 0.23±0.33 mg-N/L and 0.28±0.35 mg-N/L for the zeolite-coated and control carrier reactors, respectively (Figure10). This suggests that denitrification was occurring in both treatments. Not surprisingly, denitrifiers, quantified by the number of *nirK*, *nirS* and *nosZ* gene copies per mL or per carrier present, were detected in the bulk liquid and carrier biofilm samples in both reactors. The *nirS* (P=0.037) and *nosZ* (P=0.0071) genes were significantly enriched in the reactors containing zeolite-coated carriers (Figure 4.12), with the carrier biofilm samples containing average log *nirS* and log *nosZ* gene copies of 8.93±0.66 and 8.79±0.58 per zeolite-coated carrier, respectively, compared to 8.78±0.34 and 8.62±0.26 per control carrier, respectively (Figure 4.12). On Day 25, *nirK, nirS,* and *nosZ* copies per mL in the liquid decreased in the zeolite-coated carrier reactors, likely from the lack of nitrite in the influent. A similar decrease was not observed in the carrier biofilm samples, suggesting, as with the anammox bacteria, that the denitrifying communities on the carriers were more stable. Again, as observed with the Amx genes, a similar decrease was not observed in the control carrier reactors.

Another group of nitrogen-cycling bacteria that was analyzed in these reactors was the ammonium oxidizing bacteria, specifically, the *amoA* gene. Interestingly, even with no oxygen supplied to the reactors, the log *amoA* gene copies per mL in the bulk liquid of the zeolite-coated carrier reactors (5.24±0.29/mL) was significantly higher than that in the control reactors (4.83±0.37/mL) (P=0.009) (Figure 4.12). The carrier biofilm samples themselves did not have significantly different numbers of *amoA* gene copies per carrier (P=0.50), perhaps because of the lack of oxygen supply within the reactors. There was no significant difference in log 16S rRNA gene copies per mL or per carrier in either the bulk liquid or carrier biofilm samples between the

zeolite-coated carrier and control carrier reactors (P=0.9244 for the carrier biofilm samples and P=0.1810 for the bulk liquid samples).

Overall, Amx genes were in higher abundance in the carrier biofilm samples and bulk liquid samples in the zeolite-coated carrier reactors compared to the control reactors, with some denitrifying genes, *nirS* and *nosZ*, also in greater abundance in these samples (Figure 4.12). The bulk liquid in the reactors containing zeolite-coated carriers also had higher numbers of *amoA* genes compared to the liquid in the control reactors. This indicates that the presence of the zeolite coating on these novel carriers did attract a unique microbial community, not only on the carrier surface, but also within the reactor bulk liquid. This provides evidence that the combination of zeolite-facilitated abiotic ammonium sorption with the apparent zeolite-enhanced retention/enrichment of N-cycling bacteria improves total nitrogen removal under appropriate operating conditions (Figure 4.10).

Aerated carrier flow-through reactors. To determine whether operating the system with active aeration would encourage more substantial colonization of AOB in the reactors containing zeolite-coated carriers, the experiment was repeated with no added nitrite in the influent and with active aeration within each reactor. DO levels were high in the bulk reactor liquid throughout the experiment, with 95.1±6.5% and 89.9±20.0% of DO saturation measured in the zeolite-coated carrier and control carrier reactors, respectively. Over the course of the 30-day experiment, the reactors containing zeolite-coated carriers again removed significantly more ammonium and TN, and therefore had much lower effluent ammonium (2.1±1.9 mg-N/L) and TN (6.5±3.6 mg-N/L) concentrations compared to control reactors (9.1±3.7 mg-N/L and 12.7±3.7 mg-N/L for ammonium and TN, respectively) (P<0.0001 for ammonium and P=0.0012 for TN) (Figure 4.12). As with the previous experiment, effluent nitrite and nitrate concentrations were low and very similar in the two types of reactors (P=0.85 and P=0.83 for nitrite and nitrate respectively), which

suggests that either ammonium sorption or ammonium sorption, oxidation, and rapid denitrification on the carrier surface was occurring in the zeolite-coated carrier reactors (Figure 4.13). Log *amoA* copies were 5.55±0.24/mL and 5.41±0.15 per carrier in the reactor samples containing zeolite-coated carriers and 5.20±0.40/mL and 4.79±0.67 per carrier in the control reactor samples (Figure 4.14). As with the CFTR experiments, the log *amoA* copies per mL or per carrier were only higher in the bulk liquid of the zeolite-coated carrier reactors, and at only a 90% confidence interval, and not within the biofilm on the carriers (P=0.065 and P=0.132 for the liquid and carrier samples, respectively) (Figure 4.14), which suggests that ammonium oxidation was occurring in the bulk liquid, but was not significantly enhanced on the surface of the zeolite-coated carriers.

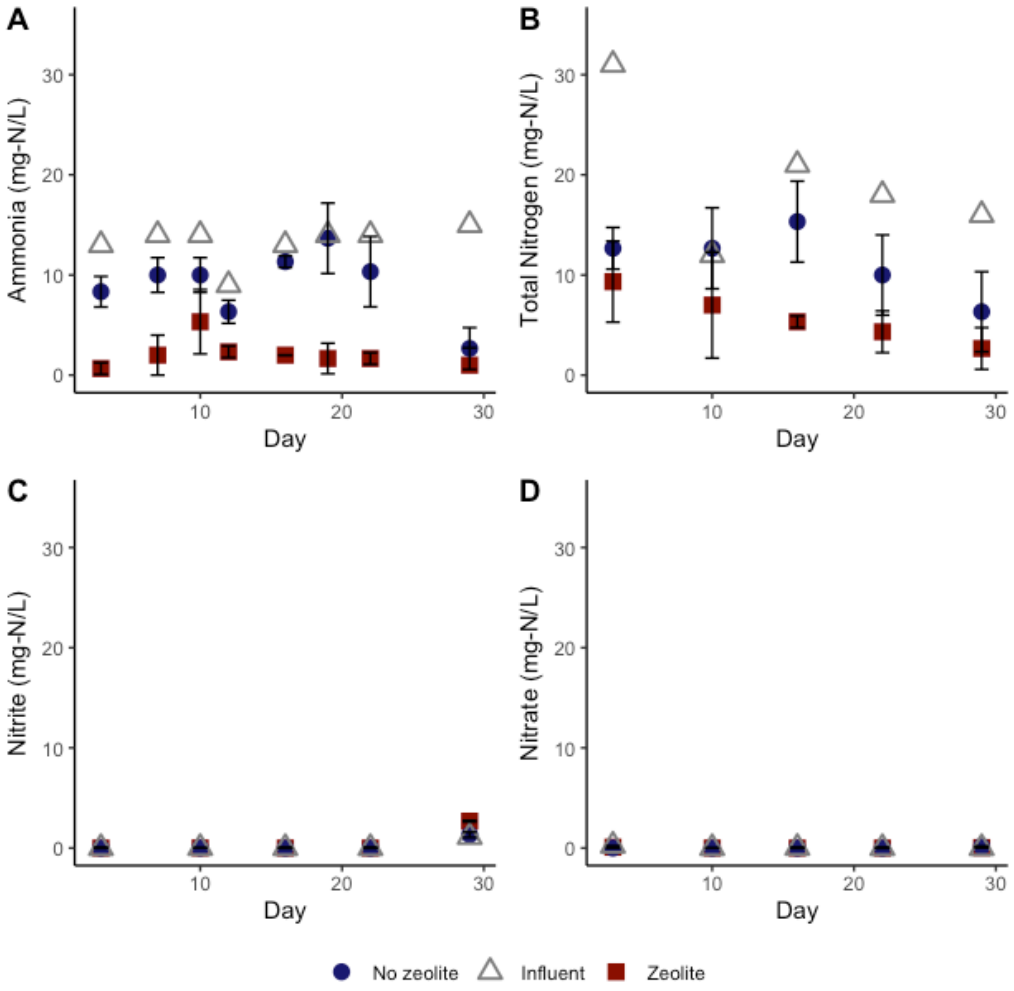

Figure 4.13. Influent and effluent concentrations of A) Ammonium, B) TN, C) Nitrite, and D) Nitrate in the ACFTR experiment. Error bars indicate the standard deviation of triplicate reactors.

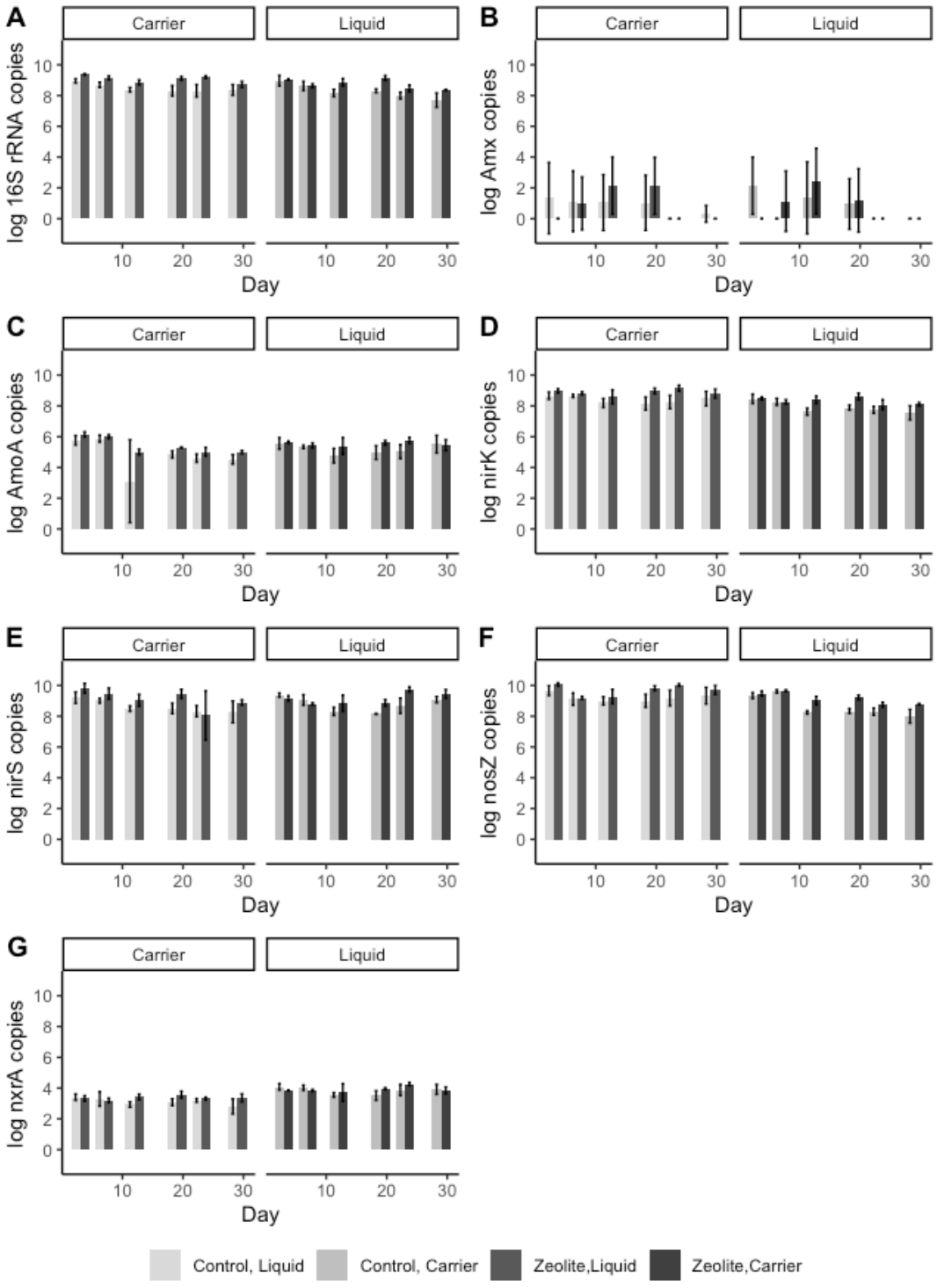

Figure 4.14. qPCR results from the ACFTR experiment for the A) 16S rRNA, B) Amx, C) *amoA*, D) *nirK,* E) *nirS, and* F) *nosZ*, and G) *nxrA* genes, showing the log number copies per carrier for the carrier biofilm samples and the log number copies

per mL for the reactor liquid from ACFTR. Light grey indicates samples from control carrier rectors and dark grey indicates samples collected from zeolite-coated carrier reactors. Error bars show the standard deviation of the reactors run in triplicate.

Unexpectedly, 16S rRNA gene copies per carrier were significantly higher in the carrier biofilm and were also higher at the 90% confidence interval in the reactor bulk liquid in samples taken from the reactors containing zeolite-coated carriers compared to samples taken from control reactors (P=0.0087 and P=0.065 and for carrier biofilm and reactor liquid samples, respectively) (Figure 4.14). In addition, the zeolite-coated carriers had higher quantities of *nirK* (P=0.009), *nosZ* (P=0.026), and *nxrA* (P=0.0411) per carrier than the control carriers (Figure 4.14). In the liquid samples, only *nirK* was in higher quantities per mL, and only at a 90% confidence interval, in the zeolite-coated carrier reactors compared to the control reactors (P=0.065). Consistent with these higher biomass numbers, effluent DOC was significantly lower (P<0.0001) in the zeolite-coated carrier reactors (18.1±13.0 mg/L) compared to that in the control carrier reactors (40.6±14.3 mg/L) (Figure 4.15).

The higher DOC and HRT of 17 hours might not have facilitated substantial autotrophic ammonium oxidation (Figure 4.13) in this experiment but did appear to lead to abundant heterotrophic growth. Indeed, the zeolite-coated carriers did accumulate greater quantities of bacteria when compared to the control carriers, and this community included denitrifiers and nitrite oxidizing bacteria. More research is needed to understand exactly how best to use the zeolite-coated carriers under aerated conditions to enhance the enrichment, retention, and activity of AOB, nitrite oxidizing bacteria, and denitrifiers to enhance shortcut nitrogen removal under highly aerobic conditions that are less amenable to anammox activity. Nevertheless, these zeolite-coated carriers appear to be promising for deployment in both anaerobic and aerated environments.

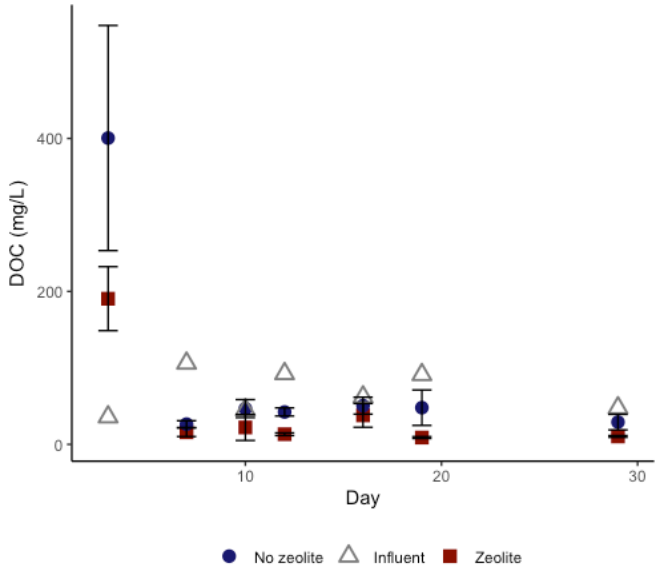

Figure 4.15. Influent and effluent DOC concentrations in the ACFTR experiment. Error bars indicate standard deviation of triplicate experiments.

Membrane flow-through bioreactors. The zeolite-coated hollow fiber membranes offer another material that shows promise with respect to its ability to sorb ammonium and retain anammox bacteria (Chapter 3).[18] The ability of these materials to enrich and retain anammox bacteria as well as AOB under a variety of operating conditions, however, is important for understanding how best to deploy and utilize these fibers for enhancing shortcut nitrogen removal in mainstream wastewater treatment. These experiments were not designed to achieve substantial nitrogen removal, with an HRT=bulk SRT of 23 hr and a single membrane serving as the only mechanism for aerating the reactor, but rather, to determine whether differential microbial growth, particularly of AOB, could occur on the membrane surface because of the membrane's ability to both sorb ammonium and transfer oxygen. Nitrogen removal results from the final day of each experiment (Figure 4.16) suggest that there is perhaps some nitrification occurring, although neither the nitrite nor the nitrate effluent concentrations correlate with experiment length or

membrane lumen oxygen concentration. Additionally, there was no difference in performance between the reactors containing zeolite-coated versus plain alumina membranes. In a full-scale application, a much larger quantity of membrane surface area would need to be added to stimulate substantial ammonium oxidation.

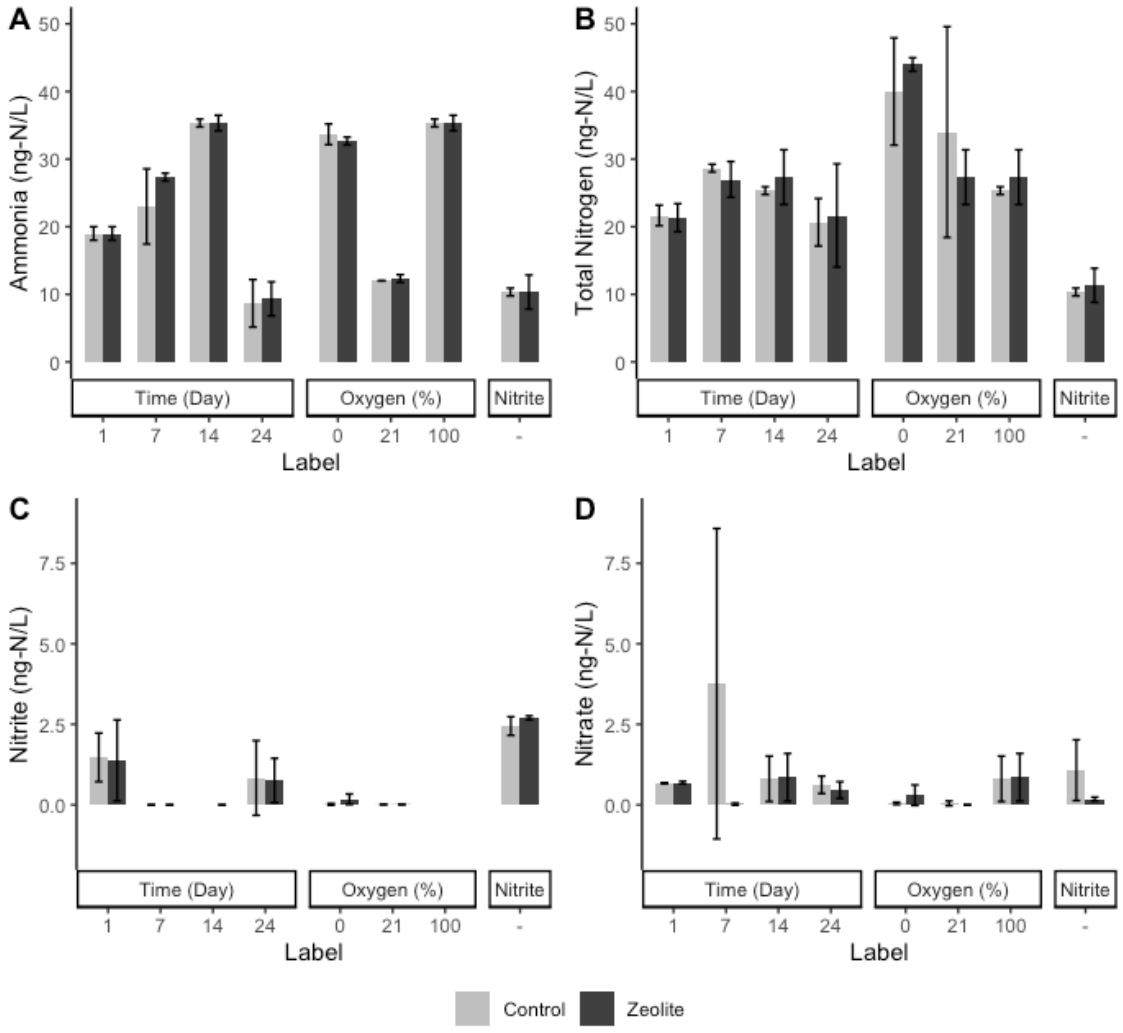

Figure 4.16. Effluent concentrations of A) Ammonium, B) TN, C) Nitrite, and D) Nitrate at the end of each of the MFTR experiments. Labels at the bottom of each panel indicate the experiment performed. "Time (days)" indicates experiments operated for different durations of time, "Oxygen (%)" indicates the oxygen concentration supplied to the membrane lumen, and "Nitrite" indicates the experiment in which nitrite

was added to the influent. The data from the 14 day and 100% oxygen experiments are the same. Light grey indicates samples from control membranes and dark grey indicates samples collected from zeolite-coated membranes. Error bars show the standard deviation of the reactors run in triplicate.

With respect to biomass growth on the membrane surface, the results are varied, with the zeolite-coated membranes only having higher quantities of total bacteria (16S rRNA gene copies per membrane) in one experiment, the 1-week experiment (P=0.044), and only having higher quantities of *amoA* copies at the 90% confidence interval (P=0.056) in the two-week, 100% oxygen experiment (Figure 4.17). The quantities of anammox bacteria generally increased in both the plain alumina membrane reactors and in the zeolite-coated membrane reactors with operation time (Figure 4.17). As observed previously (Chapter 3),[18] anammox bacteria were generally retained/enriched on the zeolite-coated membranes, with higher quantities measured in the 1-day experiment (P=0.09195) and significantly higher quantities measured in the two-week experiment (P=0.02704), as well as in the two-week experiment to which nitrite was added (P=0.04128). As observed with the carrier experiments, the zeolite coating only retained anammox bacteria and did not preferentially retain AOB.

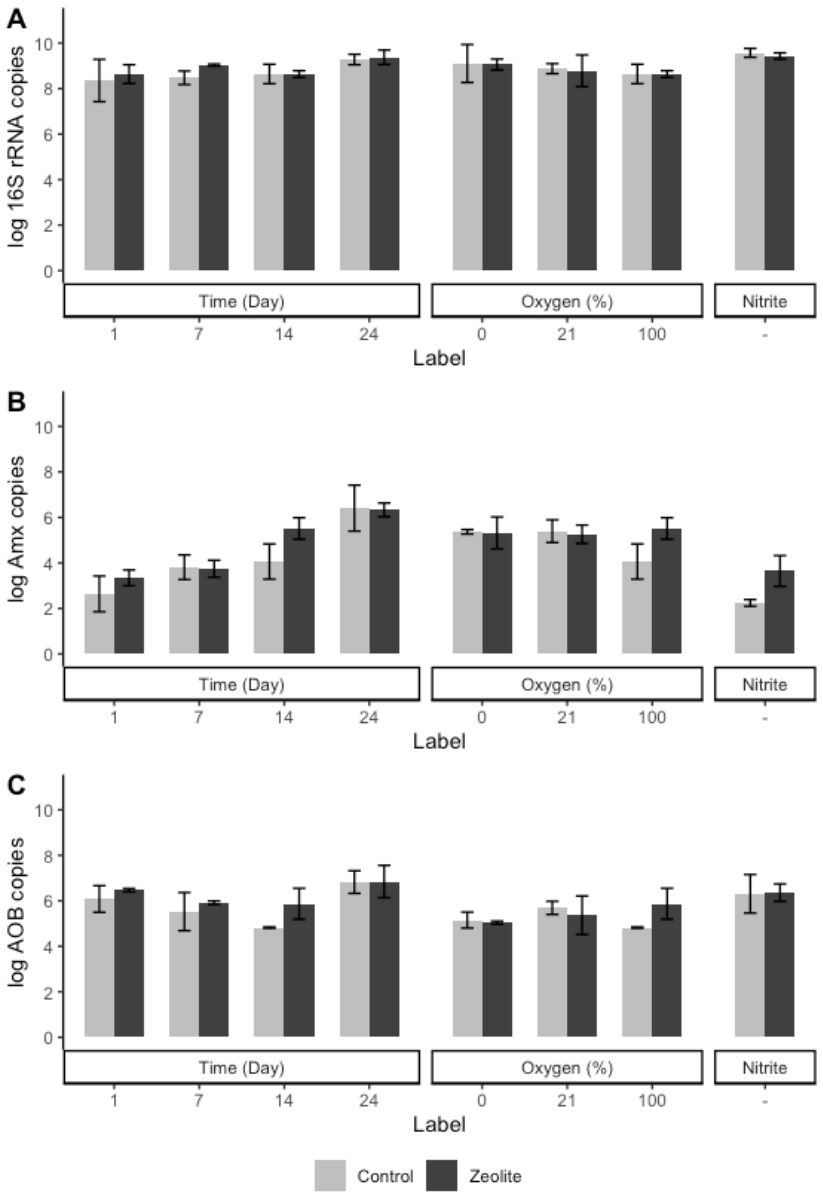

Figure 4.17. qPCR results from the MFTR experiments for the A) 16S rRNA, B) Amx, and C) *amoA* genes, showing the log number copies per membrane. Experiments included varied operation time, varied membrane lumen oxygen concentrations, and an experiment to which nitrite was added in the influent. Light grey indicates samples from control membranes (plain alumina hollow fibers) and dark grey indicates samples from zeolite-coated membranes (alumina hollow fiber core with zeolite coating). The data from the 14-day experiment and the 100% oxygen experiment are the

same but are shown twice for comparison to other experiments. Error bars show the standard deviation of triplicate experimental replicates.

Implications for the use of biofilm supports incorporating zeolite coatings. Under most of the conditions tested, anammox bacteria were retained/enriched at higher quantities on zeolite-coated surfaces compared to control surfaces. This was likely a result of the zeolite-coatings concentrating ammonium at their surface as the ammonium exchanged into the zeolite cages. Anammox bacteria were also retained to a greater degree and under more experimental conditions than AOB. Even though the half saturation constant (K_s) for anammox bacteria is low (0.07 g N/m^3)[7] compared to that for AOB (2.4 g N/m^3),[28] anammox bacteria seem to grow much more effectively on surfaces with high ammonium concentrations. A possible explanation for the different behavior of anammox bacteria and AOB is the strong tendency for anammox to grow in biofilms or granules.[29] Additionally, while the half saturation constant for AOB is slightly higher than that for anammox bacteria, it is still low, indicating AOB can function well in low ammonium environments. An unexpected finding from this work was the apparent preferential retention/enrichment of denitrifiers on zeolite-coated carriers under both aerated and anaerobic conditions. This indicates that these zeolite-coated carriers should facilitate a range of shortcut nitrogen processes, including the bypass of nitrate production and denitrification via the nitrite shunt, as long as PN could be encouraged. More work is needed to better understand why denitrifying communities are retained and under what conditions AOB can be enriched and retained on zeolite-coated surfaces.

Others have also investigated zeolite particles[16,30–32] and zeolite carriers[33] as a way to retain anammox bacteria in target environments and have reported results where similar to our study. When zeolite particles were added as media for a continuous-flow fixed bed biofilter, not only was an increase in the retention of anammox bacteria observed, but consistent, high rates of

nitrogen removal (95%) were achieved and maintained over the course of 570 days.[32] Another study added zeolite particles to sequencing batch reactors, and again, not only was anammox biomass retention improved, but the specific anammox activity in the system also increased.[16] A study using small spherical cages with zeolite particles inside as biofilm carriers also found increased retention of anammox bacteria compared to control carriers when operating a PNA system.[33] AOB were also successfully retained in this system, making up 19% of the total biomass in the carrier biofilm. In our work we were specifically trying to create surfaces that could be economically mass produced (*e.g.*, PE carriers) (Appendix A)[19] and also could be easily retained within a system that might otherwise allow zeolite particles to wash out. Nevertheless, the results of other researchers[16,30–33] are consistent with our findings and offer additional exciting possibilities for the application of zeolite-modified surfaces for enhanced nitrogen removal.

Potential applications for these biofilm support technologies are systems with low ammonium concentrations that would benefit from the localized concentration of ammonium and increased retention of anammox bacteria, such as mainstream wastewater treatment operated at low DO concentrations. The carbon amended in these experiments did not appear to negatively affect the selection and retention of anammox on zeolite surfaces, in fact, it appeared to facilitate greater growth of the overall carrier-supported biomass and the retention of denitrifiers. IFAS systems may be of particular interest for this type of zeolite-coated carrier, providing the recycling of solids, and therefore AOB, along with the carrier biofilm-based retention of anammox bacteria.[13] Such systems could be retrofitted into existing activated sludge processes, reducing the need to continuously bioaugment anammox sludge for full-scale mainstream anammox nitrogen removal, as well as improve start up times for anammox activity. It is possible that other applications where ammonium concentrations are low, such as in some treatment wetlands or stormwater systems, could also benefit from the use of zeolite-coated biofilm supports and the retention of

anammox and denitrifying bacteria.[1] These systems typically are anoxic,[34] indicating they would also be an ideal for application of this technology.

References

(1) Li, X.; Klaus, S.; Bott, C.; He, Z. Status, Challenges, and Perspectives of Mainstream Nitritation-Anammox for Wastewater Treatment. *Water Environ. Res.* **2018**, *90* (7), 634–649. https://doi.org/10.2175/106143017x15131012153112.

(2) Gu, J.; Zhang, M.; Liu, Y. A Review on Mainstream Deammonification of Municipal Wastewater: Novel Dual Step Process. *Bioresour. Technol.* **2020**, *299*, 122674. https://doi.org/10.1016/j.biortech.2019.122674.

(3) Mulder, A. The Quest for Sustainable Nitrogen Removal Technologies. *Water Sci. Technol.* **2003**, *48* (1), 67–75.

(4) Zhu, G.; Peng, Y. Biological Nitrogen Removal with Nitrification and Denitrification via Nitrite Pathway. *Harbin Gongye Daxue XuebaoJournal Harbin Inst. Technol.* **2008**, *40* (10), 1552–1557. https://doi.org/10.1007/s00253-006-0534-z.

(5) Delgado Vela, J.; Stadler, L. B.; Martin, K. J.; Raskin, L.; Bott, C. B.; Love, N. G. Prospects for Biological Nitrogen Removal from Anaerobic Effluents during Mainstream Wastewater Treatment. *Environ. Sci. Technol. Lett.* **2015**, *2* (9), 234–244. https://doi.org/10.1021/acs.estlett.5b00191.

(6) Metcalf and Eddy. *Wastewater Engineering Treatment and Reuse*; 1991.

(7) Strous, M.; Heijnen, J. J.; Kuenen, J. G.; Jetten, M. S. M. The Sequencing Batch Reactor as a Powerful Tool for the Study of Slowly Growing Anaerobic Ammonium-Oxidizing Microorganisms. *Appl. Microbiol. Biotechnol.* **1998**, *50* (5), 589–596. https://doi.org/10.1007/s002530051340.

(8) Jetten, M. S. M.; Cirpus, I.; Kartal, B.; van Niftrik, L.; van de Pas-Schoonen, K. T.; Sliekers, O.; Haaijer, S.; van der Star, W.; Schmid, M.; van de Vossenberg, J.; Schmidt, I.; Harhangi, H.; van Loosdrecht, M.; Gijs Kuenen, J.; Op den Camp, H.; Strous, M. 1994–2004: 10 Years of Research on the Anaerobic Oxidation of Ammonium. *Biochem. Soc. Trans.* **2005**, *33* (1), 119–123. https://doi.org/10.1042/BST0330119.

(9) Zhang, L.; Okabe, S. Ecological Niche Differentiation among Anammox Bacteria. *Water Res.* **2020**, *171*, 115468. https://doi.org/10.1016/j.watres.2020.115468.

(10) Kosgey, K.; Chandran, K.; Gokal, J.; Kiambi, S. L.; Bux, F.; Kumari, S. Critical Analysis of Biomass Retention Strategies in Mainstream and Sidestream ANAMMOX-Mediated Nitrogen Removal Systems. *Environ. Sci. Technol.* **2021**, *55* (1), 9–24. https://doi.org/10.1021/acs.est.0c00276.

(11) Vlaeminck, S. E.; Terada, A.; Smets, B. F.; De Clippeleir, H.; Schaubroeck, T.; Bolca, S.; Demeestere, L.; Mast, J.; Boon, N.; Carballa, M.; Verstraete, W. Aggregate Size and Architecture Determine Microbial Activity Balance for One-Stage Partial Nitritation and Anammox. *Appl. Environ. Microbiol.* **2010**, *76* (3), 900–909. https://doi.org/10.1128/AEM.02337-09.

(12) Pellicer-Nàcher, C.; Franck, S.; Gülay, A.; Ruscalleda, M.; Terada, A.; Al-Soud, W. A.; Hansen, M. A.; Sørensen, S. J.; Smets, B. F. Sequentially Aerated Membrane Biofilm Reactors for Autotrophic Nitrogen Removal: Microbial Community Composition and Dynamics. *Microb. Biotechnol.* **2014**, *7* (1), 32–43. https://doi.org/10.1111/1751-7915.12079.

(13) Zhang, L.; Liu, M.; Zhang, S.; Yang, Y.; Peng, Y. Integrated Fixed-Biofilm Activated Sludge Reactor as a Powerful Tool to Enrich Anammox Biofilm and Granular Sludge. **2015**. https://doi.org/10.1016/j.chemosphere.2015.02.001.
(14) Li, T.; Liu, J.; Bai, R. Membrane Aerated Biofilm Reactors: A Brief Current Review. *Recent Pat. Biotechnol.* **2008**, *2* (2), 88–93. https://doi.org/10.2174/187220808784619739.
(15) Wagner, B. M.; Daigger, G. T.; Love, N. G. Assessing Membrane Aerated Biofilm Reactor Configurations in Mainstream Anammox Applications. *Water Sci. Technol.* **2022**, wst2022013. https://doi.org/10.2166/wst.2022.013.
(16) Fernández, I.; Vázquez-Padín, J. R.; Mosquera-Corral, A.; Campos, J. L.; Méndez, R. Biofilm and Granular Systems to Improve Anammox Biomass Retention. *Biochem. Eng. J.* **2008**, *42* (3), 308–313. https://doi.org/10.1016/j.bej.2008.07.011.
(17) Egli, K.; Fanger, U.; Alvarez, P. J. J.; Siegrist, H.; van der Meer, J. R.; Zehnder, A. J. B. Enrichment and Characterization of an Anammox Bacterium from a Rotating Biological Contactor Treating Ammonium-Rich Leachate. *Arch. Microbiol.* **2001**, *175* (3), 198–207. https://doi.org/10.1007/s002030100255.
(18) Huff Chester, A. L.; Eum, K.; Tsapatsis, M.; Hillmyer, M. A.; Novak, P. J. Enhanced Nitrogen Removal and Anammox Bacteria Retention with Zeolite-Coated Membrane in Simulated Mainstream Wastewater. *Environ. Sci. Technol. Lett.* **2021**, *8* (6), 468–473. https://doi.org/10.1021/acs.estlett.1c00154.
(19) Feinberg, E. C.; Chester, A. L. H.; Novak, P. J.; Hillmyer, M. A. Porous Polyethylene-Supported Zeolite Carriers for Improved Wastewater Deammonification. *ACS EST Eng.* **2021**, *1* (7), 1104–1112. https://doi.org/10.1021/ACSESTENGG.1C00077.
(20) Kulak, A.; Lee, Y.-J.; Park, Y. S.; Yoon, K. B. Orientation-Controlled Monolayer Assembly of Zeolite Crystals on Glass and Mica by Covalent Linkage of Surface-Bound Epoxide and Amine Groups. *Angew. Chem.* **2000**, *112* (5), 980–983. https://doi.org/10.1002/(SICI)1521-3757(20000303)112:5<980::AID-ANGE980>3.0.CO;2-5.
(21) Wuolo-Journey, K.; BinAhmed, S.; Linna, E.; Romero-Vargas Castrillón, S. Do Graphene Oxide Nanostructured Coatings Mitigate Bacterial Adhesion? *Environ. Sci. Nano* **2019**, *6* (9), 2863–2875. https://doi.org/10.1039/C9EN00499H.
(22) Peterson, K. N.; Tan, D. T.; Bezares-Cruz, J. C.; Novak, P. J. Estrone Biodegradation in Laboratory-Scale Systems Designed for Total Nitrogen Removal from Wastewater. *Environ. Sci. Water Res. Technol.* **2017**, *3* (6), 1051–1060. https://doi.org/10.1039/C7EW00164A.
(23) Ahmed, T.; Semmens, M. J. Use of Sealed End Hollow Fibers for Bubbleless Membrane Aeration: Experimental Studies. *J. Membr. Sci.* **1992**, *69* (1–2), 1–10. https://doi.org/10.1016/0376-7388(92)80162-D.
(24) Feinberg, E. C. *SEM Image of Porous Polyethylene-Supported Zeolite Carriers*; 2021.
(25) Lahav, O.; Green, M. Bioregenerated Ion-Exchange Process: The Effect of the Biofilm on the Ion-Exchange Capacity and Kinetics. **2000**.
(26) Martins, T. H.; Souza, T. S. O.; Foresti, E. Ammonium Removal from Landfill Leachate by Clinoptilolite Adsorption Followed by Bioregeneration. *J. Environ. Chem. Eng.* **2017**, *5* (1), 63–68. https://doi.org/10.1016/j.jece.2016.11.024.
(27) Lahav, O.; Green, M. Ammonium Removal from Primary and Secondary Effluents Using a Bioregenerated Ion - Exchange Process. *Water Sci. Technol.* **2000**, *42* (1–2), 179–185.
(28) Wiesmann, U. Biological Nitrogen Removal from Wastewater. In *Biotechnics/Wastewater*; Fiechter, A., Blanch, H. W., Bungay, H. R., Cooney, Ch. L., Demain, A. L., Enfors, S.-O., Eriksson, K.-E. L., Kieslich, K., Klibanov, A. M., Lafferty, R. M., Mattiasson, B., Primrose, S. B., Rehm, H. J., Rogers, P. L., Sahm, H., Schügerl, K., von Stockar, U., Tsao, G. T., Venkat, K., Wandrey, C., Series Eds.; Advances in

Biochemical Engineering/Biotechnology; Springer Berlin Heidelberg: Berlin, Heidelberg, 1994; Vol. 51, pp 113–154. https://doi.org/10.1007/BFb0008736.

(29) Wells, G. F.; Shi, Y.; Laureni, M.; Rosenthal, A.; Sziva, I.; Weissbrodt, D. G.; Joss, A.; Buergmann, H.; Johnson, D. R.; Morgenroth, E. Comparing the Resistance, Resilience, and Stability of Replicate Moving Bed Biofilm and Suspended Growth Combined Nitritation− Anammox Reactors. *Environ. Sci. Technol.* **2017**, *51*, 5108–5117. https://doi.org/10.1021/acs.est.6b05878.

(30) Pei, Y.; Wang, J.; Wang, Z.; Tian, B. Anammox Bacteria Community and Nitrogen Removal in a Strip-like Wetland in the Riparian Zone. *J. Environ. Sci. Health Part A* **2011**, *46* (7), 715–722. https://doi.org/10.1080/10934529.2011.571582.

(31) Collison, R. S.; Grismer, M. E. Nitrogen and Chemical Oxygen Demand Removal from Septic Tank Wastewater in Subsurface Flow Constructed Wetlands: Substrate (Cation Exchange Capacity) Effects. *Water Environ. Res.* **2014**, *86* (4), 314–323. https://doi.org/10.2175/106143013X13736496908627.

(32) Yapsakli, K.; Aktan, C. K.; Mertoglu, B. Anammox-Zeolite System Acting as Buffer to Achieve Stable Effluent Nitrogen Values. *Biodegradation* **2017**, *28* (1), 69–79. https://doi.org/10.1007/s10532-016-9778-1.

(33) Lv, Y.; Pan, J.; Huo, T.; Zhao, Y.; Liu, S. Enhanced Microbial Metabolism in One Stage Partial Nitritation-Anammox System Treating Low Strength Wastewater by Novel Composite Carrier. *Water Res.* **2019**, *163*, 114872. https://doi.org/10.1016/j.watres.2019.114872.

(34) Janke, B. D.; Finlay, J. C.; Taguchi, V. J.; Gulliver, J. S. Hydrologic Processes Regulate Nutrient Retention in Stormwater Detention Ponds. *Sci. Total Environ.* **2022**, *823*, 153722. https://doi.org/10.1016/j.scitotenv.2022.153722.

Chapter 5: Applications of zeolite-coated biofilm carriers: low concentration ammonium and PFAS removal

Introduction

Stormwater runoff from urban areas contains a variety of pollutants, including sediments, nutrients, hydrocarbons, metals, and contaminants of emerging concern (CECs); if not mitigated, these pollutants can reach surface water and impact the ecological health of the system.[1–4] Nutrients, such as nitrogen, are of increasing concern as they can cause eutrophication and loss of aquatic diversity.[5–8] A national study in 2004 found that the average concentrations of ammonia, combined nitrite and nitrate, and Total Kjeldahl Nitrogen (TKN) in stormwater were 0.44±1.4 mg/L, 0.60±0.97 mg/L, and 1.4 ±1.2 mg/L, respectively.[9] Although much lower than other sources of nitrogen pollution to the environment,[10,11] nitrogen species in stormwater can still have impacts on aquatic systems.[12,13] Stormwater also serves as a major source of PFAS, including PFOA and PFOS, in some surface water systems, which is cause for concern as these CECs are ubiquitous in the environment, and, although easily transported, do not degrade.[3,11,14,10]

As stated above, average nitrogen concentrations in stormwater are relatively low; nevertheless, they can increase with storm event size, rain intensity, first flush, land use type, and season, impacting the overall nitrogen loads from stormwater into surface water systems.[16–18] According to the National Stormwater Quality Database, freeways had the highest concentrations of ammonia runoff, at an average of 1.07±1.3 mg/L.[9] During peak flows, runoff from freeways has been reported to have ammonia concentrations as high as

12 mg/L and runoff from residential areas have had measured nitrite plus nitrate concentrations as high as 18 mg/L; stormwater from both freeways and residential areas have reported TKN concentrations as high as 36 mg/L.[9] Seasonal affects, such as snow melt and dry and wet seasons, can also cause spikes in nitrogen loading. For example, in Minnesota, winter and spring seasons had the highest runoff nitrogen concentrations, with average total nitrogen (TN) of 3.4 mg/L and combined nitrite and nitrate of 0.71 mg/L.[16] Other studies in the Southeast and Mid-Atlantic have also reported higher concentrations of ammonia in stormwater in the early wet season and during first flushes.[19]

The Clean Water Act requires all states to control urban stormwater discharge and reduce pollutant loading prior to entering receiving water bodies.[17,20] Examples of control measures include stormwater ponds, wetlands, swales, rain gardens, bioretention systems, and vegetated biofilters.[9,21] It is assumed that once nitrogen enters these stormwater control structures/systems, it will be biologically degraded to harmless N_2.[22] More recent studies are finding that long-term, stormwater control systems can actually export nitrogen, increasing nitrogen loading to receiving waters via incomplete denitrification, temporary nitrogen removal via plant uptake, and re-mineralization of biologically incorporated nitrogen by primary producers.[3,17,18] With climate change, increasing storm sizes and frequency are compounding this problem, leading to washout, nitrogen exports, and overall increases in urban stormwater nitrogen loading.[21]

Alternative anaerobic nitrogen removal processes are being explored to enhance nitrogen removal in stormwater systems.[5,22] Two such processes include anaerobic ammonium oxidation (anammox)[8,23] and anoxic ferric ammonium oxidation (feammox).[24,25] Anammox is the autotrophic, anaerobic conversion of ammonium to nitrogen gas, with nitrite as the electron acceptor (Eq. 1); this process is performed by anammox bacteria.[26] Anammox are slow growing[27] but have been found in many environments, including wetlands.[28,29] These bacteria partner with aerobic ammonium oxidizing bacteria (AOB), which produce nitrite from some of the ammonium, facilitating the anammox process (Eq. 2). The feammox process, performed by organisms such as *Acidimicrobiaceae* sp. strain A6 (A6), is also an autotrophic anaerobic process for ammonium oxidation, but instead of nitrite, Fe(III) (ferrihydrite) serves as the electron acceptor (Eq. 3).[30] Feammox bacteria were initially discovered in New Jersey riparian wetlands,[30] but since have been detected in wetlands and soils globally.[31,32] Of particular importance is the fact that one feammox strain, A6, has been found to reductively deflourinate PFOS and PFOA,[33,34] which could have substantial implications for treating PFOS and PFOA *in situ*.

(Eq. 1) $2NH_4^+ + 3O_2 \rightarrow 2NO_2^- + 4H^+ + 2H_2O$

(Eq. 2) $2NH_4^+ + 2NO_2^- \rightarrow 2N_2 + 2H_2O$

(Eq. 3) $3Fe_2O_3 \cdot 0.5H_2O + 10H^+ + NH_4^+ \rightarrow 6Fe^{2+} + 8.5H_2O + NO_2^-$

In this study, we tested zeolite-coated carriers in a stormwater application, both in the field and in the laboratory. This study focused on whether the zeolite carriers could remove ammonium quickly enough to be useful in a stormwater treatment context and whether anammox, AOB, and feammox bacteria could be retained by zeolite or zeolite-coated carriers in the field and/or the laboratory. Zeolite-coated and control carriers were studied, as well as carriers pre-seeded with anammox biomass and unseeded carriers. It

was hypothesized that the presence of zeolite on the carriers would quickly remove ammonium from low-strength waste streams and increase colonization of anammox bacteria, AOB, and feammox bacteria compared to control carriers. We also hypothesized that pre-seeded zeolite carriers would better retain anammox bacteria when deployed in the field and tested in reactor systems.

Materials and Methods

Zeolite coated biofilm support carriers. Zeolite-coated carriers made of porous, low density polyethylene were made as previously described (Appendix A).[35] Control carriers were also made as previously described (Appendix A).[35]

Chemicals, reactor influent media, and reactor inoculum. Ammonium chloride (Sigma Aldrich) was used for preparation of ammonium chloride solutions for carrier sorption testing. Additionally, ammonium chloride was supplemented into Mississippi River Water, which has been previously used as model stormwater[36] and served as the influent to the laboratory-scale reactors described below. River water was collected in carboys at the Saint Anthony Falls Laboratory, Minneapolis, Minnesota, and stored in the dark at 4°C until use. The final target ammonium concentration in the influent was 3 mg/L. Media was also prepared for feammox batch experiments, as previously described by Huang and Jaffé, 2018.[30] Ammonium concentrations for the feammox media were modified to reflect peak stormwater concentrations, at a target concentration of 7 mg/L. The pH was 8.6±0.4 for the model stormwater and 6.1±0.3 for the feammox medium.

Feammox reactors were immediately pH adjusted to 4 with H_3PO_4 (Sigma Aldrich, diluted to 10% with MilliQ) after fresh media was added.

Carriers, both control and zeolite-coated, were pre-seeded with biofilm containing anammox bacteria. Carriers were placed in mesh bags then submerged into an anammox enrichment deammonification (DEMON) reactor that had been operated for 6 years (described previously by Peterson et al.[37]). Pre-seeded carriers deployed in the field study were submerged in the DEMON reactor for 23 days and pre-seeded carriers used in laboratory-scale reactor experiments were submerged in the DEMON reactor for one week. Carriers, again, both control and zeolite-coated, were also submerged for one week in pond water collected on December 31, 2021 from Maryland stormwater pond, to pre-seed the carriers with pond bacteria prior to use in laboratory-scale reactor experiments. This stormwater pond was also used in the field deployment of the pre-seeded and unseeded control and zeolite-coated carriers, as described below. A6-containing enrichment cultures were provided by the Jaffé research group, Princeton University. Details of the culture have been previously described.[30]

Experimental set up and carrier deployment.

Carrier ammonium removal rate tests. Different quantities of zeolite-coated carriers (1, 3, 5, or 10) were placed in 20 mL of 3 mg-N/L ammonium chloride solution and mixed on a rotator. Samples were taken after 5, 10, 20 and 60 minutes and ammonium was measured by an ammonium probe (Orion) to determine the rate of ammonium removal by the zeolite-coated carriers. Each quantity of carrier was tested in triplicate.

Field deployment of carriers in full-scale stormwater treatment systems. Carriers, including zeolite-coated pre-seeded carriers (ZP carriers), zeolite-coated unseeded carriers (Z carriers), control pre-seeded carriers (CP carriers), and control unseeded carriers (C carriers) were deployed in two full-scale stormwater treatment systems: a stormwater pond and a raingarden. The two deployment locations selected were approximately 4 miles apart from one another (Figure 5.1). The raingarden was the South Pascal raingarden, located at the intersection of McKinley St. and Pascal St., St. Paul, Minnesota, and surrounded by with residential land use (Figure 5.2). The stormwater treatment pond was the Maryland stormwater pond at the intersection of Maryland Ave. and interstate highway I35E in St. Paul, Minnesota, surrounded by mixed land use (Figure 5.2). Locations of both sites are shown in Figure 5.1.

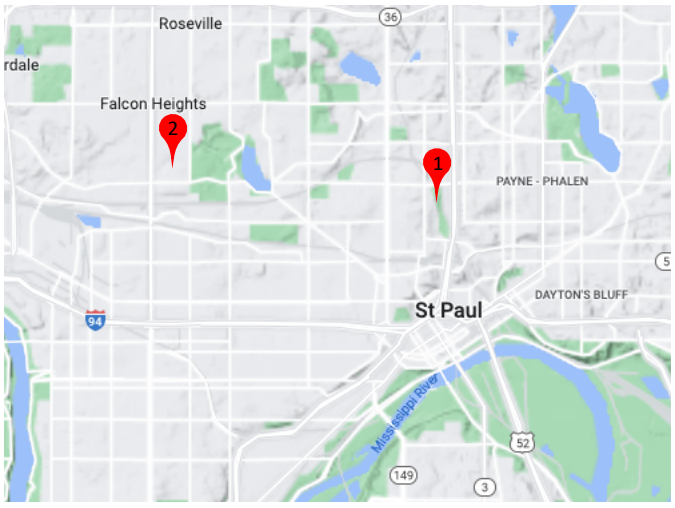

Figure 5.1. Locations of the stormwater systems in which the carriers were deployed. The number 1 indicates the Maryland stormwater pond and the number 2 indicates the South Pascal raingarden.

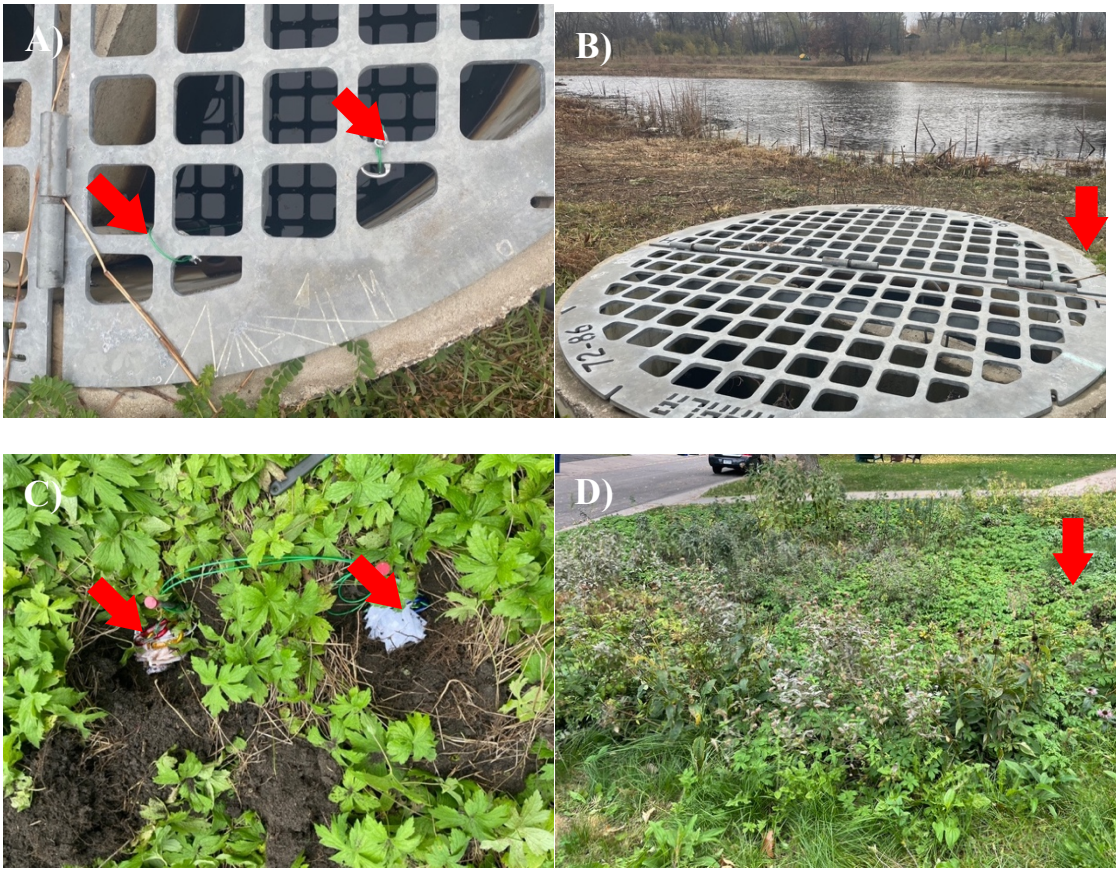

Figure 5.2. Images of the carrier installation field sites. A) Carrier installation at the outlet control box of the Maryland stormwater pond. B) Image of the Maryland stormwater pond. C) Installation of carriers at the South Pascal raingarden; carriers were covered with 4 inches of soil. D) Image of the South Pascal raingarden.

For both the stormwater pond and raingarden installation, all carriers were deployed in mesh bags for ease of retrieval with five carriers per bag. In the pond, mesh bags of carriers were suspended by a wire in the outlet structure, submerged on the pond side of the outlet structure weir. The average ammonium concentration for this pond, measured from storm events that occurred within the year prior to the experiment, was 0.112 mg/L,

with a peak concentration of 0.36 mg/L measured in the outlet structure.[38] The average TKN in the pond was 2.35 mg/L, with a maximum concentration of 3.5 mg/L.[38] Carriers deployed in the raingarden were buried in the soil, in their mesh bags, 4 inches below ground surface. Water temperature and discharge volume data for the Maryland Pond during the carrier deployment was available.[39] No data was available for the raingarden. Each time samples were collected, one bag of each carrier type (ZP, Z, CP, and C carriers) was collected at each site with the exception of the pre-seeded carriers that were collected every other time. Carriers were installed on September 30th, 2021 with final samples collected on December 16th, 2021. Once collected, samples were immediately taken back to the laboratory and frozen.

Flow-through stormwater reactor experiments. Laboratory-scale, flow-through reactors were designed and tested to monitor ammonium removal and the retention and/or enrichment of anammox bacteria and AOB at varying flow rates, designed to simulate storm events. Reactors were packed with 80 ZP or CP carriers or 80 Z or C carriers pre-seeded with pond water. The reactor configuration was identical to that shown previously (Figure 4.4, Chapter 4). Triplicate reactors were operated for experimental replication. Experiments were operated for 6 days and HRTs varied between batch operation with an HRT of up to 2 days to 10 minutes, to simulate a storm. Operation was as follows: 22 hours operated in batch mode, 47 hours operated with an HRT of 12 hours, 21 hours operated in batch mode, 6 hours operated with HRT of 30 minutes, 45 hours operated in batch mode, 3 hours operated in HRT of 10 minutes. The HRTs were selected to simulate rain events, based on the Minnesota Stormwater Manual guidelines[40] and other studies.[41]

The average influent ammonium concentration was 2.8±0.55 mg-N/L, amended into Mississippi River water, as described previously.[36] Effluent samples were collected and analyzed (see below) and carrier samples were harvested through a side port and analyzed (see below).

Feammox enrichment batch experiments. Two experiments were performed with triplicate reactors for each. In the first, reactors were amended with 2.0±0.001g particles of faujasite-type zeolite (Sigma Aldrich); in the second, reactors were amended with 105 zeolite-coated carriers as biofilm supports. Glass particles (Sigma Aldrich) and uncoated PE carriers were used as support media in control reactors for the first experiment and second experiment, respectively. Reactors consisted of 50-mL serum bottles containing 15 mL of feammox medium. The headspace (35 mL) was filled with 20% CO_2:80% N_2 gas. One third of the reactor volume was exchanged with fresh medium every 5 days for an HRT=SRT of 15 days. The average influent ammonium concentration was 7.7±3.2 mg-N/L for the particle experiment and 6.2 ±0.84 mg-N/L for the carrier experiment. Ammonium and pH were measured from the collected effluent (see below). Carriers were collected as biomass samples for further analysis.

Sample Analysis

Molecular methods. Single carriers were collected for DNA extractions. DNA extraction and quantitative polymerase chain reaction (qPCR) methods for 16S rRNA, 16S Amx (Amx), and *amoA* genes are described previously in Chapter 3. The qPCR primers and protocols for A6 were based on previous work by Ruiz-Urigüen et al.[34] Briefly, primer

set acm_v1F (5′-GGCGGCGTGCTTAACACAT-3’) and acm_v1R (5′-GAGCCCGTCCCAGAGTGATA-3) were used for quantification of A6. The thermal cycling (CFX Connect, Biorad) protocol was as follows: 3 min at 95ºC, followed by 40 cycles of 5 s at 95ºC, 30 s at 55ºC. qPCR reaction mixtures for all of the targets were prepared with ratios as described previously (Chapter 3).[42] Each qPCR assay was run with no-template negative controls and a standard curve made from a serial dilution of at least 5 different gene quantities.

Chemical analysis. Liquid samples for chemical analysis were immediately filtered (0.45 μm) after collection and were stored at 4ºC until analysis. An ammonium probe was used for ammonium measurement, a colorimetric ammonium assay was also used for ammonium measurement. Ion chromatography was used to quantify nitrate and nitrite. pH was measured with a pH probe. All chemical analysis methods are described previously in Chapter 3.[42]

Statistical Analysis.

Data for a single type of treatment (*e.g.*, CP carriers) was averaged across all time points throughout a given experiment for comparison to other treatments and Wilcoxon rank sum tests were used for statistical comparisons unless otherwise indicated. Student’s t test was only used for the feammox carrier experiment to compare data on specific days and is clearly indicated. Shapiro-Wilk test was used to confirm normality of the data before using Student’s t test. P-values less than 0.05 were considered significant.

Results and Discussion

Removal rate of ammonium by zeolite-coated carriers. Z Carriers were tested for the rate of ammonium sorption to determine if they would remove ammonium fast enough to be useful for stormwater applications. Ammonium concentrations over the 60-minute experiment with sorption to 1, 3, 5, and 10 carriers is shown in Figure 5.3. The reactors containing 10 carriers removed the ammonium quickly, with 63.5 ± 9.1% of the ammonium removed after only 5 minutes (Figure 5.3). The ammonium removed appeared to reach or begin to reach equilibrium after approximately 20 minutes (Figure 5.3). This indicated that with the amendment of enough zeolite-coated carriers, ammonium could be rapidly removed from stormwater. All of the experiments showed substantial removal of ammonium within 60 minutes, with 1 carrier removing 59 ± 6%, 3 carriers removing 83 ± 3%, 5 carriers removing 90 ± 3%, and 10 carriers removing 91 ± 3% of the ammonium added (Figure 5.3). Retention times in stormwater structures depend on the type of system, but systems such as outlet boxes and swales can be designed to have a minimum retention time of 9 minutes.[43] Retention times in stormwater ponds or retention basins are typically around 12 hours.[40]

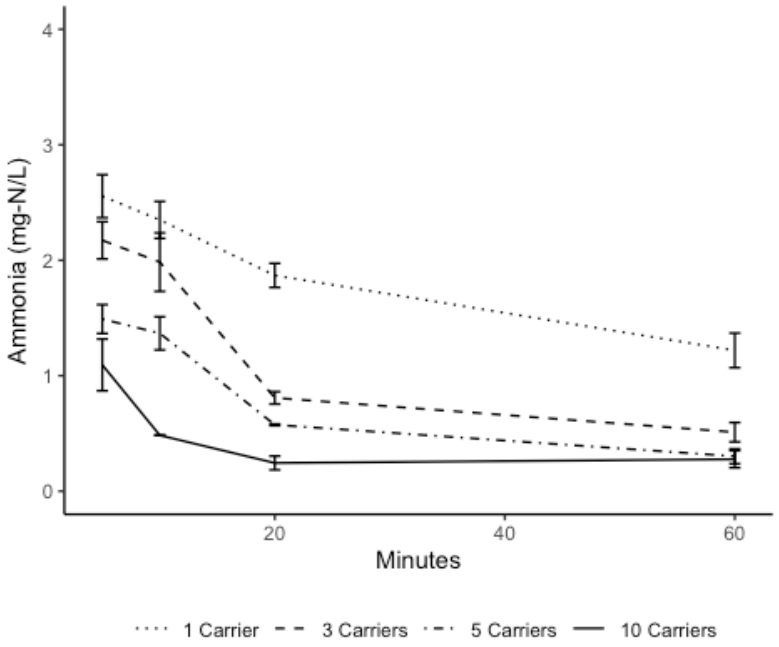

Figure 5.3. Rapid abiotic ammonium removal by 1, 3, 5, or 10 zeolite-coated carriers. Error bars indicate the standard deviation of triplicate experiments.

Field deployment of carriers in stormwater systems. The water temperature and discharge events in the Maryland stormwater pond were recorded by a monitoring station operated by CRWD from the date of carrier deployment (September 30) to November 1, when monitoring was stopped as a result of cold weather (Figure 5.4). A monitoring station was not located at the raingarden; therefore, no temperature or event data was available. Given the close proximity of the two sites, the temperature was assumed to be similar to that measured at the pond.

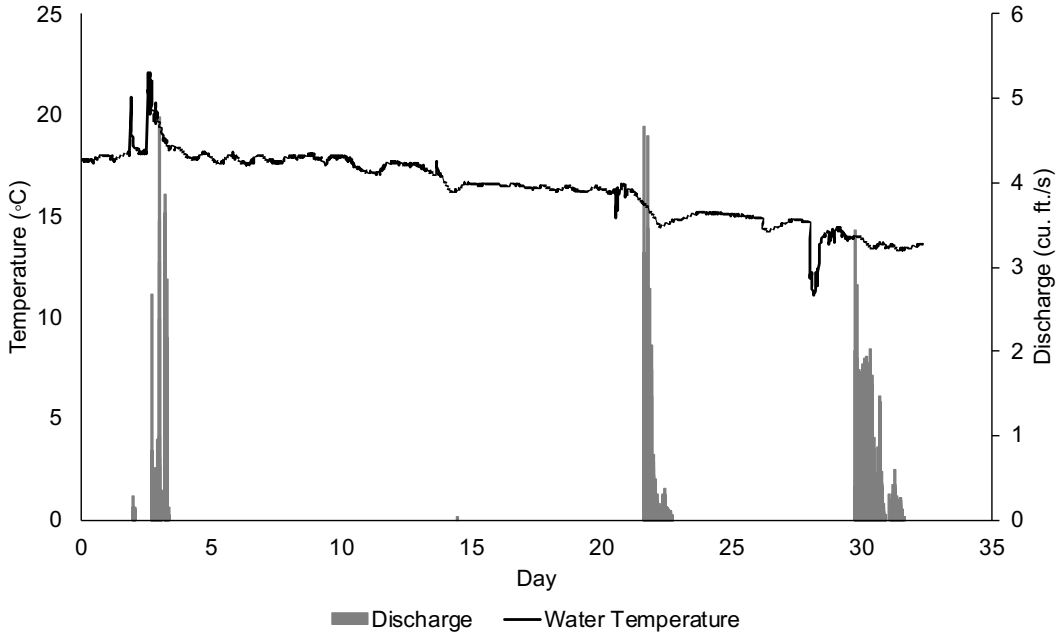

Figure 5.4. Temperature and discharge at the Maryland stormwater pond. Records were collected from the CRWD website from September 30 (date of deployment) to November 1.[39]

The average log 16S rRNA gene copy number for total bacteria (16S rRNA), 16S rRNA gene copy number for anammox bacteria (Amx), and *amoA* gene copy number extracted from carriers deployed in the raingarden and the stormwater pond are shown in Figures 5.5 and 5.6, respectively. Pre-seeding carriers had the intended benefit of increasing the anammox biomass in both the raingarden and pond systems compared to biofilms grown naturally (Figures 5.5 and 5.6). For carriers deployed in the raingarden, there were more Amx and *amoA* gene copies detected on pre-seeded carriers compared to unseeded carriers (Figure 5.5). The average log Amx copies/carrier on seeded carriers was 5.65±0.66 compared to 2.09±1.48 on the unseeded carriers ($P<0.0001$). The average log *amoA* copies/carrier was 6.18±0.51 on pre-seeded and 4.60±0.69 on unseeded carriers

(P<0.0001). A similar pattern was observed for the carriers deployed in the stormwater pond (Figure 5.6). Seeded carriers had more log Amx copies, at 5.22±0.88, and more log *amoA* copies/carrier, at 5.85±0.93, while unseeded carriers had 1.38±1.09 log Amx copies/carrier and 3.92±0.85 log *amoA* copies/carrier (P<0.0001 for both Amx and *amoA* genes). 16S rRNA copies followed a similar trend to that observed with the Amx and *amoA* genes, with more copies on the pre-seeded carriers in both systems (P<0.0001 for both the raingarden and pond). Because the results were averaged across time for each carrier type, this suggests that the pre-seeded carriers did retain the biofilm on the carriers for at least two and a half months, which is promising for the use of such pre-seeded carriers in the future.

With respect to carrier type, Z and ZP carriers did not always retain more of the target organisms when compared to the C and CP carriers. Z and ZP carriers retained more Amx and *amoA* gene copies when deployed in the raingarden, suggesting that the zeolite coating provided an advantage with respect to the enrichment and retention of these organisms (Figure 5.5). ZP carriers had 5.84±0.81 log Amx copies/carrier and 6.32±0.54 log *amoA* copies/carrier, while CP carriers had 5.47±0.42 log Amx copies/carrier and 6.05±0.54 log *amoA* copies/carrier (P=0.024 and P= 0.033, for Amx and *amoA,* respectively). The Z carriers deployed in the raingarden did have more *amoA* copies (4.74±0.63) than the C carriers (4.45 ±0.71) (P=0.01), but the number of Amx genes on both carriers was statistically equivalent (P=0.20). For the carriers deployed in the pond, there was not a significant difference between the number of Amx or *amoA* copies/carrier between the ZP and CP carriers (P=0.76 and P=0.34, for Amx and *amoA,* respectively).

With respect to the unseeded Z and C carriers, the number of log *amoA* copies on the C carriers (4.13±0.71) was statistically greater than that on the Z carriers (3.71±0.93) (P=0.041), whereas the number of Amx genes was statistically the same on both carriers (P=0.37) (Figure 5.6). C carriers had a larger number of log 16S copies than the Z carriers in both systems (P=0.0067 for the raingarden and P=0.0092 for the pond).

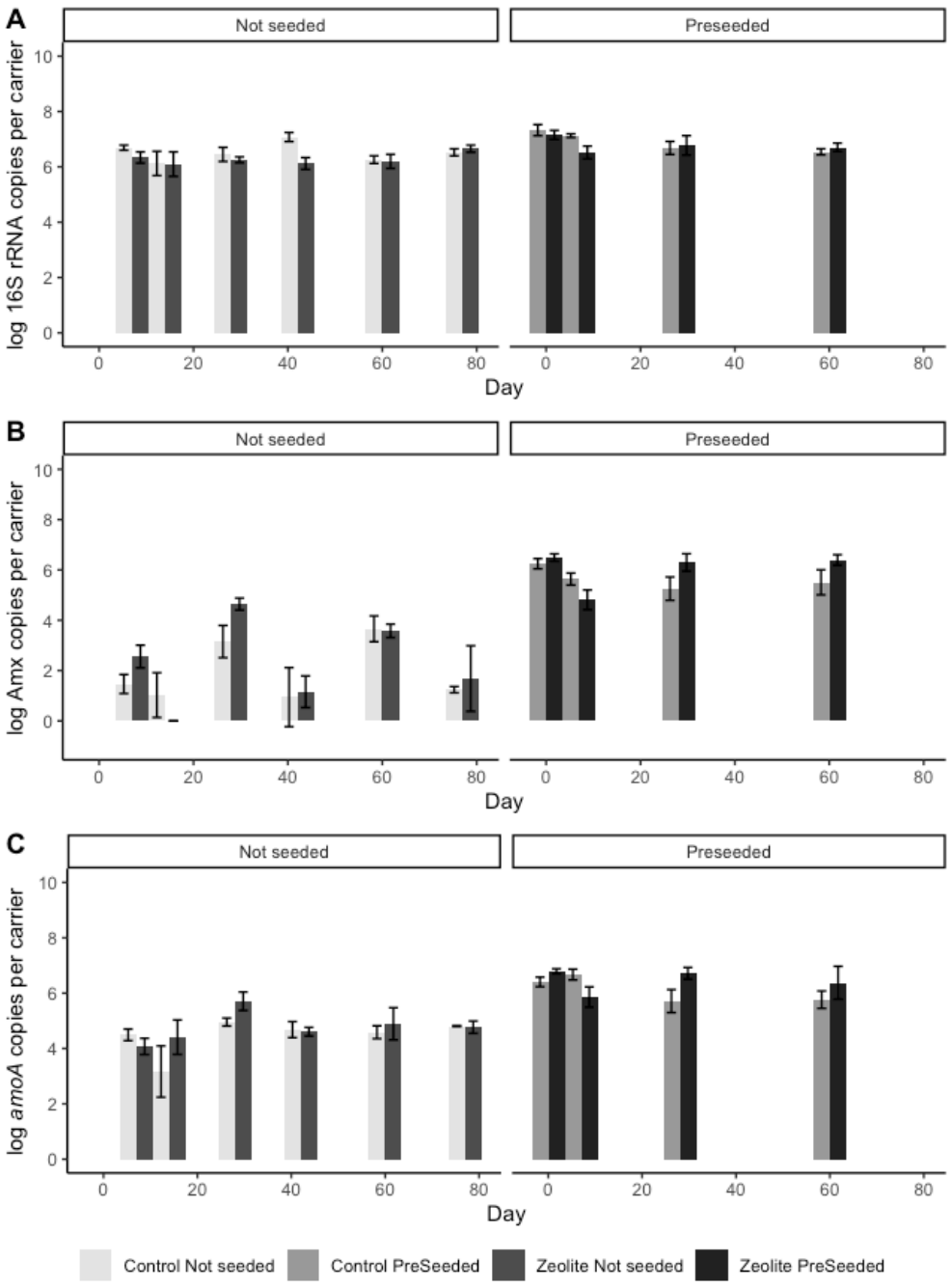

Figure 5.5. qPCR results from the carrier samples retrieved from the raingarden deployment. A) 16S rRNA B) Amx C) *amoA.* Error bars indicate standard deviation from five replicate samples. Pre-seeded samples on Day 0 indicate log copies present on the carriers immediately after harvesting from the DEMON reactor and before deployment in the field.

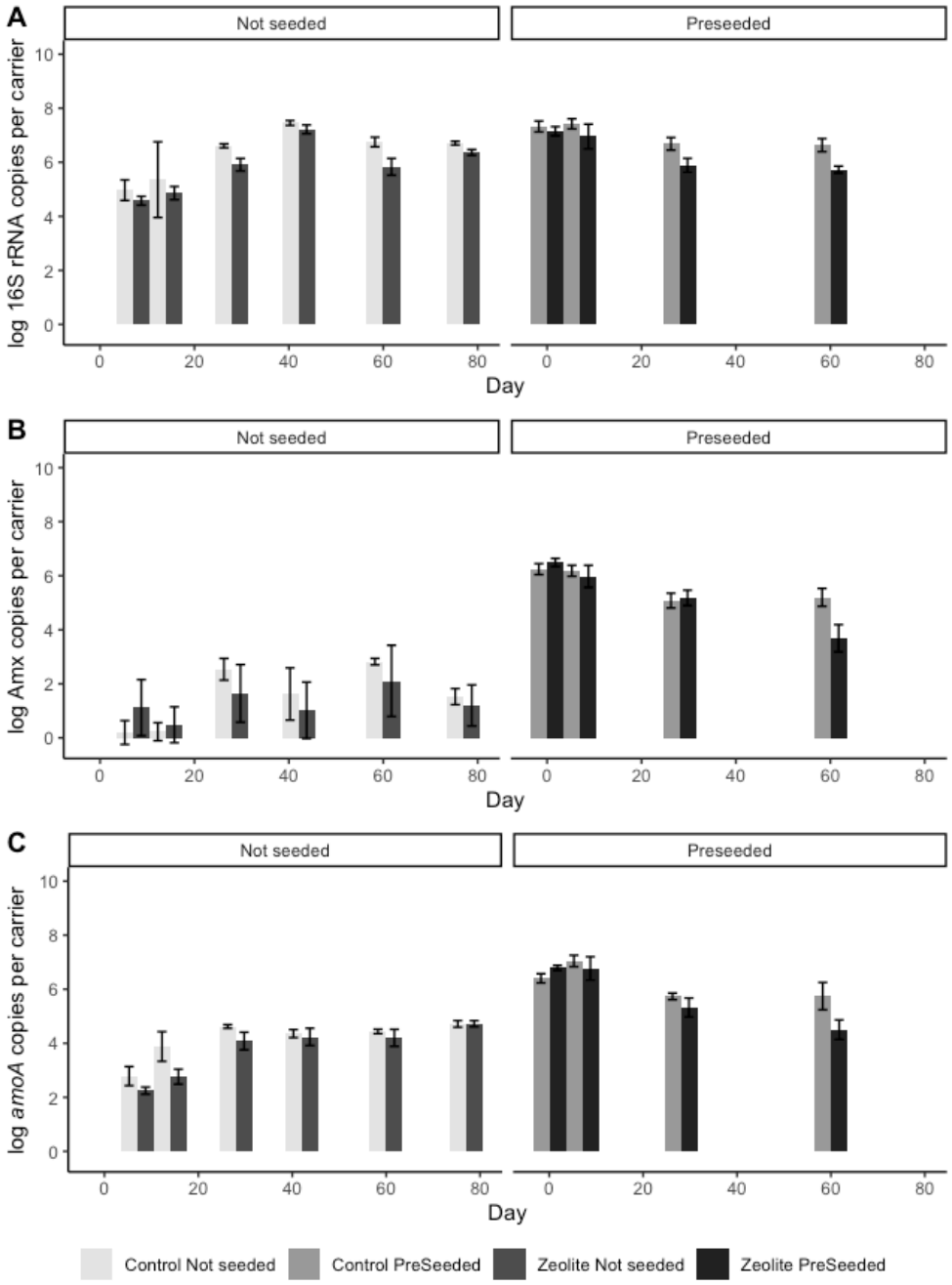

Figure 5.6. qPCR results of carrier samples from stormwater pond. A) 16S rRNA B) 16S Amx C) *amoA*. Error bars indicate standard deviation from five sample replicates. Pre-seeded samples on Day 0 indicate log copies immediately after harvesting from the DEMON reactor and before deployment in the field.

These finding indicate that pre-seeding in an anammox enrichment reactor prior to deployment will increase nitrogen cycling biomass, but that the carrier material may not matter as much. ZP carriers did retain more anammox bacteria and AOB in the raingarden system, but not the pond system. One explanation for this is that pond samples were constantly subjected to flowing water, making it more difficult to retain anammox bacteria and AOB, especially in cold conditions, while raingarden samples were able to better retain the pre-seeded biofilm in the soil. Another potential explanation is the availability of ammonium in the soil of the raingarden, providing more favorable conditions for anammox bacteria and AOB on the ZP carrier surface.[44] Overall, the number of gene quantities on the pre-seeded carriers did not dramatically fluctuate over time, indicating that the carriers were able to roughly maintain the biomass that had grown during the pre-seeding period, even when discharge events occurred (*e.g.*, around Days 3, 22, and 30) (Figure 5.4) and temperatures were cold. This is promising and suggests that more research under a wider variety of conditions may be warranted to further identify when and where such carriers should be deployed for the most effective nitrogen removal.

It was expected that the Z carriers would encourage the colonization of more nitrogen cycling microbes compared to the C carriers, but this was not consistently seen. Amx and *amoA* genes were detected on both the Z and C carriers deployed at the raingarden and pond sites, however. This indicated that anammox bacteria and AOB were present in both locations and were able to readily colonize the carriers, again, even under cold conditions that were likely unfavorable for growth (Figures 5.5 and 5.6). The presence of *amoA*

genes suggests that at least nitritation in these environments, notably in the anaerobic environment of the stormwater treatment pond, was possible. The biomass that colonized the unseeded carriers did appear to fluctuate over time, especially the numbers of Amx genes on the raingarden carriers. An unexpected observation was that the C carriers occasionally had increased numbers of total bacteria and AOB present on the carriers deployed in the pond. Further work is needed to determine why this occurred.

Lab-scale stormwater experiments. Ammonium removal and the log number of 16S rRNA, Amx, and *amoA* gene copies over time in reactors containing Z and C carriers incubated with the pond water are shown in Figure 5.7. The reactors containing Z carriers removed more ammonium throughout all stages of the experiment compared to the reactors containing C carriers, with average ammonium effluent concentrations of 0.84 ± 0.81 mg-N/L versus 1.96 ± 0.82 mg-N/L in the reactors containing the Z versus C carriers, respectively ($P<0.0001$). The effluent ammonium concentrations during each of the operational stages of varying HRT (12 hr, 30 min, 10 min) are summarized in Table 5.1, which again showed lower effluent ammonium concentrations in all stages in the reactors containing Z carriers versus those containing C carriers (See Table 5.1 for P-values). Although ammonium removal decreased in both sets of reactors when the HRT decreased to 30 min and 10 min, removal rebounded after the simulated storm event. It is unclear whether this removal was primarily abiotic sorption or whether some biological removal of ammonium also occurred. No nitrite was detected in the influent or effluent to the reactors over time, suggesting that if ammonium oxidation occurred, any nitrite produced was either further oxidized to nitrate or reduced to nitrogen gas. Nitrate was

detected in the reactor influent, at 1.31 ± 0.27 mg-N/L, decreasing in the effluent over the 12 hr HRT period and again after the 30 min HRT (Figure 5.8). This suggests that some denitrification was occurring in the reactors. Although it is difficult to determine whether anammox or ammonium oxidation was active on the carriers, based on previous observations of enhanced biological ammonium degradation under simulated mainstream wastewater conditions (Chapters 3 and 4), it is likely that given time and development of more robust biofilm on the carriers, the biological component of ammonium removal in actual or simulated stormwater treatment systems would increase.

With respect to the quantities of bacteria and nitrogen-cycling genes present on the carriers pre-seeded with pond water, the two different types of carriers, Z and C, performed similarly for most of the 6-day experiment (Figure 5.7), with no significant differences observed between the two carrier types for any of the genes. Only for the carrier samples taken after the 12 hr HRT period (at Experiment Hour 70) was there more *amoA* on the Z carriers than the C carriers (3.18±0.08 vs 2.49±0.16 log copy numbers) (P=0.0024). Despite the periodic increases in flow rate, the total number of bacteria (via 16S rRNA gene copy number) and AOB (via *amoA* gene copy number) were well retained on the carriers (Figure 5.7).

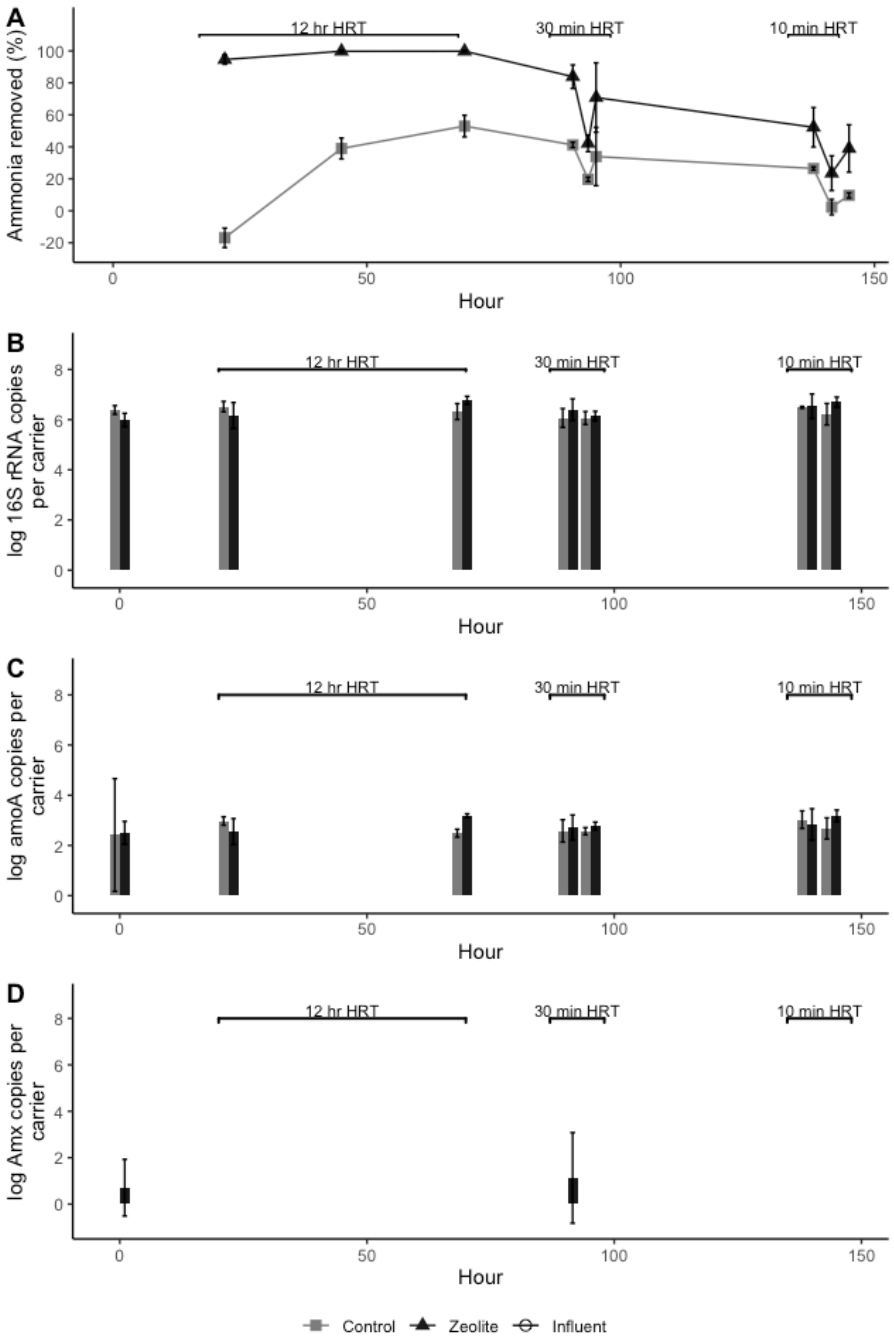

Figure 5.7. Ammonium removal and qPCR results for lab scale carrier reactors pre-seeded via incubation with the Maryland stormwater pond water. A) Ammonium removal [$(C_i-C_o)/C_i$], B) Log 16S rRNA copies per carrier, C) Log *amoA* copies per carrier, D) Log Amx copies per carrier. Error bars indicate the standard deviation from triplicate experimental replicates.

Table 5.1. Ammonium effluent concentrations in mg-N/L and removal (%) from stormwater carrier reactors seeded with pond water and with an anammox enrichment culture from a DEMON reactor over operational periods with different HRTs. Average values ± the standard deviation from triplicate experimental replicates is shown.

	Ammonium effluent (mg-N/L)			**Ammonium Removal (%)**	
	Zeolite-coated carrier reactors	Control carrier reactors	P-values	Zeolite-coated carrier reactors	Control carrier reactors
	Reactors pre-seeded with pond water				
12 hr HRT	0.054 ± 0.085	1.99 ± 1.09	0.0004	98 ± 3	25 ± 32
30 min HRT	0.74 ± 0.50	1.44 ± 0.37	0.013	61 ± 27	26 ± 20
10 min HRT	1.73± 0.51	2.56 ± 0.50	0.016	38 ± 17	13 ± 11
	Reactors pre-seeded with anammox culture				
12 hr HRT	0.72 ± 1.05	0.98 ± 1.31	0.51	78 ± 32	70 ± 35
30 min HRT	1.80 ± 0.44	2.11 ± 0.38	0.58	41 ± 15	31 ± 13
10 min HRT	2.0 ± 0.45	2.14 ± 0.45	0.63	26 ± 17	21 ± 17

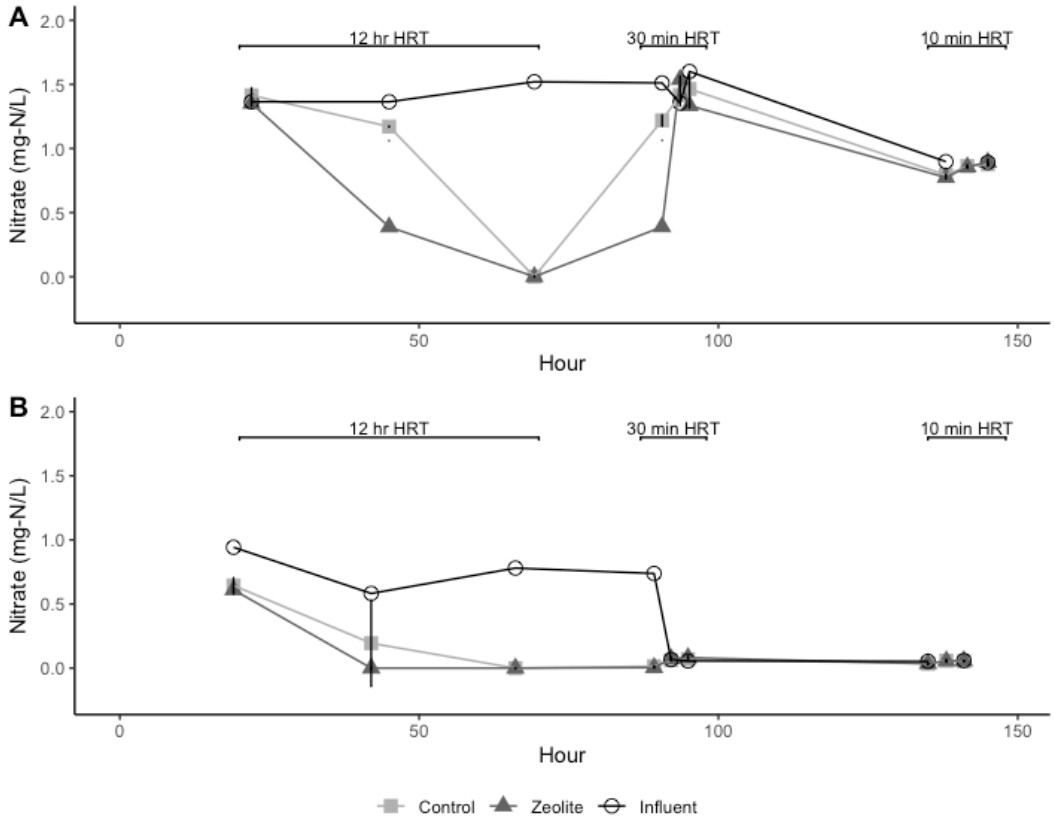

Figure 5.8. Nitrate influent and effluent concentration in the laboratory-scale carrier reactors. A) Z and C carriers pre-seeded with pond water, B) ZP and CP carriers pre-seeded in anammox enrichment reactor. Error bars represent the standard deviation from triplicate experimental replicates.

Reactors containing ZP and CP carriers (again, carriers seeded in the anammox enrichment reactor) performed differently than those containing Z and C carriers seeded with pond water, in that they removed similar quantities of ammonium, with statistically similar effluent concentrations (P=0.14) (Figure 5.9). Similarly, the effluent ammonium concentrations during each of the operational stages (HRT of 12 hr, 30 min, or 10 min) were not significantly different between the reactors containing the two different types of carriers (Table 5.1). This suggests that when pre-seeded, the carrier type did not

significantly influence ammonium removal at these short HRTs. This differs from what one might expect based on previous research that showed that zeolite was still capable of exchanging ammonium when covered by biofilm (Chapter 4). Nevertheless, those results were obtained under equilibrium conditions and not under conditions that were dominated by sorption kinetics (Chapter 4). As with the Z and C carrier-containing reactors, no nitrite was detected in the influent or the effluent, however nitrate was detected in the influent to the reactors at 0.47±0.40 mg-N/L. Nitrate concentrations decreased in the effluent of both the Z and C carrier reactors (Figure 5.8), again indicating that some denitrification was occurring in the reactors.

With respect to the quantities of bacteria and nitrogen-cycling genes present, the two different types of carriers, ZP and CP, performed relatively similarly for the 7-day experiment (Figure 5.9), with the log number of 16S gene copies higher on the ZP carriers than on the CP carriers (P=0.003), but Amx and *amoA* copes statistically the same between the two (P=0.44 and P=0.23). As with the experiment containing the Z and C carriers pre-seeded with pond water, the total number of bacteria, anammox bacteria, and AOB were all well-retained on the carriers over the course of the 7-day experiment, with only a slight drop in the *amoA* and 16S rRNA copy numbers after the 30 minute HRT operating period (Figure 5.9).

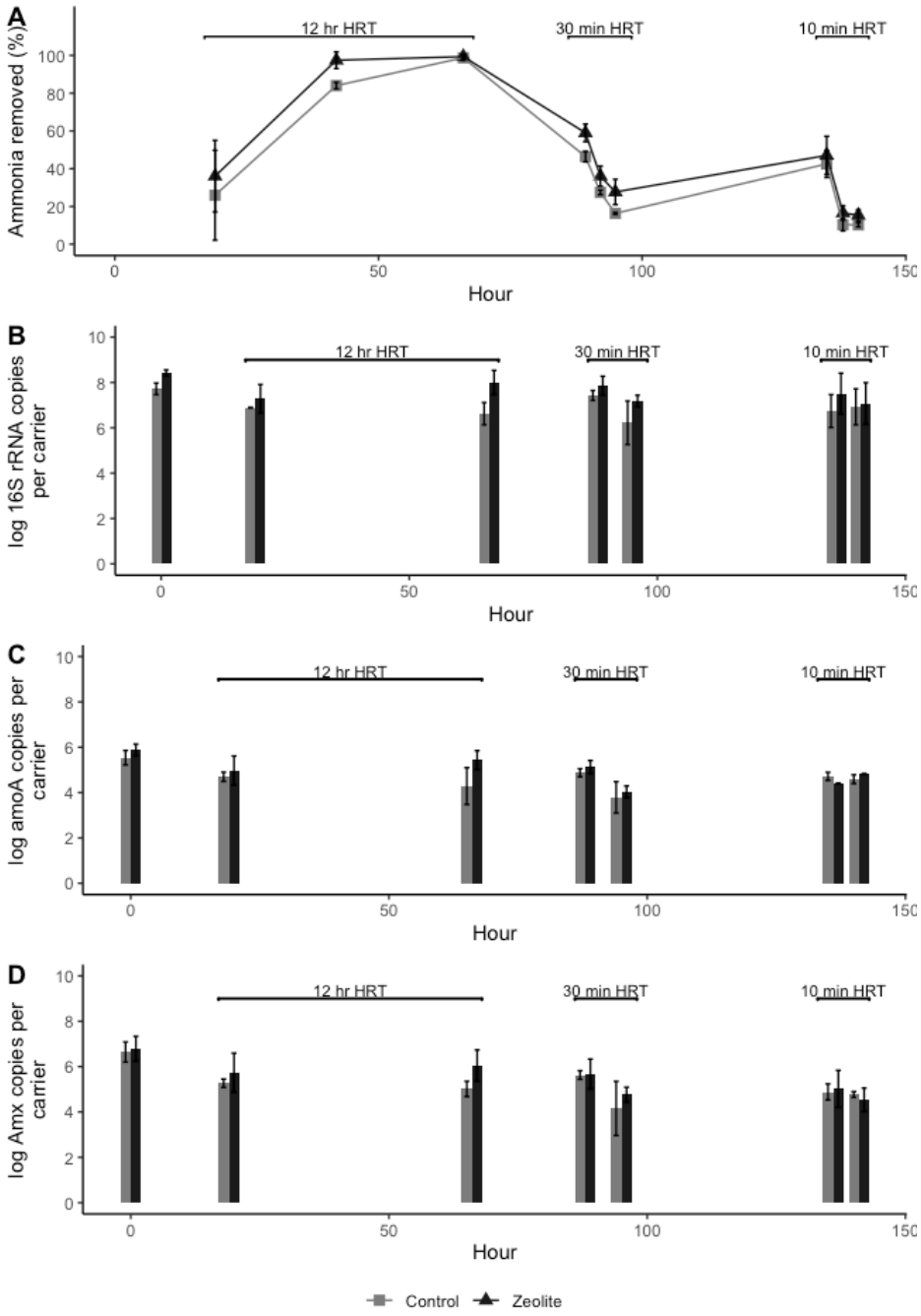

Figure 5.9. Ammonium removal and qPCR results for the laboratory-scale reactors containing carriers pre-seeded in the DEMON reactor. A) Ammonium removal [$(C_i-C_o)/C_i$], B) Log 16S rRNA copies per carrier, C) Log *amoA* copies per carrier, D) Log Amx copies per carrier. Error bars indicate the standard deviation of triplicate experimental replicates.

Feammox enrichment batch experiment. Feammox enrichment experiments were operated using both zeolite particles and the recently developed Z carriers.[42] Influent ammonium concentrations in these experiments ranged from 3 to 11 mg-N/L, simulating peak stormwater ammonium conditions.[9] Figure 5.10 shows the effluent ammonium concentrations, pH values, and the qPCR results for the 16S rRNA gene and the A6 16S rRNA gene for the experiments amended with zeolite particles. Effluent ammonium concentrations for the 55-day experiment remained very low in the zeolite reactors (3.8 ± 1.3 mg-N/L) compared to the control reactors (6.9 ±2.6 mg-N/L) (P=0.0004). While ammonium removal is typically an indication of feammox activity, one cannot distinguish between abiotic ammonium sorption and microbial ammonium oxidation in this case. Nevertheless, the increased pH of 7.48 ± 0.28 in the zeolite particle reactors (adjusted to a pH of 4 every 2.5 days) was an indication of feammox activity, as these organisms actively consume H^+ (Eq. 3).[34] Control reactors maintained an average pH of 3.58 ± 0.41 (P<0.0001), suggesting that feammox activity was not as significant in those reactors.

As hypothesized and expected based on the increase in pH, A6 was enriched in reactors containing zeolite particles, with an average of 2.21±0.44 log A6 16S rRNA copies compared to only 0.53±0.86 log copies in the control reactors containing glass particles (P<0.0001). Total bacteria also increased in the reactors containing zeolite particles, with 7.17 ±0.96 log 16S rRNA copies present compared to only 5.57 ±1.6 log 16S rRNA

copies present in the control reactors (P=0.0001). These results show the great benefits of zeolite for retaining the PFAS-degrading feammox bacterium A6, and strongly suggest that the zeolite-coated carriers should also be able to enrich and retain these important feammox bacteria.

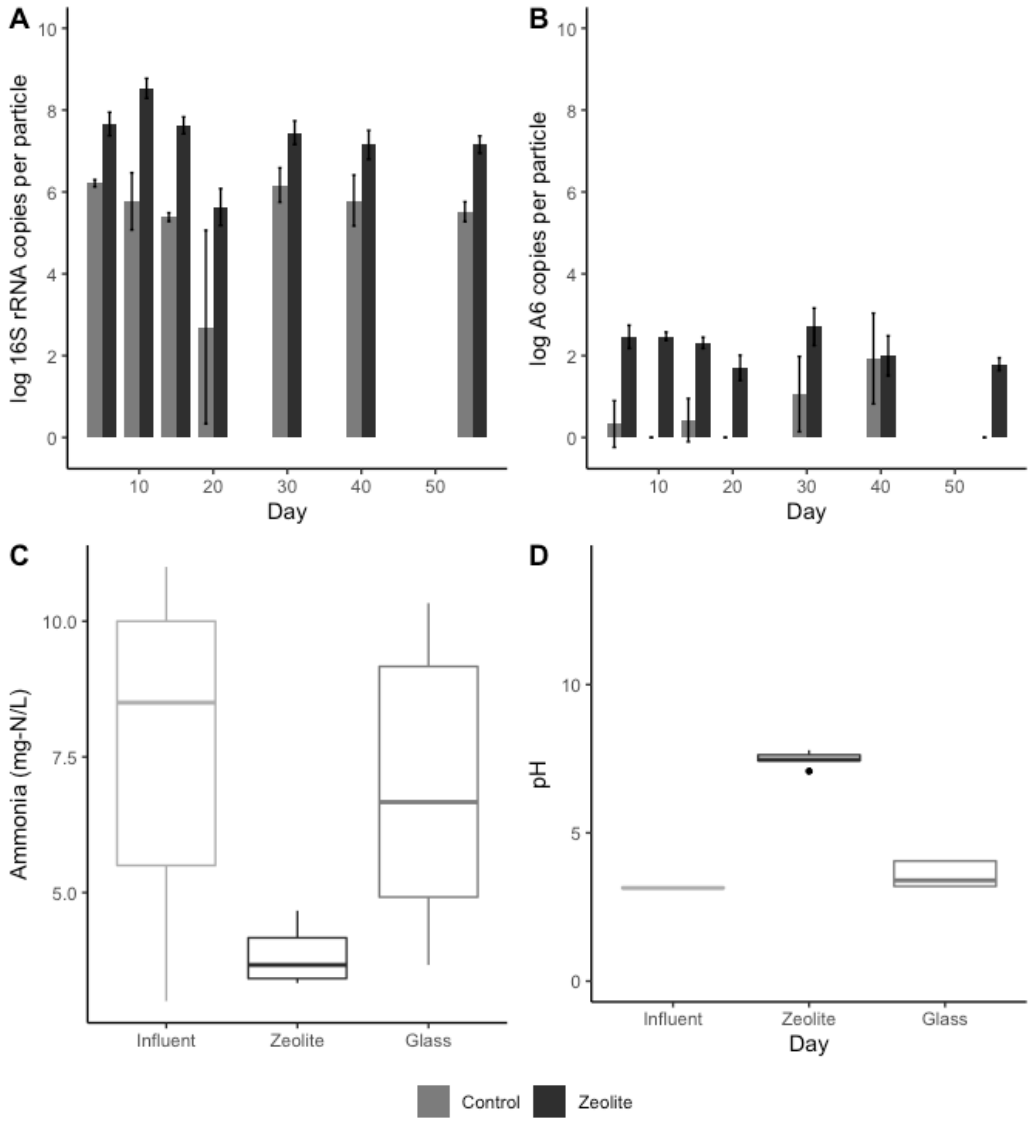

Figure 5.10. Effluent ammonium, pH, and qPCR results for the feammox enrichment experiment amended with zeolite or glass particles. A) log 16S rRNA gene copies, B) log A6 16S rRNA gene copies, C) influent and effluent

ammonium concentrations (mg/L), and D) influent pH and effluent pH prior to adjustment every 2.5 days. Error bars indicate the standard deviation of triplicate experimental replicates.

Because of the exciting results obtained with zeolite particles, zeolite-coated carriers were also studied to determine if they could stimulate feammox activity and enrich A6 in a similar manner. Effluent ammonium in the reactors containing Z carriers was very low, at 0.2 ± 0.35 mg-N/L, with influent ammonium at 6.2 ± 0.85 mg-N/L. Reactors containing control carriers had higher effluent ammonium concentrations, at 12.3 ± 0.95 mg-N/L ($P<0.0001$), than those in the influent, which may have been a result of high ammonium concentrations in the initial inoculum or the production of microbial decay products in the reactor over time. The pH in the Z carrier reactors was high, at 6.7 ± 0.2, compared to 4.8 ± 0.1 in the control reactors ($P<0.0001$), again indicating higher feammox activity in the Z carrier reactors, though likely not as high as in the zeolite particle reactors (average pH 7.48 ± 0.28).

When pooled with time, the C carrier reactors and Z carrier reactors performed similarly with respect to log A6 ($P= 0.51$) and log 16S rRNA ($P= 0.59$) copies/carrier (Figure 5.10). When comparing results for individual sampling dates, however, the reactors containing Z carriers contained significantly more A6 than the C carriers on Day 10 (Student's t test, $P=0.007$) and Day 25 ($P=0.045$), with Days 5 ($P=0.75$), 15 ($P=0.26$), and 20 ($P=0.67$) being statistically similar (Figure 5.10). 16S rRNA was only significantly higher on Z carriers on Day 25 ($P=0.016$). Although the results were not as unequivocal

as those obtained with the zeolite particles, they are promising and suggest that more work should be performed to identify how best to manufacture and deploy the Z carriers to enrich and retain A6 and stimulate PFAS degradation long-term. Additional research on the carriers themselves, incorporating regions capable of sorbing PFAS in addition to ammonium, could also improve the ability of these novel carriers to facilitate ammonium and PFAS removal.

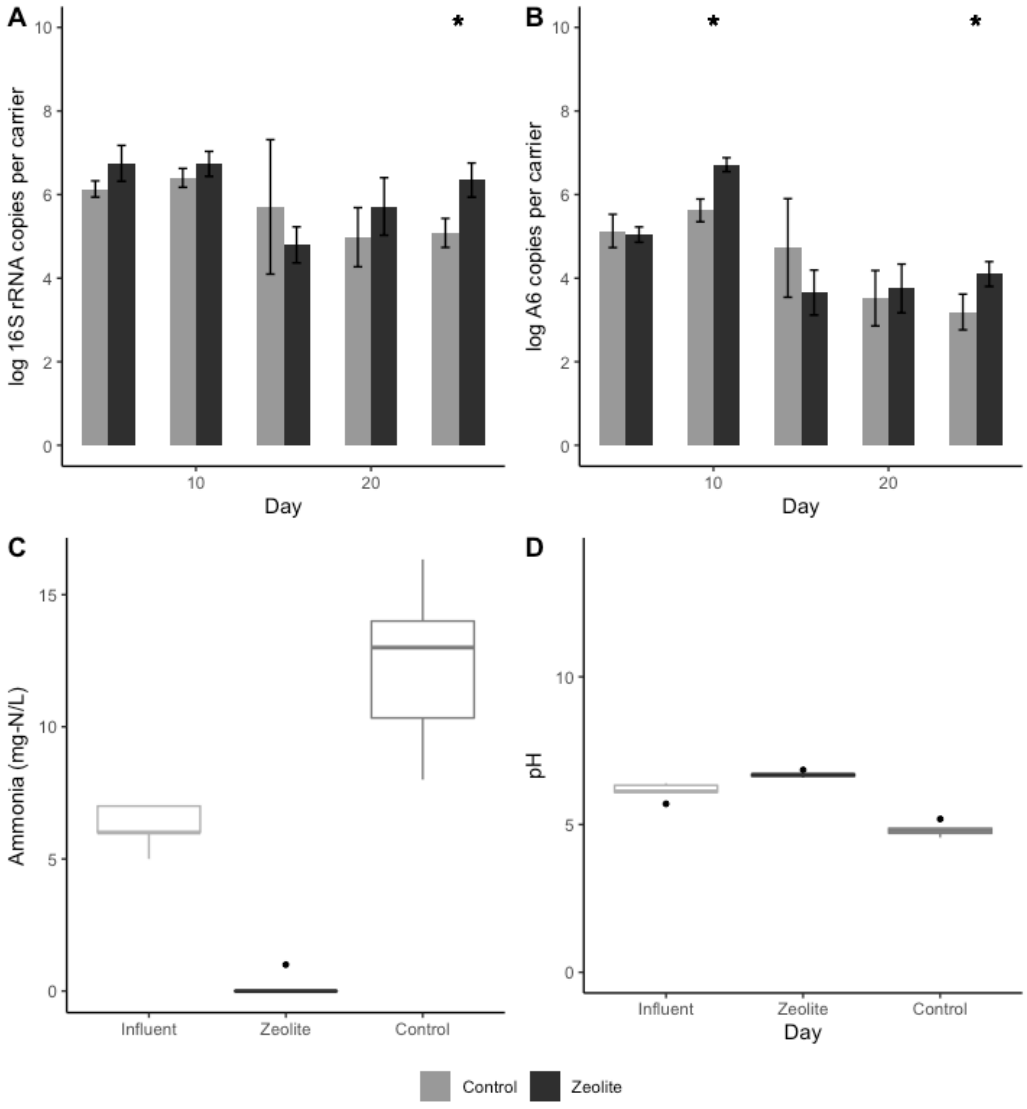

Figure 5.11. Zeolite and control carrier feammox experiment qPCR and effluent results. A) 16S rRNA qPCR B) A6 qPCR C) Influent and effluent ammonium (mg/L). D) Influent and effluent pH before pH adjusting to 4. Error bars indicate standard deviation from triplicate experimental replicates.
* indicates those treatments that are significantly different from the control.

Implications of zeolite-coated carrier technologies for stormwater applications. For the anaerobic oxidation of ammonium via the activity of anammox bacteria to occur in

stormwater systems, or even PFAS degradation via the activity of feammox bacteria to occur in stormwater, these slow growing bacteria need to be retained. Zeolite is one potential solution to retain anammox and feammox bacteria in a variety of environments. Recent work, described in Chapters 3 and 4, has shown that engineered zeolite materials, such as zeolite-coated biofilm carriers, can retain anammox bacteria in mainstream wastewater environments.[42] Other studies have also found that zeolite particles and spherical polymer cages containing zeolite retain anammox biomass, enhance nitrogen removal, and even increase specific anammox activity in wastewater environments.[45–47] In stormwater, the use of zeolite for abiotic ammonium removal has been reported[48,49] as well as the use of zeolite particles[28,50] and other carrier materials such as biochar[41,51,52] for the enrichment and/or retention of nitrogen-cycling microbial communities in wetland and stormwater bioretention systems. No work has been reported on efforts to retain feammox bacteria in stormwater treatment systems, or to study the retention of A6 in the presence of a biofilm carrier. Perhaps longer-lasting polymer carriers modified with zeolites can also work in stormwater treatment systems to retain anammox and feammox for long-term and self-sustaining treatment. Such technologies, combining rapid zeolite-driven abiotic sorption[48] followed by slow biological ammonium degradation,[53] may be particularly useful in a stormwater application, as stormwater systems can have periods of high flow rates and low retention times followed by periods of slow-to-no flow.[41,43] This type of a system may even provide treatment during winter months when microbial metabolism is extremely slow.

In this research zeolite-coated carriers were able to remove ammonium from influent water rapidly, and at time frames relevant for sizable storm events;[41,43] this indicates that if paired with the bio-regeneration of the zeolite via ammonium oxidizing microbes, ideally anammox for complete nitrogen removal, these novel carriers could offer a method of mitigating nitrogen pollution from stormwater or stormwater treatment systems that might otherwise export excess nitrogen.[5,22] Pre-seeded carriers were able to retain their biofilm during an 11-week field deployment in a raingarden system and a stormwater treatment pond over a period of low temperatures. In this study the zeolite coating did not always help to enrich or retain anammox bacteria and/or AOB, possibly because some minimum quantity of zeolite is required for enrichment/retention, as observed in a previous study (Chapter 3).[42] In addition, laboratory-scale experiments demonstrated that the zeolite-coated carriers were better able to remove ammonium from the influent during a simulated storm event when not pre-seeded with an anammox biofilm (Table 5.1). As mentioned above, this differs from what was observed in previous research, in which zeolite-coated carriers were still capable of exchanging ammonium when covered by biofilm (Chapter 4); nevertheless, those results were obtained under equilibrium conditions, and not under conditions that were kinetically controlled (Chapter 4). Pre-seeded carriers, regardless of whether they were control or zeolite-coated, did contain a greater quantity of nitrogen-cycling bacteria in the carrier biofilm than unseeded carriers. These results suggest that a combination of anammox-pre-seeded carriers (control or zeolite-coated) and zeolite-coated unseeded carriers may be ideal for deployment in a stormwater treatment system, achieving both rapid abiotic ammonium removal and enhanced biological nitrogen degradation. Longer term studies are needed to

determine if anammox bacteria recover from washout events on zeolite-coated carriers more quickly and if unseeded zeolite-coated carriers enrich and retain more nitrogen cycling bacteria long-term, as was observed in a simulated mainstream wastewater treatment system (Chapters 3 and 4). Additionally, carriers should be tested during different seasons when ammonium concentrations are slightly higher and when rain events may be more frequent. Carriers should also be analyzed for retention of denitrifying genes such as *nirK, nirS*, and *nosZ* as previous work (Chapter 4) demonstrated retention of these genes in wastewater systems.

The performance of reactors containing zeolite particles or zeolite-coated carriers amended with feammox was particularly exciting. Both systems showed evidence of ammonium sorption and enhanced feammox activity, via increased pH, and although the results from the zeolite-coated carrier reactors were less dramatic compared to those from the zeolite particle reactors, A6 appeared to be retained and/or enriched in the presence of zeolite. More research is clearly needed to understand how to deploy zeolite or zeolite-modified carriers for enhanced A6 activity, particularly for enhanced A6-mediated PFOS and PFOA biodegradation,[33,34] but these results are extremely promising and offer the potential for targeted A6 deployment for remediation purposes in addition to the potential for the removal of PFAS in stormwater. More research focused on modifying the zeolite-coated carriers for enhanced PFAS sorption might be a way to further improve the activity and utility of this system for PFAS remediation.

References

(1) LeFevre Gregory H.; Paus Kim H.; Natarajan Poornima; Gulliver John S.; Novak Paige J.; Hozalski Raymond M. Review of Dissolved Pollutants in Urban Storm Water and Their Removal and Fate in Bioretention Cells. *J. Environ. Eng.* 2015, *141* (1), 04014050. https://doi.org/10.1061/(ASCE)EE.1943-7870.0000876.

(2) Xu, D.; Lee, L. Y.; Lim, F. Y.; Lyu, Z.; Zhu, H.; Ong, S. L.; Hu, J. Water Treatment Residual: A Critical Review of Its Applications on Pollutant Removal from Stormwater Runoff and Future Perspectives. *J. Environ. Manage.* 2020, *259*, 109649. https://doi.org/10.1016/j.jenvman.2019.109649.

(3) Fairbairn, D. J.; Elliott, S. M.; Kiesling, R. L.; Schoenfuss, H. L.; Ferrey, M. L.; Westerhoff, B. M. Contaminants of Emerging Concern in Urban Stormwater: Spatiotemporal Patterns and Removal by Iron-Enhanced Sand Filters (IESFs). *Water Res.* 2018, *145*, 332–345. https://doi.org/10.1016/j.watres.2018.08.020.

(4) Tian, Z.; Peter, K. T.; Gipe, A. D.; Zhao, H.; Hou, F.; Wark, D. A.; Khangaonkar, T.; Kolodziej, E. P.; James, C. A. Suspect and Nontarget Screening for Contaminants of Emerging Concern in an Urban Estuary. *Environ. Sci. Technol.* 2020, *54* (2), 889–901. https://doi.org/10.1021/acs.est.9b06126.

(5) Gold, A. C.; Thompson, S. P.; Piehler, M. F. Nitrogen Cycling Processes within Stormwater Control Measures: A Review and Call for Research. *Water Res.* 2019, *149*, 578–587. https://doi.org/10.1016/j.watres.2018.10.036.

(6) Lusk, M. G.; Toor, G. S.; Inglett, P. W. Organic Nitrogen in Residential Stormwater Runoff: Implications for Stormwater Management in Urban Watersheds. *Sci. Total Environ.* 2020, *707*, 135962. https://doi.org/10.1016/j.scitotenv.2019.135962.

(7) Hathaway, J. M.; Moore, T. L. C.; Burkholder, J. M.; Hunt, W. F. Temporal Analysis of Stormwater Control Measure Effluent Based on Windows of Harmful Algal Bloom (HAB) Sensitivity: Are Annual Nutrient EMCs Appropriate during HAB-Sensitive Seasons? *Ecol. Eng.* 2012, *49*, 41–47. https://doi.org/10.1016/j.ecoleng.2012.08.014.

(8) Biswal, B. K.; Vijayaraghavan, K.; Adam, M. G.; Lee Tsen-Tieng, D.; Davis, A. P.; Balasubramanian, R. Biological Nitrogen Removal from Stormwater in Bioretention Cells: A Critical Review. *Crit. Rev. Biotechnol.* 2021, 1–23. https://doi.org/10.1080/07388551.2021.1969888.

(9) Pitt, R.; Maestre, A.; Morquecho, R. National Stormwater Quality Database. Version 1.1. 2004.

(10) Van Drecht, G.; Bouwman, A. F.; Harrison, J.; Knoop, J. M. Global Nitrogen and Phosphate in Urban Wastewater for the Period 1970 to 2050: N AND P IN URBAN WASTE WATER. *Glob. Biogeochem. Cycles* 2009, *23* (4), n/a-n/a. https://doi.org/10.1029/2009GB003458.

(11) Howarth, R. W. Human Acceleration of the Nitrogen Cycle: Drivers, Consequences, and Steps toward Solutions. *Water Sci. Technol.* 2004, *49* (5–6), 7–13. https://doi.org/10.2166/wst.2004.0731.

(12) Paul, M. J.; Meyer, J. L. Streams in the Urban Landscape. *Annu. Rev. Ecol. Syst.* 2001, *32* (1), 333–365. https://doi.org/10.1146/annurev.ecolsys.32.081501.114040.

(13) Walsh, C. J.; Roy, A. H.; Feminella, J. W.; Cottingham, P. D.; Groffman, P. M.; Morgan, R. P. The Urban Stream Syndrome: Current Knowledge and the Search for a Cure. *J. North Am. Benthol. Soc.* 2005, *24* (3), 706–723. https://doi.org/10.1899/04-028.1.

(14) Pramanik, B. K.; Roychand, R.; Monira, S.; Bhuiyan, M.; Jegatheesan, V. Fate of Road-Dust Associated Microplastics and per- and Polyfluorinated Substances in Stormwater. *Process Saf. Environ. Prot.* 2020, *144*, 236–241. https://doi.org/10.1016/j.psep.2020.07.020.

(15) Codling, G.; Yuan, H.; Jones, P. D.; Giesy, J. P.; Hecker, M. Metals and PFAS in Stormwater and Surface Runoff in a Semi-Arid Canadian City Subject to Large Variations in Temperature among Seasons. *Environ. Sci. Pollut. Res.* 2020, *27* (15), 18232–18241. https://doi.org/10.1007/s11356-020-08070-2.
(16) Brezonik, P. L.; Stadelmann, T. H. Analysis and Predictive Models of Stormwater Runoff Volumes, Loads, and Pollutant Concentrations from Watersheds in the Twin Cities Metropolitan Area, Minnesota, USA. *Water Res.* 2002, *36* (7), 1743–1757. https://doi.org/10.1016/S0043-1354(01)00375-X.
(17) Kayhanian, M.; Fruchtman, B. D.; Gulliver, J. S.; Montanaro, C.; Ranieri, E.; Wuertz, S. Review of Highway Runoff Characteristics: Comparative Analysis and Universal Implications. *Water Res.* 2012, *46* (20), 6609–6624. https://doi.org/10.1016/j.watres.2012.07.026.
(18) Mayer, T.; Marsalek, J.; Reyes, E. D. Nutrients and Metal Contaminants Status of Urban Stormwater Ponds. *Lake Reserv. Manag.* 1996, *12* (3), 348–363. https://doi.org/10.1080/07438149609354276.
(19) Hathaway, J. M.; Tucker, R. S.; Spooner, J. M.; Hunt, W. F. A Traditional Analysis of the First Flush Effect for Nutrients in Stormwater Runoff from Two Small Urban Catchments. *Water. Air. Soil Pollut.* 2012, *223* (9), 5903–5915. https://doi.org/10.1007/s11270-012-1327-x.
(20) US EPA. Clean Water Act (CWA) Compliance Monitoring. July 13, 2021.
(21) Koch, B. J.; Febria, C. M.; Gevrey, M.; Wainger, L. A.; Palmer, M. A. Nitrogen Removal by Stormwater Management Structures: A Data Synthesis. *JAWRA J. Am. Water Resour. Assoc.* 2014, *50* (6), 1594–1607. https://doi.org/10.1111/jawr.12223.
(22) Burgin, A. J.; Hamilton, S. K. Have We Overemphasized the Role of Denitrification in Aquatic Ecosystems? A Review of Nitrate Removal Pathways. *Front. Ecol. Environ.* 2007, *5* (2), 89–96. https://doi.org/10.1890/1540-9295(2007)5[89:HWOTRO]2.0.CO;2.
(23) Sawayama, S. Possibility of Anoxic Ferric Ammonium Oxidation. *J. Biosci. Bioeng.* 2006, *101* (1), 70–72. https://doi.org/10.1263/jbb.101.70.
(24) Huang, S.; Jaffé, P. R. Characterization of Incubation Experiments and Development of an Enrichment Culture Capable of Ammonium Oxidation under Iron-Reducing Conditions. *Biogeosciences* 2015, *12* (3), 769–779. https://doi.org/10.5194/bg-12-769-2015.
(25) Shrestha, J.; Rich, J. J.; Ehrenfeld, J. G.; Jaffe, P. R. Oxidation of Ammonium to Nitrite Under Iron-Reducing Conditions in Wetland Soils: Laboratory, Field Demonstrations, and Push-Pull Rate Determination. *Soil Sci.* 2009, *174* (3), 156–164. https://doi.org/10.1097/SS.0b013e3181988fbf.
(26) Strous, M.; Heijnen, J. J.; Kuenen, J. G.; Jetten, M. S. M. The Sequencing Batch Reactor as a Powerful Tool for the Study of Slowly Growing Anaerobic Ammonium-Oxidizing Microorganisms. *Appl. Microbiol. Biotechnol.* 1998, *50* (5), 589–596. https://doi.org/10.1007/s002530051340.
(27) Jetten, M. S. M.; Cirpus, I.; Kartal, B.; van Niftrik, L.; van de Pas-Schoonen, K. T.; Sliekers, O.; Haaijer, S.; van der Star, W.; Schmid, M.; van de Vossenberg, J.; Schmidt, I.; Harhangi, H.; van Loosdrecht, M.; Gijs Kuenen, J.; Op den Camp, H.; Strous, M. 1994–2004: 10 Years of Research on the Anaerobic Oxidation of Ammonium. *Biochem. Soc. Trans.* 2005, *33* (1), 119–123. https://doi.org/10.1042/BST0330119.
(28) Pei, Y.; Wang, J.; Wang, Z.; Tian, B. Anammox Bacteria Community and Nitrogen Removal in a Strip-like Wetland in the Riparian Zone. *J. Environ. Sci. Health Part A* 2011, *46* (7), 715–722. https://doi.org/10.1080/10934529.2011.571582.
(29) Wang, Y.; Xu, L.; Wang, S.; Ye, F.; Zhu, G. Global Distribution of Anaerobic Ammonia Oxidation (Anammox) Bacteria – Field Surveys in Wetland, Dryland, Groundwater Aquifer and Snow. *Front. Microbiol.* 2019, *10*, 2583. https://doi.org/10.3389/fmicb.2019.02583.

(30) Huang, S.; Jaffé, P. R. Isolation and Characterization of an Ammonium-Oxidizing Iron Reducer: Acidimicrobiaceae Sp. A6. *PLoS ONE* 2018, *13* (4), 8–10. https://doi.org/10.1371/journal.pone.0194007.
(31) Huang, S.; Chen, C.; Peng, X.; Jaffé, P. R. Environmental Factors Affecting the Presence of Acidimicrobiaceae and Ammonium Removal under Iron-Reducing Conditions in Soil Environments. *Soil Biol. Biochem.* 2016, *98*, 148–158. https://doi.org/10.1016/j.soilbio.2016.04.012.
(32) Yang, W. H.; Weber, K. A.; Silver, W. L. Nitrogen Loss from Soil through Anaerobic Ammonium Oxidation Coupled to Iron Reduction. *Nat. Geosci.* 2012, *5* (8), 538–541. https://doi.org/10.1038/ngeo1530.
(33) Huang, S.; Jaffé, P. R. Defluorination of Perfluorooctanoic Acid (PFOA) and Perfluorooctane Sulfonate (PFOS) by Acidimicrobium Sp. Strain A6. *Environ. Sci. Technol.* 2019. https://doi.org/10.1021/acs.est.9b04047.
(34) Ruiz-Urigüen, M.; Shuai, W.; Huang, S.; Jaffé, P. R. Biodegradation of PFOA in Microbial Electrolysis Cells by Acidimicrobiaceae Sp. Strain A6. *Chemosphere* 2022, *292*, 133506. https://doi.org/10.1016/j.chemosphere.2021.133506.
(35) Feinberg, E. C.; Chester, A. L. H.; Novak, P. J.; Hillmyer, M. A. Porous Polyethylene-Supported Zeolite Carriers for Improved Wastewater Deammonification. *ACS EST Eng.* 2021, *1* (7), 1104–1112. https://doi.org/10.1021/ACSESTENGG.1C00077.
(36) Erickson, A.; Kozarek, J.; Kramarczuk, K.; Lewis, L. *Biofiltration Media Optimization – Phase I Final Report*; University of Minnesota Water Resources Center, Minnesota Stormwater Research Council; Project Report 593; 2021.
(37) Peterson, K. N.; Tan, D. T.; Bezares-Cruz, J. C.; Novak, P. J. Estrone Biodegradation in Laboratory-Scale Systems Designed for Total Nitrogen Removal from Wastewater. *Environ. Sci. Water Res. Technol.* 2017, *3* (6), 1051–1060. https://doi.org/10.1039/C7EW00164A.
(38) Wein, S., Monitoring Coordinator. 2021.
(39) Capitol Region Watershed District. Water Data Reporting Tool. 2022.
(40) Minnesota Pollution Control Agency. Design Criteria for Stormwater Ponds. May 25, 2021.
(41) Smith, D. P. Sorptive Media Biofiltration for Inorganic Nitrogen Removal from Storm Water. *J. Irrig. Drain. Eng.* 2008, *134* (5), 624–629. https://doi.org/10.1061/(ASCE)0733-9437(2008)134:5(624).
(42) Huff Chester, A. L.; Eum, K.; Tsapatsis, M.; Hillmyer, M. A.; Novak, P. J. Enhanced Nitrogen Removal and Anammox Bacteria Retention with Zeolite-Coated Membrane in Simulated Mainstream Wastewater. *Environ. Sci. Technol. Lett.* 2021, *8* (6), 468–473. https://doi.org/10.1021/acs.estlett.1c00154.
(43) MassDEP. Volume 2 Chapter 2: Structural BMP Specifications for the Massachusetts Stormwater Handbook. February 2020.
(44) Zhang, B.; Chen, L.; Guo, Q.; Lian, J.; Ye Yao. Evaluation of Ammonia and Nitrate Distribution and Reduction within Stormwater Green Infrastructure with Different Woody Plants under Multiple Influencing Factors. *J. Environ. Manage.* 2022, *302*, 114086. https://doi.org/10.1016/j.jenvman.2021.114086.
(45) Fernández, I.; Vázquez-Padín, J. R.; Mosquera-Corral, A.; Campos, J. L.; Méndez, R. Biofilm and Granular Systems to Improve Anammox Biomass Retention. *Biochem. Eng. J.* 2008, *42* (3), 308–313. https://doi.org/10.1016/j.bej.2008.07.011.
(46) Lv, Y.; Pan, J.; Huo, T.; Zhao, Y.; Liu, S. Enhanced Microbial Metabolism in One Stage Partial Nitritation-Anammox System Treating Low Strength Wastewater by Novel Composite Carrier. *Water Res.* 2019, *163*, 114872. https://doi.org/10.1016/j.watres.2019.114872.

(47) Yapsakli, K.; Aktan, C. K.; Mertoglu, B. Anammox-Zeolite System Acting as Buffer to Achieve Stable Effluent Nitrogen Values. *Biodegradation* 2017, *28* (1), 69–79. https://doi.org/10.1007/s10532-016-9778-1.
(48) Widiastuti, N.; Wu, H.; Ang, H. M.; Zhang, D. Removal of Ammonium from Greywater Using Natural Zeolite. *Desalination* 2011, *277* (1–3), 15–23. https://doi.org/10.1016/j.desal.2011.03.030.
(49) Reddy, K. R.; Xie, T.; Dastgheibi, S. Nutrients Removal from Urban Stormwater by Different Filter Materials. *Water. Air. Soil Pollut.* 2014, *225* (1), 1778. https://doi.org/10.1007/s11270-013-1778-8.
(50) Collison, R. S.; Grismer, M. E. Nitrogen and Chemical Oxygen Demand Removal from Septic Tank Wastewater in Subsurface Flow Constructed Wetlands: Substrate (Cation Exchange Capacity) Effects. *Water Environ. Res.* 2014, *86* (4), 314–323. https://doi.org/10.2175/106143013X13736496908627.
(51) Rahman, M. Y. A.; Nachabe, M. H.; Ergas, S. J. Biochar Amendment of Stormwater Bioretention Systems for Nitrogen and Escherichia Coli Removal: Effect of Hydraulic Loading Rates and Antecedent Dry Periods. *Bioresour. Technol.* 2020, *310*, 123428. https://doi.org/10.1016/j.biortech.2020.123428.
(52) Peng, Y.; Deng, S.; Kong, Z.; Yuan, Y.; Long, H.; Fang, J.; Ma, H.; Shao, Z.; He, Q.; Chai, H. Biochar and Woodchip Amended Bioreactor Extending Reactive Volume for Enhanced Denitrification in Stormwater Runoff. *J. Water Process Eng.* 2022, *46*, 102541. https://doi.org/10.1016/j.jwpe.2021.102541.
(53) Lahav, O.; Green, M. Ammonium Removal from Primary and Secondary Effluents Using a Bioregenerated Ion - Exchange Process. *Water Sci. Technol.* 2000, *42* (1–2), 179–185.

Chapter 6: Conclusions and recommendations

Several recommendations and conclusions can be offered from the findings of this work:

First, the water quality parameters, detection of contaminants of emerging concern (CECs), and spikes in antibiotic resistance genes found along the Volta River, Ghana indicate impacts of anthropogenic activities such as urban development, sand mining, agriculture, shellfish processing, and agriculture. While the overall low concentrations of CECs detected is encouraging, continued monitoring is recommended to better understand impacts of future mitigation measures that can hopefully improve environmental and human health.

Second, nitrogen removal is enhanced in the presence of zeolite particles and zeolite-coated materials. Additionally, anammox bacteria are preferentially retained on zeolite surfaces in mainstream-like wastewater systems and in some stormwater-like systems. Nevertheless, it is not well understood how the ammonium substrate profiles develop and change once biofilms are established. Determination of the distribution of ammonium in an established biofilm could lead to improved modeling and design of systems with zeolite materials.

To achieve retention of anammox and enhance nitrogen removal, a minimum amount of zeolite, or ammonium sorption capacity, in a system is needed. The reason for a minimum sorption capacity is not understood. It is recommended that additional research obtain a better understanding the impacts of zeolite and localized increased ammonium concentrations on microbial communities not only on the zeolite surfaces themselves, but also the impacts to the bulk liquid of the system.

Zeolite carriers and membranes did not preferentially retain ammonia oxidizing bacteria on their surfaces compared to control materials. Ammonia oxidizing bacteria were only retained under some conditions, and mostly in the reactor liquid. Further investigation of how to better

retain ammonia oxidizing bacteria and why they were not retained on zeolite surfaces is essential if mainstream partial nitritation-anammox is to occur in a single system.

Pre-seeding carriers with target biomass before deployment helped to retain and stabilize microbial communities in stormwater environments, both in field deployments and laboratory scale studies. No significant difference was detected between the performance of zeolite and control carriers when pre-seeded at the time frames tested. It is recommended that carriers are tested for longer durations to determine if zeolite-coating is needed when carriers are pre-seeded with biofilms, as this could result in substantial cost if scaled.

Finally, other microbes were found to be preferentially retained along with anammox bacteria including denitrifiers (*nirS, nirK* and *nosZ*) and feammox bacteria. This indicates that other potential applications of this technology continue to be explored. Further testing should determine if other constituents are being sorbed to the zeolite surfaces and why denitrifiers are being retained. Additionally, further work of whether defluorination of PFAO/PFOS with feammox culture retained on zeolite carriers can occur.

Cumulative Bibliography

(1) Fekadu, S.; Alemayehu, E.; Dewil, R.; Van der Bruggen, B. Pharmaceuticals in Freshwater Aquatic Environments: A Comparison of the African and European Challenge. *Science of The Total Environment* 2019, *654*, 324–337. https://doi.org/10.1016/j.scitotenv.2018.11.072.

(2) Bradley, P. M.; Journey, C. A.; Romanok, K. M.; Barber, L. B.; Buxton, H. T.; Foreman, W. T.; Furlong, E. T.; Glassmeyer, S. T.; Hladik, M. L.; Iwanowicz, L. R.; Jones, D. K.; Kolpin, D. W.; Kuivila, K. M.; Loftin, K. A.; Mills, M. A.; Meyer, M. T.; Orlando, J. L.; Reilly, T. J.; Smalling, K. L.; Villeneuve, D. L. Expanded Target-Chemical Analysis Reveals Extensive Mixed-Organic-Contaminant Exposure in U.S. Streams. *Environ. Sci. Technol.* 2017, *51* (9), 4792–4802. https://doi.org/10.1021/acs.est.7b00012.

(3) Kolpin, D. W.; Furlong, E. T.; Meyer, M. T.; Thurman, E. M.; Zaugg, S. D.; Barber, L. B.; Buxton, H. T. Pharmaceuticals, Hormones, and Other Organic Wastewater Contaminants in U.S. Streams, 1999−2000: A National Reconnaissance. *Environ. Sci. Technol.* 2002, *36* (6), 1202–1211. https://doi.org/10.1021/es011055j.

(4) Ongley, E. D.; Xiaolan, Z.; Tao, Y. Current Status of Agricultural and Rural Non-Point Source Pollution Assessment in China. *Environmental Pollution* 2010, *158* (5), 1159–1168. https://doi.org/10.1016/j.envpol.2009.10.047.

(5) Hua, L.; Li, W.; Zhai, L.; Yen, H.; Lei, Q.; Liu, H.; Ren, T.; Xia, Y.; Zhang, F.; Fan, X. An Innovative Approach to Identifying Agricultural Pollution Sources and Loads by Using Nutrient Export Coefficients in Watershed Modeling. *Journal of Hydrology* 2019, *571*, 322–331. https://doi.org/10.1016/j.jhydrol.2019.01.043.

(6) US EPA. National Management Measures to Control Nonpoint Source Pollution from Agriculture, 2003.

(7) Scavia, D.; Kalcic, M.; Muenich, R. L.; Read, J.; Aloysius, N.; Bertani, I.; Boles, C.; Confesor, R.; DePinto, J.; Gildow, M.; Martin, J.; Redder, T.; Robertson, D.; Sowa, S.; Wang, Y.; Yen, H. Multiple Models Guide Strategies for Agricultural Nutrient Reductions. *Front Ecol Environ* 2017, *15* (3), 126–132. https://doi.org/10.1002/fee.1472.

(8) Petrucci, G.; Gromaire, M.-C.; Shorshani, M. F.; Chebbo, G. Nonpoint Source Pollution of Urban Stormwater Runoff: A Methodology for Source Analysis. *Environ Sci Pollut Res* 2014, *21* (17), 10225–10242. https://doi.org/10.1007/s11356-014-2845-4.

(9) Janke, B. D.; Finlay, J. C.; Hobbie, S. E. Trees and Streets as Drivers of Urban Stormwater Nutrient Pollution. *Environ. Sci. Technol.* 2017, *51* (17), 9569–9579. https://doi.org/10.1021/acs.est.7b02225.

(10) Nilsen, E.; Smalling, K. L.; Ahrens, L.; Gros, M.; Miglioranza, K. S. B.; Picó, Y.; Schoenfuss, H. L. Critical Review: Grand Challenges in Assessing the Adverse Effects of Contaminants of Emerging Concern on Aquatic Food Webs. *Environmental Toxicology and Chemistry* 2019, *38* (1), 46–60. https://doi.org/10.1002/etc.4290.

(11) Arnold, K. E.; Brown, A. R.; Ankley, G. T.; Sumpter, J. P. Medicating the Environment: Assessing Risks of Pharmaceuticals to Wildlife and Ecosystems. *Phil. Trans. R. Soc. B* 2014, *369* (1656), 20130569. https://doi.org/10.1098/rstb.2013.0569.
(12) Corcoran, J.; Winter, M. J.; Tyler, C. R. Pharmaceuticals in the Aquatic Environment: A Critical Review of the Evidence for Health Effects in Fish. *Critical Reviews in Toxicology* 2010, *40* (4), 287–304. https://doi.org/10.3109/10408440903373590.
(13) Gwenzi, W.; Chaukura, N. Organic Contaminants in African Aquatic Systems: Current Knowledge, Health Risks, and Future Research Directions. *Science of The Total Environment* 2018, *619–620*, 1493–1514. https://doi.org/10.1016/j.scitotenv.2017.11.121.
(14) Asem-Hiablie, S.; Church, C. D.; Elliott, H. A.; Shappell, N. W.; Schoenfuss, H. L.; Drechsel, P.; Williams, C. F.; Knopf, A. L.; Dabie, M. Y. Serum Estrogenicity and Biological Responses in African Catfish Raised in Wastewater Ponds in Ghana. *Science of The Total Environment* 2013, *463–464*, 1182–1191. https://doi.org/10.1016/j.scitotenv.2013.06.032.
(15) Parkinson, J.; Tayler, K. Decentralized Wastewater Management in Peri-Urban Areas in Low-Income Countries. *Environment and Urbanization* 2003, *15* (1), 75–90. https://doi.org/10.1177/095624780301500119.
(16) Bouwman, A. F.; Van Drecht, G.; Knoop, J. M.; Beusen, A. H. W.; Meinardi, C. R. Exploring Changes in River Nitrogen Export to the World's Oceans. *Global Biogeochem. Cycles* 2005, *19* (1). https://doi.org/10.1029/2004GB002314.
(17) Van Drecht, G.; Bouwman, A. F.; Harrison, J.; Knoop, J. M. Global Nitrogen and Phosphate in Urban Wastewater for the Period 1970 to 2050: N AND P IN URBAN WASTE WATER. *Global Biogeochem. Cycles* 2009, *23* (4), n/a-n/a. https://doi.org/10.1029/2009GB003458.
(18) Glüge, J.; Scheringer, M.; Cousins, I. T.; DeWitt, J. C.; Goldenman, G.; Herzke, D.; Lohmann, R.; Ng, C. A.; Trier, X.; Wang, Z. An Overview of the Uses of Per- and Polyfluoroalkyl Substances (PFAS). *Environ. Sci.: Processes Impacts* 2020, *22* (12), 2345–2373. https://doi.org/10.1039/D0EM00291G.
(19) Podder, A.; Sadmani, A. H. M. A.; Reinhart, D.; Chang, N.-B.; Goel, R. Per and Poly-Fluoroalkyl Substances (PFAS) as a Contaminant of Emerging Concern in Surface Water: A Transboundary Review of Their Occurrences and Toxicity Effects. *Journal of Hazardous Materials* 2021, *419*, 126361. https://doi.org/10.1016/j.jhazmat.2021.126361.
(20) Crone, B. C.; Speth, T. F.; Wahman, D. G.; Smith, S. J.; Abulikemu, G.; Kleiner, E. J.; Pressman, J. G. Occurrence of Per- and Polyfluoroalkyl Substances (PFAS) in Source Water and Their Treatment in Drinking Water. *Critical Reviews in Environmental Science and Technology* 2019, *49* (24), 2359–2396. https://doi.org/10.1080/10643389.2019.1614848.
(21) Baabish, A.; Sobhanei, S.; Fiedler, H. Priority Perfluoroalkyl Substances in Surface Waters - A Snapshot Survey from 22 Developing Countries. *Chemosphere* 2021, *273*, 129612. https://doi.org/10.1016/j.chemosphere.2021.129612.

(22) Lenka, S. P.; Kah, M.; Padhye, L. P. A Review of the Occurrence, Transformation, and Removal of Poly- and Perfluoroalkyl Substances (PFAS) in Wastewater Treatment Plants. *Water Research* 2021, *199*, 117–187. https://doi.org/10.1016/j.watres.2021.117187.
(23) Phong Vo, H. N.; Ngo, H. H.; Guo, W.; Hong Nguyen, T. M.; Li, J.; Liang, H.; Deng, L.; Chen, Z.; Hang Nguyen, T. A. Poly-and Perfluoroalkyl Substances in Water and Wastewater: A Comprehensive Review from Sources to Remediation. *Journal of Water Process Engineering* 2020, *36*, 101393. https://doi.org/10.1016/j.jwpe.2020.101393.
(24) Castiglioni, S.; Valsecchi, S.; Polesello, S.; Rusconi, M.; Melis, M.; Palmiotto, M.; Manenti, A.; Davoli, E.; Zuccato, E. Sources and Fate of Perfluorinated Compounds in the Aqueous Environment and in Drinking Water of a Highly Urbanized and Industrialized Area in Italy. *Journal of Hazardous Materials* 2015, *282*, 51–60. https://doi.org/10.1016/j.jhazmat.2014.06.007.
(25) Sharma, B. M.; Bharat, G. K.; Tayal, S.; Larssen, T.; Bečanová, J.; Karásková, P.; Whitehead, P. G.; Futter, M. N.; Butterfield, D.; Nizzetto, L. Perfluoroalkyl Substances (PFAS) in River and Ground/Drinking Water of the Ganges River Basin: Emissions and Implications for Human Exposure. *Environmental Pollution* 2016, *208*, 704–713. https://doi.org/10.1016/j.envpol.2015.10.050.
(26) Pramanik, B. K.; Roychand, R.; Monira, S.; Bhuiyan, M.; Jegatheesan, V. Fate of Road-Dust Associated Microplastics and per- and Polyfluorinated Substances in Stormwater. *Process Safety and Environmental Protection* 2020, *144*, 236–241. https://doi.org/10.1016/j.psep.2020.07.020.
(27) Jiménez, B.; Mara, D.; Carr, R.; Brissaud, F. Wastewater Treatment for Pathogen Removal and Nutrient Conservation: Suitable Systems for Use in Developing Countries. *Wastewater Irrigation and Health. Assessing and Mitigating Risk in Low-Income Countries* 2010, 149–169.
(28) Rahman, S. M.; Eckelman, M. J.; Onnis-Hayden, A.; Gu, A. Z. Comparative Life Cycle Assessment of Advanced Wastewater Treatment Processes for Removal of Chemicals of Emerging Concern. *Environ. Sci. Technol.* 2018, *52* (19), 11346–11358. https://doi.org/10.1021/acs.est.8b00036.
(29) Li, Y.; Li, H.; Xu, X.; Xiao, S.; Wang, S.; Xu, S. Fate of Nitrogen in Subsurface Infiltration System for Treating Secondary Effluent. *Water Science and Engineering* 2017, *10* (3), 217–224. https://doi.org/10.1016/j.wse.2017.10.002.
(30) Delgado Vela, J.; Stadler, L. B.; Martin, K. J.; Raskin, L.; Bott, C. B.; Love, N. G. Prospects for Biological Nitrogen Removal from Anaerobic Effluents during Mainstream Wastewater Treatment. *Environ. Sci. Technol. Lett.* 2015, *2* (9), 234–244. https://doi.org/10.1021/acs.estlett.5b00191.
(31) Howarth, R. W. Coastal Nitrogen Pollution: A Review of Sources and Trends Globally and Regionally. *Harmful Algae* 2008, *8* (1), 14–20. https://doi.org/10.1016/j.hal.2008.08.015.
(32) Smetacek, V.; Zingone, A. Green and Golden Seaweed Tides on the Rise. *Nature* 2013, *504* (7478), 84–88. https://doi.org/10.1038/nature12860.
(33) Ansa-Asare, O.; Mensah, E.; Entsua-Mensah, M.; Biney, C. Impact of Human Activities on Nutrient and Trophic Status of Some Selected Lagoons in Ghana.

West African Journal of Applied Ecology 2009, *12* (1). https://doi.org/10.4314/wajae.v12i1.45761.
(34) Mojiri, A.; Bashir, M. J. K. Wastewater Treatment: Current and Future Techniques. *Water* 2022, *14* (3), 448. https://doi.org/10.3390/w14030448.
(35) Water Quality: Two Year Milestones, 2015.
(36) Li, X.; Klaus, S.; Bott, C.; He, Z. Status, Challenges, and Perspectives of Mainstream Nitritation-Anammox for Wastewater Treatment. *Water Environment Research* 2018, *90* (7), 634–649. https://doi.org/10.2175/106143017x15131012153112.
(37) Hu, Z.; Houweling, D.; Dold, P. Biological Nutrient Removal in Municipal Wastewater Treatment: New Directions in Sustainability. *J. Environ. Eng.* 2012, *138* (3), 307–317. https://doi.org/10.1061/(ASCE)EE.1943-7870.0000462.
(38) Mamais, D.; Noutsopoulos, C.; Dimopoulou, A.; Stasinakis, A.; Lekkas, T. D. Wastewater Treatment Process Impact on Energy Savings and Greenhouse Gas Emissions. *Water Science and Technology* 2015, *71* (2), 303–308. https://doi.org/10.2166/wst.2014.521.
(39) Crawford, G.; Sandino, J. *Energy Efficiency in Wastewater Treatment in North America: A Compendium of Best Practices and Case Studies of Novel Approaches*; 2010.
(40) Gu, J.; Zhang, M.; Liu, Y. A Review on Mainstream Deammonification of Municipal Wastewater: Novel Dual Step Process. *Bioresource Technology* 2020, *299*, 122674. https://doi.org/10.1016/j.biortech.2019.122674.
(41) Tarallo, S. *A Guide to Net-Zero Energy Solutions for Water Resource Recovery Facilities*; 2015; Vol. 14. https://doi.org/10.2166/9781780407685.
(42) Jetten, M. S. M.; Cirpus, I.; Kartal, B.; van Niftrik, L.; van de Pas-Schoonen, K. T.; Sliekers, O.; Haaijer, S.; van der Star, W.; Schmid, M.; van de Vossenberg, J.; Schmidt, I.; Harhangi, H.; van Loosdrecht, M.; Gijs Kuenen, J.; Op den Camp, H.; Strous, M. 1994–2004: 10 Years of Research on the Anaerobic Oxidation of Ammonium. *Biochemical Society Transactions* 2005, *33* (1), 119–123. https://doi.org/10.1042/BST0330119.
(43) Mulder, A.; van de Graaf, A. A.; Robertson, L. A.; Kuenen, J. G. Anaerobic Ammonium Oxidation Discovered in a Denitrifying Fluidized Bed Reactor. *FEMS Microbiology Ecology* 1995, *16* (3).
(44) Zhang, L.; Narita, Y.; Gao, L.; Ali, M.; Oshiki, M.; Ishii, S.; Okabe, S. Microbial Competition among Anammox Bacteria in Nitrite-Limited Bioreactors. *Water Research* 2017, *125*, 249–258. https://doi.org/10.1016/J.WATRES.2017.08.052.
(45) Wang, S.; Peng, Y.; Ma, B.; Wang, S.; Zhu, G. Anaerobic Ammonium Oxidation in Traditional Municipal Wastewater Treatment Plants with Low-Strength Ammonium Loading: Widespread but Overlooked. *Water Research* 2015, *84*, 66–75. https://doi.org/10.1016/j.watres.2015.07.005.
(46) Qiao, L.; Ning, X.; Li, Y.; Zhang, Y. A Kinetics Study on Anammox Bacteria with a Disproportionate Substrate Concentration. *Journal of Chemical Technology & Biotechnology* 2017. https://doi.org/10.1002/jctb.5229.
(47) Schmidt, I.; Sliekers, O.; Schmid, M.; Cirpus, I.; Strous, M.; Bock, E.; Kuenen, J. G.; Jetten, M. S. M. Aerobic and Anaerobic Ammonia Oxidizing Bacteria –

Competitors or Natural Partners? *FEMS Microbiology Ecology* 2002, *39* (3), 175–181. https://doi.org/10.1016/S0168-6496(01)00208-2.

(48) Jin, R.-C.; Yang, G.-F.; Yu, J.-J.; Zheng, P. The Inhibition of the Anammox Process: A Review. *Chemical Engineering Journal* 2012, *197*, 67–79. https://doi.org/10.1016/J.CEJ.2012.05.014.

(49) Laureni, M.; Weissbrodt, D. G.; Szivák, I.; Robin, O.; Nielsen, J. L.; Morgenroth, E.; Joss, A. Activity and Growth of Anammox Biomass on Aerobically Pre-Treated Municipal Wastewater. *Water Research* 2015, *80*, 325–336. https://doi.org/10.1016/j.watres.2015.04.026.

(50) Wang, Y.; Xu, L.; Wang, S.; Ye, F.; Zhu, G. Global Distribution of Anaerobic Ammonia Oxidation (Anammox) Bacteria – Field Surveys in Wetland, Dryland, Groundwater Aquifer and Snow. *Front. Microbiol.* 2019, *10*, 2583. https://doi.org/10.3389/fmicb.2019.02583.

(51) Zhang, J.; Zhang, Y.; Li, Y.; Zhang, L.; Qiao, S.; Yang, F.; Quan, X. Enhancement of Nitrogen Removal in a Novel Anammox Reactor Packed with Fe Electrode. *Bioresource Technology* 2012, *114*, 102–108. https://doi.org/10.1016/j.biortech.2012.03.018.

(52) Akaboci, T. R. V.; Gich, F.; Ruscalleda, M.; Balaguer, M. D.; Colprim, J. Assessment of Operational Conditions towards Mainstream Partial Nitritation-Anammox Stability at Moderate to Low Temperature: Reactor Performance and Bacterial Community. *Chemical Engineering Journal* 2018, *350* (May), 192–200. https://doi.org/10.1016/j.cej.2018.05.115.

(53) Wells, G. F.; Shi, Y.; Laureni, M.; Rosenthal, A.; Sziva, I.; Weissbrodt, D. G.; Joss, A.; Buergmann, H.; Johnson, D. R.; Morgenroth, E. Comparing the Resistance, Resilience, and Stability of Replicate Moving Bed Biofilm and Suspended Growth Combined Nitritation− Anammox Reactors. *Environmental Science & Technology* 2017, *51*, 5108–5117. https://doi.org/10.1021/acs.est.6b05878.

(54) Wagner, B. M.; Daigger, G. T.; Love, N. G. Assessing Membrane Aerated Biofilm Reactor Configurations in Mainstream Anammox Applications. *Water Science and Technology* 2022, wst2022013. https://doi.org/10.2166/wst.2022.013.

(55) Mulder, A. The Quest for Sustainable Nitrogen Removal Technologies. *Water Science & Technology* 2003, *48* (1), 67–75.

(56) The Development of Simultaneous Partial Nitrification, ANAMMOX and Denitrification (SNAD) Process in a Single Reactor for Nitrogen Removal. *Bioresource Technology* 2009, *100* (4), 1548–1554. https://doi.org/10.1016/J.BIORTECH.2008.09.003.

(57) Bagchi, S.; Biswas, R.; Nandy, T. Alkalinity and Dissolved Oxygen as Controlling Parameters for Ammonia Removal through Partial Nitritation and ANAMMOX in a Single-Stage Bioreactor. *Journal of Industrial Microbiology and Biotechnology* 2010, *37* (8), 871–876. https://doi.org/10.1007/s10295-010-0744-3.

(58) Zhu, G.; Peng, Y. Biological Nitrogen Removal with Nitrification and Denitrification via Nitrite Pathway. *Harbin Gongye Daxue Xuebao/Journal of Harbin Institute of Technology* 2008, *40* (10), 1552–1557. https://doi.org/10.1007/s00253-006-0534-z.

(59) Ni, B.-J.; Ruscalleda, M.; Smets, B. F. Evaluation on the Microbial Interactions of Anaerobic Ammonium Oxidizers and Heterotrophs in Anammox Biofilm. *Water Research* 2012, *46* (15), 4645–4652. https://doi.org/10.1016/J.WATRES.2012.06.016.
(60) Li, X.; Peng, Y.; Zhang, J.; Du, R. Highly Efficient and Synchronous Nitrogen Removal from Ammonia-Rich Wastewater and Domestic Wastewater via a Novel Anammox Coupled with Double-Nitrite-Shunt Process at Low Temperature. *Chemical Engineering Journal* 2021, *425*, 131449. https://doi.org/10.1016/j.cej.2021.131449.
(61) Singh, V.; Ormeci, B.; Mishra, S.; Hussain, A. Simultaneous Partial Nitrification, ANAMMOX and Denitrification (SNAD) – A Review of Critical Operating Parameters and Reactor Configurations. *Chemical Engineering Journal* 2022, *433*, 133677. https://doi.org/10.1016/j.cej.2021.133677.
(62) Wang, X.; Gao, D. The Transformation from Anammox Granules to Deammonification Granules in Micro-Aerobic System by Facilitating Indigenous Ammonia Oxidizing Bacteria. *Bioresource Technology* 2018, *250* (November 2017), 439–448. https://doi.org/10.1016/j.biortech.2017.11.046.
(63) Lackner, S.; Gilbert, E. M.; Vlaeminck, S. E.; Joss, A.; Horn, H.; van Loosdrecht, M. C. M. Full-Scale Partial Nitritation/Anammox Experiences - An Application Survey. *Water Research* 2014, *55* (2014), 292–303. https://doi.org/10.1016/j.watres.2014.02.032.
(64) Mulder, J. W.; Van Loosdrecht, M. C. M.; Hellinga, C.; Van Kempen, R. Full-Scale Application of the SHARON Process for Treatment of Rejection Water of Digested Sludge Dewatering. *Water Science and Technology* 2001, *43* (11), 127–134. https://doi.org/10.2166/wst.2001.0675.
(65) Kosgey, K.; Chandran, K.; Gokal, J.; Kiambi, S. L.; Bux, F.; Kumari, S. Critical Analysis of Biomass Retention Strategies in Mainstream and Sidestream ANAMMOX-Mediated Nitrogen Removal Systems. *Environ. Sci. Technol.* 2021, *55* (1), 9–24. https://doi.org/10.1021/acs.est.0c00276.
(66) Environmental Protection Agency EPA. Wastewater Management Fact Sheet: Energy Conservation. 2006.
(67) Hubaux, N.; Wells, G.; Morgenroth, E. Impact of Coexistence of Flocs and Biofilm on Performance of Combined Nitritation-Anammox Granular Sludge Reactors. *Water Research* 2015, *68*, 127–139. https://doi.org/10.1016/j.watres.2014.09.036.
(68) Winkler, M. K. H.; Kleerebezem, R.; Van Loosdrecht, M. C. M. Integration of Anammox into the Aerobic Granular Sludge Process for Main Stream Wastewater Treatment at Ambient Temperatures. *Water Research* 2012, *46* (1), 136–144. https://doi.org/10.1016/j.watres.2011.10.034.
(69) Magrí, A.; Vanotti, M. B.; Szögi, A. A. Anammox Sludge Immobilized in Polyvinyl Alcohol (PVA) Cryogel Carriers. *Bioresource Technology* 2012, *114*, 231–240. https://doi.org/10.1016/j.biortech.2012.03.077.
(70) Vlaeminck, S. E.; Terada, A.; Smets, B. F.; De Clippeleir, H.; Schaubroeck, T.; Bolca, S.; Demeestere, L.; Mast, J.; Boon, N.; Carballa, M.; Verstraete, W. Aggregate Size and Architecture Determine Microbial Activity Balance for One-

Stage Partial Nitritation and Anammox. *Applied and environmental microbiology* 2010, *76* (3), 900–909. https://doi.org/10.1128/AEM.02337-09.
(71) van Dongen, U.; Jetten, M. S. M.; van Loosdrecht, M. C. M. The SHARON®-Anammox® Process for Treatment of Ammonium Rich Wastewater. *Water Science and Technology* 2001, *44* (1), 153–160.
(72) Ma, Y.; Domingo-Félez, C.; Plósz, B. Gy.; Smets, B. F. Intermittent Aeration Suppresses Nitrite-Oxidizing Bacteria in Membrane-Aerated Biofilms: A Model-Based Explanation. *Environmental Science & Technology* 2017, *51* (11), 6146–6155. https://doi.org/10.1021/acs.est.7b00463.
(73) Ma, B.; Bao, P.; Wei, Y.; Zhu, G.; Yuan, Z.; Peng, Y. Suppressing Nitrite-Oxidizing Bacteria Growth to Achieve Nitrogen Removal from Domestic Wastewater via Anammox Using Intermittent Aeration with Low Dissolved Oxygen. *Nature Publishing Group* 2015. https://doi.org/10.1038/srep13048.
(74) Isanta, E.; Reino, C.; An Carrera, J.; Erez, J. P. Stable Partial Nitritation for Low-Strength Wastewater at Low Temperature in an Aerobic Granular Reactor. 2015. https://doi.org/10.1016/j.watres.2015.04.028.
(75) Kuenen, J. G. Anammox Bacteria: From Discovery to Application. *Nature Reviews Microbiology* 2008, *6* (4), 320. https://doi.org/10.1038/nrmicro1857.
(76) Egli, K.; Fanger, U.; Alvarez, P. J. J.; Siegrist, H.; van der Meer, J. R.; Zehnder, A. J. B. Enrichment and Characterization of an Anammox Bacterium from a Rotating Biological Contactor Treating Ammonium-Rich Leachate. *Archives of Microbiology* 2001, *175* (3), 198–207. https://doi.org/10.1007/s002030100255.
(77) Joss, A.; Derlon, N.; Cyprien, C.; Burger, S.; Szivak, I.; Traber, J.; Siegrist, H.; Morgenroth, E. Combined Nitritation-Anammox: Advances in Understanding Process Stability. *Environmental Science and Technology* 2011, *45* (22), 9735–9742. https://doi.org/10.1021/es202181v.
(78) Mehrabi, S.; Houweling, D.; Dagnew, M. Establishing Mainstream Nitrite Shunt Process in Membrane Aerated Biofilm Reactors: Impact of Organic Carbon and Biofilm Scouring Intensity. *Journal of Water Process Engineering* 2020, *37*, 101460. https://doi.org/10.1016/j.jwpe.2020.101460.
(79) Langeveld, J. G.; Liefting, H. J.; Boogaard, F. C. Uncertainties of Stormwater Characteristics and Removal Rates of Stormwater Treatment Facilities: Implications for Stormwater Handling. *Water Research* 2012, *46* (20), 6868–6880. https://doi.org/10.1016/j.watres.2012.06.001.
(80) Lee, H.; Swamikannu, X.; Radulescu, D.; Kim, S.; Stenstrom, M. K. Design of Stormwater Monitoring Programs. *Water Research* 2007, *41* (18), 4186–4196. https://doi.org/10.1016/j.watres.2007.05.016.
(81) US EPA. Hourly Diurnal Flow Variation in Publically-Owned Wasetwater Treatment Facilities, 1981.
(82) Metcalf and Eddy. *Wastewater Engineering Treatment and Reuse*; 1991.
(83) Pitt, R.; Maestre, A.; Morquecho, R. National Stormwater Quality Database. Version 1.1. 2004.
(84) Zeiger, S.; Hubbart, J. Urban Stormwater Temperature Surges: A Central US Watershed Study. *Hydrology* 2015, *2* (4), 193–209. https://doi.org/10.3390/hydrology2040193.

(85) Brezonik, P. L.; Stadelmann, T. H. Analysis and Predictive Models of Stormwater Runoff Volumes, Loads, and Pollutant Concentrations from Watersheds in the Twin Cities Metropolitan Area, Minnesota, USA. *Water Research* 2002, *36* (7), 1743–1757. https://doi.org/10.1016/S0043-1354(01)00375-X.
(86) Kayhanian, M.; Fruchtman, B. D.; Gulliver, J. S.; Montanaro, C.; Ranieri, E.; Wuertz, S. Review of Highway Runoff Characteristics: Comparative Analysis and Universal Implications. *Water Research* 2012, *46* (20), 6609–6624. https://doi.org/10.1016/j.watres.2012.07.026.
(87) Koch, B. J.; Febria, C. M.; Gevrey, M.; Wainger, L. A.; Palmer, M. A. Nitrogen Removal by Stormwater Management Structures: A Data Synthesis. *J Am Water Resour Assoc* 2014, *50* (6), 1594–1607. https://doi.org/10.1111/jawr.12223.
(88) Gold, A. C.; Thompson, S. P.; Piehler, M. F. Nitrogen Cycling Processes within Stormwater Control Measures: A Review and Call for Research. *Water Research* 2019, *149*, 578–587. https://doi.org/10.1016/j.watres.2018.10.036.
(89) Burgin, A. J.; Hamilton, S. K. Have We Overemphasized the Role of Denitrification in Aquatic Ecosystems? A Review of Nitrate Removal Pathways. *Frontiers in Ecology and the Environment* 2007, *5* (2), 89–96. https://doi.org/10.1890/1540-9295(2007)5[89:HWOTRO]2.0.CO;2.
(90) Sun, Y.; Zhang, D.; Wang, Z.-W. The Potential of Using Biological Nitrogen Removal Technique for Stormwater Treatment. *Ecological Engineering* 2017, *106*, 482–495. https://doi.org/10.1016/j.ecoleng.2017.05.045.
(91) Carvajal-Arroyo, J. M.; Sun, W.; Sierra-Alvarez, R.; Field, J. A. Inhibition of Anaerobic Ammonium Oxidizing (Anammox) Enrichment Cultures by Substrates, Metabolites and Common Wastewater Constituents. *Chemosphere* 2013, *91* (1), 22–27. https://doi.org/10.1016/j.chemosphere.2012.11.025.
(92) Trigo, C.; Campos, J. L.; Garrido, J. M.; Méndez, R. Start-up of the Anammox Process in a Membrane Bioreactor. *Journal of Biotechnology* 2006, *126*, 475–487. https://doi.org/10.1016/j.jbiotec.2006.05.008.
(93) Siegrist, H.; Gujer, W. Demonstration of Mass Transfer and PH Effects in a Nitrifying Biofilm. *Water Research* 1987, *21* (12), 1481–1487. https://doi.org/10.1016/0043-1354(87)90131-X.
(94) Kuenen, J. G.; Jorgi~nsen, B.; Revsnech, N. P. OXYGEN MICROPROFILES OF TRICKLING FILTER BIOFILMS. *Wat. Res* 1986, *20* (12), 1589–1598.
(95) Zhang, L.; Liu, M.; Zhang, S.; Yang, Y.; Peng, Y. Integrated Fixed-Biofilm Activated Sludge Reactor as a Powerful Tool to Enrich Anammox Biofilm and Granular Sludge. 2015. https://doi.org/10.1016/j.chemosphere.2015.02.001.
(96) Frankel, T. How to Select the Right MBBR Media, 2020.
(97) Picioreanu, C.; Kreft, J.-U.; Mark C. M. van Loosdrecht. Particle Based Multidimensional Multispecies Biofilm Model. *Applied and Environmental Microbiology* 2004, *70* (5), 3024–3040. https://doi.org/10.1128/AEM.70.5.3024.
(98) Xavier, B.; Picioreanu, C.; M van Loosdrecht, M. C.; Xavier, J. B.; Picioreanu, C.; M van Loosdrecht, M. C. A Framework for Multidimensional Modelling of Activity and Structure of Multispecies Biofilms. *Environmental Microbiology* 2005, *7* (8), 1085–1103. https://doi.org/10.1111/j.1462-2920.2005.00787.x.
(99) Wanner, O.; Gujer, W. A Multispecies Biofilm Model. *Biotechnology and Bioengineering* 1986, *28* (3), 314–328. https://doi.org/10.1002/bit.260280304.

(100) Horn, H.; Lackner, S. Modeling of Biofilm Systems: A Review; Springer International Publishing, 2014; pp 53–76. https://doi.org/10.1007/10_2014_275.
(101) Horn, H.; Reiff, H.; Morgenroth, E. Simulation of Growth and Detachment in Biofilm Systems under Defined Hydrodynamic Conditions. *Biotechnology and Bioengineering* 2003, *81* (5), 607–617. https://doi.org/10.1002/bit.10503.
(102) Casey, E.; Glennon, B.; Hamer, G. Biofilm Development in a Membrane-Aerated Biofilm Reactor: Effect of Flow Velocity on Performance. *Biotechnology and Bioengineering* 2000, *67* (4), 476–486. https://doi.org/10.1002/(SICI)1097-0290(20000220)67:4<476::AID-BIT11>3.0.CO;2-2.
(103) Cole, A. C.; Semmens, M. J.; LaPara, T. M. Stratification of Activity and Bacterial Community Structure in Biofilms Grown on Membranes Transferring Oxygen. *Applied and Environmental Microbiology* 2004, *70* (4), 1982–1989. https://doi.org/10.1128/AEM.70.4.1982-1989.2004.
(104) Rittmann, B. E.; Manem, J. A. Development and Experimental Evaluation of a Steady-state, Multispecies Biofilm Model. *Biotechnology and Bioengineering* 1992, *39* (9), 914–922. https://doi.org/10.1002/bit.260390906.
(105) LaPara, T. M.; Cole, A. C.; Shanahan, J. W.; Semmens, M. J. The Effects of Organic Carbon, Ammoniacal-Nitrogen, and Oxygen Partial Pressure on the Stratification of Membrane-Aerated Biofilms. *Journal of Industrial Microbiology and Biotechnology* 2006, *33* (4), 315–323. https://doi.org/10.1007/s10295-005-0052-5.
(106) Shanahan, J. W.; Semmens, M. J. Multipopulation Model of Membrane-Aerated Biofilms. *Environmental Science & Technology* 2004, *38* (11), 3176–3183. https://doi.org/10.1021/es034809y.
(107) Kindaichi, T.; Tsushima, I.; Ogasawara, Y.; Shimokawa, M.; Ozaki, N.; Satoh, H.; Okabe, S. In Situ Activity and Spatial Organization of Anaerobic Ammonium-Oxidizing (Anammox) Bacteria in Biofilms. *Applied and environmental microbiology* 2007, *73* (15), 4931–4939. https://doi.org/10.1128/AEM.00156-07.
(108) van der Star, W. R. L.; Miclea, A. I.; van Dongen, U. G. J. M.; Muyzer, G.; Picioreanu, C.; van Loosdrecht, M. C. M. The Membrane Bioreactor: A Novel Tool to Grow Anammox Bacteria as Free Cells. *Biotechnol. Bioeng.* 2008, *101* (2), 286–294. https://doi.org/10.1002/bit.21891.
(109) Fernández, I.; Vázquez-Padín, J. R.; Mosquera-Corral, A.; Campos, J. L.; Méndez, R. Biofilm and Granular Systems to Improve Anammox Biomass Retention. *Biochemical Engineering Journal* 2008, *42*, 308–313. https://doi.org/10.1016/j.bej.2008.07.011.
(110) Bagchi, S.; Lamendella, R.; Strutt, S.; Van Loosdrecht, M. C. M.; Saikaly, P. E. Metatranscriptomics Reveals the Molecular Mechanism of Large Granule Formation in Granular Anammox Reactor. *Scientific Reports* 2016, *6* (1), 28327. https://doi.org/10.1038/srep28327.
(111) Brindle, K.; Stephenson, T.; Semmens, M. J. Nitrification and Oxygen Utilisation in a Membrane Aeration Bioreactor. *Journal of Membrane Science* 1998, *144* (1–2), 197–209. https://doi.org/10.1016/S0376-7388(98)00047-7.
(112) Pellicer-Nàcher, C.; Franck, S.; Gülay, A.; Ruscalleda, M.; Terada, A.; Al-Soud, W. A.; Hansen, M. A.; Sørensen, S. J.; Smets, B. F. Sequentially Aerated Membrane Biofilm Reactors for Autotrophic Nitrogen Removal: Microbial

Community Composition and Dynamics. *Microbial Biotechnology* 2014, *7* (1), 32–43. https://doi.org/10.1111/1751-7915.12079.
(113) Semmens, M. J.; Dahm, K.; Shanahan, J.; Christianson, A. COD and Nitrogen Removal by Biofilms Growing on Gas Permeable Membranes. *Water Research* 2003, *37* (18), 4343–4350. https://doi.org/10.1016/S0043-1354(03)00416-0.
(114) Ahmadi Motlagh, A. R.; LaPara, T. M.; Semmens, M. J. Ammonium Removal in Advective-Flow Membrane-Aerated Biofilm Reactors (AF-MABRs). *Journal of Membrane Science* 2008, *319* (1–2), 76–81. https://doi.org/10.1016/j.memsci.2008.03.020.
(115) Uri-Carreño, N.; Nielsen, P. H.; Gernaey, K. V.; Flores-Alsina, X. Long-Term Operation Assessment of a Full-Scale Membrane-Aerated Biofilm Reactor under Nordic Conditions. *Science of The Total Environment* 2021, *779*, 146366. https://doi.org/10.1016/j.scitotenv.2021.146366.
(116) He, H.; Wagner, B. M.; Carlson, A. L.; Yang, C.; Daigger, G. T. Recent Progress Using Membrane Aerated Biofilm Reactors for Wastewater Treatment. *Water Science and Technology* 2021, *84* (9), 2131–2157. https://doi.org/10.2166/wst.2021.443.
(117) LaPara, T. M.; Cole, A. C.; Shanahan, J. W.; Semmens, M. J. The Effects of Organic Carbon, Ammoniacal-Nitrogen, and Oxygen Partial Pressure on the Stratification of Membrane-Aerated Biofilms. *Journal of Industrial Microbiology and Biotechnology* 2006, *33* (4), 315–323. https://doi.org/10.1007/s10295-005-0052-5.
(118) Soliman, M.; Eldyasti, A. Development of Partial Nitrification as a First Step of Nitrite Shunt Process in a Sequential Batch Reactor (SBR) Using Ammonium Oxidizing Bacteria (AOB) Controlled by Mixing Regime. *Bioresource Technology* 2016, *221*, 85–95. https://doi.org/10.1016/j.biortech.2016.09.023.
(119) Pollice, A.; Tandoi, V.; Lestingi, C. Influence of Aeration and Sludge Retention Time on Ammonium Oxidation to Nitrite and Nitrate. *Water Research* 2002, *36* (10), 2541–2546. https://doi.org/10.1016/S0043-1354(01)00468-7.
(120) Winkler, M. K. H.; Kleerebezem, R.; Kuenen, J. G.; Yang, J.; Van Loosdrecht, M. C. M. Segregation of Biomass in Cyclic Anaerobic/Aerobic Granular Sludge Allows the Enrichment of Anaerobic Ammonium Oxidizing Bacteria at Low Temperatures. *Environ. Sci. Technol* 2011, *45*, 7330–7337. https://doi.org/10.1021/es201388t.
(121) Li, J.; Zhu, L. P.; Xu, Y. Y.; Zhu, B. K. Oxygen Transfer Characteristics of Hydrophilic Treated Polypropylene Hollow Fiber Membranes for Bubbleless Aeration. *Journal of Membrane Science* 2010, *362* (1–2), 47–57. https://doi.org/10.1016/j.memsci.2010.06.013.
(122) Ahmed, T.; Semmens, M. J. Use of Sealed End Hollow Fibers for Bubbleless Membrane Aeration: Experimental Studies. *Journal of Membrane Science* 1992, *69* (1–2), 1–10. https://doi.org/10.1016/0376-7388(92)80162-D.
(123) Mery, C.; Guerrero, L.; Alonso-Gutiérrez, J.; Figueroa, M.; Lema, J. M.; Montalvo, S.; Borja, R. Evaluation of Natural Zeolite as Microorganism Support Medium in Nitrifying Batch Reactors: Influence of Zeolite Particle Size. *Journal of Environmental Science and Health, Part A* 2012, *47* (3), 420–427. https://doi.org/10.1080/10934529.2012.646129.

(124) Huang, X.; Liu, C.; Gao, C.; Wang, Z.; Zhu, G.; Liu, L.; Lin, G. Comparison of Nutrient Removal and Bacterial Communities between Natural Zeolite-Based and Volcanic Rock-Based Vertical Flow Constructed Wetlands Treating Piggery Wastewater. 2013. https://doi.org/10.1080/19443994.2012.747422.
(125) Zhu, X.; Tian, J.; Liu, C.; Chen, L. Composition and Dynamics of Microbial Community in a Zeolite Biofilter-Membrane Bioreactor Treating Coking Wastewater. *Applied Microbiology and Biotechnology* 2013, *97* (19), 8767–8775. https://doi.org/10.1007/s00253-012-4558-2.
(126) Miazga-Rodriguez, M.; Han, S.; Yakiwchuk, B.; Wei, K.; English, C.; Bourn, S.; Bohnert, S.; Stein, L. Y. Enhancing Nitrification at Low Temperature with Zeolite in a Mining Operations Retention Pond. *Frontiers in Microbiology* 2012, *3* (JUL), 1–9. https://doi.org/10.3389/fmicb.2012.00271.
(127) Semmens, M. J.; Goodrich, R. R. Biological Regeneration of Ammonium-Saturated Clinoptilolite. I. Initial Observations. *Environ. Sci. Technol.* 1977, *11* (3), 255–259. https://doi.org/10.1021/es60126a010.
(128) Yapsakli, K.; Aktan, C. K.; Mertoglu, B. Anammox-Zeolite System Acting as Buffer to Achieve Stable Effluent Nitrogen Values. *Biodegradation* 2017, *28* (1), 69–79. https://doi.org/10.1007/s10532-016-9778-1.
(129) Grismer, M. E.; Collison, R. S. The Zeolite-Anammox Treatment Process for Nitrogen Removal from Wastewater-A Review. *Water (Switzerland)* 2017, *9* (11). https://doi.org/10.3390/w9110901.
(130) Pei, Y.; Wang, J.; Wang, Z.; Tian, B. Anammox Bacteria Community and Nitrogen Removal in a Strip-like Wetland in the Riparian Zone. *Journal of Environmental Science and Health, Part A* 2011, *46* (7), 715–722. https://doi.org/10.1080/10934529.2011.571582.
(131) Yapsakli, K.; Aktan, C. K.; Mertoglu, B. Anammox-Zeolite System Acting as Buffer to Achieve Stable Effluent Nitrogen Values. *Biodegradation* 2017, *28* (1), 69–79. https://doi.org/10.1007/s10532-016-9778-1.
(132) Montalvo, S.; Guerrero, L.; Borja, R.; Sánchez, E.; Milán, Z.; Cortés, I.; Angeles de la la Rubia, M. Application of Natural Zeolites in Anaerobic Digestion Processes: A Review. *Applied Clay Science* 2012, *58*, 125–133. https://doi.org/10.1016/j.clay.2012.01.013.
(133) Chen, S.; Sun, D.; Chung, J.-S. Simultaneous Removal of COD and Ammonium from Landfill Leachate Using an Anaerobic–Aerobic Moving-Bed Biofilm Reactor System. *Waste Management* 2008, *28* (2), 339–346. https://doi.org/10.1016/j.wasman.2007.01.004.
(134) Lv, P.; Luo, J.; Zhuang, X.; Zhang, D.; Huang, Z.; Bai, Z. Diversity of Culturable Aerobic Denitrifying Bacteria in the Sediment, Water and Biofilms in Liangshui River of Beijing, China. *Scientific Reports* 2017, *7* (1), 10032. https://doi.org/10.1038/s41598-017-09556-9.
(135) Klieve, J. R.; Semmens, M. J. An Evaluation of Pretreated Natural Zeolites for Ammonium Removal. *Water Research* 1980, *14* (2), 161–168. https://doi.org/10.1016/0043-1354(80)90232-8.
(136) Martin, K. J.; Nerenberg, R. The Membrane Biofilm Reactor (MBfR) for Water and Wastewater Treatment: Principles, Applications, and Recent Developments.

Bioresource Technology 2012, *122*, 83–94. https://doi.org/10.1016/j.biortech.2012.02.110.
(137) Huff Chester, A. L.; Eum, K.; Tsapatsis, M.; Hillmyer, M. A.; Novak, P. J. Enhanced Nitrogen Removal and Anammox Bacteria Retention with Zeolite-Coated Membrane in Simulated Mainstream Wastewater. *Environ. Sci. Technol. Lett.* 2021, *8* (6), 468–473. https://doi.org/10.1021/acs.estlett.1c00154.
(138) Borchardt, D.; Gordon, C.; Alcamo, J.; Dannis, J.; Müller, R.; Mensah, A. *Solutions to the Water Quality Challenge: A Preliminary Review.*; UNEP, A Snapshot of the World's Water Quality: Towards a Global Assessment; 162p; United Nations Environment Programme: Nairobi; pp 81–93.
(139) Arnold, K. E.; Brown, A. R.; Ankley, G. T.; Sumpter, J. P. Medicating the Environment: Assessing Risks of Pharmaceuticals to Wildlife and Ecosystems. *Phil. Trans. R. Soc. B* 2014, *369* (1656), 20130569. https://doi.org/10.1098/rstb.2013.0569.
(140) de Jongh, C. M.; Kooij, P. J.; de Voogt, P.; ter Laak, T. L. Screening and Human Health Risk Assessment of Pharmaceuticals and Their Transformation Products in Dutch Surface Waters and Drinking Water. *Science of the Total Environment* 2012, *427*, 70–77.
(141) Kostich, M. S.; Batt, A. L.; Lazorchak, J. M. Concentrations of Prioritized Pharmaceuticals in Effluents from 50 Large Wastewater Treatment Plants in the US and Implications for Risk Estimation. *Environmental Pollution* 2014, *184*, 354–359.
(142) Egbi, C. D.; Anornu, G. K.; Ganyaglo, S. Y.; Appiah-Adjei, E. K.; Li, S.-L.; Dampare, S. B. Nitrate Contamination of Groundwater in the Lower Volta River Basin of Ghana: Sources and Related Human Health Risks. *Ecotoxicology and environmental safety* 2020, *191*, 110227.
(143) Vikesland, P.; Garner, E.; Gupta, S.; Kang, S.; Maile-Moskowitz, A.; Zhu, N. Differential Drivers of Antimicrobial Resistance across the World. *Accounts of chemical research* 2019, *52* (4), 916–924.
(144) Agramont, J.; Gutiérrez-Cortez, S.; Joffré, E.; Sjöling, Å.; Calderon Toledo, C. Fecal Pollution Drives Antibiotic Resistance and Class 1 Integron Abundance in Aquatic Environments of the Bolivian Andes Impacted by Mining and Wastewater. *Microorganisms* 2020, *8* (8), 1122. https://doi.org/10.3390/microorganisms8081122.
(145) Ho, J. Y.; Jong, M.-C.; Acharya, K.; Liew, S. S. X.; Smith, D. R.; Noor, Z. Z.; Goodson, M. L.; Werner, D.; Graham, D. W.; Eswaran, J. Multidrug-Resistant Bacteria and Microbial Communities in a River Estuary with Fragmented Suburban Waste Management. *Journal of hazardous materials* 2021, *405*, 124687.
(146) Thongsamer, T.; Neamchan, R.; Blackburn, A.; Acharya, K.; Sutheeworapong, S.; Tirachulee, B.; Pattanachan, P.; Vinitnantharat, S.; Zhou, X.-Y.; Su, J.-Q. Environmental Antimicrobial Resistance Is Associated with Faecal Pollution in Central Thailand's Coastal Aquaculture Region. *Journal of Hazardous Materials* 2021, *416*, 125718.

(147) Aneck-Hahn, N.; Bornman, M.; De Jager, C. Oestrogenic Activity in Drinking Waters from a Rural Area in the Waterberg District, Limpopo Province, South Africa. *WSA* 2012, *35* (3). https://doi.org/10.4314/wsa.v35i3.76760.
(148) Larsson, D. J. Pollution from Drug Manufacturing: Review and Perspectives. *Philosophical Transactions of the Royal Society B: Biological Sciences* 2014, *369* (1656), 20130571.
(149) Ahrens, L.; Xie, Z.; Ebinghaus, R. Distribution of Perfluoroalkyl Compounds in Seawater from Northern Europe, Atlantic Ocean, and Southern Ocean. *Chemosphere* 2010, *78* (8), 1011–1016. https://doi.org/10.1016/j.chemosphere.2009.11.038.
(150) González-Gaya, B.; Casal, P.; Jurado, E.; Dachs, J.; Jiménez, B. Vertical Transport and Sinks of Perfluoroalkyl Substances in the Global Open Ocean. *Environmental Science: Processes & Impacts* 2019, *21* (11), 1957–1969. https://doi.org/10.1039/C9EM00266A.
(151) González-Gaya, B.; Dachs, J.; Roscales, J. L.; Caballero, G.; Jiménez, B. Perfluoroalkylated Substances in the Global Tropical and Subtropical Surface Oceans. *Environmental Science & Technology* 2014, *48* (22), 13076–13084. https://doi.org/10.1021/es503490z.
(152) Alves, D. D.; Riegel, R. P.; de Quevedo, D. M.; Osório, D. M. M.; da Costa, G. M.; do Nascimento, C. A.; Telöken, F. Seasonal Assessment and Apportionment of Surface Water Pollution Using Multivariate Statistical Methods: Sinos River, Southern Brazil. *Environmental Monitoring and Assessment* 2018, *190* (7), 384. https://doi.org/10.1007/s10661-018-6759-3.
(153) Campo, J.; Lorenzo, M.; Pérez, F.; Picó, Y.; Farré, Marinel. la; Barceló, D. Analysis of the Presence of Perfluoroalkyl Substances in Water, Sediment and Biota of the Jucar River (E Spain). Sources, Partitioning and Relationships with Water Physical Characteristics. *Environmental Research* 2016, *147*, 503–512. https://doi.org/10.1016/j.envres.2016.03.010.
(154) MacInnis, J. J.; French, K.; Muir, D. C. G.; Spencer, C.; Criscitiello, A.; De Silva, A. O.; Young, C. J. Emerging Investigator Series: A 14-Year Depositional Ice Record of Perfluoroalkyl Substances in the High Arctic. *Environ. Sci.: Processes Impacts* 2017, *19* (1), 22–30. https://doi.org/10.1039/C6EM00593D.
(155) Butt, C. M.; Berger, U.; Bossi, R.; Tomy, G. T. Levels and Trends of Poly- and Perfluorinated Compounds in the Arctic Environment. *Science of The Total Environment* 2010, *408* (15), 2936–2965. https://doi.org/10.1016/j.scitotenv.2010.03.015.
(156) Muir, D.; Bossi, R.; Carlsson, P.; Evans, M.; De Silva, A.; Halsall, C.; Rauert, C.; Herzke, D.; Hung, H.; Letcher, R.; Rigét, F.; Roos, A. Levels and Trends of Poly- and Perfluoroalkyl Substances in the Arctic Environment – An Update. *Emerging Contaminants* 2019, *5*, 240–271. https://doi.org/10.1016/j.emcon.2019.06.002.
(157) Vento, S. D.; Halsall, C.; Gioia, R.; Jones, K.; Dachs, J. Volatile Per- and Polyfluoroalkyl Compounds in the Remote Atmosphere of the Western Antarctic Peninsula: An Indirect Source of Perfluoroalkyl Acids to Antarctic Waters? *Atmospheric Pollution Research* 2012, *3* (4), 450–455. https://doi.org/10.5094/APR.2012.051.

(158) Mensah, A.; Gordon, C. Water Pollution in River Basins: River Basin 3-Volta, In UNEP, A Snapshot of the World's Water Quality: Towards a Global Assessment. *United Nations Environment Programme: Nairobi*. 2016, pp 59–62.
(159) Codjoe, S. N. A.; Appeaning Addo, K.; Addoquaye Tagoe, C.; Nyarko, B. K.; Martey, F.; Nelson, W. A.; Jayson-Quashigah, P.-N.; Atiglo, D. Y.; Adjei, P. O.-W.; Anderson, K. The Volta Delta, Ghana: Challenges in an African Setting. In *Deltas in the Anthropocene*; Palgrave Macmillan, Cham, 2020; pp 79–102.
(160) Karikari, A. Assessment of Environmental Impacts of Cage Aquaculture on Lake Volta of Ghana. *University of Science and Technology, Kumasi, Ghana (Doctoral dissertation)* 2017.
(161) CSIR, W. *Annual Report 2016*; 2016.
(162) Xiong, W.; Sun, Y.; Zhang, T.; Ding, X.; Li, Y.; Wang, M.; Zeng, Z. Antibiotics, Antibiotic Resistance Genes, and Bacterial Community Composition in Fresh Water Aquaculture Environment in China. *Microb Ecol* 2015, *70* (2), 425–432. https://doi.org/10.1007/s00248-015-0583-x.
(163) Clottey, M.; Asmah, R.; Ofori-Danson, P.; Ameworwor, M.; Karikari, A. Impacts of Cage Culture on Physico-Chemical and Bacteriological Water Quality in Lake Volta, Ghana. *African Journal of Aquatic Science* 2016, *41* (4), 473–480.
(164) Han, Y.; Wang, J.; Zhao, Z.; Chen, J.; Lu, H.; Liu, G. Fishmeal Application Induces Antibiotic Resistance Gene Propagation in Mariculture Sediment. *Environmental Science and Technology* 2017, *51* (18), 10850–10860. https://doi.org/10.1021/acs.est.7b02875.
(165) Konadu, L. Effects of Fish Cage Culture on Sediment and Water Quality in the Gorge Area of the Volta Lake. 2017.
(166) Gao, Q.; Li, Y.; Qi, Z.; Yue, Y.; Min, M.; Peng, S.; Shi, Z.; Gao, Y. Diverse and Abundant Antibiotic Resistance Genes from Mariculture Sites of China's Coastline. *Science of the Total Environment* 2018, *630*, 117–125.
(167) Liyanage, G. Y.; Manage, P. M. Occurrence and Distribution of Tetracycline Resistance Determinants and Their Pollution Profile in Selected Aquaculture Environments in Sri Lanka. 2019.
(168) Andah, W.; Van de Giesen, N.; Biney, C. Water, Climate, Food, and Environment in the Volta Basin, 2004.
(169) Egbi, C. D.; Anornu, G.; Appiah-Adjei, E. K.; Ganyaglo, S. Y.; Dampare, S. B. Evaluation of Water Quality Using Hydrochemistry, Stable Isotopes, and Water Quality Indices in the Lower Volta River Basin of Ghana. *Environment, Development and Sustainability* 2019, *21* (6), 3033–3063.
(170) Ashraf, M. A.; Maah, M. J.; Yusoff, I.; Wajid, A.; Mahmood, K. Sand Mining Effects, Causes and Concerns: A Case Study from Bestari Jaya, Selangor, Peninsular Malaysia. *Scientific Research and Essays* 2011, *6* (6), 1216–1231.
(171) Kim, S.-C.; Carlson, K. Quantification of Human and Veterinary Antibiotics in Water and Sediment Using SPE/LC/MS/MS. *Analytical and bioanalytical chemistry* 2007, *387* (4), 1301–1315.
(172) Zhou, Z.; Liang, Y.; Shi, Y.; Xu, L.; Cai, Y. Occurrence and Transport of Perfluoroalkyl Acids (PFAAs), Including Short-Chain PFAAs in Tangxun Lake, China. *Environmental science & technology* 2013, *47* (16), 9249–9257.

(173) Schymanski, E. L.; Jeon, J.; Gulde, R.; Fenner, K.; Ruff, M.; Singer, H. P.; Hollender, J. Identifying Small Molecules via High Resolution Mass Spectrometry: Communicating Confidence. 2014.
(174) LaPara, T. M.; Wilkinson, K. H.; Strait, J. M.; Hozalski, R. M.; Sadowksy, M. J.; Hamilton, M. J. The Bacterial Communities of Full-Scale Biologically Active, Granular Activated Carbon Filters Are Stable and Diverse and Potentially Contain Novel Ammonia-Oxidizing Microorganisms. *Applied and Environmental Microbiology* 2015, *81* (19), 6864–6872. https://doi.org/10.1128/AEM.01692-15.
(175) Callahan, B. J.; McMurdie, P. J.; Rosen, M. J.; Han, A. W.; Johnson, A. J. A.; Holmes, S. P. DADA2: High-Resolution Sample Inference from Illumina Amplicon Data. *Nature Methods* 2016, *13* (7), 581–583. https://doi.org/10.1038/nmeth.3869.
(176) Quast, C.; Pruesse, E.; Yilmaz, P.; Gerken, J.; Schweer, T.; Yarza, P.; Peplies, J.; Glöckner, F. O. The SILVA Ribosomal RNA Gene Database Project: Improved Data Processing and Web-Based Tools. *Nucleic Acids Research* 2013, *41* (D1), 590–596. https://doi.org/10.1093/nar/gks1219.
(177) Kasprzyk-Hordern, B.; Dinsdale, R. M.; Guwy, A. J. The Occurrence of Pharmaceuticals, Personal Care Products, Endocrine Disruptors and Illicit Drugs in Surface Water in South Wales, UK. *Water research* 2008, *42* (13), 3498–3518.
(178) Kairigo, P.; Ngumba, E.; Sundberg, L.-R.; Gachanja, A.; Tuhkanen, T. Occurrence of Antibiotics and Risk of Antibiotic Resistance Evolution in Selected Kenyan Wastewaters, Surface Waters and Sediments. *Science of the Total Environment* 2020, *720*, 137580.
(179) Kemper, N. Veterinary Antibiotics in the Aquatic and Terrestrial Environment. *Ecological Indicators* 2008, *8* (1), 1–13. https://doi.org/10.1016/j.ecolind.2007.06.002.
(180) Zou, S.; Xu, W.; Zhang, R.; Tang, J.; Chen, Y.; Zhang, G. Occurrence and Distribution of Antibiotics in Coastal Water of the Bohai Bay, China: Impacts of River Discharge and Aquaculture Activities. *Environmental Pollution* 2011, *159* (10), 2913–2920.
(181) Muziasari, W. I.; Managaki, S.; Pärnänen, K.; Karkman, A.; Lyra, C.; Tamminen, M.; Suzuki, S.; Virta, M. Sulphonamide and Trimethoprim Resistance Genes Persist in Sediments at Baltic Sea Aquaculture Farms but Are Not Detected in the Surrounding Environment. *PLoS One* 2014, *9* (3), e92702.
(182) Defoirdt, T.; Sorgeloos, P.; Bossier, P. Alternatives to Antibiotics for the Control of Bacterial Disease in Aquaculture. *Current opinion in microbiology* 2011, *14* (3), 251–258.
(183) Chen, H.; Liu, S.; Xu, X.-R.; Diao, Z.-H.; Sun, K.-F.; Hao, Q.-W.; Liu, S.-S.; Ying, G.-G. Tissue Distribution, Bioaccumulation Characteristics and Health Risk of Antibiotics in Cultured Fish from a Typical Aquaculture Area. *Journal of hazardous materials* 2018, *343*, 140–148.
(184) Dawood, M. A.; Koshio, S.; Esteban, M. Á. Beneficial Roles of Feed Additives as Immunostimulants in Aquaculture: A Review. *Reviews in Aquaculture* 2018, *10* (4), 950–974.
(185) Elliott, S. M.; Brigham, M. E.; Lee, K. E.; Banda, J. A.; Choy, S. J.; Gefell, D. J.; Minarik, T. A.; Moore, J. N.; Jorgenson, Z. G. Contaminants of Emerging

Concern in Tributaries to the Laurentian Great Lakes: I. Patterns of Occurrence. *PloS one* 2017, *12* (9), e0182868.
(186) Zhao, P.; Xia, X.; Dong, J.; Xia, N.; Jiang, X.; Li, Y.; Zhu, Y. Short- and Long-Chain Perfluoroalkyl Substances in the Water, Suspended Particulate Matter, and Surface Sediment of a Turbid River. *Science of The Total Environment* 2016, *568*, 57–65. https://doi.org/10.1016/j.scitotenv.2016.05.221.
(187) Lam, N.-H.; Cho, C.-R.; Lee, J.-S.; Soh, H.-Y.; Lee, B.-C.; Lee, J.-A.; Tatarozako, N.; Sasaki, K.; Saito, N.; Iwabuchi, K.; Kannan, K.; Cho, H.-S. Perfluorinated Alkyl Substances in Water, Sediment, Plankton and Fish from Korean Rivers and Lakes: A Nationwide Survey. *Science of The Total Environment* 2014, *491–492*, 154–162. https://doi.org/10.1016/j.scitotenv.2014.01.045.
(188) Möller, A.; Ahrens, L.; Surm, R.; Westerveld, J.; van der Wielen, F.; Ebinghaus, R.; de Voogt, P. Distribution and Sources of Polyfluoroalkyl Substances (PFAS) in the River Rhine Watershed. *Environmental Pollution* 2010, *158* (10), 3243–3250. https://doi.org/10.1016/j.envpol.2010.07.019.
(189) Van Leeuwen, S.; De Boer, J. Extraction and Clean-up Strategies for the Analysis of Poly-and Perfluoroalkyl Substances in Environmental and Human Matrices. *Journal of Chromatography A* 2007, *1153* (1–2), 172–185.
(190) Almakki, A.; Jumas-Bilak, E.; Marchandin, H.; Licznar-Fajardo, P. Antibiotic Resistance in Urban Runoff. *Science of The Total Environment* 2019, *667*, 64–76. https://doi.org/10.1016/j.scitotenv.2019.02.183.
(191) Han, Y.; Zhou, Z.-C.; Zhu, L.; Wei, Y.-Y.; Feng, W.-Q.; Xu, L.; Liu, Y.; Lin, Z.-J.; Shuai, X.-Y.; Zhang, Z.-J. The Impact and Mechanism of Quaternary Ammonium Compounds on the Transmission of Antibiotic Resistance Genes. *Environmental Science and Pollution Research* 2019, *26* (27), 28352–28360.
(192) Nnadozie, C. F.; Odume, O. N. Freshwater Environments as Reservoirs of Antibiotic Resistant Bacteria and Their Role in the Dissemination of Antibiotic Resistance Genes. *Environmental Pollution* 2019, *254*, 113067.
(193) Devarajan, N.; Laffite, A.; Mulaji, C. K.; Otamonga, J.-P.; Mpiana, P. T.; Mubedi, J. I.; Prabakar, K.; Ibelings, B. W.; Poté, J. Occurrence of Antibiotic Resistance Genes and Bacterial Markers in a Tropical River Receiving Hospital and Urban Wastewaters. *PloS one* 2016, *11* (2), e0149211.
(194) Gao, P.; Mao, D.; Luo, Y.; Wang, L.; Xu, B.; Xu, L. Occurrence of Sulfonamide and Tetracycline-Resistant Bacteria and Resistance Genes in Aquaculture Environment. *Water research* 2012, *46* (7), 2355–2364.
(195) Fang, H.; Huang, K.; Yu, J.; Ding, C.; Wang, Z.; Zhao, C.; Yuan, H.; Wang, Z.; Wang, S.; Hu, J. Metagenomic Analysis of Bacterial Communities and Antibiotic Resistance Genes in the Eriocheir Sinensis Freshwater Aquaculture Environment. *Chemosphere* 2019, *224*, 202–211.
(196) Sauvé, S.; Desrosiers, M. A Review of What Is an Emerging Contaminant. *Chemistry Central Journal* 2014, *8* (1), 15. https://doi.org/10.1186/1752-153X-8-15.
(197) Dekić, S.; Klobučar, G.; Ivanković, T.; Zanella, D.; Vucić, M.; Bourdineaud, J.-P.; Hrenović, J. Emerging Human Pathogen Acinetobacter Baumannii in the Natural Aquatic Environment: A Public Health Risk? *International Journal of Environmental Health Research* 2018, *28* (3), 315–322.

(198) Ouyang, L.; Chen, H.; Liu, X.; Wong, M. H.; Xu, F.; Yang, X.; Xu, W.; Zeng, Q.; Wang, W.; Li, S. Characteristics of Spatial and Seasonal Bacterial Community Structures in a River under Anthropogenic Disturbances. *Environmental Pollution* 2020, *264*. https://doi.org/10.1016/j.envpol.2020.114818.
(199) Ott, A.; O'Donnell, G.; Tran, N. H.; Mohd Haniffah, M. R.; Su, J.-Q.; Zealand, A. M.; Gin, K. Y.-H.; Goodson, M. L.; Zhu, Y.-G.; Graham, D. W. Developing Surrogate Markers for Predicting Antibiotic Resistance "Hot Spots" in Rivers Where Limited Data Are Available. *Environmental Science & Technology* 2021, *55* (11), 7466–7478. https://doi.org/10.1021/acs.est.1c00939.
(200) Fairbairn, D. J.; Karpuzcu, M. E.; Arnold, W. A.; Barber, B. L.; Kaufenberg, E. F.; Koskinen, W. C.; Novak, P. J.; Rice, P. J.; Swackhamer, D. L. Sources and Transport of Contaminants of Emerging Concern: A Two-Year Study of Occurrence and Spatiotemporal Variation in a Mixed Land Use Watershed. *Science of the Total Environment* 2016, *551*, 605–613.
(201) Li, X.; Klaus, S.; Bott, C.; He, Z. Status, Challenges, and Perspectives of Mainstream Nitritation-Anammox for Wastewater Treatment. *Water Environment Research* 2018, *90* (7), 634–649. https://doi.org/10.2175/106143017x15131012153112.
(202) Xu, G.; Zhou, Y.; Yang, Q.; Lee, Z. M.-P.; Gu, J.; Lay, W.; Cao, Y.; Liu, Y. The Challenges of Mainstream Deammonification Process for Municipal Used Water Treatment. *Applied Microbiology and Biotechnology* 2015, *99* (6), 2485–2490. https://doi.org/10.1007/s00253-015-6423-6.
(203) Winkler, M. K.; Straka, L. New Directions in Biological Nitrogen Removal and Recovery from Wastewater. *Current Opinion in Biotechnology* 2019, *57*, 50–55. https://doi.org/10.1016/j.copbio.2018.12.007.
(204) Jin, R.-C.; Yang, G.-F.; Yu, J.-J.; Zheng, P. The Inhibition of the Anammox Process: A Review. *Chemical Engineering Journal* 2012, *197*, 67–79. https://doi.org/10.1016/J.CEJ.2012.05.014.
(205) Wells, G. F.; Shi, Y.; Laureni, M.; Rosenthal, A.; Sziva, I.; Weissbrodt, D. G.; Joss, A.; Buergmann, H.; Johnson, D. R.; Morgenroth, E. Comparing the Resistance, Resilience, and Stability of Replicate Moving Bed Biofilm and Suspended Growth Combined Nitritation− Anammox Reactors. *Environmental Science & Technology* 2017, *51*, 5108–5117. https://doi.org/10.1021/acs.est.6b05878.
(206) Van Der Star, W. R. L.; Miclea, A. I.; Van Dongen, U. G. J. M.; Muyzer, G.; Picioreanu, C.; Van Loosdrecht, M. C. M. The Membrane Bioreactor: A Novel Tool to Grow Anammox Bacteria as Free Cells. *Biotechnology and Bioengineering* 2008, *101* (2), 286–294. https://doi.org/10.1002/bit.21891.
(207) Abbassi, R.; Yadav, A. K.; Huang, S.; Jaffé, P. R. Laboratory Study of Nitrification, Denitrification and Anammox Processes in Membrane Bioreactors Considering Periodic Aeration. *Journal of Environmental Management* 2014, *142*, 53–59. https://doi.org/10.1016/j.jenvman.2014.03.013.
(208) Wett, B.; Omari, A.; Podmirseg, S. M.; Han, M.; Akintayo, O.; Gómez Brandón, M.; Murthy, S.; Bott, C.; Hell, M.; Takács, I.; Nyhuis, G.; O'Shaughnessy, M. Going for Mainstream Deammonification from Bench to Full Scale for

Maximized Resource Efficiency. *Water Science and Technology* 2013, *68* (2), 283–289. https://doi.org/10.2166/wst.2013.150.
(209) Ma, Y.; Domingo-Félez, C.; Plósz, B. Gy.; Smets, B. F. Intermittent Aeration Suppresses Nitrite-Oxidizing Bacteria in Membrane-Aerated Biofilms: A Model-Based Explanation. *Environmental Science & Technology* 2017, *51* (11), 6146–6155. https://doi.org/10.1021/acs.est.7b00463.
(210) Johnson, D. W.; Semmens, M. J.; Gulliver, J. S. A Rotating Membrane Contactor: Application to Biologically Active Systems. *Water Environment Research* 1999, *71* (2), 163–168. https://doi.org/10.2175/106143099x121382.
(211) Li, J.; Zhu, L. P.; Xu, Y. Y.; Zhu, B. K. Oxygen Transfer Characteristics of Hydrophilic Treated Polypropylene Hollow Fiber Membranes for Bubbleless Aeration. *Journal of Membrane Science* 2010, *362* (1–2), 47–57. https://doi.org/10.1016/j.memsci.2010.06.013.
(212) Li, T.; Liu, J.; Bai, R. Membrane Aerated Biofilm Reactors: A Brief Current Review. *Recent Patents on Biotechnology* 2008, *2* (2), 88–93. https://doi.org/10.2174/187220808784619739.
(213) Lackner, S.; Terada, A.; Horn, H.; Henze, M.; Smets, B. F. Nitritation Performance in Membrane-Aerated Biofilm Reactors Differs from Conventional Biofilm Systems. *Water Research* 2010, *44* (20), 6073–6084. https://doi.org/10.1016/J.WATRES.2010.07.074.
(214) Pellicer-Nàcher, C.; Sun, S.; Lackner, S.; Terada, A.; Schreiber, F.; Zhou, Q.; Smets, B. F. Sequential Aeration of Membrane-Aerated Biofilm Reactors for High-Rate Autotrophic Nitrogen Removal: Experimental Demonstration. *Environmental Science and Technology* 2010, *44* (19), 7628–7634. https://doi.org/10.1021/es1013467.
(215) Pellicer-Nàcher, C.; Franck, S.; Gülay, A.; Ruscalleda, M.; Terada, A.; Al-Soud, W. A.; Hansen, M. A.; Sørensen, S. J.; Smets, B. F. Sequentially Aerated Membrane Biofilm Reactors for Autotrophic Nitrogen Removal: Microbial Community Composition and Dynamics. *Microbial Biotechnology* 2014, *7* (1), 32–43. https://doi.org/10.1111/1751-7915.12079.
(216) Ahmadi Motlagh, A. R.; LaPara, T. M.; Semmens, M. J. Ammonium Removal in Advective-Flow Membrane-Aerated Biofilm Reactors (AF-MABRs). *Journal of Membrane Science* 2008, *319* (1–2), 76–81. https://doi.org/10.1016/j.memsci.2008.03.020.
(217) Margeta, K.; Zabukovec, N.; Siljeg, M.; Farkas, A. Natural Zeolites in Water Treatment – How Effective Is Their Use. In *Water Treatment*; InTech, 2013. https://doi.org/10.5772/50738.
(218) Martins, T. H.; Souza, T. S. O.; Foresti, E. Ammonium Removal from Landfill Leachate by Clinoptilolite Adsorption Followed by Bioregeneration. *Journal of Environmental Chemical Engineering* 2017, *5* (1), 63–68. https://doi.org/10.1016/j.jece.2016.11.024.
(219) Lahav, O.; Green, M. Ammonium Removal from Primary and Secondary Effluents Using a Bioregenerated Ion-Exchange Process. In *Water Science & Technology*; Int Water Assoc, 2000; Vol. 42, pp 179–185. https://doi.org/10.2166/wst.2000.0311.

(220) Fernández, I.; Vázquez-Padín, J. R.; Mosquera-Corral, A.; Campos, J. L.; Méndez, R. Biofilm and Granular Systems to Improve Anammox Biomass Retention. *Biochemical Engineering Journal* 2008, *42*, 308–313. https://doi.org/10.1016/j.bej.2008.07.011.
(221) Novak, P.; Romero-Vargas Castrillón, S.; Huff, A.; Hillmyer, M.; Tsapatsis, M. SYSTEMS AND METHODS FOR TREATING WASTEWATER. 16/433,915, 2019.
(222) Shao, J.; Zhan, Z.; Li, J.; Wang, Z.; Li, K.; Yan, Y. Zeolite NaA Membranes Supported on Alumina Hollow Fibers: Effect of Support Resistances on Pervaporation Performance. *Journal of Membrane Science journal* 2013, *451* (2014), 10–17. https://doi.org/10.1016/j.memsci.2013.09.049.
(223) Eum, K.; Hayashi, M.; De Mello, M. D.; Xue, F.; Kwon, H. T.; Tsapatsis, M. ZIF-8 Membrane Separation Performance Tuning by Vapor Phase Ligand Treatment. *Angewandte Chemie* 2019, *131* (46), 16542–16546. https://doi.org/10.1002/ange.201909490.
(224) Peterson, K. N.; Tan, D. T.; Bezares-Cruz, J. C.; Novak, P. J. Estrone Biodegradation in Laboratory-Scale Systems Designed for Total Nitrogen Removal from Wastewater. *Environmental Science: Water Research & Technology* 2017, *3* (6), 1051–1060. https://doi.org/10.1039/C7EW00164A.
(225) Han, P.; Gu, J.-D. More Refined Diversity of Anammox Bacteria Recovered and Distribution in Different Ecosystems. *Applied Microbiology and Biotechnology* 2013, *97* (8), 3653–3663. https://doi.org/10.1007/s00253-013-4756-6.
(226) Karolewski, J. S.; Sutherland, K. M.; Hansel, C. M.; Wankel, S. D. An Isotopic Study of Abiotic Nitrite Oxidation by Ligand-Bound Manganese (III). *Geochimica et Cosmochimica Acta* 2021, *293*, 365–378. https://doi.org/10.1016/j.gca.2020.11.004.
(227) Lim, N. Y. N.; Frostegård, Å.; Bakken, L. R. Nitrite Kinetics during Anoxia: The Role of Abiotic Reactions versus Microbial Reduction. *Soil Biology and Biochemistry* 2018, *119* (January), 203–209. https://doi.org/10.1016/j.soilbio.2018.01.006.
(228) Choi, E. Y.; Nam, I. S.; Kim, Y. G. TPD Study of Mordenite-Type Zeolites for Selective Catalytic Reduction of NO by NH3. *Journal of Catalysis* 1996, *161* (2), 597–604. https://doi.org/10.1006/jcat.1996.0222.
(229) Centi, G.; Perathoner, S.; Biglino, D.; Giamello, E. Adsorption and Reactivity of NO on Copper-on-Alumina Catalysts: I. Formation of Nitrate Species and Their Influence on Reactivity in NO and NH3 Conversion. *Journal of Catalysis* 1995, *152* (1), 75–92. https://doi.org/10.1006/jcat.1995.1062.
(230) Lu, D.; Bai, H.; Kong, F.; Liss, S. N.; Liao, B. Recent Advances in Membrane Aerated Biofilm Reactors. *Critical Reviews in Environmental Science and Technology* 2020. https://doi.org/10.1080/10643389.2020.1734432.
(231) Augusto, M. R.; Camiloti, P. R.; Souza, T. S. O. de. Fast Start-up of the Single-Stage Nitrogen Removal Using Anammox and Partial Nitritation (SNAP) from Conventional Activated Sludge in a Membrane-Aerated Biofilm Reactor. *Bioresource Technology* 2018, *266*, 151–157. https://doi.org/10.1016/j.biortech.2018.06.068.

(232) Mulder, A. The Quest for Sustainable Nitrogen Removal Technologies. *Water Science & Technology* 2003, *48* (1), 67–75.
(233) Zhu, G.; Peng, Y. Biological Nitrogen Removal with Nitrification and Denitrification via Nitrite Pathway. *Harbin Gongye Daxue Xuebao/Journal of Harbin Institute of Technology* 2008, *40* (10), 1552–1557. https://doi.org/10.1007/s00253-006-0534-z.
(234) Strous, M.; Heijnen, J. J.; Kuenen, J. G.; Jetten, M. S. M. The Sequencing Batch Reactor as a Powerful Tool for the Study of Slowly Growing Anaerobic Ammonium-Oxidizing Microorganisms. *Applied Microbiology and Biotechnology* 1998, *50* (5), 589–596. https://doi.org/10.1007/s002530051340.
(235) Zhang, L.; Okabe, S. Ecological Niche Differentiation among Anammox Bacteria. *Water Research* 2020, *171*, 115468. https://doi.org/10.1016/j.watres.2020.115468.
(236) Vlaeminck, S. E.; Terada, A.; Smets, B. F.; De Clippeleir, H.; Schaubroeck, T.; Bolca, S.; Demeestere, L.; Mast, J.; Boon, N.; Carballa, M.; Verstraete, W. Aggregate Size and Architecture Determine Microbial Activity Balance for One-Stage Partial Nitritation and Anammox. *Applied and environmental microbiology* 2010, *76* (3), 900–909. https://doi.org/10.1128/AEM.02337-09.
(237) Li, T.; Liu, J.; Bai, R. Membrane Aerated Biofilm Reactors: A Brief Current Review. *Recent Patents on Biotechnology* 2008, *2* (2), 88–93. https://doi.org/10.2174/187220808784619739.
(238) Fernández, I.; Vázquez-Padín, J. R.; Mosquera-Corral, A.; Campos, J. L.; Méndez, R. Biofilm and Granular Systems to Improve Anammox Biomass Retention. *Biochemical Engineering Journal* 2008, *42* (3), 308–313. https://doi.org/10.1016/j.bej.2008.07.011.
(239) Feinberg, E. C.; Chester, A. L. H.; Novak, P. J.; Hillmyer, M. A. Porous Polyethylene-Supported Zeolite Carriers for Improved Wastewater Deammonification. *ACS ES&T Engineering* 2021, *1* (7), 1104–1112. https://doi.org/10.1021/ACSESTENGG.1C00077.
(240) Kulak, A.; Lee, Y.-J.; Park, Y. S.; Yoon, K. B. Orientation-Controlled Monolayer Assembly of Zeolite Crystals on Glass and Mica by Covalent Linkage of Surface-Bound Epoxide and Amine Groups. *Angewandte Chemie* 2000, *112* (5), 980–983. https://doi.org/10.1002/(SICI)1521-3757(20000303)112:5<980::AID-ANGE980>3.0.CO;2-5.
(241) Wuolo-Journey, K.; BinAhmed, S.; Linna, E.; Romero-Vargas Castrillón, S. Do Graphene Oxide Nanostructured Coatings Mitigate Bacterial Adhesion? *Environ. Sci.: Nano* 2019, *6* (9), 2863–2875. https://doi.org/10.1039/C9EN00499H.
(242) Feinberg, E. C. *SEM Image of Porous Polyethylene-Supported Zeolite Carriers*; 2021.
(243) Lahav, O.; Green, M. Bioregenerated Ion-Exchange Process: The Effect of the Biofilm on the Ion-Exchange Capacity and Kinetics. 2000.
(244) Martins, T. H.; Souza, T. S. O.; Foresti, E. Ammonium Removal from Landfill Leachate by Clinoptilolite Adsorption Followed by Bioregeneration. *Journal of Environmental Chemical Engineering* 2017, *5* (1), 63–68. https://doi.org/10.1016/j.jece.2016.11.024.

(245) Lahav, O.; Green, M. Ammonium Removal from Primary and Secondary Effluents Using a Bioregenerated Ion - Exchange Process. *Water Science & Technology* 2000, *42* (1–2), 179–185.
(246) Wiesmann, U. Biological Nitrogen Removal from Wastewater. In *Biotechnics/Wastewater*; Fiechter, A., Blanch, H. W., Bungay, H. R., Cooney, Ch. L., Demain, A. L., Enfors, S.-O., Eriksson, K.-E. L., Kieslich, K., Klibanov, A. M., Lafferty, R. M., Mattiasson, B., Primrose, S. B., Rehm, H. J., Rogers, P. L., Sahm, H., Schügerl, K., von Stockar, U., Tsao, G. T., Venkat, K., Wandrey, C., Series Eds.; Advances in Biochemical Engineering/Biotechnology; Springer Berlin Heidelberg: Berlin, Heidelberg, 1994; Vol. 51, pp 113–154. https://doi.org/10.1007/BFb0008736.
(247) Pei, Y.; Wang, J.; Wang, Z.; Tian, B. Anammox Bacteria Community and Nitrogen Removal in a Strip-like Wetland in the Riparian Zone. *Journal of Environmental Science and Health, Part A* 2011, *46* (7), 715–722. https://doi.org/10.1080/10934529.2011.571582.
(248) Collison, R. S.; Grismer, M. E. Nitrogen and Chemical Oxygen Demand Removal from Septic Tank Wastewater in Subsurface Flow Constructed Wetlands: Substrate (Cation Exchange Capacity) Effects. *Water Environment Research* 2014, *86* (4), 314–323. https://doi.org/10.2175/106143013X13736496908627.
(249) Lv, Y.; Pan, J.; Huo, T.; Zhao, Y.; Liu, S. Enhanced Microbial Metabolism in One Stage Partial Nitritation-Anammox System Treating Low Strength Wastewater by Novel Composite Carrier. *Water Research* 2019, *163*, 114872. https://doi.org/10.1016/j.watres.2019.114872.
(250) Janke, B. D.; Finlay, J. C.; Taguchi, V. J.; Gulliver, J. S. Hydrologic Processes Regulate Nutrient Retention in Stormwater Detention Ponds. *Science of The Total Environment* 2022, *823*, 153722. https://doi.org/10.1016/j.scitotenv.2022.153722.
(251) LeFevre Gregory H.; Paus Kim H.; Natarajan Poornima; Gulliver John S.; Novak Paige J.; Hozalski Raymond M. Review of Dissolved Pollutants in Urban Storm Water and Their Removal and Fate in Bioretention Cells. *Journal of Environmental Engineering* 2015, *141* (1), 04014050. https://doi.org/10.1061/(ASCE)EE.1943-7870.0000876.
(252) Xu, D.; Lee, L. Y.; Lim, F. Y.; Lyu, Z.; Zhu, H.; Ong, S. L.; Hu, J. Water Treatment Residual: A Critical Review of Its Applications on Pollutant Removal from Stormwater Runoff and Future Perspectives. *Journal of Environmental Management* 2020, *259*, 109649. https://doi.org/10.1016/j.jenvman.2019.109649.
(253) Fairbairn, D. J.; Elliott, S. M.; Kiesling, R. L.; Schoenfuss, H. L.; Ferrey, M. L.; Westerhoff, B. M. Contaminants of Emerging Concern in Urban Stormwater: Spatiotemporal Patterns and Removal by Iron-Enhanced Sand Filters (IESFs). *Water Research* 2018, *145*, 332–345. https://doi.org/10.1016/j.watres.2018.08.020.
(254) Tian, Z.; Peter, K. T.; Gipe, A. D.; Zhao, H.; Hou, F.; Wark, D. A.; Khangaonkar, T.; Kolodziej, E. P.; James, C. A. Suspect and Nontarget Screening for Contaminants of Emerging Concern in an Urban Estuary. *Environ. Sci. Technol.* 2020, *54* (2), 889–901. https://doi.org/10.1021/acs.est.9b06126.
(255) Lusk, M. G.; Toor, G. S.; Inglett, P. W. Organic Nitrogen in Residential Stormwater Runoff: Implications for Stormwater Management in Urban

Watersheds. *Science of The Total Environment* 2020, *707*, 135962. https://doi.org/10.1016/j.scitotenv.2019.135962.
(256) Hathaway, J. M.; Moore, T. L. C.; Burkholder, J. M.; Hunt, W. F. Temporal Analysis of Stormwater Control Measure Effluent Based on Windows of Harmful Algal Bloom (HAB) Sensitivity: Are Annual Nutrient EMCs Appropriate during HAB-Sensitive Seasons? *Ecological Engineering* 2012, *49*, 41–47. https://doi.org/10.1016/j.ecoleng.2012.08.014.
(257) Biswal, B. K.; Vijayaraghavan, K.; Adam, M. G.; Lee Tsen-Tieng, D.; Davis, A. P.; Balasubramanian, R. Biological Nitrogen Removal from Stormwater in Bioretention Cells: A Critical Review. *Critical Reviews in Biotechnology* 2021, 1–23. https://doi.org/10.1080/07388551.2021.1969888.
(258) Howarth, R. W. Human Acceleration of the Nitrogen Cycle: Drivers, Consequences, and Steps toward Solutions. *Water Science and Technology* 2004, *49* (5–6), 7–13. https://doi.org/10.2166/wst.2004.0731.
(259) Paul, M. J.; Meyer, J. L. Streams in the Urban Landscape. *Annu. Rev. Ecol. Syst.* 2001, *32* (1), 333–365. https://doi.org/10.1146/annurev.ecolsys.32.081501.114040.
(260) Walsh, C. J.; Roy, A. H.; Feminella, J. W.; Cottingham, P. D.; Groffman, P. M.; Morgan, R. P. The Urban Stream Syndrome: Current Knowledge and the Search for a Cure. *Journal of the North American Benthological Society* 2005, *24* (3), 706–723. https://doi.org/10.1899/04-028.1.
(261) Codling, G.; Yuan, H.; Jones, P. D.; Giesy, J. P.; Hecker, M. Metals and PFAS in Stormwater and Surface Runoff in a Semi-Arid Canadian City Subject to Large Variations in Temperature among Seasons. *Environ Sci Pollut Res* 2020, *27* (15), 18232–18241. https://doi.org/10.1007/s11356-020-08070-2.
(262) Mayer, T.; Marsalek, J.; Reyes, E. D. Nutrients and Metal Contaminants Status of Urban Stormwater Ponds. *Lake and Reservoir Management* 1996, *12* (3), 348–363. https://doi.org/10.1080/07438149609354276.
(263) Hathaway, J. M.; Tucker, R. S.; Spooner, J. M.; Hunt, W. F. A Traditional Analysis of the First Flush Effect for Nutrients in Stormwater Runoff from Two Small Urban Catchments. *Water Air Soil Pollut* 2012, *223* (9), 5903–5915. https://doi.org/10.1007/s11270-012-1327-x.
(264) US EPA. Clean Water Act (CWA) Compliance Monitoring, 2021.
(265) Sawayama, S. Possibility of Anoxic Ferric Ammonium Oxidation. *Journal of Bioscience and Bioengineering* 2006, *101* (1), 70–72. https://doi.org/10.1263/jbb.101.70.
(266) Huang, S.; Jaffé, P. R. Characterization of Incubation Experiments and Development of an Enrichment Culture Capable of Ammonium Oxidation under Iron-Reducing Conditions. *Biogeosciences* 2015, *12* (3), 769–779. https://doi.org/10.5194/bg-12-769-2015.
(267) Shrestha, J.; Rich, J. J.; Ehrenfeld, J. G.; Jaffe, P. R. Oxidation of Ammonium to Nitrite Under Iron-Reducing Conditions in Wetland Soils: Laboratory, Field Demonstrations, and Push-Pull Rate Determination. *Soil Science* 2009, *174* (3), 156–164. https://doi.org/10.1097/SS.0b013e3181988fbf.

(268) Huang, S.; Jaffé, P. R. Isolation and Characterization of an Ammonium-Oxidizing Iron Reducer: Acidimicrobiaceae Sp. A6. *PLoS ONE* 2018, *13* (4), 8–10. https://doi.org/10.1371/journal.pone.0194007.
(269) Huang, S.; Chen, C.; Peng, X.; Jaffé, P. R. Environmental Factors Affecting the Presence of Acidimicrobiaceae and Ammonium Removal under Iron-Reducing Conditions in Soil Environments. *Soil Biology and Biochemistry* 2016, *98*, 148–158. https://doi.org/10.1016/j.soilbio.2016.04.012.
(270) Yang, W. H.; Weber, K. A.; Silver, W. L. Nitrogen Loss from Soil through Anaerobic Ammonium Oxidation Coupled to Iron Reduction. *Nature Geosci* 2012, *5* (8), 538–541. https://doi.org/10.1038/ngeo1530.
(271) Huang, S.; Jaffé, P. R. Defluorination of Perfluorooctanoic Acid (PFOA) and Perfluorooctane Sulfonate (PFOS) by Acidimicrobium Sp. Strain A6. *Environmental Science and Technology* 2019. https://doi.org/10.1021/acs.est.9b04047.
(272) Ruiz-Urigüen, M.; Shuai, W.; Huang, S.; Jaffé, P. R. Biodegradation of PFOA in Microbial Electrolysis Cells by Acidimicrobiaceae Sp. Strain A6. *Chemosphere* 2022, *292*, 133506. https://doi.org/10.1016/j.chemosphere.2021.133506.
(273) Erickson, A.; Kozarek, J.; Kramarczuk, K.; Lewis, L. *Biofiltration Media Optimization – Phase I Final Report*; University of Minnesota Water Resources Center, Minnesota Stormwater Research Council; Project Report 593; 2021.
(274) Peterson, K. N.; Tan, D. T.; Bezares-Cruz, J. C.; Novak, P. J. Estrone Biodegradation in Laboratory-Scale Systems Designed for Total Nitrogen Removal from Wastewater. *Environmental Science: Water Research & Technology* 2017, *3* (6), 1051–1060. https://doi.org/10.1039/C7EW00164A.
(275) Wein, S., Monitoring Coordinator. 2021.
(276) Capitol Region Watershed District. Water Data Reporting Tool, 2022.
(277) Minnesota Pollution Control Agency. Design Criteria for Stormwater Ponds, 2021.
(278) Smith, D. P. Sorptive Media Biofiltration for Inorganic Nitrogen Removal from Storm Water. *J. Irrig. Drain Eng.* 2008, *134* (5), 624–629. https://doi.org/10.1061/(ASCE)0733-9437(2008)134:5(624).
(279) MassDEP. Volume 2 Chapter 2: Structural BMP Specifications for the Massachusetts Stormwater Handbook, 2020.
(280) Zhang, B.; Chen, L.; Guo, Q.; Lian, J.; Ye Yao. Evaluation of Ammonia and Nitrate Distribution and Reduction within Stormwater Green Infrastructure with Different Woody Plants under Multiple Influencing Factors. *Journal of Environmental Management* 2022, *302*, 114086. https://doi.org/10.1016/j.jenvman.2021.114086.
(281) Widiastuti, N.; Wu, H.; Ang, H. M.; Zhang, D. Removal of Ammonium from Greywater Using Natural Zeolite. *Desalination* 2011, *277* (1–3), 15–23. https://doi.org/10.1016/j.desal.2011.03.030.
(282) Reddy, K. R.; Xie, T.; Dastgheibi, S. Nutrients Removal from Urban Stormwater by Different Filter Materials. *Water Air Soil Pollut* 2014, *225* (1), 1778. https://doi.org/10.1007/s11270-013-1778-8.
(283) Rahman, M. Y. A.; Nachabe, M. H.; Ergas, S. J. Biochar Amendment of Stormwater Bioretention Systems for Nitrogen and Escherichia Coli Removal:

Effect of Hydraulic Loading Rates and Antecedent Dry Periods. *Bioresource Technology* 2020, *310*, 123428. https://doi.org/10.1016/j.biortech.2020.123428.

(284) Peng, Y.; Deng, S.; Kong, Z.; Yuan, Y.; Long, H.; Fang, J.; Ma, H.; Shao, Z.; He, Q.; Chai, H. Biochar and Woodchip Amended Bioreactor Extending Reactive Volume for Enhanced Denitrification in Stormwater Runoff. *Journal of Water Process Engineering* 2022, *46*, 102541. https://doi.org/10.1016/j.jwpe.2021.102541.

Appendix A: Porous Polyethylene-Supported Zeolite Carriers for Improved Wastewater Deammonification

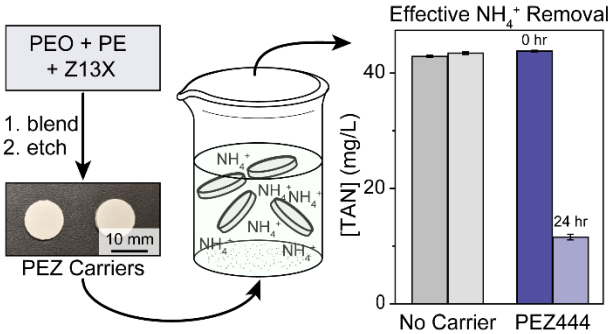

This chapter has been published in the journal *ACS ES&T Engineering* and is cited as:

Feinberg, E. C., Huff Chester, A. L., Novak, P. J., & Hillmyer, M. A. (2021). Porous Polyethylene-Supported Zeolite Carriers for Improved Wastewater Deammonification. *ACS ES&T Engineering*, 1(7), 1104-1112.

Abstract:

Wastewater treatment is increasingly important as anthropogenic activities continue to stress our water systems. Ammonium is one of the most common pollutants in wastewater streams and is typically oxidized to nitrate during treatment, which still results in the discharge of reactive nitrogen to the environment. Anaerobic ammonium oxidation (anammox) can completely remove reactive nitrogen, forming dinitrogen, and also decrease the cost of ammonium removal compared to conventional activated sludge wastewater treatment systems. Anammox faces challenges in mainstream implementation, however, as a result of the slow growth rates of anammox bacteria, narrow ideal growth conditions, and competition with other taxa. Addition of zeolite, such as faujasite, into low ammonium waste streams improves ammonium removal and locally concentrates ammonium ions, which in turn can improve the proliferation of anammox bacteria. Here we report the development of a scalable approach to plastic carriers for potential use in mainstream anammox reactors that combines the processability of thermoplastics and the ammonium sequestration ability of zeolites. Carriers were prepared by melt-blending polyethylene (PE), microparticulate zeolite 13X (Z13X, a faujasite), and a sacrificial poly(ethylene oxide) (PEO) template. Removal of the PEO template by solvent etching in water exposed a percolating pore network within the PE support structure and the particulate zeolite trapped within to the exterior. A pore size in the range of 10–25 μm was typical, with zeolite loadings as high as 45% by mass in the final product. The hybrid inorganic-polymer carriers were highly effective in sequestering ammonium, capable of removing >75% of ammonium from a 45 mg/L TAN aqueous environment in 24 h at less than 1% mass loading of carriers as compared to solution mass. Ammonium removal by ion exchange was confirmed by spectrophotometric methods and by energy-dispersive x-ray spectroscopy, and the kinetics of ammonium sequestration were zeroth-order with respect to ammonium and first-order with respect to zeolite. The materials described in this manuscript are expected to find utility in future bioreactor development.

Introduction:

Ammonium removal from wastewater is an energy intensive, yet necessary, process to protect our waters from excess nitrogenous oxygen demand and ammonium toxicity.[1,2] In the United States, wastewater treatment accounts for 2% of total energy consumption,[3] about 30 terawatt hours annually, and costs an estimated 2 billion USD per year.[4] Over half of the energy consumed by conventional treatment facilities goes to aeration of the activated sludge process for ammonium oxidation,[5] making it the most energy intensive treatment process in a conventional treatment facility.[6] If complete nitrogen removal is required, multistage treatment, where nitrification (autotrophic aerobic ammonia and nitrite oxidation) is followed by denitrification (heterotrophic anaerobic reduction of nitrate) to yield dinitrogen, is needed, further increasing treatment costs and complexity.[7,8]

An alternative to conventional activated sludge nitrogen removal, anaerobic ammonium oxidation (anammox) was first observed in a fluidized bed reactor in 1995.[9] Anammox bacteria are capable of autotrophic anaerobic deammonification of wastewater in a metabolic process where near equimolar equivalents of ammonium and nitrite comproportionate to yield dinitrogen and water.[10] The anammox process does not require oxygen,[11] reducing the oxygen demand by up to 60%.[12,13] Additionally, the anammox process eliminates the cost of carbon addition and reduces sludge production, thereby significantly reducing CO_2 emissions and improving the economic and environmental sustainability of wastewater treatment.[5,14] Unfortunately, in mainstream wastewater conditions, anammox bacteria are out-competed due to high carbon loading and relatively low ammonium concentrations of 30–80 mg/L total ammonium nitrogen (TAN),[15,16] compared to a TAN content 400-1000 mg/L where anammox bacteria have been observed to thrive.[17] A potential route to mitigate this challenge is the creation of microenvironments of high TAN on biofilm

carriers to attract and retain anammox bacteria in reactors, such as by the addition of zeolite, as in the zeolite-anammox process.[18]

Zeolites, and specifically faujasite-type zeolites such as zeolite 13X (Z13X), readily sequester ammonium through a cation exchange process.[19] In the presence of zeolites, anammox bacteria proliferate on the ammonium-rich surface of the mineral, forming a robust biofilm.[20] Microbial carriers can also be used for biofilm formation, with anammox biofilm on carriers significantly more stable than granular anammox aggregates and also proliferating more quickly under a broader range on conditions, resulting in more efficient deammonification in less time.[21,22] The addition of zeolite to a bioreactor in the form of large mineral aggregates, however, limits the available surface area, and therefore the degree of process improvement. Additionally, zeolite is friable and can wash out of the system over time.[23] In this research we envisioned the development of a hybrid polymer-zeolite system to address these limitations. By embedding particulate zeolite within a porous polymer matrix, retention and accessibility of the zeolite can be optimized, resulting in efficient ammonium concentration, which should in turn encourage anammox biofilm proliferation. These carriers could, in principle, be deployed in compact moving bed biofilm reactor (MBBR) or integrated fixed-film activated sludge (IFAS) systems for treatment of mainstream wastewater.

It has been previously demonstrated that ternary blends of two immiscible polymers with a particulate filler will form cocontinuous polymer domains.[24–27] Localization of the filler material varies, but it has been shown that addition of inorganic clays to polyethlene/poly(ethylene oxide) (PE-PEO) blends results in preferential localization of the filler component to the interface.[28] We sought to produce, by analogy, a cocontinuous PE-PEO-Z13X system which would then be solvent-etched in water to remove the sacrificial PEO domain, exposing the surface of the PEO domain throughout. We hypothesized that, by analogy to the PE-PEO-clay blends, zeolite would localize at the PE-PEO interface and be fully exposed by PEO removal.

In this article, we describe a novel, hybrid polymer-inorganic material system comprising a particulate zeolite within a polyethylene support matrix. Our approach uses inexpensive materials and scalable methods to produce a hybrid material in the form of a ~1 cm diameter disk that can be added directly to an aqueous system and that readily sequesters ammonium ions. Here, we present the manufacture of these materials by melt blending polyethylene, poly(ethylene oxide), and particulate zeolite, followed by solvent etching in water to afford the final porous product. A formulation screening process led to the selection of 3 materials for larger scale material manufacture. Subsequent testing in aqueous solution showed rapid (<24 h) removal of 75% of ammonium at typical municipal wastewater concentrations at a loading below 10 g carrier per L (~1000 g) of influent. This approach is scalable, tunable, and relies solely on readily available commercial materials, allowing for the rapid future incorporation of such carriers into existing wastewater treatment infrastructure.

Methods:

Materials and instrumentation

An Xplore MC 5 microcompounder was used to melt blend small batches for formulation screening. Large batches (~40 g) of blended materials were processed using a HAAKE Rheomix Lab Mixer (Thermo Fisher Scientific). Compression molding was performed in a Wabash Genesis (G15H-12-CLX) hot press. Attenuated total reflection Fourier transform infrared spectroscopy (ATR-FTIR) spectra were collected on a Bruker Alpha II with a Platinum ATR attachment; spectra were collected at a resolution of 1 cm^{-1} and for a minimum of 32 average scans. UV-visible absorption spectra were collected using a double-beam Shimadzu UV-1800 Spectrophotometer; spectra were collected at medium scan speed with 1 nm resolution with an empty reference beam, and samples were prepared in Starstedt polystyrene cuvettes (10 mm path length) and blanked against deionized water. Total organic carbon (TOC) measurements were taken using a Shimadzu TOC-L Total Organic Carbon Analyzer with ASI-L Autosampler attachment. Thermogravimetric

analysis (TGA) traces were collected using a TA Instruments Q500 Thermogravimetric Analyzer with 12 pan autosampler platter. Scanning electron microscopy (SEM) was conducted at the University of Minnesota Characterization Facility Labs using a Hitachi SU8230 Field Emission Gun Scanning Electron Microscope; energy-dispersive X-ray (EDX) spectroscopy was conducted using the attached Thermo Noran System 7 EDS.

Low-density polyethylene (Dowlex 955I) and poly(ethylene oxide) (Polyox N10) were provided by the Dow Chemical Company. Zeolite 13X (molecular sieves, 2 μm average size), sodium salicylate, sodium nitroprusside dihydrate, sodium citrate (tribasic, monohydrate), and methanol (ACS reagent grade) were purchased from MilliporeSigma and used without further purification. Ammonium chloride and sodium hydroxide were purchased from Fisher Scientific and used without further purification. Polyguard Blast Bleach (3%) was used as the commercial bleach source. Kapton sheets were purchased from McMaster-Carr and cut into appropriate size for use as release liners.

Small-scale PEZ manufacture

Initial formulation screening samples were manufactured on the 4.5 g scale in a DSM microcompounder. Poly(ethylene oxide) and zeolite 13X powder were loaded into a 5 g twin screw microcompounder at 75 °C and 100 rpm screw speed. After addition of PEO and Z13X powder, the barrel temperature was increased to 150 °C and the PE was loaded. The ternary mixture was blended for 10 min at 100 rpm screw speed and 150 °C, at which point the screw speed was reduced to 50 rpm, and the recirculating loop was opened, extruding the blended material as a cylindrical rod which was then air-cooled. The extruded material was sectioned into ~1 cm long rods for further testing.

The sectioned rods (1.0 g total) were then submerged in a scintillation vial with 20 mL of deionized water and a 3×10 mm magnetic stir bar and stirred for one week. Aliquots (100 μL) were

removed at 0, 1, 2, 3, 4, and 7, days for TOC analysis. After 7 d, the water etchant was exchanged for methanol, and the samples were stirred an additional 48 h. After solvent exchange, the etched materials were air dried for 4 h and further dried under reduced pressure for 24 h to remove residual solvent.

Large-batch PEZ manufacture

Large batches (~40 g) of blended material were prepared in a HAAKE batch compounder. PE, PEO and Z13X were loaded in one shot at 150 °C with 100 rpm screw speed. After loading, the mixture was blended for 10 min at 150 °C and 100 rpm. After blending, the batch compounder was disassembled, and the hot blend was scraped out with a wooden scraper. The blend was then immediately compacted to a 1.5 mm thickness in a Wabash hot press at 150 °C and 1 ton of compaction force. After holding for roughly 30 s, the platens were transferred to a cooling plate with a 20 lb weight on top. After 15 min, the material sheet was removed from the Kapton release liner and manually punched into 11 mm diameter × 1.5 mm thick disks (disk volume = 0.26 cm^3).

Disks (~16.0 g, total) were then etched in 500 mL deionized water for 48 h, at which point the water was exchanged for 200 mL methanol. After 24 h in methanol, the etched disks were removed, air-died for 24 h, and dried under reduced pressure for 24 h to afford the final carrier disk product.

Ammonium sequestration kinetics

The spectrophotometric salicylate method for determining ammonium concentration in aqueous solution was adapted from Le and Boyd.[29] Briefly, a 45 mg/L total ammonium nitrogen (TAN) solution was prepared by diluting 153 mg ammonium chloride to a total volume of 1000 mL in deionized water. Glass vials were then charged with 10, 20, or 40 mL of the ammonium chloride solution and a PTFE-coated magnetic stir bar. To each vial was added a single carrier disk of PEZ444, each with a mass of ~125 mg. Aliquots (250 μL) were taken immediately upon mixing

and after stirring for 0.5, 1, 2, 3, 6, and 24 h. Each aliquot was diluted to 10.0 mL total volume with deionized water. A sodium salicylate solution was prepared by dissolving 44.0 g sodium salicylate and 0.028 g sodium nitroprusside in 100 g deionized water; an alkaline citrate solution was prepared by dissolving 1.85 g sodium hydroxide and 10.0 g sodium citrate (tribasic, monohydrate) in 100 g deionized water; and alkaline hypochlorite solution was prepared by gently mixing 90 mL of the alkaline citrate solution and 10 mL of commercial bleach (3%). To each diluted aliquot was added 1.2 mL of the sodium salicylate solution and 2.0 mL of the alkaline hypochlorite solution. The samples were then thoroughly mixed and set in a dark enclosure for 1 h. After 1 h, the UV-Vis absorption spectra were measured for each sample, and the concentration of ammonium was determined by comparison of the optical density at 640 nm with the optical density of known standards at the same wavelength.

Twenty-four four ammonium sequestration efficiency

The measurement of ammonium sequestration by PEZ carriers follows the same basic procedure outlined in the preceding section. A 45 mg/L TAN solution was prepared as above, and a series of scintillation vials was charged with 20 mL of the ammonium chloride solution and a PTFE-coated 3×10 mm magnetic stir bar. To each vial was added a whole number of carriers (PEZ480, PEZ441, and PEZ444) such that the total mass of carriers in each vial was 100–125 mg. One set of vials was reserved with no added carrier. Aliquots (250 μL) were taken from each sample immediately upon mixing and stored overnight in a –20 °C freezer. After 24 h, a second set of aliquots was taken. Workup and analysis of the aliquots followed the same procedure detailed in the previous section.

Forty-eight hour ammonium sequestration in synthetic wastewater

Measurement of ammonium sequestration in synthetic wastewater followed a modified protocol, owing to potential interference of wastewater constituents on the spectroscopic method.

Synthetic wastewater was produced using the formulation given in Table S12 for 1L of synthetic wastewater. For each experiment, one carrier (PEZ480, PEZ441, or PEZ444) was used to sequester ammonium from 10 mL of synthetic wastewater. Ammonium was measured via an ammonium probe (Orion, Thermo Scientific) at the end of the 48-hour period. A 5-point standard curve, ranging from 0.1 to 50 mg-N/L (typical R^2 values of 0.99 or higher), was used for quantification. Standards were made gravimetrically with NH_4Cl in ultrapure (MilliQ, Millipore) water.

Results and Discussion:

The goal of this research was to combine the desirable processability and durability of plastic MBBR or IFAS carriers and the ammonium sequestration ability of faujasite-type zeolites to produce a carrier that could be used to improve the retention of anammox bacteria, and as a result, the efficiency of anaerobic ammonia oxidation in mainstream wastewater. To do this, we envisioned the development of a hybrid material: micron-scale particulate zeolite embedded within macroporous polyethylene (PE). Previous work has shown that melt blending ternary polymer-polymer-filler blends is facile[24–27], and that addition of inorganic clays to blends of PE and poly(ethylene oxide) (PEO) results in a preferential localization of clay at the blend interface.[30] We hypothesized that addition of microparticulate zeolite 13X (Z13X) to PE-PEO blends would similarly result in localization of Z13X at the PE-PEO interface, and that etching the PEO with water would result in a porous PE framework decorated with Z13X on the pore walls. This manufacturing process is shown schematically in **Figure A.1**.

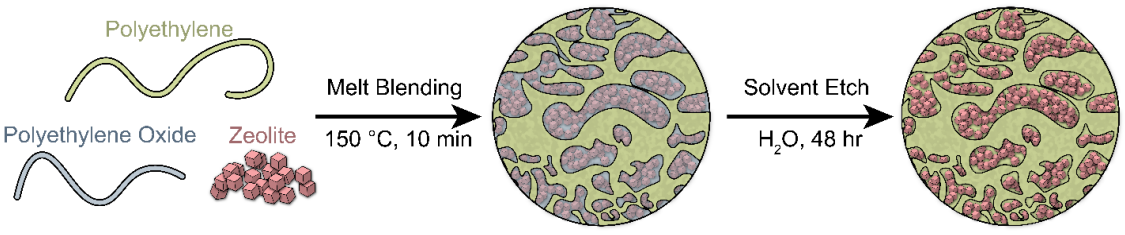

Figure A.1 Material fabrication scheme. Melt blending of polyethylene (PE), poly(ethylene oxide) (PEO) and zeolite 13X (Z13X) at 150 °C results in a macrophase separated polymer blend with

Z13X largely segregated into the PEO phase. Solvent etching in H_2O for up to 7 d results in removal of solvent-accessible PEO while Z13X particulate is physically trapped in the pore structure.

Formulation Screening

Sixteen formulations were targeted, with PE:PEO mass ratios of 4:1, 4:2, 4:4, and 4:8 as well as PE/Z13X mass ratios of 4:0, 4:1, 4:2, and 4:4. A naming convention is described in **Table A.1** where each ternary blend is labeled by the prefix TB (ternary blend) and a three digit suffix denoting the relative parts, by mass, of polyethylene, poly(ethylene oxide), and zeolite 13X, respectively. For example, TB421 is a ternary blend comprising 4 parts PE, 2 parts PEO, and 1 part Z13X, by mass. Ternary blends were prepared by melt compounding in a DSM twin screw microcompounder in 4.5 g batches. Blending was performed at 150 °C, and materials were extruded with air cooling. The resulting extrudate was cut into 1 cm sections for further processing and analysis. Three of the sixteen formulations were not processable; blends with a greater mass of Z13X than PEO (TB412, 414, and 424) jammed in the compounder and did not result in fully blended material.

Table A.1: List of formulation numbers, composition, morphology, and mass fraction of zeolite in etched material

BLEND#	PARTS PEO*	PARTS Z13X*	MORPHOLOGY	$Z13X_{THEO}$ (%)	$Z13X_F$ (%)
410	1	0	Spheres	0	0
411	1	1	Spheres	20	14
412†	1	2	Spheres	33	15
414†	1	4	---	50	---
420	2	0	Spheres	0	0
421	2	1	Partly Continuous	20	13
422	2	2	Partly Continuous	33	22
424†	2	4	---	50	---
440	4	0	Partly Continuous	0	0
441	4	1	Cocontinuous	20	15
442	4	2	Cocontinuous	33	26
444	4	4	Cocontinuous	50	42
480	8	0	Cocontinuous	0	0
481	8	1	Cocontinuous	20	12
482	8	2	Cocontinuous	33	22

484	8	4	Partly Continuous	50	36

* PEO and Z13X ratios are listed versus 4 parts, by weight of PE in each formulation.

† Samples with a greater mass loading of Z31X than PEO were not processable. An attempt was made to process formula 412 which resulted in significant jamming of the microcompounder and macroscale inhomogeneity.

After melt compounding, the processable blends were etched for one week in a deionized water bath to remove PEO, yielding a PE-Z13X material, following the TB naming convention and given the prefix PEZ. Etching in water was followed by solvent exchange in methanol for 24 h and drying under reduced pressure at room temperature for an additional 24 h. The kinetics of solvent etching were monitored by TOC, as it provided a means to measure both the overall kinetics and the total amount of PEO removed during the etching process. In general, etching followed first-order kinetics, shown by the time evolution of organic carbon in the natant solution (**Figure A.2**). As shown in **Figure A.2**, the kinetics of PEO etching varied substantially with formulation, providing a useful reporter on pore continuity. Complete removal of PEO in the blend necessitates a continuous structure; a depressed TOC measurement indicates incomplete removal of PEO and possibly a discontinuous pore network. Of the 16 formulations, 2 were not processable, 4 formed fully discontinuous blends, and 10 formed partially or fully cocontinuous networks (**see Appendix B**). The presence of cocontinuous morphologies was concluded by the appearance of a mechanically integral PE network and complete etching of PEO. TOC analysis indicated that for samples with cocontinuous networks, etching was complete in approximately 48 h; for samples with discontinuous morphologies, complete etching was not observed within one week.

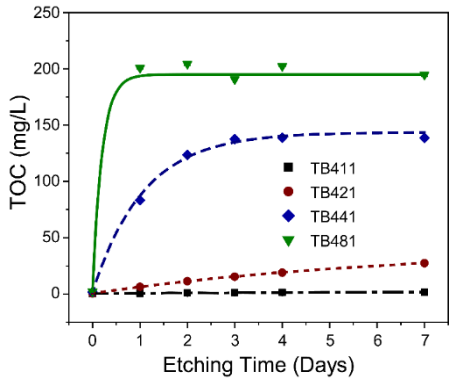

Figure A.2 TOC analysis of TB4X1 series etching process. 100 µL aliquots were taken at the same time each day and diluted to 10 mL in deionized water. Carbon content was then measured by a TOC analyzer. Individual points represent the average of three measurements; error bars (occluded by data points) represent the standard deviation. Fitted curves are first order exponential functions. Theoretical TOC levels for complete etching of TB411, 421, 441, and 481 are 46, 77, 121, and 171 mg/L, respectively. Maximum TOC levels for TB411 and 421 are significantly below the theoretical levels. Maximum levels for TB441 and 481 are slightly above the theoretical levels, which is likely a combination of accumulated volume error from sampling and release of small (<1 µm) PE discontinuities.

Fourier transform infrared spectroscopy (FTIR), TGA, and SEM provided further insight into the chemical and physical structure of the materials. FTIR spectroscopy was used to determine the ratio of PE to PEO before and after etching samples. This was done by fitting FTIR spectra of the blends to linear combinations of spectra for PE, PEO, and Z13X. The exact procedure for this analysis is detailed in the **Appendix B**. For example, in **Figure A.3**, the FTIR spectra of TB444 and PEZ444 are shown along with the calculated curves of best fit. FTIR analysis suggests that the polymer component of TB444 comprises 44% PE and 56% PEO, comparable to the expected 50:50 ratio. After etching, the PEO polymer component composition is calculated at 98% PE and 2% PEO, indicative of nearly complete etching, consistent with TOC measurements.

FTIR analysis was not feasible for particulate zeolite and resulted in artificially elevated measures for Z13X loading due to imperfect compaction during standard measurement. Therefore, the mass fraction of zeolite in samples before and after etching was determined by TGA experiments at a 10 °C/min ramp rate up to 550 °C under air. These conditions were sufficient to pyrolyze the polymer

matrices, and the mass fraction of zeolite in each material was then determined from the residual mass after pyrolysis, as the zeolite itself is pyrolytically stable (**see Appendix B**). Theoretical zeolite loading in etched materials was 0, 20, 33, or 50%, depending on the PE:Z13X ratio. Samples with discontinuities exhibited substantially lower final zeolite loadings than predicted, largely as a result of the substantial amount of PEO that remained unetched. Formulations produced with equal parts PE and PEO (PEZ44X series) resulted in 75-85% zeolite loading versus the theoretical maximum; the slight depression in zeolite loading was attributed to small amounts of unetched PEO and to leaching of the zeolite, presumably near the periphery of the material where the path length out of the matrix was lower. Zeolite leaching was directly visible by the release of white, insoluble particulate, typically early in the etching process; no samples showed significant leaching after the first 2 days. Samples produced using a 2:1 ratio of PE:PEO (PEZ48X series) afforded slightly depressed final zeolite loadings, typically in the range of 60 to 70%. It is feasible that the greater porosity of the PEZ48X series led to more facile leaching of zeolite through the pore network and out of the matrix.

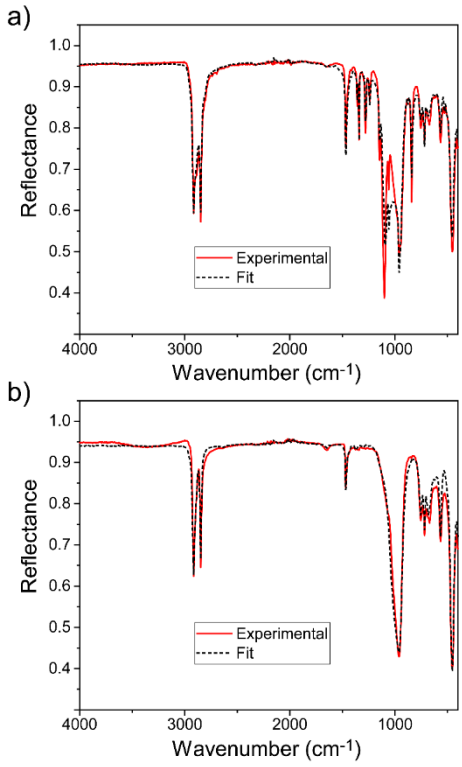

Figure A.3 FTIR spectra of TB444 (a) and PEZ444 (b) and curves of best fit calculated from linear combinations of spectra stock PE, PEO, and Z13X samples acquired under identical conditions. Before etching, TB444 shows a substantial contribution from PEO; after etching, PEZ444 shows minimal PEO contribution while retaining significant signal from Z13X.

Micrographs of the etched samples showed an unexpected result: in lieu of localization at the PE-PEO interface, the particulate Z13X instead seemed to migrate nearly exclusively to the interior of the PEO domain and remain trapped within the voids of the pore structure post etching (**Figure A.4**). This can be rationalized by considering the relative surface energies of PE, PEO, and Z13X. LDPE has a reported surface energy of 28 mJ/m^2 at 150 °C, while PEO has a reported surface energy of 33 mJ/m^2 at the same temperature.[30] Unlike previously studied inorganic additives, the surface energy of Zeolite 13X is in excess of 150 mJ/m^2,[31] accounting for the stark preference of Z13X for the more highly polar PEO phase. Also of note is that, despite not being physically or chemically bound to the PE matrix, the particulate zeolite did not appreciably leach from the system, with zeolite loadings of up to 83% of theoretical remaining after one week of vigorous stirring during the etching process for samples in the PEZ44X series. This result indicates that the zeolite was, instead, kinetically trapped within the tortuous pore network, and the micron-scale particles were unable to escape the network on timescales of days-weeks. The more open pore structure of the PEZ48X series resulted in lower zeolite retention, consistent with this explanation. In practical applications, it is likely that bacterial infiltration during use would further stabilize the material, decreasing spurious zeolite loss.

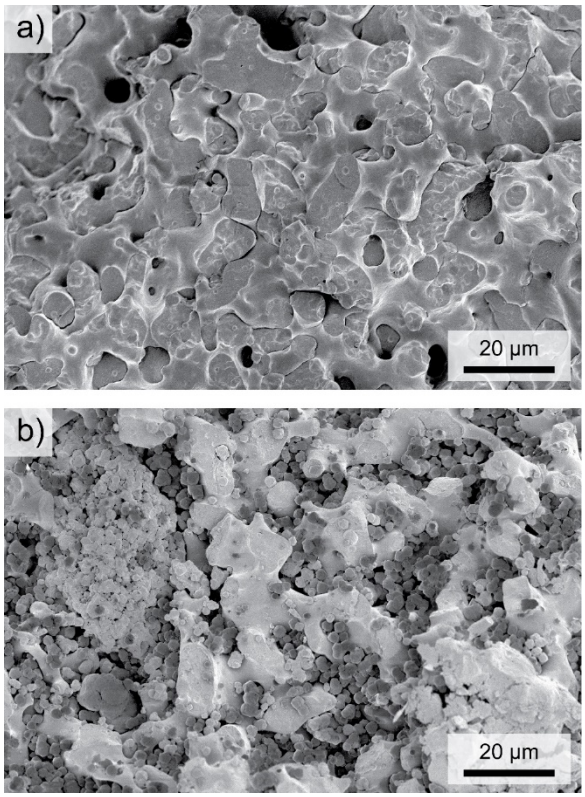

Figure A.4 SEM micrographs of TB444 (a) and PEZ444 (b). Before etching, a cocontinuous network of PE and PEO is visible in a. After etching, the PEO is fully evacuated while the particulate zeolite remains within the pore structure of the PE matrix in b.

Bulk Materials

Based on the results of the formulation screening, three formulations were chosen for further testing. PEZ444 and PEZ441 were chosen as formulations with high and low zeolite loading, respectively. PEZ480 was chosen as a zeolite-free control sample, as it was the only zeolite-free formulation with a fully continuous pore network. The overall manufacturing process for the bulk materials is outlined in **Figure A.5a**. Briefly, PE, PEO, and Z13X were loaded into a HAAKE batch compounder and mixed at 150 °C for 10 minutes, after which the blended materials was collected and pressed in a Wabash hot press at 150 °C for 60 s and then cooled between to aluminum platens. After the material was cooled, 11 mm diameter carrier disks were punched manually and solvent etched for 48 h in deionized water, followed by solvent exchange and drying.

Samples for analysis were reserved before and after the etching process. The PEZ carriers were stable to handling and were highly uniform (**Figure A.5b**).

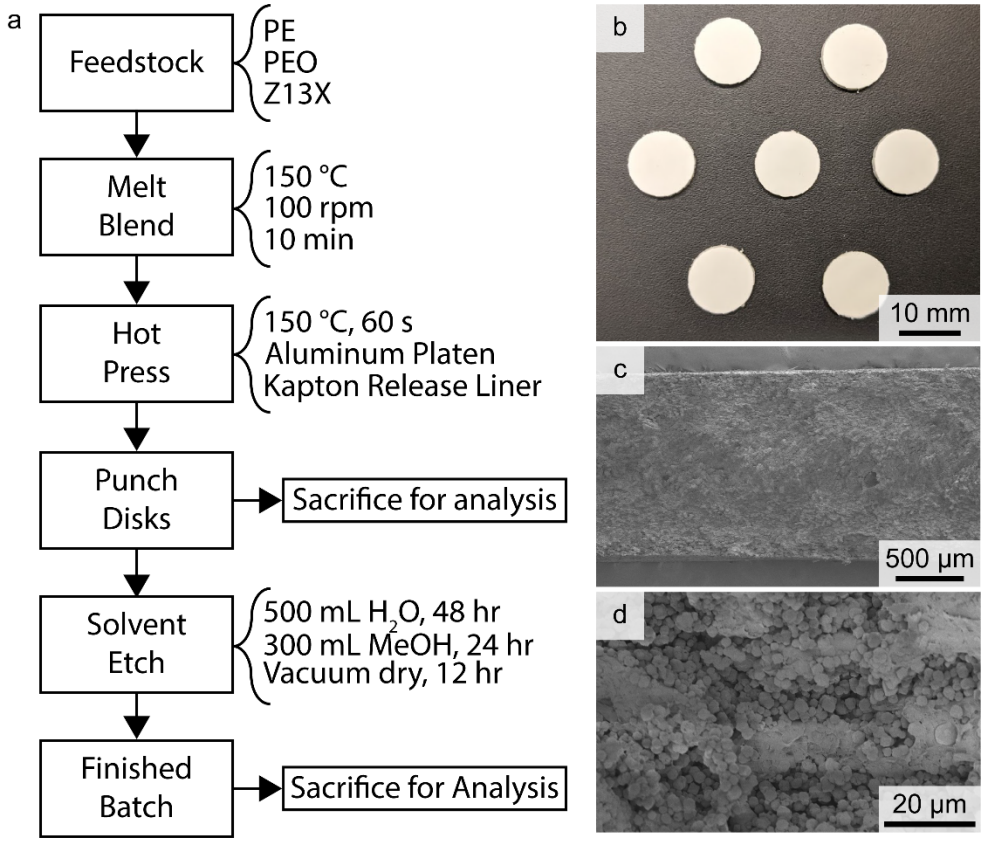

Figure A.5 Bulk material manufacturing: manufacturing scheme of the bulk PEZ carriers (a), optical photograph of PEZ444 carriers (b) showing high degree of uniformity, and scanning electron micrographs of PEZ444 carrier cross sections (c,d) showing continuous pore network and well distributed zeolite.

Like the samples prepared during the formulation screening, the bulk materials were characterized using a combination of SEM, FTIR, and TGA. Only minor differences were observed between the bulk materials used to produce the carrier disks and those manufactured during the formulation screening (**see Appendix B**). In particular, SEM characterization (**Figure A.5C,D**) showed that the PE matrix had a continuous network of pores throughout the material, and that the added zeolite was well distributed within the pore network. However, SEM characterization did

reveal quantities of zeolite embedded within the PE matrix along fracture surfaces in the bulk materials, likely due to differences in mixing.

Ammonium Absorption

Before investigating the overall efficiency of the carriers, we examined the kinetics of ammonium absorption. The kinetics of ammonium uptake by PEZ444 carriers were measured under three different carrier loadings: 100, 50, and 25 carriers per liter, corresponding to 5.0, 2.5, and 1.25 g of zeolite per liter, respectively. The solution used to test uptake was a 45 mg/L TAN solution prepared from ammonium chloride in deionized water. This concentration was chosen to mimic common TAN levels in mainstream wastewater.[17] It was found that both the overall kinetics and the amount of ammonium sequestered were dependent on carrier loading (**Figure A.6**). At the lowest loading (25 carriers per liter), the maximum nitrogen absorbed per 125 mg carrier was 0.70 mg, corresponding to ~1.4% nitrogen uptake when compared to the mass of zeolite in the carrier (50 mg Z13X, see **Appendix B** for calculation). This maximum uptake value of 1.4% is slightly lower than previously reported 2.3% (w/w) ammonium nitrogen capacity (3.0% total ammonium ion mass) for Z13X[32], but suggests that >50% of the present zeolite was available for facile ion exchange in the carrier system.

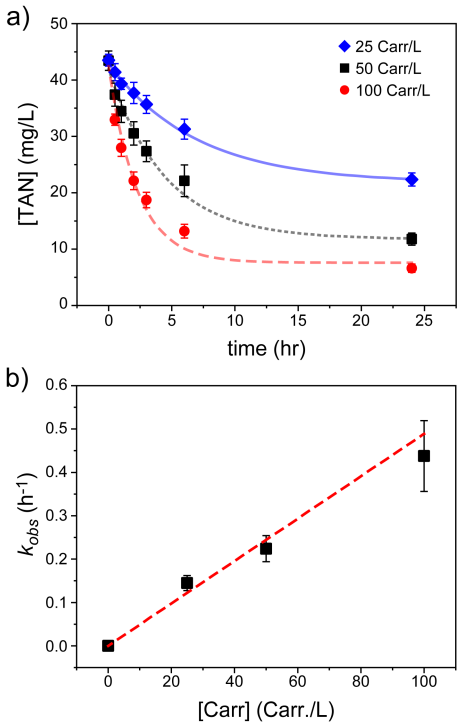

Figure A.6. Ammonium absorption kinetics of PEZ444 in aqueous 45 mgL^{-1} TAN solution prepared from ammonium chloride: (a) kinetic rate plots showing the first order absorption of ammonium over a 24 h period at three different carrier loadings and (b) plot of observed first order rate constants versus carrier loading.

Interestingly, ammonium absorption followed clear first-order kinetics, and the observed rate constant of ammonium sorption varied linearly with carrier loading, indicating that ammonium absorption is first-order with respect to zeolite. With overall first-order kinetics, these results necessitate that the ammonium absorption reaction is zero order with respect to ammonium; significant deviations from first-order kinetics would be expected if there was a greater than zeroth-order dependence on ammonium, as these experiments were not conducted under ammonium-saturated conditions. Future testing under a variety of influent ammonium concentrations will be necessary to validate these results. These kinetic results are reasonably explained only if sodium desorption from the zeolite is the rate limiting step in the ammonium absorption process; i.e., sodium desorption is relatively slow in comparison to ammonium sorption. An extension of this analysis is that the rate of ammonium uptake can be finely tuned by varying the carrier loading to

optimize processing conditions with minimal regard to initial ammonium concentration, as long the saturation regime of the zeolite is not reached.

Given the above kinetics results, it was prudent to determine the overall efficacy of ammonium removal over 24 h in comparison to control samples. A ca. 45 mg/L TAN stock solution was prepared from ammonium chloride in deionized water, as for the kinetics measurements. Samples were prepared by aliquoting 20 mL of the ammonium chloride stock solution into 12 scintillation vials and adding a 3×10 mm ($d \times l$) magnetic stir bar. One set of three samples was left stirring with no added carriers. PEZ444 and PEZ441 samples were prepared by adding a single, whole carrier to each of three scintillation vials, a loading of ~125 mg per 20 mL vial for PEZ444 and ~110 mg per 20 mg vial for PEZ441. PEZ480 was tested as a zeolite-free control by adding 4-5 whole carriers (totaling ~125 mg) to each of three scintillation vials. Immediately after preparation, aliquots were taken from each vial and stored in a freezer overnight to minimize possible evaporation. After 24 h, a second round of aliquots was taken, and the TAN was measured using the same method as in the kinetics measurements. The results of these measurements are shown in **Figure A.7**.

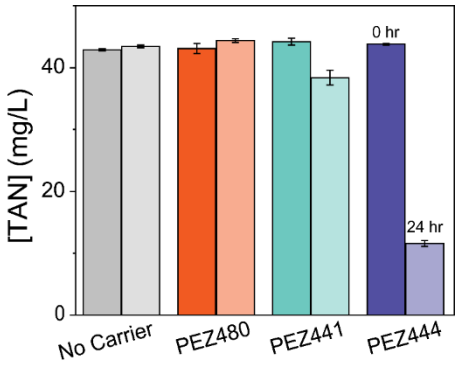

Figure A.7 Ammonium absorption efficiency of carriers manufactured in this study comparing [$NH4^+$] removal in the absence of any carrier and in the presence of ~100 mg of PEZ480, PEZ441, and PEZ444. [NH_4^+] was measured immediately after carrier addition (left columns) and after 24 hours of gentle stirring (right columns).

In the absence of added carrier, ammonium concentration was steady across the 24 h time period, as expected in the absence of evaporation or reaction. Samples containing ~125 mg of the no-zeolite control carrier, PEZ480, similarly showed no change in ammonium concentration over the 24 h sorption period. The result of the control experiment clearly indicates that ammonium removal was the result of ion exchange with the zeolite and not surface adsorption on the porous polymer system. Addition of ~115 mg PEZ441 resulted in the removal of approximately 15% of the endogenous ammonium, while 125 mg of PEZ444, with a significantly higher loading of zeolite, removed ~75% of ammonium over the same period. This indicates that, per liter of 45 mg/L TAN solution (or, theoretically, wastewater), only 6.25 g of PEZ444 would be required to remove 75% of aqueous ammonium in 24 h, creating a stable method for concentrating ammonium from wastewater and, as a result, potentially stimulating the anammox process. In the interest of studying ammonium removal in wastewater-relevant conditions, the ammonium sequestration efficiency of the carriers was further investigated in synthetic wastewater. In these experiments, PEZ480 showed no removal, as expected. In contrast, PEZ444 removed ~50% of the aqueous ammonium in a 46 mg/L TAN solution at a 1% w/w (carrier/influent) loading. (**Figure B.S57**).

Ion exchange with of ammonium for sodium in the zeolite was confirmed by SEM-EDX (**Figure A.8**). While SEM-EDX was unable to resolve the incorporation of ammonium within the PEZ444 carriers, a significant depression in the level of sodium was observed throughout the material used in the 25 Carr./L kinetics experiments. The Na Kα signal was attenuated by 25% when referenced against both Si Kα and Al Kα signals; this compares with a calculated 16±1% loss in sodium based on the stoichiometry of ammonium absorbed (**see Appendix B**). Confirmation of ion exchange by SEM-EDX indicates that the ammonium sorption is solely due to zeolite within the PE support matrix, and that the efficacy of ammonium absorption is largely unaffected by embedding within the PE matrix. Further, kinetics and overall ion capacity are readily tuned by varying the formulation of the PEZ carrier. With tunable kinetics and easily variable ammonium

ion capacity, it is expected that these carriers could be readily incorporated into an IFAS system to stimulate anammox at low cost and with relatively facile process optimization. Future investigations of the role these materials play in biologically active IFAS systems will further elucidate the utility of these hybrid carriers and aid in optimization of design, both with regard to materials formulation and form factor.

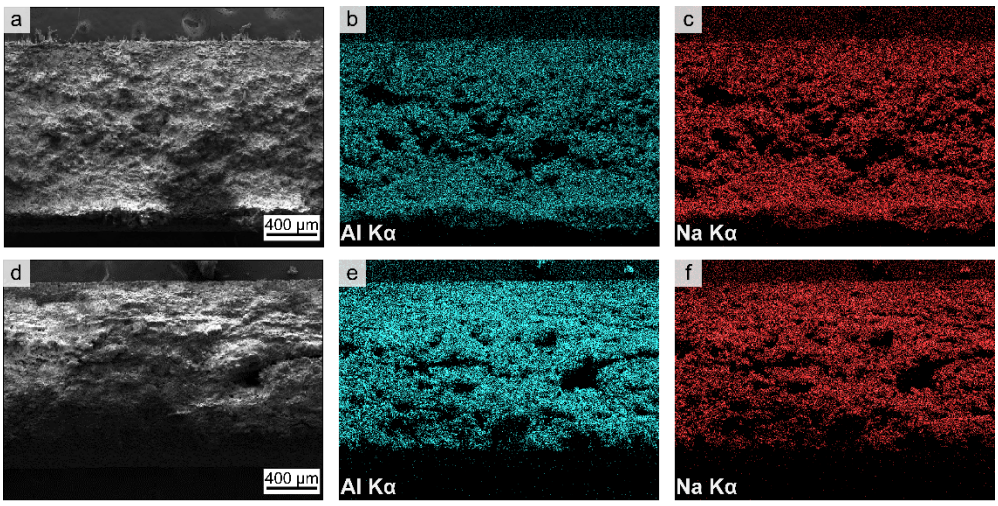

Figure A.8. Scanning electron microscopy and energy dispersive X-ray spectroscopy mapping of PEZ444 carriers before (a-c) and after (d-f) ion exchange in a 45 mg/L TAN solution. Micrographs (a,d) show the overall structure of the carriers in cross section. Maps of the Al Kα (b,e) and Na Kα (c,f) signals show thorough incorporation of the zeolite throughout the bulk of the material. The ratio of Na to Al was found to be ~24% lower after ion exchange. Further SEM and EDX characterization is available in the supporting information.

Conclusions

We have presented the design, fabrication, and ammonium removal ability of organic-inorganic hybrid carriers to be used for the enhancement of the anammox process moving bed biofilm reactor and integrated fixed-film activated sludge systems for mainstream wastewater deammonification. These carriers comprise a macroporous polyethylene support matrix and an entrapped particulate zeolite, capable of rapidly scavenging ammonium in aqueous environments. This design may provide an inexpensive and scalable solution to current challenges in mainstream anammox wastewater treatment. PEZ carriers are robust, with negligible loss of zeolite during a

week of vigorous stirring, and, at less than 1 wt.% loading, efficiently capture ~75% of ammonium in 24 h at concentrations mimicking municipal wastewater. The highly efficient ammonium sequestration was further corroborated by experiments demonstrating ~50% removal of ammonium in synthetic wastewater at similar carrier loadings. The materials presented in this manuscript are expected to serve as functional carriers for zeolite-anammox bioreactors, substantially improving the efficiency of wastewater treatment and reclamation. Further research will explore the application of these carriers in biologically active reactors, including optimization of zeolite loading and matrix pore structure to promote microbial proliferation and retention.

References

(1) Domingues, R. B.; Barbosa, A. B.; Sommer, U.; Galvão, H. M. Ammonium, Nitrate and Phytoplankton Interactions in a Freshwater Tidal Estuarine Zone: Potential Effects of Cultural Eutrophication. *Aquat. Sci.* **2011**, *73* (3), 331–343. https://doi.org/10.1007/s00027-011-0180-0.

(2) Zhang, M.; Wang, Z.; Xu, J.; Liu, Y.; Ni, L.; Cao, T.; Xie, P. Ammonium, Microcystins, and Hypoxia of Blooms in Eutrophic Water Cause Oxidative Stress and C–N Imbalance in Submersed and Floating-Leaved Aquatic Plants in Lake Taihu, China. *Chemosphere* **2011**, *82* (3), 329–339. https://doi.org/https://doi.org/10.1016/j.chemosphere.2010.10.038.

(3) Pabi, S.; Amarnath, A.; Goldstein, R.; Reekie, L. Electricity Use and Management in the Municipal Water Supply and Wastewater Industries. *Electr. Power Res. Institute, Palo Alto* **2013**, *194*.

(4) Lemar, P. *Energy Data Management Manual for the Wastewater Treatment Sector*; 2017. United States Department of Energy.

(5) Cogert, K. I.; Ziels, R. M.; Winkler, M. K. H. Reducing Cost and Environmental Impact of Wastewater Treatment with Denitrifying Methanotrophs, Anammox, and Mainstream Anaerobic Treatment. *Environ. Sci. Technol.* **2019**, *53* (21), 12935–12944. https://doi.org/10.1021/acs.est.9b04764.

(6) Mulder, A. The Quest for Sustainable Nitrogen Removal Technologies. *Water Sci. Technol.* **2003**, *48* (1), 67–75. https://doi.org/10.2166/wst.2003.0018.

(7) Ritter, W. F.; Eastburn, R. P. A Review of Denitrification in On-Site Wastewater Treatment Systems. *Environ. Pollut.* **1988**, *51* (1), 49–61. https://doi.org/https://doi.org/10.1016/0269-7491(88)90238-2.

(8) Chen, Y.; Lan, S.; Wang, L.; Dong, S.; Zhou, H.; Tan, Z.; Li, X. A Review: Driving Factors and Regulation Strategies of Microbial Community Structure and Dynamics in

Wastewater Treatment Systems. *Chemosphere* **2017**, *174*, 173–182. https://doi.org/https://doi.org/10.1016/j.chemosphere.2017.01.129.

(9) Mulder, A.; van de Graaf, A. A.; Robertson, L. A.; Kuenen, J. G. Anaerobic Ammonium Oxidation Discovered in a Denitrifying Fluidized Bed Reactor. *FEMS Microbiol. Ecol.* **1995**, *16* (3), 177–183. https://doi.org/10.1111/j.1574-6941.1995.tb00281.x.

(10) Hu, B.; Shen, L.; Xu, X.; Zheng, P. Anaerobic Ammonium Oxidation (Anammox) in Different Natural Ecosystems. *Biochem. Soc. Trans.* **2011**, *39* (6), 1811–1816. https://doi.org/10.1042/BST20110711.

(11) Lotti, T.; Kleerebezem, R.; Lubello, C.; van Loosdrecht, M. C. M. Physiological and Kinetic Characterization of a Suspended Cell Anammox Culture. *Water Res.* **2014**, *60*, 1–14. https://doi.org/https://doi.org/10.1016/j.watres.2014.04.017.

(12) Kartal, B.; Maalcke, W. J.; de Almeida, N. M.; Cirpus, I.; Gloerich, J.; Geerts, W.; Op den Camp, H. J. M.; Harhangi, H. R.; Janssen-Megens, E. M.; Francoijs, K.-J.; Stunnenberg, H. G.; Keltjens, J. T.; Jetten, M. S. M.; Strous, M. Molecular Mechanism of Anaerobic Ammonium Oxidation. *Nature* **2011**, *479* (7371), 127–130. https://doi.org/10.1038/nature10453.

(13) Van Hulle, S. W. H.; Vandeweyer, H. J. P.; Meesschaert, B. D.; Vanrolleghem, P. A.; Dejans, P.; Dumoulin, A. Engineering Aspects and Practical Application of Autotrophic Nitrogen Removal from Nitrogen Rich Streams. *Chem. Eng. J.* **2010**, *162* (1), 1–20. https://doi.org/https://doi.org/10.1016/j.cej.2010.05.037.

(14) Li, X.; Klaus, S.; Bott, C.; He, Z. Status, Challenges, and Perspectives of Mainstream Nitritation–Anammox for Wastewater Treatment. *Water Environ. Res.* **2018**, *90* (7), 634–649. https://doi.org/10.2175/106143017X15131012153112.

(15) Jin, R.-C.; Yang, G.-F.; Yu, J.-J.; Zheng, P. The Inhibition of the Anammox Process: A Review. *Chem. Eng. J.* **2012**, *197*, 67–79. https://doi.org/https://doi.org/10.1016/j.cej.2012.05.014.

(16) Xu, G.; Zhou, Y.; Yang, Q.; Lee, Z. M.-P.; Gu, J.; Lay, W.; Cao, Y.; Liu, Y. The Challenges of Mainstream Deammonification Process for Municipal Used Water Treatment. *Appl. Microbiol. Biotechnol.* **2015**, *99* (6), 2485–2490. https://doi.org/10.1007/s00253-015-6423-6.

(17) Nsenga Kumwimba, M.; Lotti, T.; Şenel, E.; Li, X.; Suanon, F. Anammox-Based Processes: How Far Have We Come and What Work Remains? A Review by Bibliometric Analysis. *Chemosphere* **2020**, *238*, 124627. https://doi.org/https://doi.org/10.1016/j.chemosphere.2019.124627.

(18) Collison, R. S.; Grismer, M. E. Nitrogen and Chemical Oxygen Demand Removal from Septic Tank Wastewater in Subsurface Flow Constructed Wetlands: Substrate (Cation Exchange Capacity) Effects. *Water Environ. Res.* **2014**, *86* (4), 314–323. https://doi.org/10.2175/106143013X13736496908627.

(19) Fletcher, P.; Townsend, R. P. Exchange of Ammonium and Sodium Ions in Synthetic Faujasites. *J. Chem. Soc. Faraday Trans. 1 Phys. Chem. Condens. Phases* **1982**, *78* (6), 1741–1753. https://doi.org/10.1039/F19827801741.

(20) Fernández, I.; Vázquez-Padín, J. R.; Mosquera-Corral, A.; Campos, J. L.; Méndez, R. Biofilm and Granular Systems to Improve Anammox Biomass Retention. *Biochem. Eng.*

J. **2008**, *42* (3), 308–313. https://doi.org/https://doi.org/10.1016/j.bej.2008.07.011.

(21) Adams, M.; Xie, J.; Xie, J.; Chang, Y.; Guo, M.; Chen, C.; Zhang, T. C. The Effect of Carrier Addition on Anammox Start-up and Microbial Community: A Review. *Rev. Environ. Sci. Bio/Technology* **2020**, *19* (2), 355–368. https://doi.org/10.1007/s11157-020-09530-4.

(22) Grismer, M. E.; Collison, R. S. The Zeolite-Anammox Treatment Process for Nitrogen Removal from Wastewater—A Review. *Water* **2017**, *9*, 901.

(23) Klieve, J. R.; Semmens, M. J. An Evaluation of Pretreated Natural Zeolites for Ammonium Removal. *Water Res.* **1980**, *14* (2), 161–168. https://doi.org/https://doi.org/10.1016/0043-1354(80)90232-8.

(24) Vermant, J.; Cioccolo, G.; Nair, K. G.; Moldenaers, P. Coalescence Suppression in Model Immiscible Polymer Blends by Nano-Sized Colloidal Particles. *Rheol. acta* **2004**, *43* (5), 529–538.

(25) Zhang, W.; Lin, M.; Winesett, A.; Dhez, O.; Kilcoyne, A. L. D.; Ade, H.; Rubinstein, M.; Shafi, K. V. P. M.; Ulman, A.; Gersappe, D.; Tenne, R.; Rafailovich, M.; Sokolov, J.; Frisch, H. L. The Use of Functionalized Nanoparticles as Non-Specific Compatibilizers for Polymer Blends. *Polym. Adv. Technol.* **2011**, *22* (1), 65–71. https://doi.org/https://doi.org/10.1002/pat.1875.

(26) Thareja, P.; Velankar, S. Particle-Induced Bridging in Immiscible Polymer Blends. *Rheol. acta* **2007**, *46* (3), 405–412.

(27) Thareja, P.; Moritz, K.; Velankar, S. S. Interfacially Active Particles in Droplet/Matrix Blends of Model Immiscible Homopolymers: Particles Can Increase or Decrease Drop Size. *Rheol. acta* **2010**, *49* (3), 285–298.

(28) Trifkovic, M.; Hedegaard, A. T.; Sheikhzadeh, M.; Huang, S.; Macosko, C. W. Stabilization of PE/PEO Cocontinuous Blends by Interfacial Nanoclays. *Macromolecules* **2015**, *48* (13), 4631–4644. https://doi.org/10.1021/acs.macromol.5b00354.

(29) Le, P. T. T.; Boyd, C. E. Comparison of Phenate and Salicylate Methods for Determination of Total Ammonia Nitrogen in Freshwater and Saline Water. *J. World Aquac. Soc.* **2012**, *43* (6), 885–889. https://doi.org/10.1111/j.1749-7345.2012.00616.x.

(30) Trifkovic, M.; Hedegaard, A. T.; Sheikhzadeh, M.; Huang, S.; Macosko, C. W. Stabilization of PE/PEO Cocontinuous Blends by Interfacial Nanoclays. *Macromolecules* **2015**, *48* (13), 4631–4644. https://doi.org/10.1021/acs.macromol.5b00354.

(31) Díaz, E.; Ordóñez, S.; Vega, A.; Coca, J. Adsorption Characterisation of Different Volatile Organic Compounds over Alumina, Zeolites and Activated Carbon Using Inverse Gas Chromatography. *J. Chromatogr. A* **2004**, *1049* (1), 139–146. https://doi.org/https://doi.org/10.1016/j.chroma.2004.07.061.

(32) Singh, G.; Prasad, B. Removal of Ammonia from Coke-Plant Wastewater by Using Synthetic Zeolite. *Water Environ. Res.* **1997**, *69* (2), 157–161. https://doi.org/10.2175/106143097X125308.

Appendix B: Supporting Information for Porous Polyethylene-Supported Zeolite Carriers for Improved Wastewater Deammonification

This chapter has been published as Supplemental Information in the journal *ACS ES&T Engineering* and is cited as:

Feinberg, E. C., Huff Chester, A. L., Novak, P. J., & Hillmyer, M. A. (2021). Porous Polyethylene-Supported Zeolite Carriers for Improved Wastewater Deammonification. *ACS ES&T Engineering*, 1(7), 1104-1112.

Table of Contents for Appendix B

Characterization of Formulation Screening Materials

This section details supplementary information for the manufacture and characterization of materials use in the formulation screening process detailed in the main text. Etching kinetics were monitored by total organic carbon analysis (TOC). Material composition before and after etching was determined by a combination of Fourier transform infrared spectroscopy (FTIR) and thermogravimetric analysis (TGA). Morphology was assessed by scanning electron microscopy (SEM).

Total Organic Carbon Analysis of Etching Process

The following pages total organic carbon (TOC) measurements taken during the solvent etching of ternary blends in deionized water. TOC measurements were taken using a Shimadzu TOC-L Total Organic Carbon Analyzer with ASI-L Autosampler attachment. Samples were prepared by taking 100 µL aliquots from the etching bath at 0, 1, 2, 3, 4, and 7 days, diluting to 10 mL total volume with deionized water, and filtering through a 0.45 µm PTFE syringe filter. Each time point was measured by TOC three times to ensure reproducibility. The plotted values are those exactly as measured from the diluted aliquots; actual TOC values in the etching bath natant are therefore 100× higher. For example, the maximum TOC for TB480 is ~200 mg/L as measured, and the actual TOC in the natant before dilution is therefore ~20 g/L. TOC measurements for each material are fit to a first-order exponential function where possible.

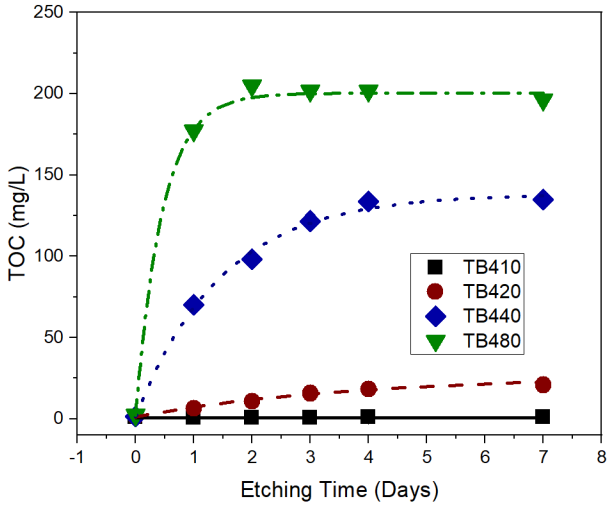

Figure B.S1. Total organic carbon analysis of TB4X0 series materials during etching in deionized water. Points represent the average of three measurements; errors bars representing the standard deviation are present but eclipsed in many cases. Curves represent a first-order exponential fit. Rate constants for etching are displayed in **Table B.S1**. The fitting for TB410 did not converge, as there was no observable etching.

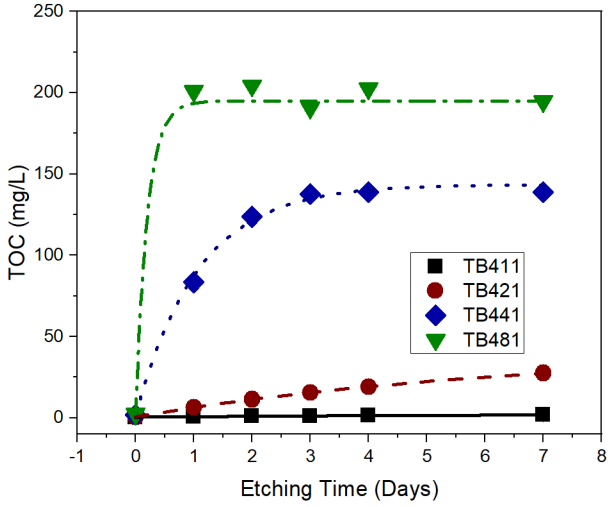

Figure B.S2. Total organic carbon analysis of TB4X1 series materials during etching in deionized water. Points represent the average of three measurements; errors bars representing the standard deviation are present but eclipsed in many cases. Curves represent a first-order exponential fit. Rate constants for etching are displayed in **Table B.S1**. The fitting for TB411 did not converge, as there was minimal observable etching.

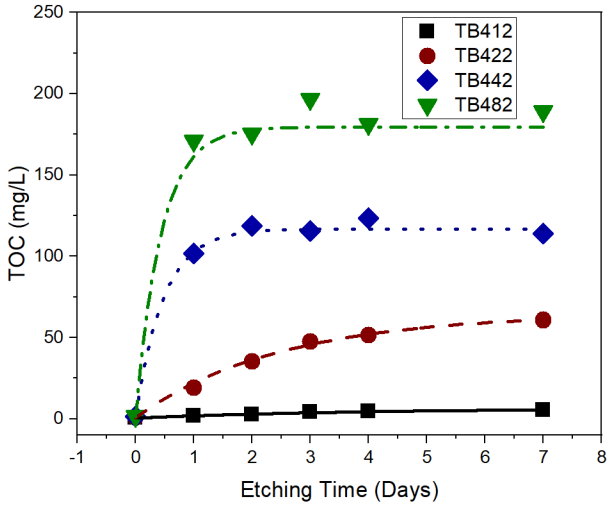

Figure B.S3. Total organic carbon analysis of TB4X2 series materials during etching in deionized water. Points represent the average of three measurements; errors bars representing the standard deviation are present but eclipsed in many cases. Curves represent a first-order exponential fit. Rate constants for etching are displayed in **Table B.S1**.

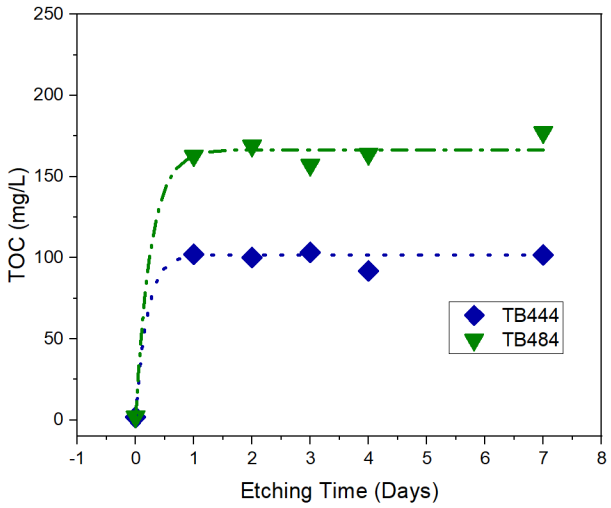

Figure B.S4. Total organic carbon analysis of TB4X4 series materials during etching in deionized water. Points represent the average of three measurements; errors bars representing the standard deviation are present but eclipsed in many cases. Curves represent a first-order exponential fit. Rate constants for etching are displayed in **Table B.S1**. Blends TB414 and TB424 were not etched, as they could not be fabricated due to jamming of the compounder at <1:1 PEO:Z13X ratios.

Table B.S1. Rate constants for PEO solvent etching measured by TOC.

Sample	k(day^{-1})
TB410	---
TB420	0.275
TB440	0.676
TB480	2.19
TB411	---
TB421	0.148
TB441	0.927
TB481	>3.0
TB412	0.254
TB422	0.405
TB442	2.08
TB482	>3.0
TB414	---
TB424	---
TB444	>3.0
TB484	>3.0

Scanning electron micrograph of formulation screening materials

The following pages present scanning electron micrographs (SEMs) of ternary blends and etched materials used in the formulation screening section of this manuscript. All micrographs were acquired on an Hitachi SU8230 Field Emission Gun Scanning Electron Microscope at the Characterization Facility Labs at the University of Minnesota. All samples were dried at room temperature under reduced pressure for 24 hr before sample preparation. All samples were sputter coated with 5 nm iridium. Unless otherwise noted, all images were acquired at a 1.0 kV accelerating voltage using both upper and lower detectors for image acquisition. Image contrast of some micrographs has been adjusted for clarity in print; no other modifications (other than cropping to fit) were made.

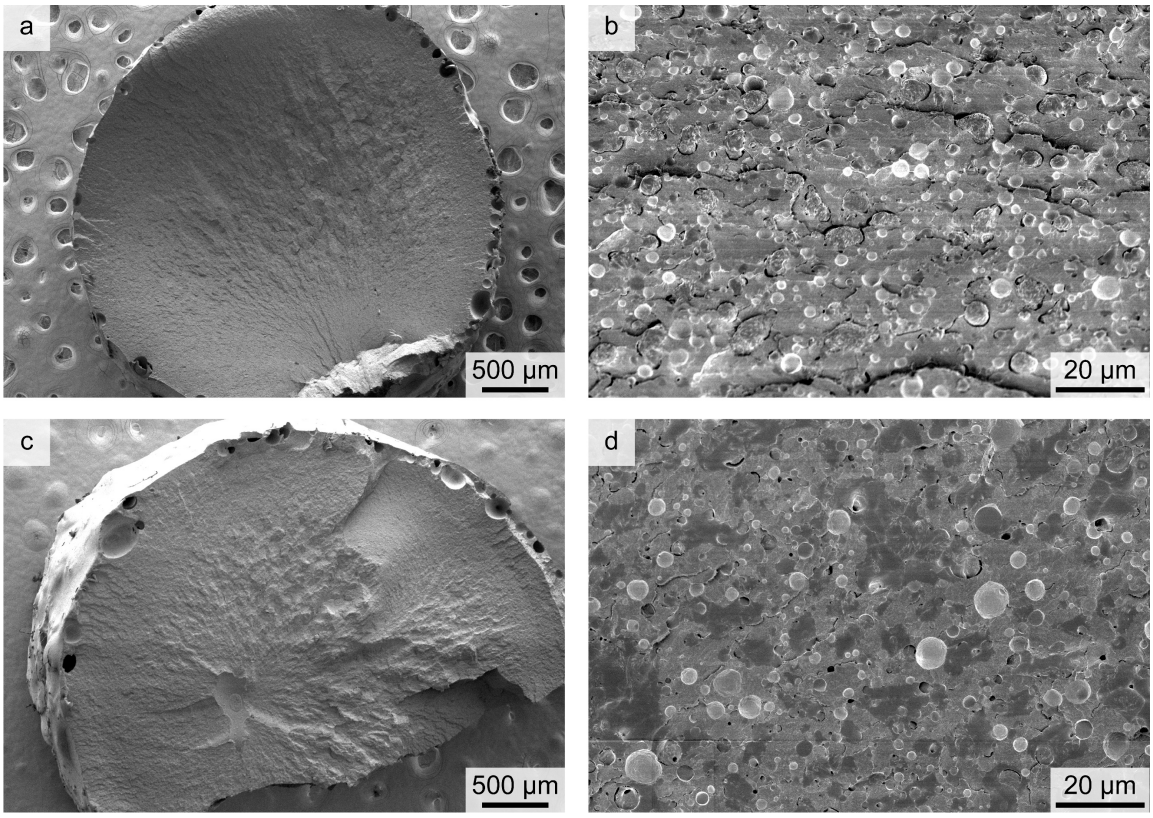

Figure B.S5. Scanning electron micrographs of formulation 410. Micrographs were collected of TB410 before (a,b) and PEZ410 after (c,d) solvent etching in deionized water. PEO is visible as spheres within the PE matrix. Due to lack of connectivity of PEO domains, there is no observable etching within the bulk of the material.

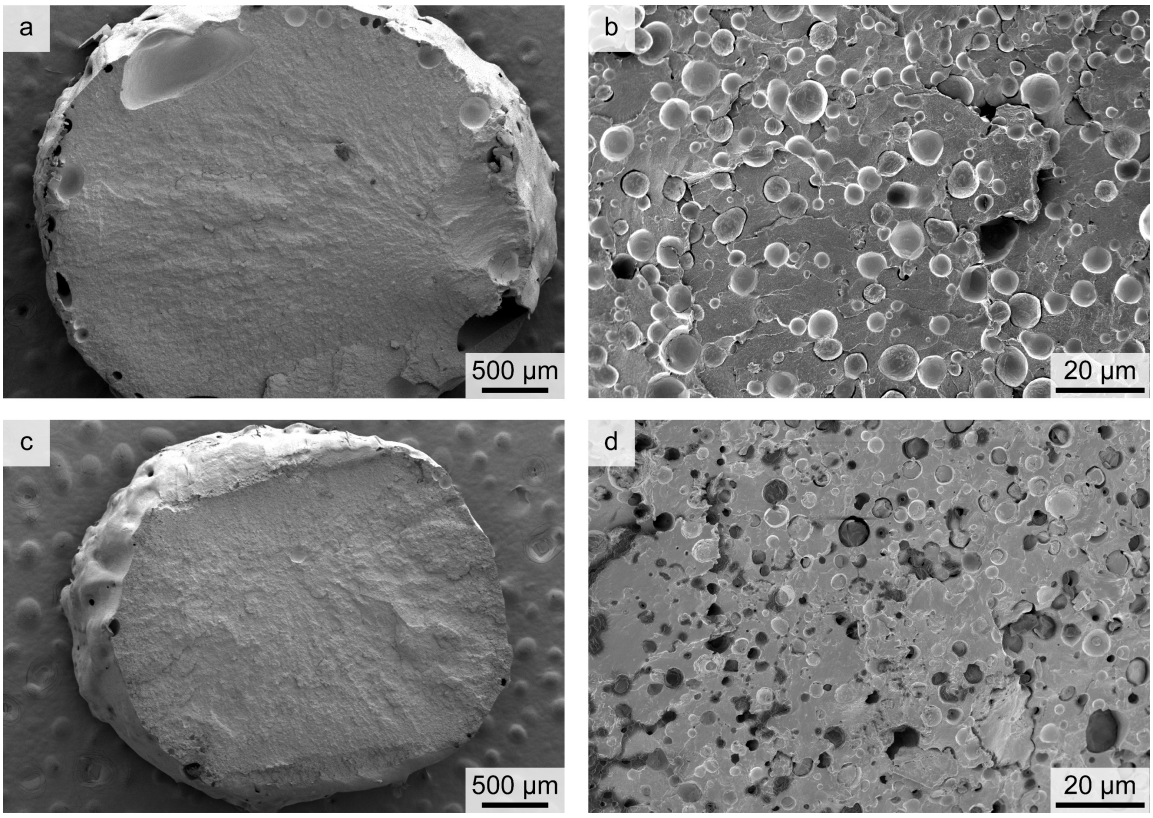

Figure B.S6. Scanning electron micrographs of formulation 420. Micrographs were collected of TB420 before (a,b) and PEZ420 after (c,d) solvent etching in deionized water. PEO is visible as spheres within the PE matrix. Due to general lack of connectivity of PEO domains, there is minimal observable etching within the bulk of the material.

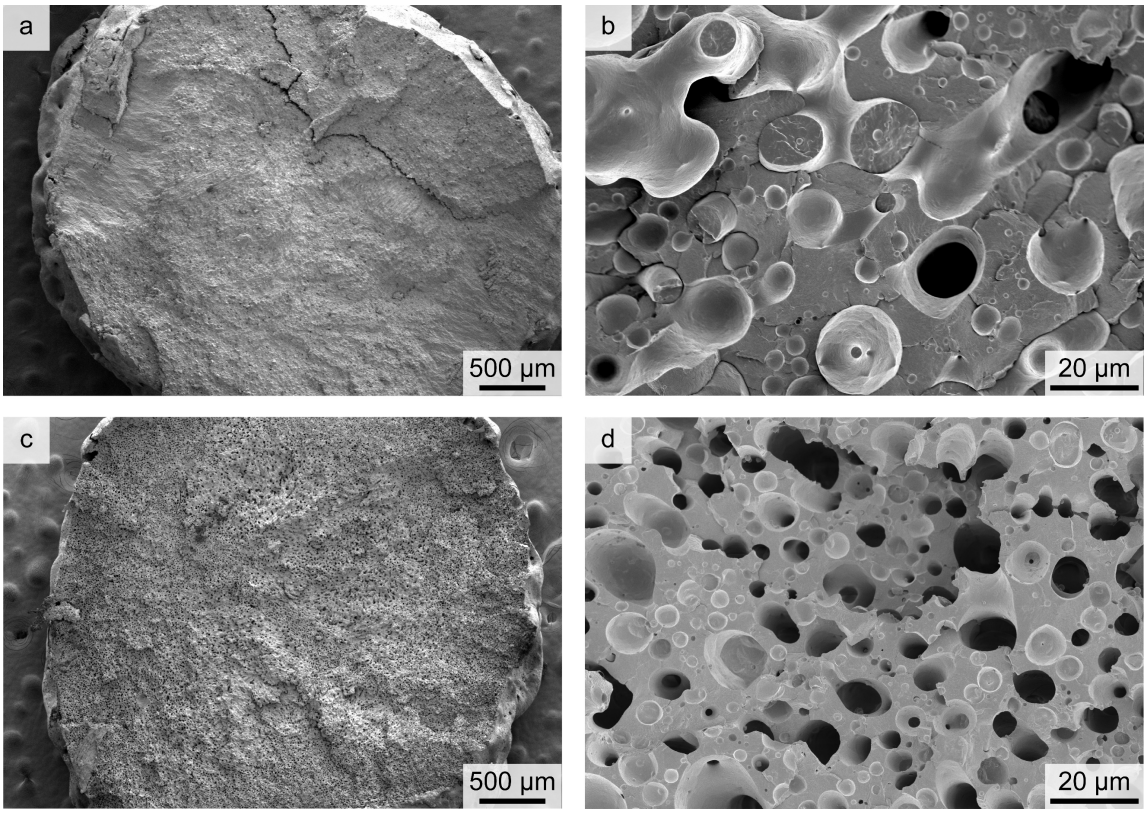

Figure B.S7. Scanning electron micrographs of formulation 440. Micrographs were collected of TB440 before (a,b) and PEZ440 after (c,d) solvent etching in deionized water. A largely co-continuous network of PE and PEO is visible before etching, with some discontinuous PEO domains. Co-continuous PEO domains are readily evacuated during solvent etching, while some PEO remains in the solvent-inaccessible discontinuous PEO domains.

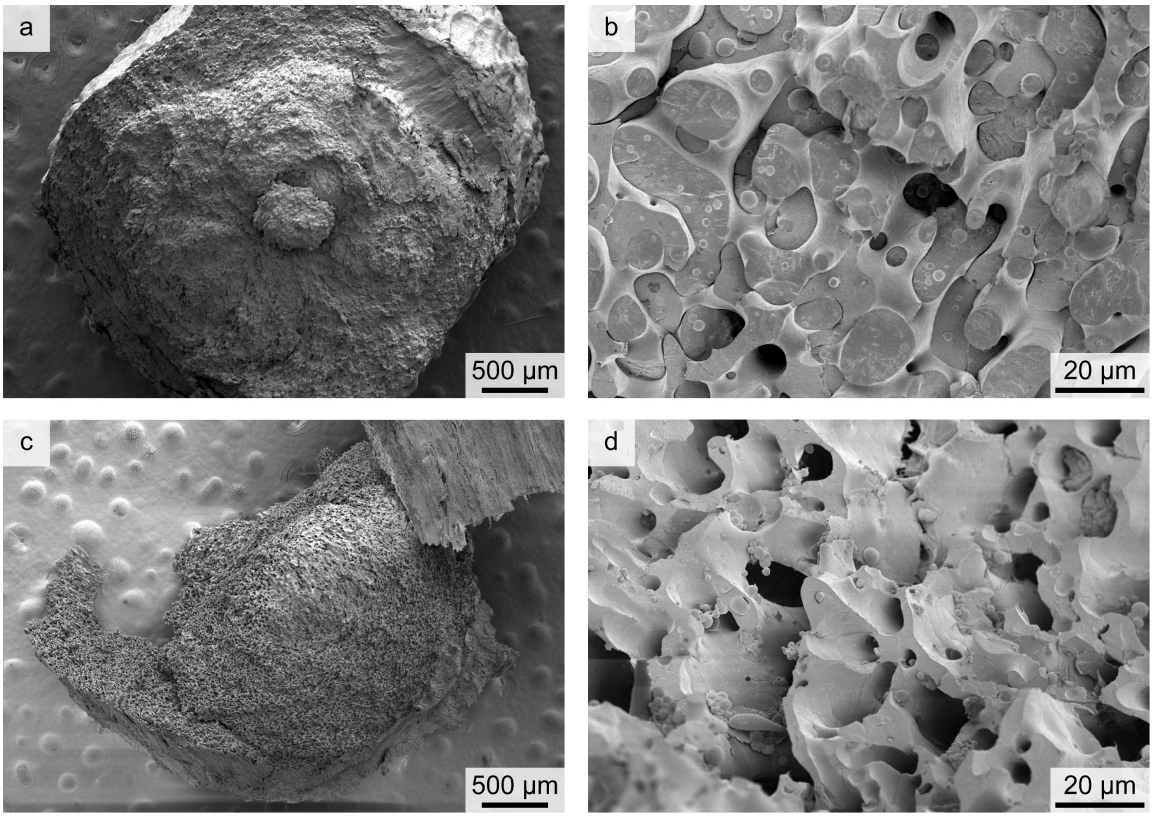

Figure B.S8. Scanning electron micrographs of formulation 480. Micrographs were collected of TB480 before (a,b) and PEZ480 after (c,d) solvent etching in deionized water. A co-continuous network of PE and PEO is visible before etching. The PEO domains are readily evacuated during solvent etching. Due to the high void content after etching, the PE matrix is not mechanically robust on the macroscale, as observed in the damage to the PEX480 SEM sample during freeze fracture. Also of note is the presence of small amounts of PE spheres, indicating some number of discontinuous PE domains in TB480.

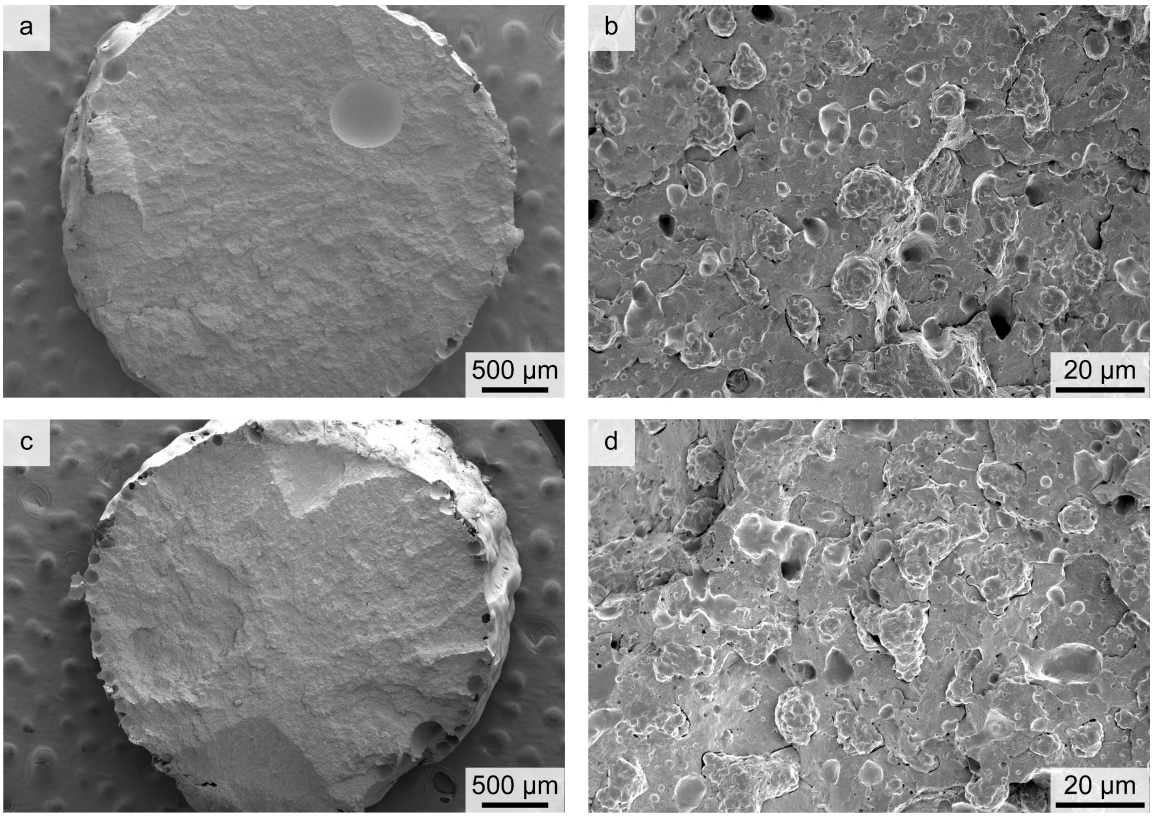

Figure B.S9. Scanning electron micrographs of formulation 411. Micrographs were collected of TB411 before (a,b) and PEZ411 after (c,d) solvent etching in deionized water. PEO and Z13X form a single phase of discontinuous domains within a PE matrix. Due to the high discontinuity, no significant evacuation of PEO is observed.

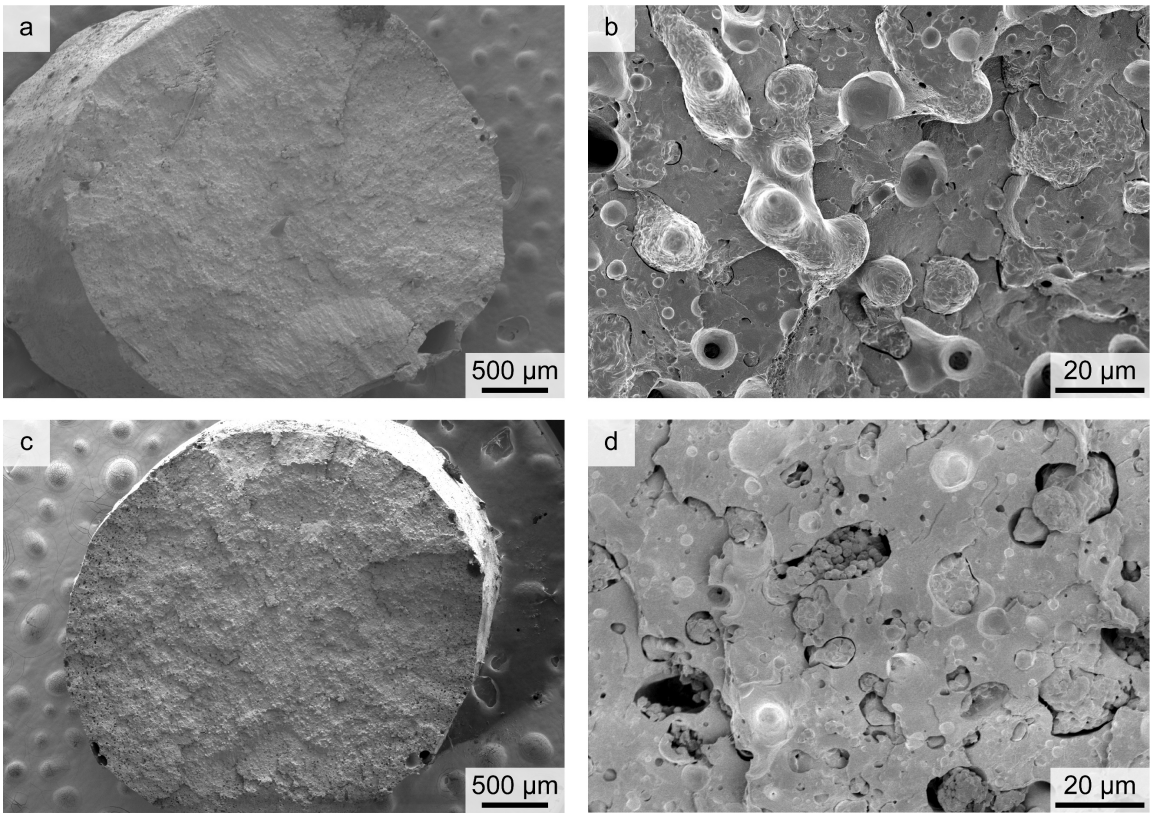

Figure B.S10. Scanning electron micrographs of formulation 421. Micrographs were collected of TB421 before (a,b) and PEZ421 after (c,d) solvent etching in deionized water. PEO and Z13X form a single phase of partly continuous domains before etching. After etching, a mixture of unetched PEO-Z13X domains and etched pores with entrapped Z13X is visible.

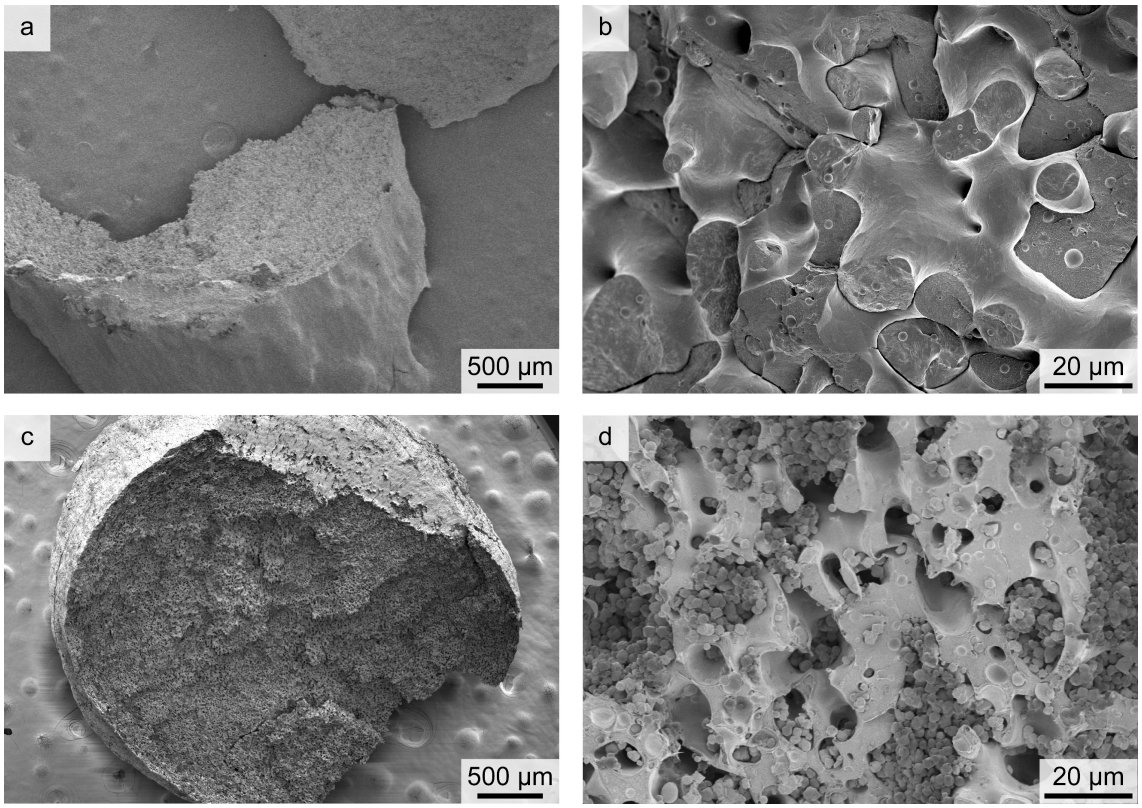

Figure B.S11. Scanning electron micrographs of formulation 441. Micrographs were collected of TB441 before (a,b) and PEZ441 after (c,d) solvent etching in deionized water. Before etching, the PEO-Z13X domain is fully co-continuous with the PE domain. Etching of the PEO network results in effectively complete evacuation of PEO. After etching, the Z13X is clearly visible within the pore network of the PE support matrix.

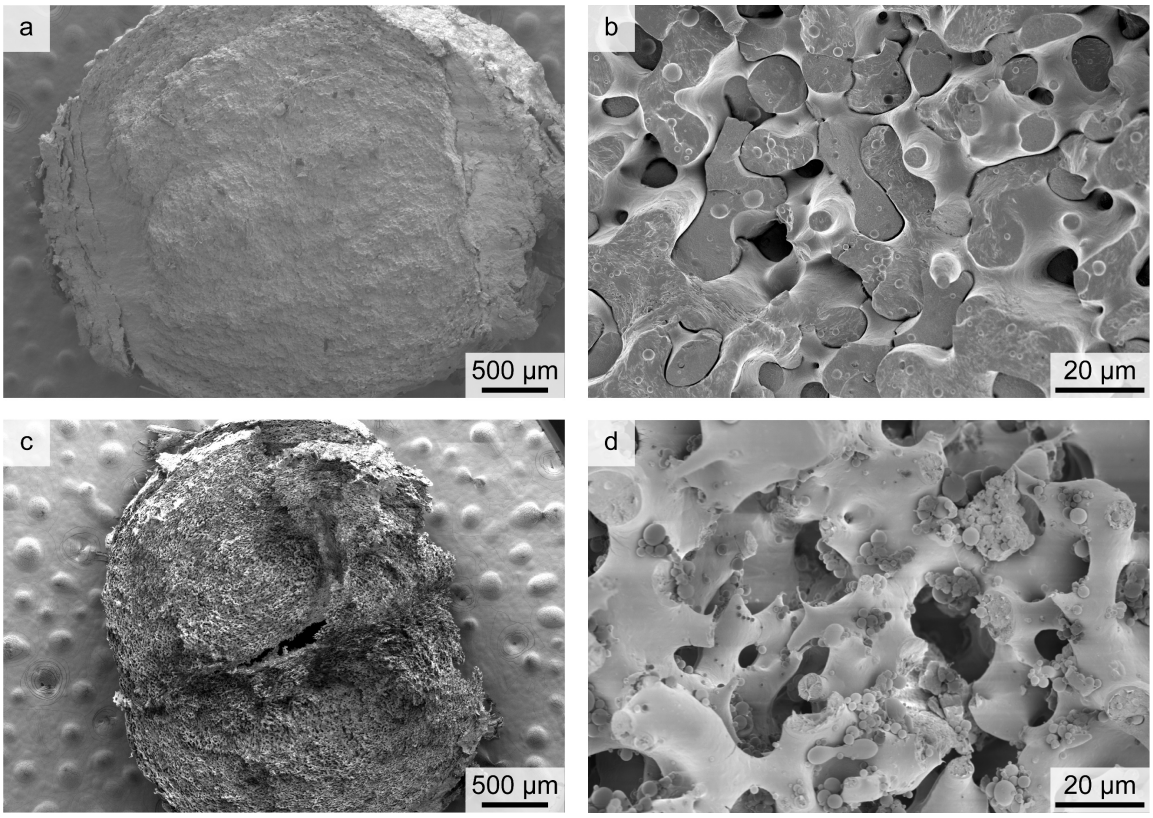

Figure B.S12. Scanning electron micrographs of formulation 481. Micrographs were collected of TB481 before (a,b) and PEZ481 after (c,d) solvent etching in deionized water. Before etching, the PEO-Z13X domain is co-continuous with the PE domain. Etching of the PEO network results in effectively complete evacuation of PEO. After etching, both Z13X and PEP droplets are visible within the pore network of the PE support matrix. In contrast to PEZ441, the pores of PEZ481 are significantly more open-structured, with lower overall retention of zeolite within the support matrix.

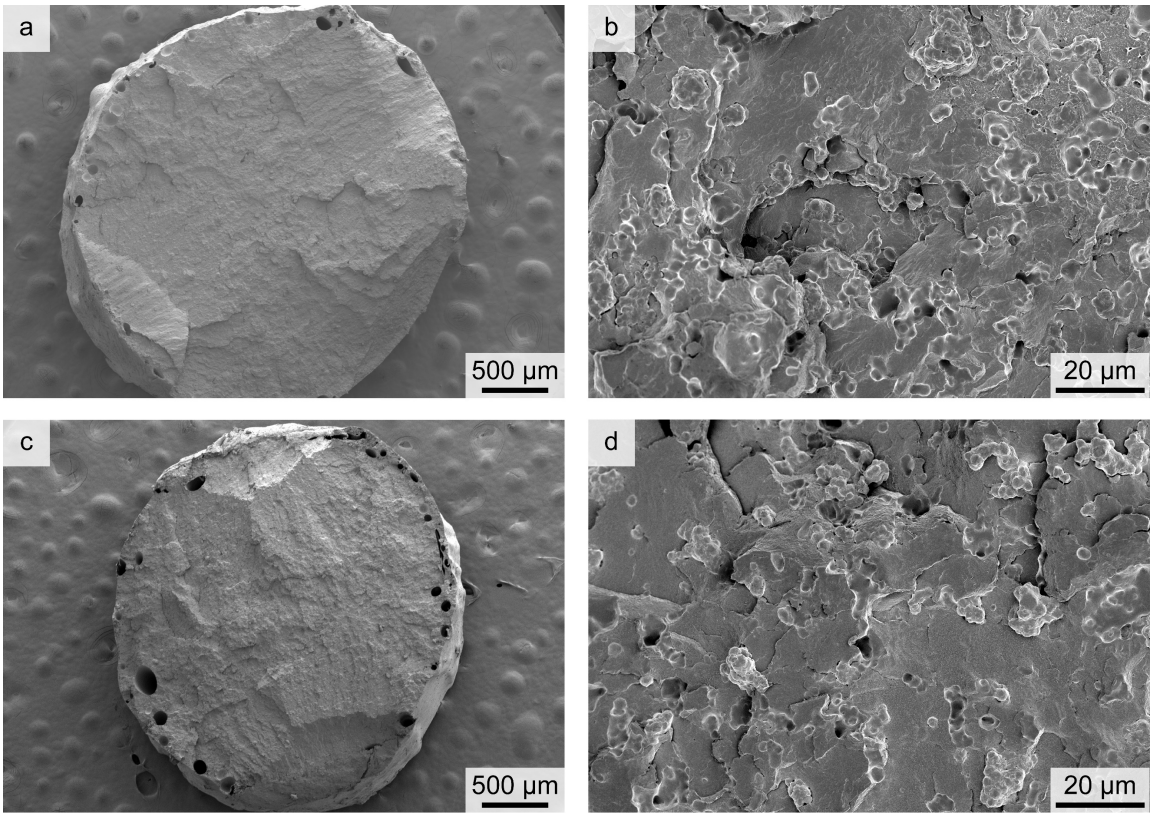

Figure B.S13. Scanning electron micrographs of formulation 412. Micrographs were collected of TB412 before (a,b) and PEZ412 after (c,d) solvent etching in deionized water. TB412 was not readily processable, due to significant jamming within the microcompounder. An attempt was made to recover the TB412 material, which exhibited significant macroscale void formation and inhomogeneity. The PEO-Z13X phase is visible as discreet domains withing the PE matrix, and etching was found to have little effect due to discontinuity.

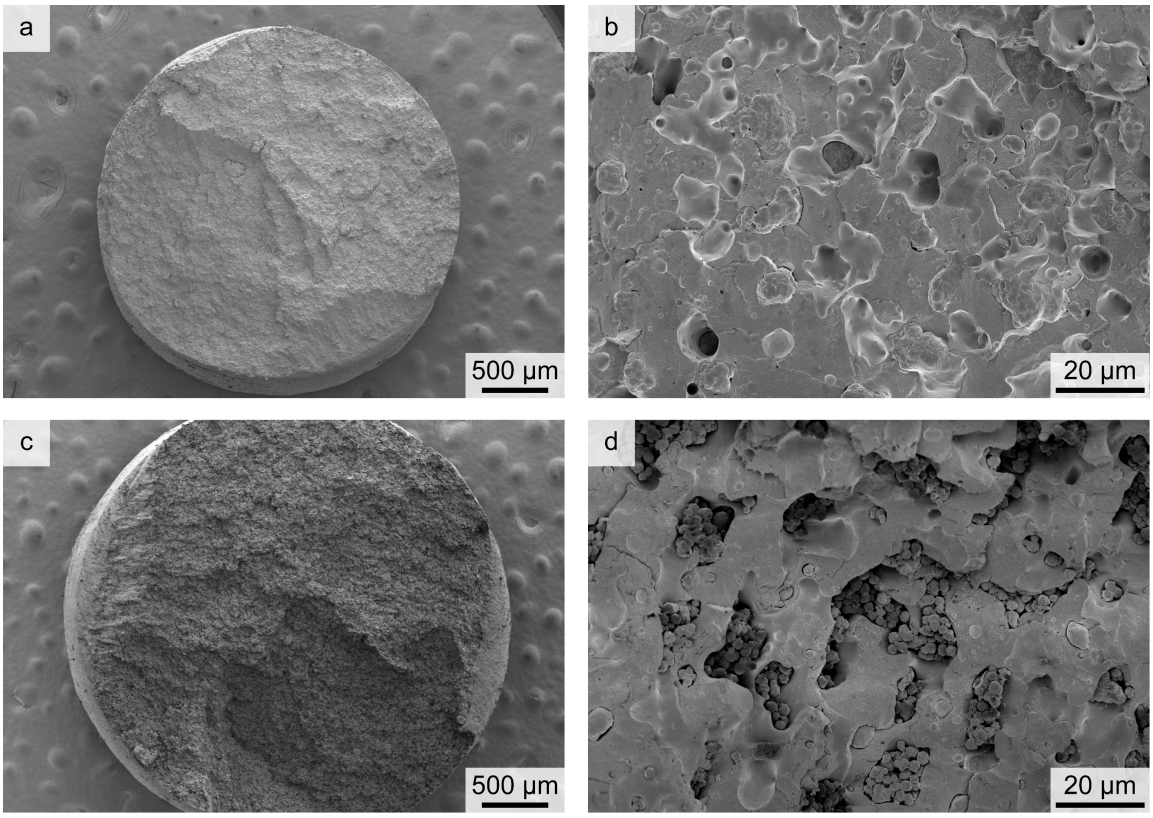

Figure B.S14. Scanning electron micrographs of formulation 422. Micrographs were collected of TB422 before (a,b) and PEZ422 after (c,d) solvent etching in deionized water. Before etching, the PEO-Z13X domain is partly continuous with the PE domain. Etching of the PEO network results in evacuation of PEO from the solvent-accessible domains. After etching, Z13X particles are visible within the pore network of the PE support matrix, while some unetched PEO-Z13X domains are still visible.

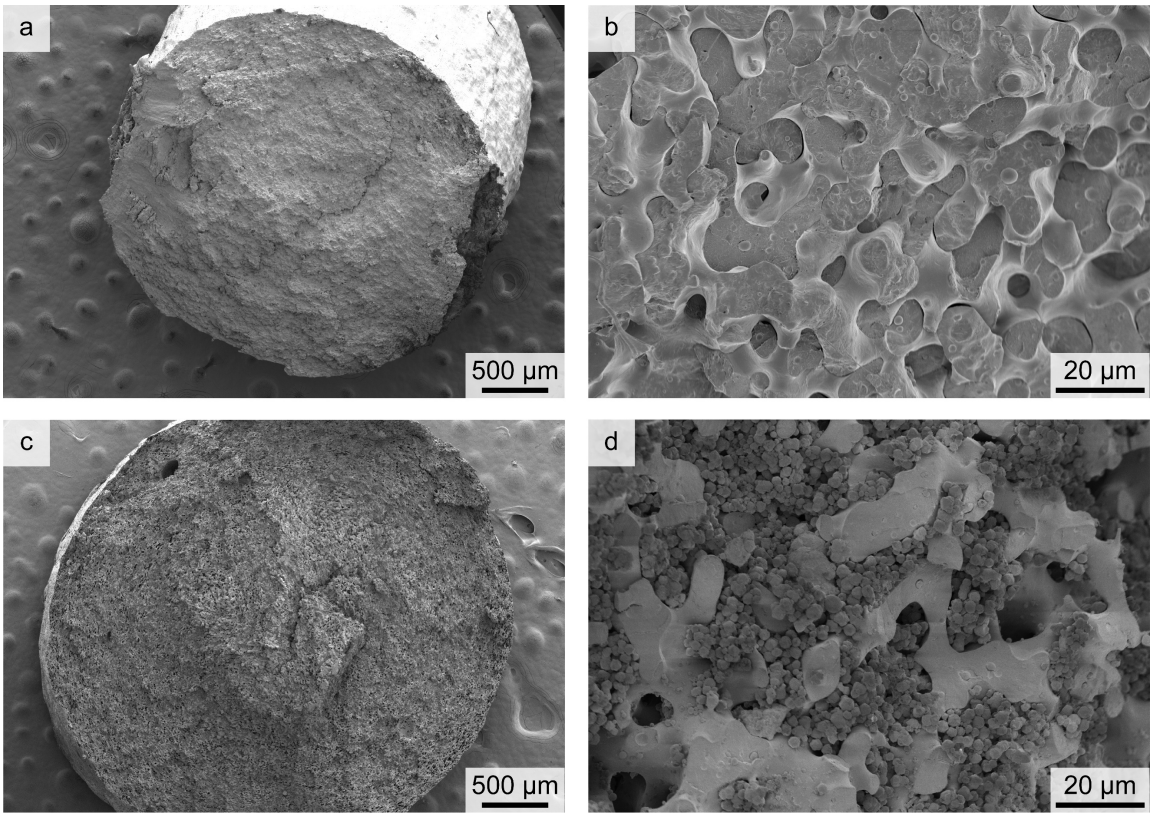

Figure B.S15. Scanning electron micrographs of formulation 442. Micrographs were collected of TB442 before (a,b) and PEZ442 after (c,d) solvent etching in deionized water. Before etching, the PEO-Z13X domain is co-continuous with the PE domain. Etching of the PEO network results in effectively complete evacuation of the PEO network. After etching, Z13X particles are visible within the pore network of the PE support matrix.

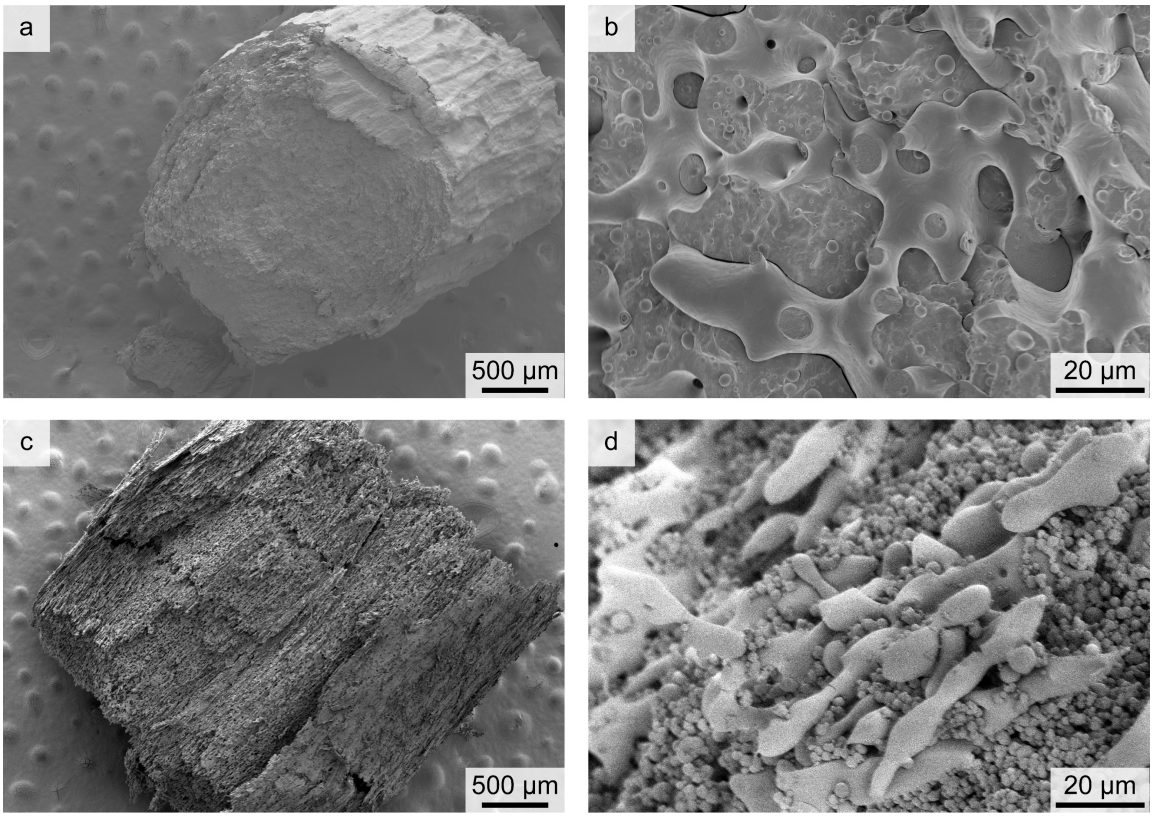

Figure B.S16. Scanning electron micrographs of formulation 482. Micrographs were collected of TB482 before (a,b) and PEZ482 after (c,d) solvent etching in deionized water. Before etching, the PEO-Z13X domain is fully continuous. Etching of the PEO network results in effectively complete evacuation of the PEO network. After etching, Z13X particles are visible within the pore network of the PE support matrix, though discontinuity in the PE network is visible. The PE discontinuity is further evidenced by the lack of mechanical integrity in the SEM samples during the freeze fracture process.

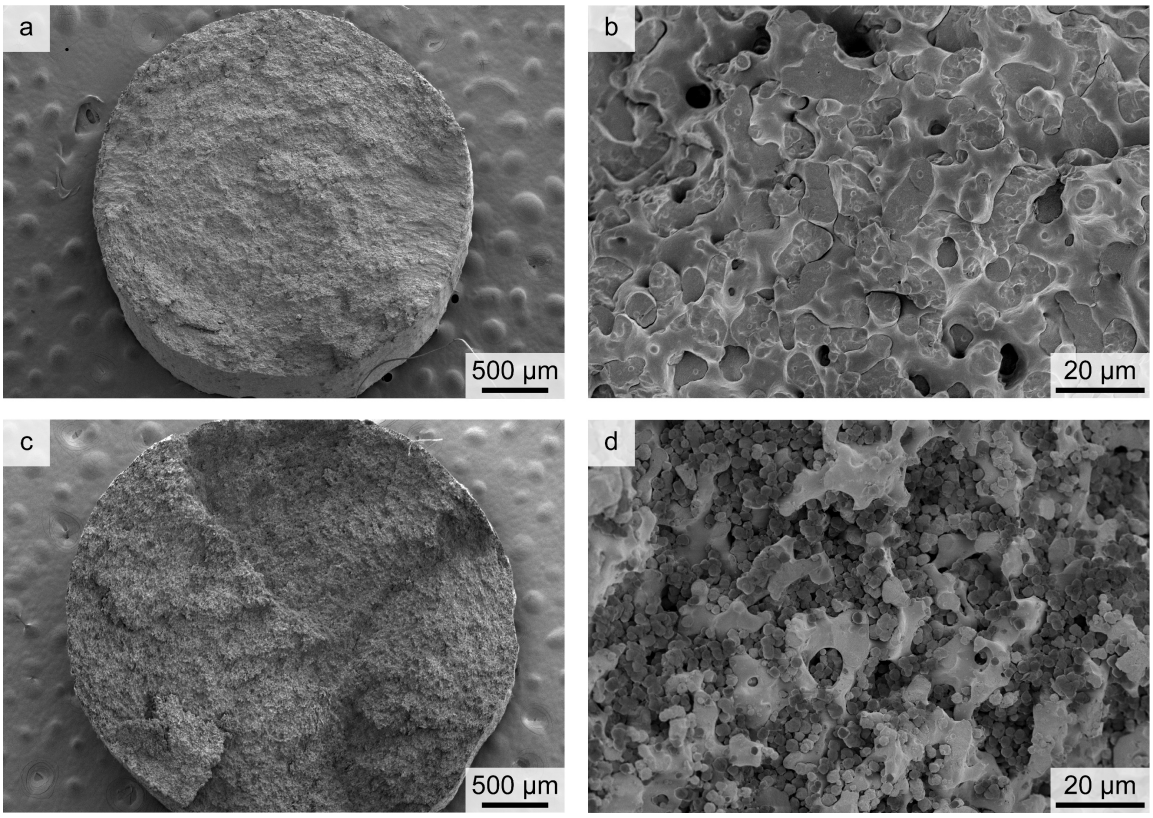

Figure B.S17. Scanning electron micrographs of formulation 444. Micrographs were collected of TB444 before (a,b) and PEZ444 after (c,d) solvent etching in deionized water. Before etching, the PEO-Z13X domain is co-continuous with the PE domain. Etching of the PEO network results in effectively complete evacuation of the PEO network. After etching, Z13X particles are visible within the pore network of the PE support matrix.

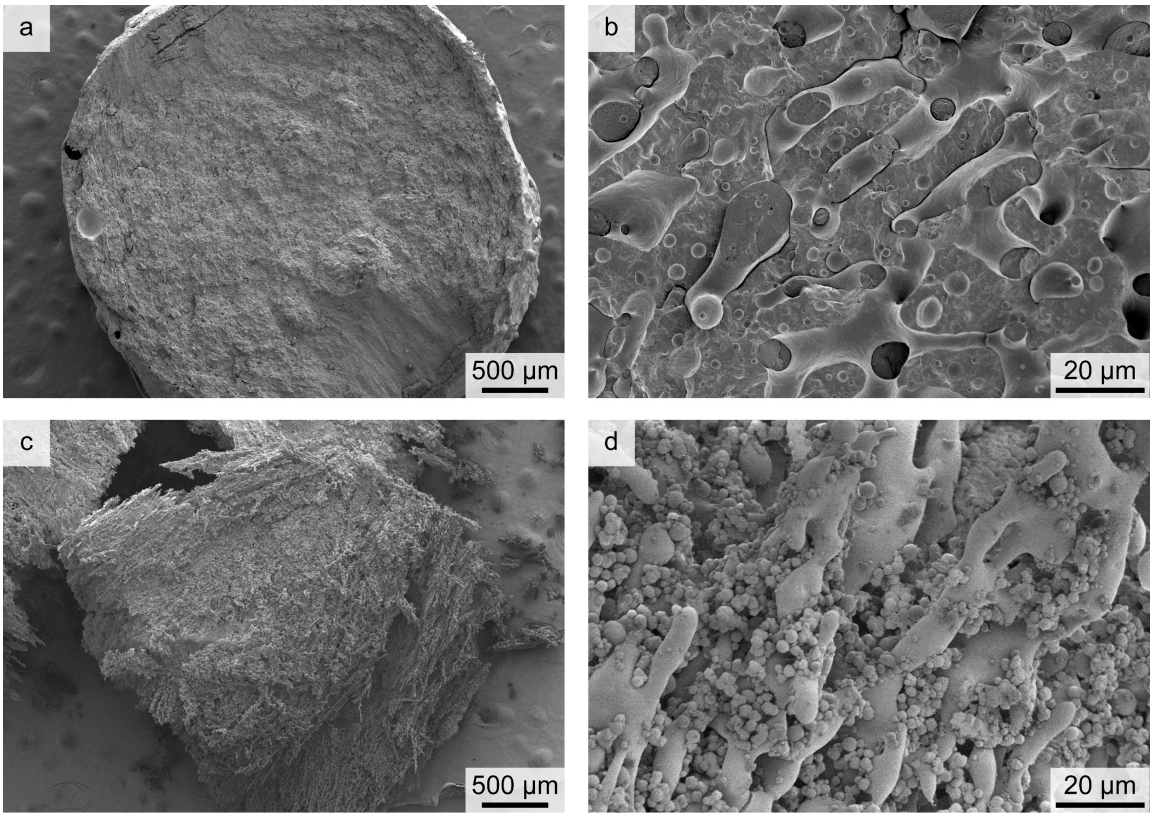

Figure B.S18. Scanning electron micrographs of formulation 484. Micrographs were collected of TB484 before (a,b) and PEZ484 after (c,d) solvent etching in deionized water. Before etching, the PEO-Z13X domain is fully continuous. Etching of the PEO network results in effectively complete evacuation of the PEO network. After etching, Z13X particles are visible within the pore network of the PE support matrix, though discontinuity in the PE network is visible. The PE discontinuity is further evidenced by the lack of mechanical integrity in the SEM samples during the freeze fracture process.

ATR-FTIR analysis of formulation screening materials

ATR-FTIR spectra of complex mixtures can be fit to a linear combination of spectra of the constituent materials, within some degree of error, when in the absorption, rather than reflectance, domain. In the absorption domain, this is represented by the following equation:

$$A_{m,i} = C_a \cdot A_{a,i} + C_b \cdot A_{b,i} + C_c \cdot A_{c,i} + \cdots$$

Where $A_{m,i}$ is the measured absorption of the mixture at the wavelength i; $A_{a,i}$ is the measured absorption of the ath component of the mixture at the ith wavelength; C_a is the coefficient of the ath component spectrum. In dilute solutions, the above equation holds rigorously true were the coefficient C_a is equal to the relative concentration of the Cth component. In solid mixtures, the above relationship is *qualitatively* accurate, but not rigorously so due to fluctuations in bulk density, morphology, and penetration depth. For reflectance FTIR, it is necessary to account for the relationship between absorbance (A) and reflectance (R), as below:

$$A_{a,i} = -\log\left(R_{a,i}\right)$$

Therefore, the equation for linear combination of spectra in ATR-FTIR becomes:

$$-\log\left(R_{m,i}\right) = C_a \cdot -\log\left(R_{a,i}\right) + C_b \cdot -\log\left(R_{b,i}\right) + C_c \cdot -\log\left(R_{c,i}\right) + \cdots$$

Again, it is critical to emphasize that this equation is not rigorously quantitative for use in ATR-FTIR, nor in any other reflectance mode spectroscopy with bulk materials. However, it is sufficient to provide *relative* and *qualitative* assessments of the components of a mixture. In regard to relative PE and PEO fractional composition, the fitting function generally agrees with expected results; however, it fails quite spectacularly in the estimation of zeolite loading—an example of the aforementioned challenges arising from differences in packing and bulk density. Therefore, only PE:PEO ratios are estimated from ATR-FTIR, while zeolite loading is determined by TGA.

ATR-FTIR analysis of materials produced in the formulation screening process is shown on the following pages:

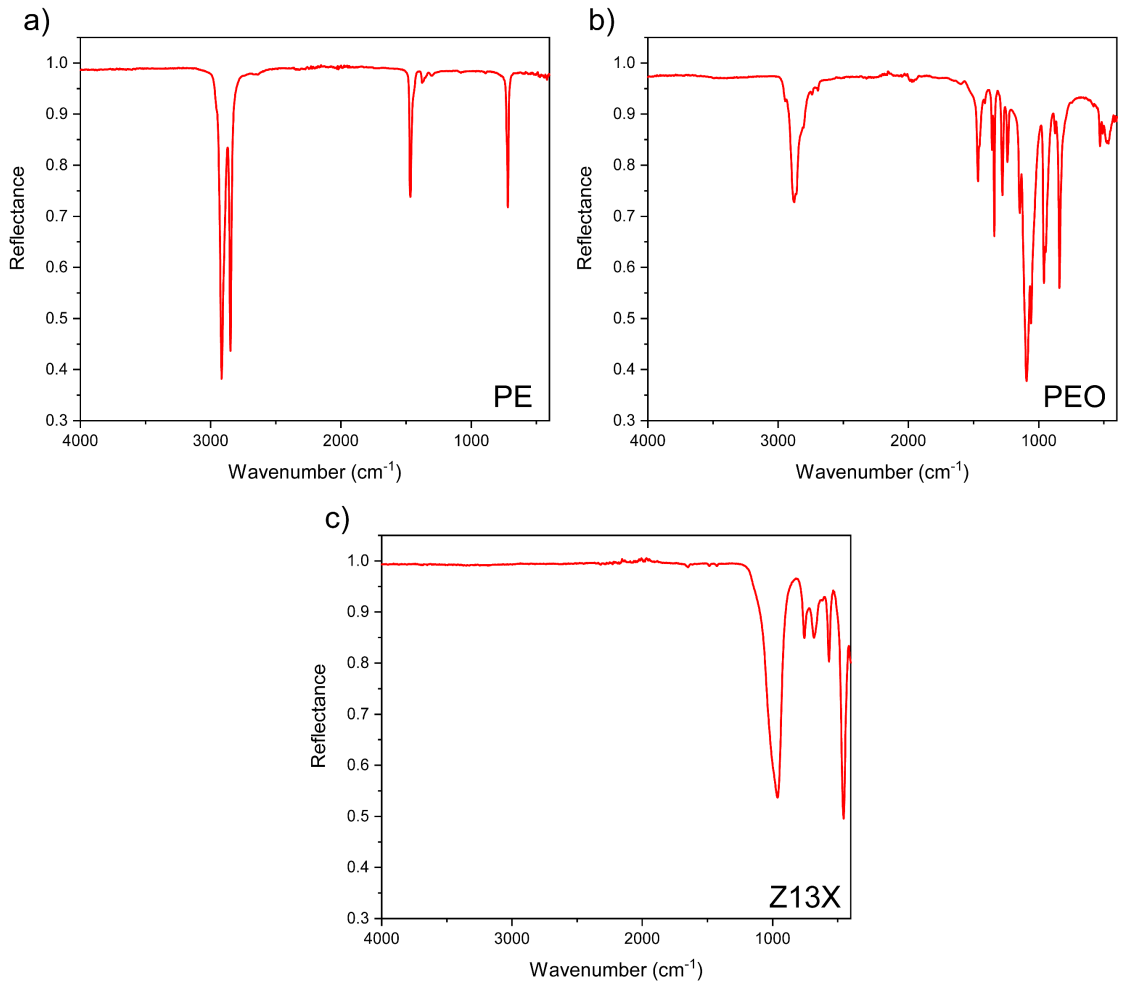

Figure B.S19. ATR FTIR spectra of polyethylene (a), polyethylene oxide (b), and zeolite 13X (c) used in this study.

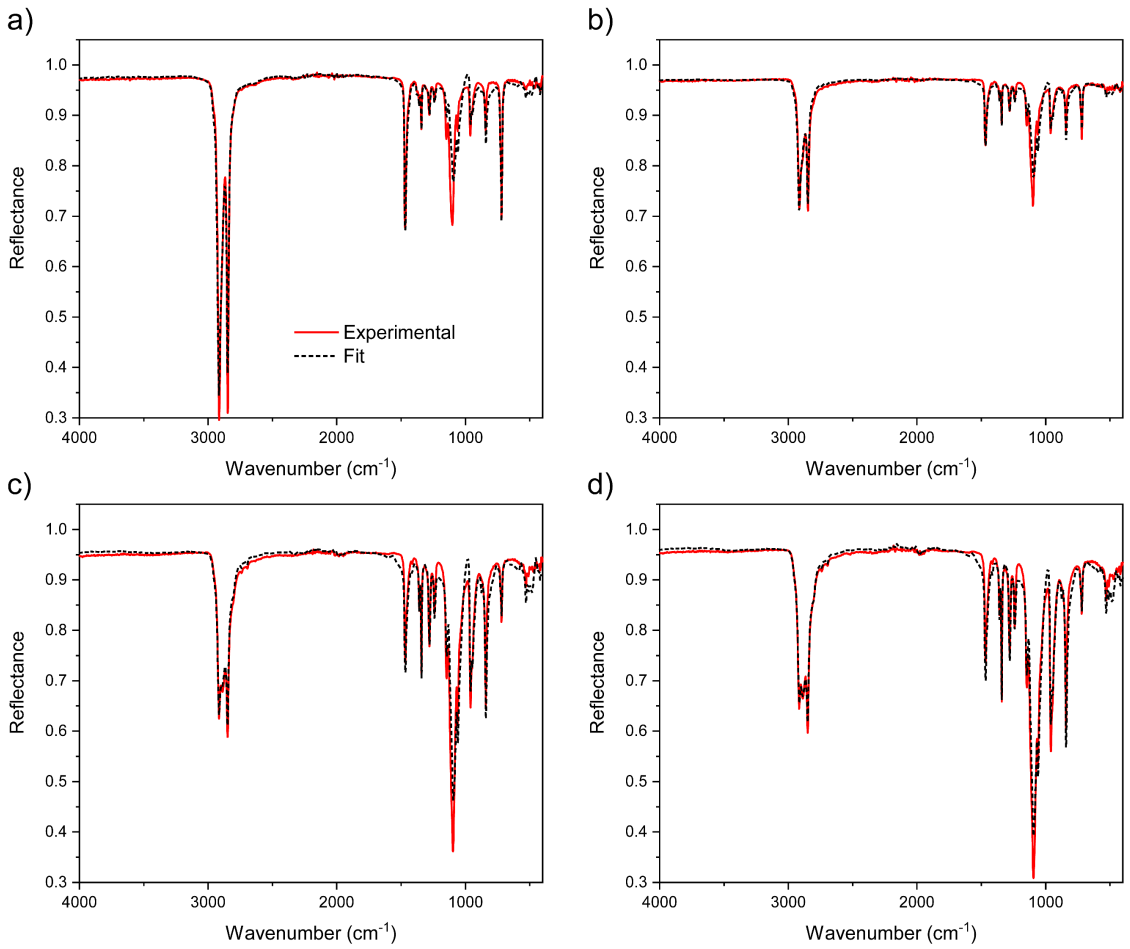

Figure B.S20. Measured ATR FTIR spectra for TB4X0 series materials and curves of best fit calculated from combinations of standard PE, PEO and Z13X spectra: TB410 (a), TB420 (b), TB440 (c), and TB480 (d).

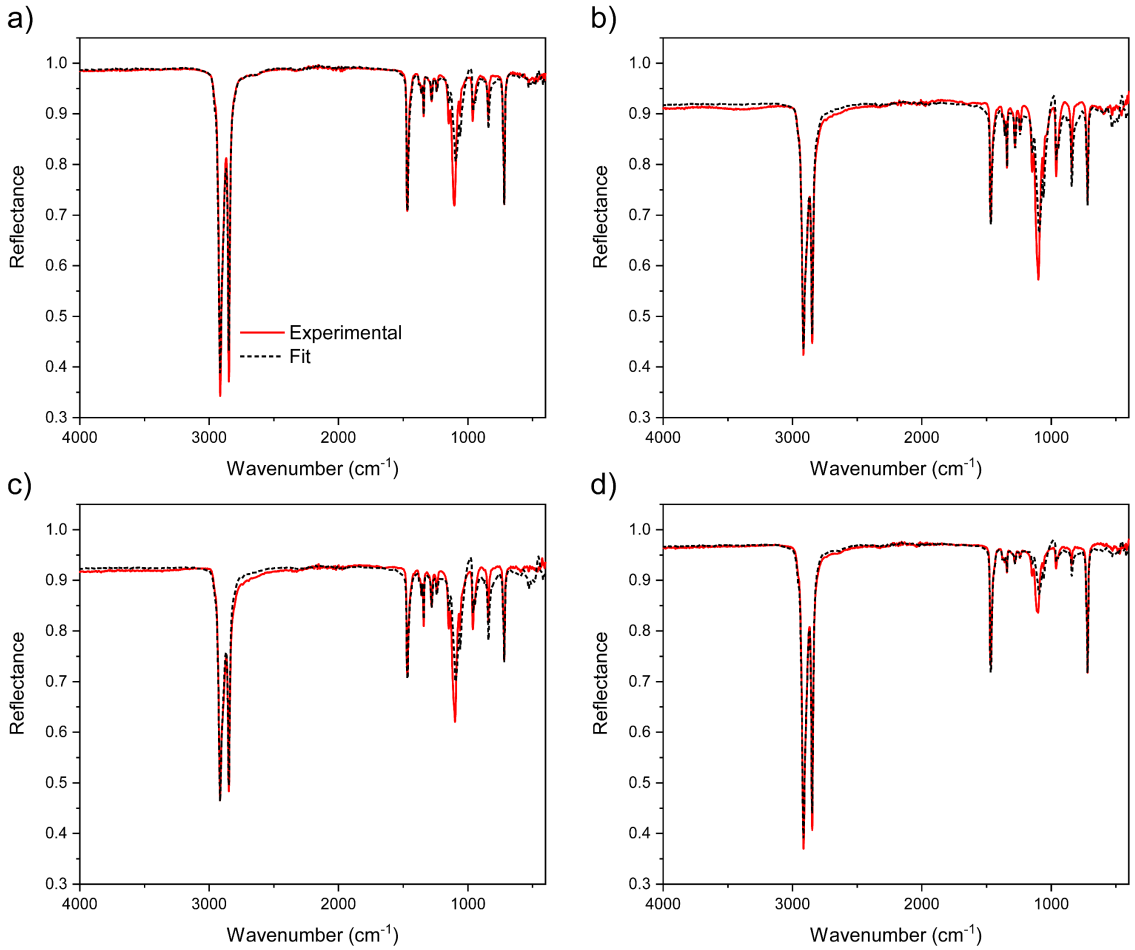

Figure B.S21. Measured ATR FTIR spectra for PEZ4X0 series materials and curves of best fit calculated from combinations of standard PE, PEO and Z13X spectra: PEZ410 (a), PEZ420 (b), PEZ440 (c), and PEZ480 (d).

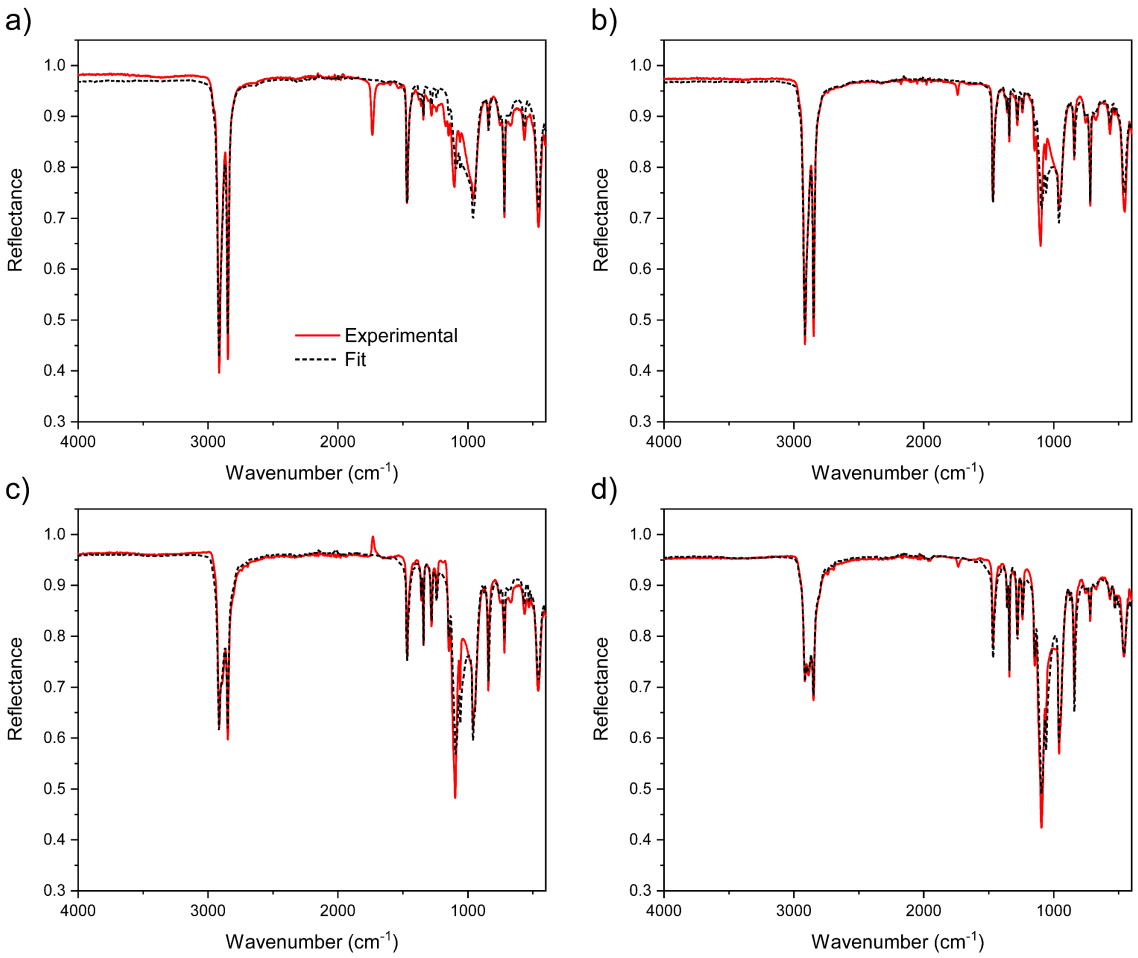

Figure B.S22. Measured ATR FTIR spectra for TB4X1 series materials and curves of best fit calculated from combinations of standard PE, PEO and Z13X spectra: TB411 (a), TB421 (b), TB441 (c), and TB481 (d).

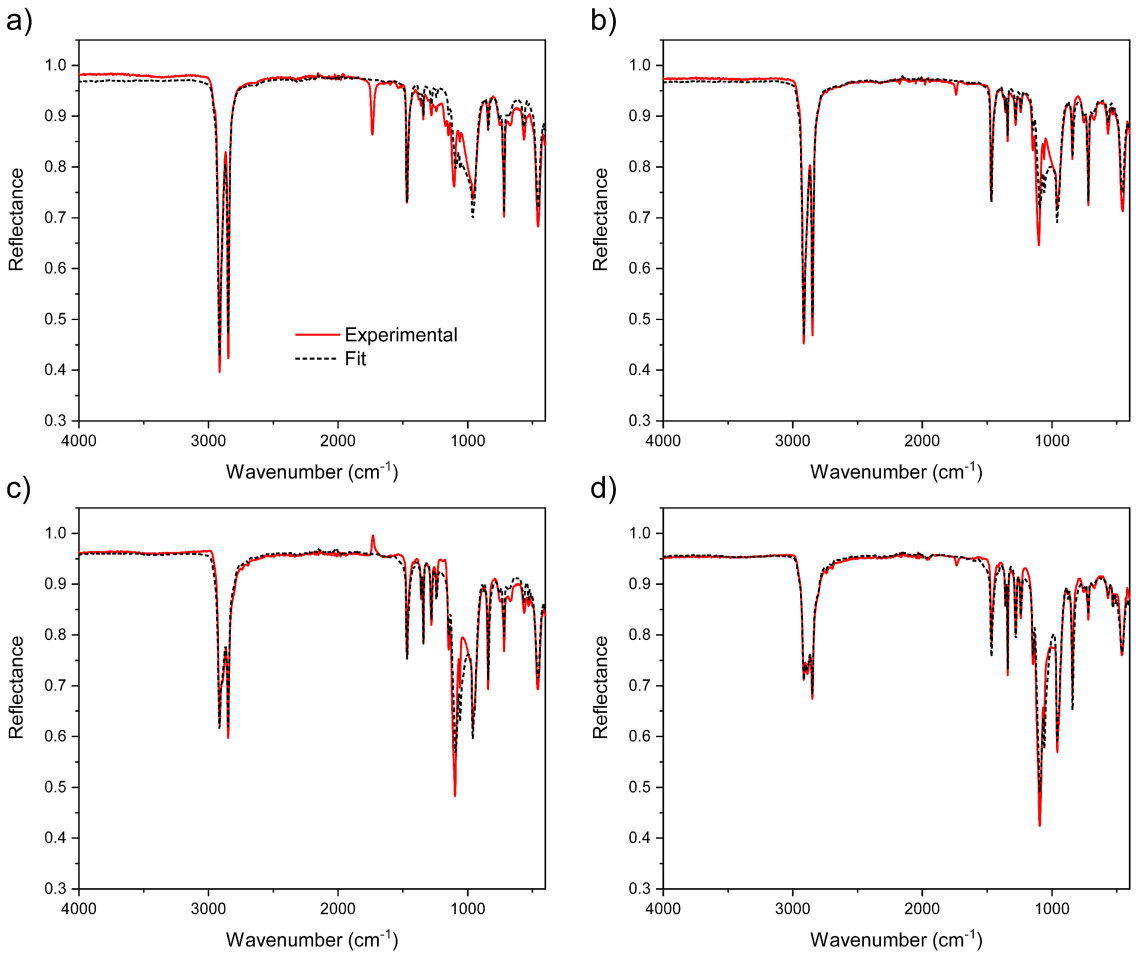

Figure B.S23. Measured ATR FTIR spectra for PEZ4X1 series materials and curves of best fit calculated from combinations of standard PE, PEO and Z13X spectra: PEZ411 (a), PEZ421 (b), PEZ441 (c), and PEZ481 (d).

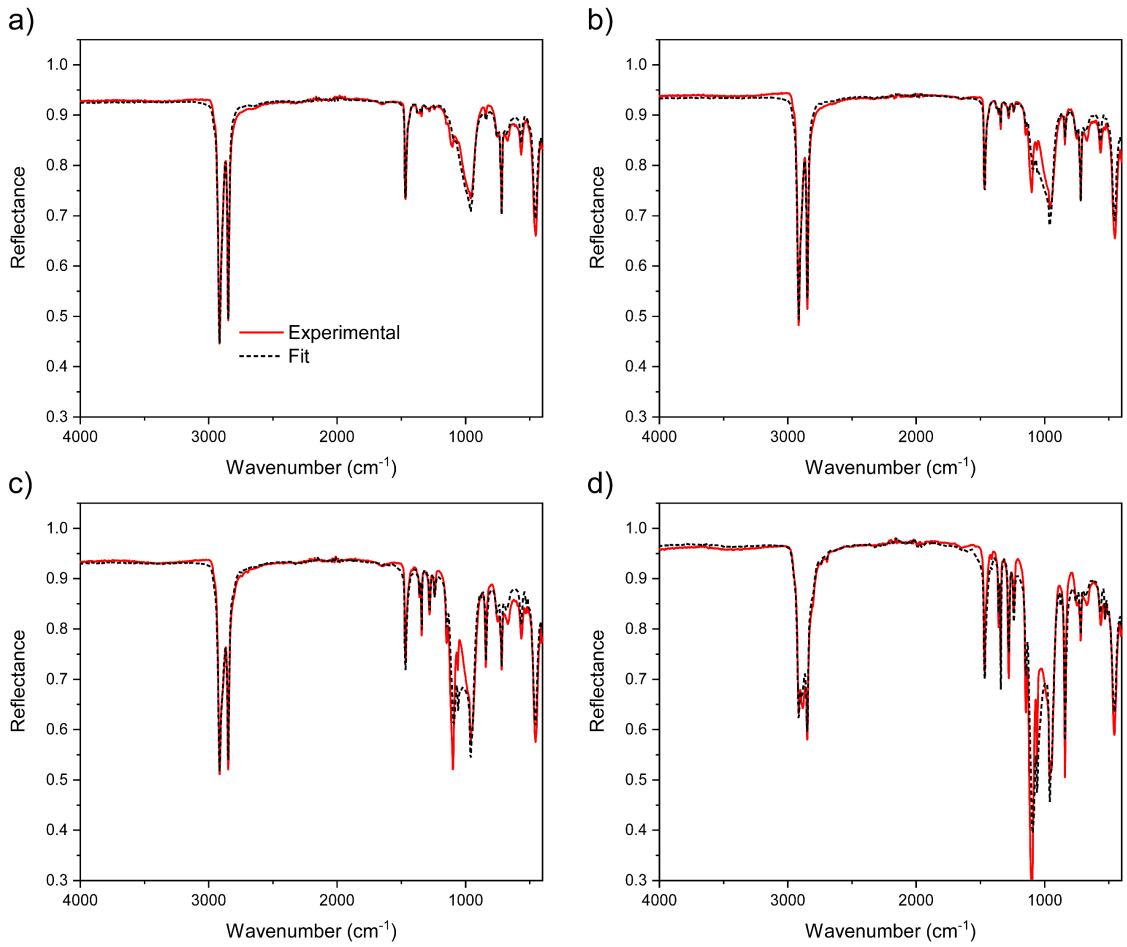

Figure B.S24. Measured ATR FTIR spectra for TB4X2 series materials and curves of best fit calculated from combinations of standard PE, PEO and Z13X spectra: TB412 (a), TB422 (b), TB442 (c), and TB482 (d).

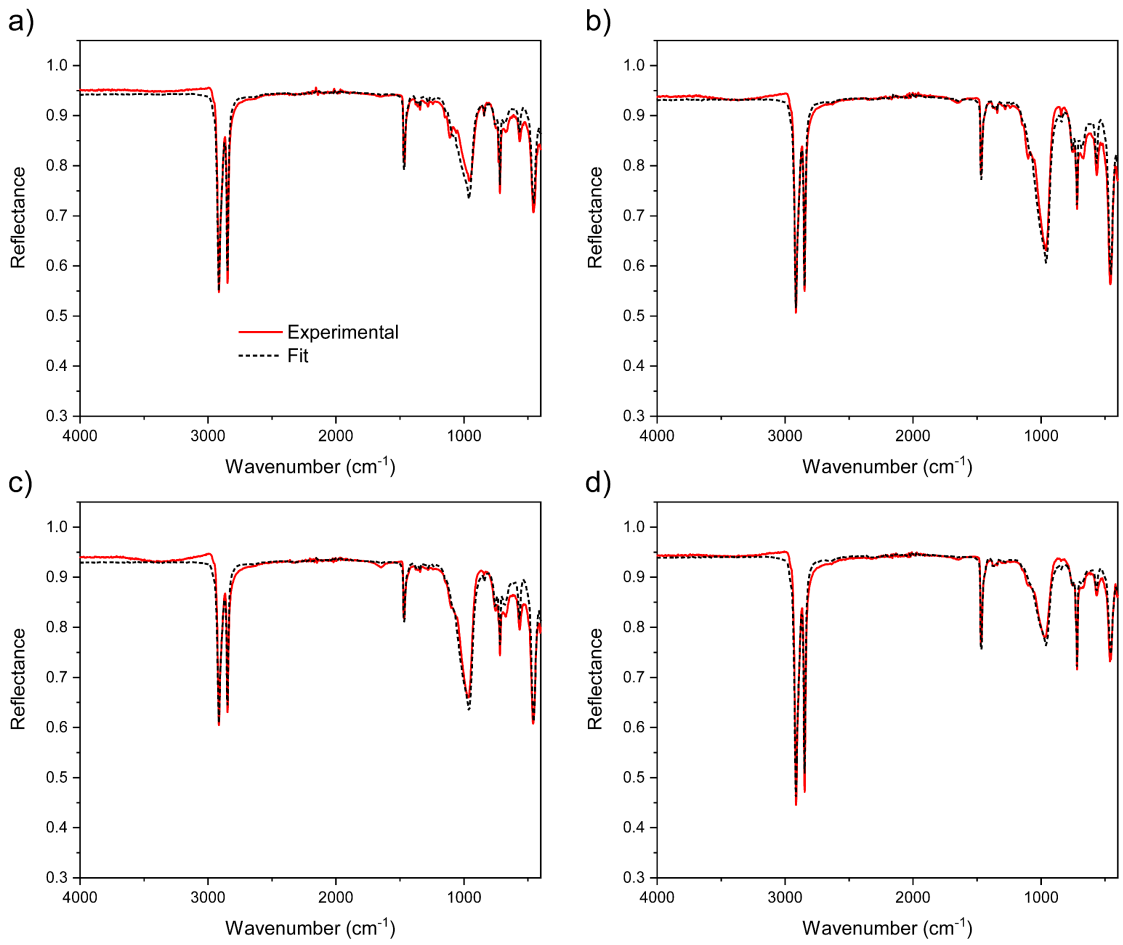

Figure B.S25. Measured ATR FTIR spectra for PEZ4X2 series materials and curves of best fit calculated from combinations of standard PE, PEO and Z13X spectra: PEZ412 (a), PEZ422 (b), PEZ442 (c), and PEZ482 (d).

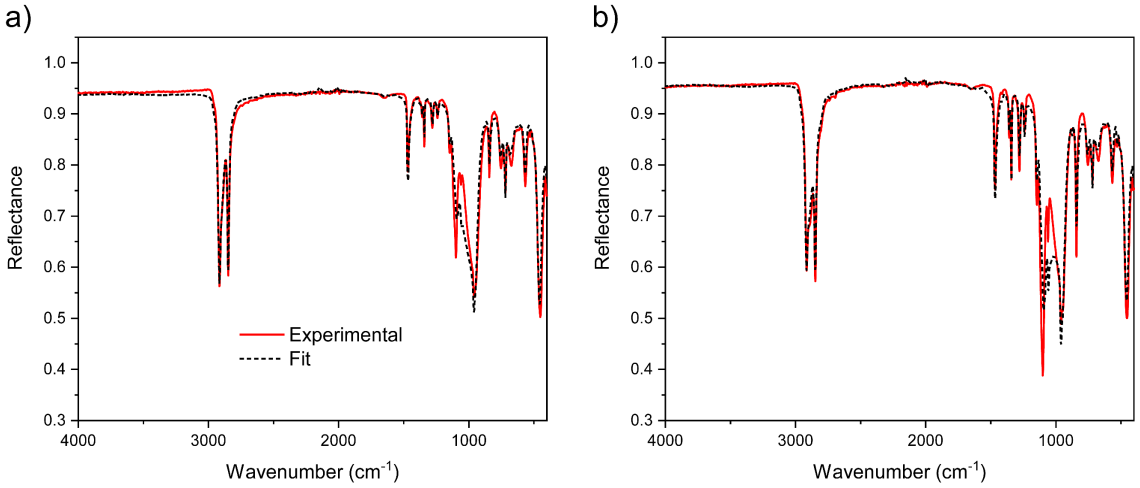

Figure B.S26. Measured ATR FTIR spectra for TB4X4 series materials and curves of best fit calculated from combinations of standard PE, PEO and Z13X spectra: TB444 (a) and TB484 (b).

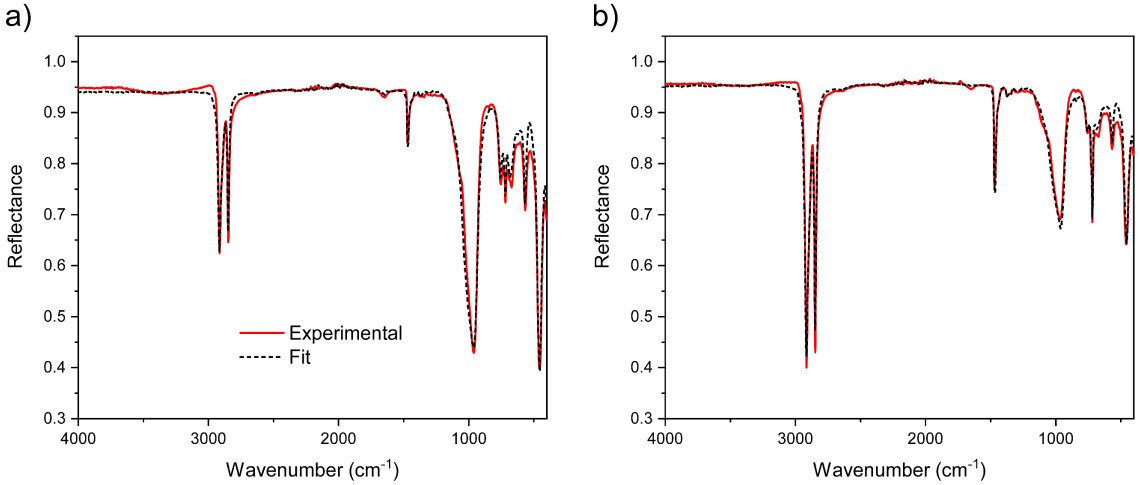

Figure B.S27. Measured ATR FTIR spectra for PEZ4X4 series materials and curves of best fit calculated from combinations of standard PE, PEO and Z13X spectra: PEZ444 (a) and PEZ484 (b).

Table B.S2. Fitted Spectrum Components and PE:PEO ratios for formulation screening materials

	Spectral Coefficient			Polymer Fraction (%)	
Sample	f_{PE}	f_{PEO}	f_{Z13X}	PE_{meas}	PEO_{meas}
TB410	0.46	0.11	0.03	81	19
TB420	0.13	0.10	0.02	56	44
TB440	0.15	0.33	0.05	32	68
TB480	0.14	0.41	0.04	25	75
PEZ410	0.42	0.09	0.02	82	18
PEZ420	0.30	0.14	0.04	68	32
PEZ440	0.28	0.12	0.04	70	30
PEZ480	0.40	0.05	0.02	90	10
TB411	0.36	0.07	0.17	84	16
TB421	0.31	0.12	0.13	73	27
TB441	0.18	0.22	0.14	45	55
TB481	0.11	0.28	0.08	27	73
PEZ411	0.38	0.05	0.16	88	12
PEZ421	0.17	0.10	0.11	62	38
PEZ441	0.29	0.03	0.18	90	10
PEZ481	0.35	0.02	0.10	95	5
TB412[†]	0.30	0.02	0.16	95	5
TB422	0.26	0.05	0.16	84	16
TB442	0.24	0.16	0.22	60	40
TB482	0.16	0.39	0.19	30	70
PEZ412	0.23	0.02	0.15	91	9
PEZ422	0.25	0.02	0.26	93	7
PEZ442	0.18	0.01	0.24	92	8
PEZ482	0.30	0.01	0.13	97	3
TB414[†]	---	---	---	---	---
TB424[†]	---	---	---	---	---
TB444	0.21	0.09	0.32	69	31
TB484	0.19	0.24	0.31	44	56
PEZ414[†]	---	---	---	---	---
PEZ424[†]	---	---	---	---	---
PEZ444	0.18	0.00	0.50	98	2
PEZ484	0.35	0.01	0.23	98	2

† Samples were not processable due to jamming of the compounder at <1:1 PEO:Z13X ratios. Formulation TB412 was recovered from the compounder, but the material exhibited significant heterogeneity. Formulations TB414 and TB424 were not processable whatsoever.

Thermogravimetric analysis of formulation screening materials

The following pages present thermogravimetric analysis (TGA) traces for each of the materials produced in the formulation screening process. TGA traces were collected using a TA Instruments Q500 Thermogravimetric Analyzer with 12 pan autosampler platter. All dynamic TGA traces were acquired at a 10 °C/min ramp rate under 60 mL/min flowing air. Samples were first equilibrated at ~ 50 °C and heated to 550 °C to fully pyrolize the polymer component of each material. The % mass residue at the end of each heating cycle was used to determine the zeolite loading in each material.

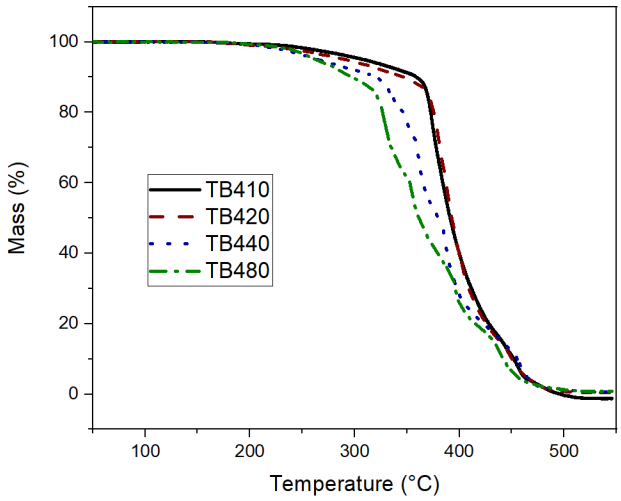

Figure B.S28. Dynamic thermogravimetric analysis scans of TB4X0 series materials. Scans were collected at a 10 °C/min ramp rate under 60 mL/min air flow.

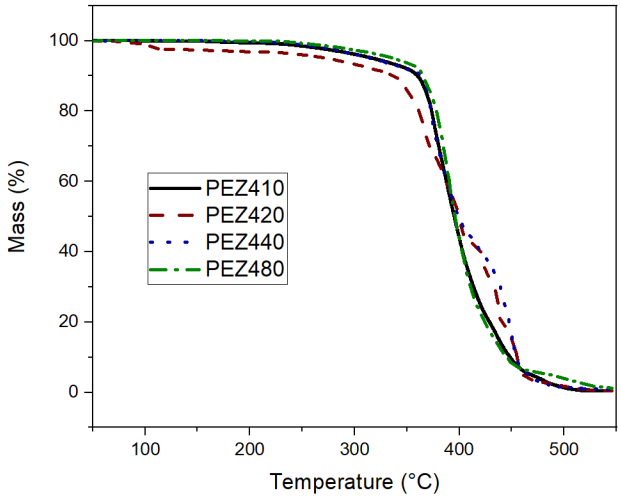

Figure B.S29. Dynamic thermogravimetric analysis scans of PEZ4X0 series materials. Scans were collected at a 10 °C/min ramp rate under 60 mL/min air flow.

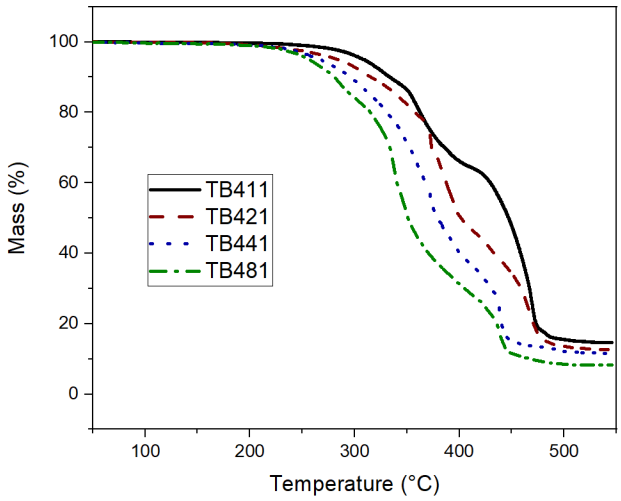

Figure B.S30. Dynamic thermogravimetric analysis scans of TB4X1 series materials. Scans were collected at a 10 °C/min ramp rate under 60 mL/min air flow.

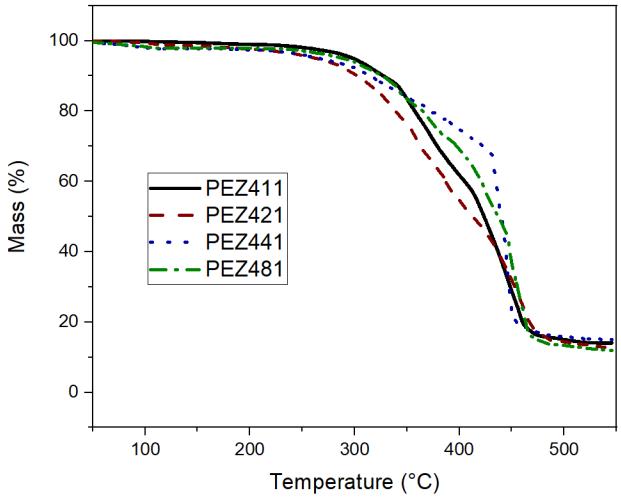

Figure B.S31. Dynamic thermogravimetric analysis scans of PEZ4X1 series materials. Scans were collected at a 10 °C/min ramp rate under 60 mL/min air flow.

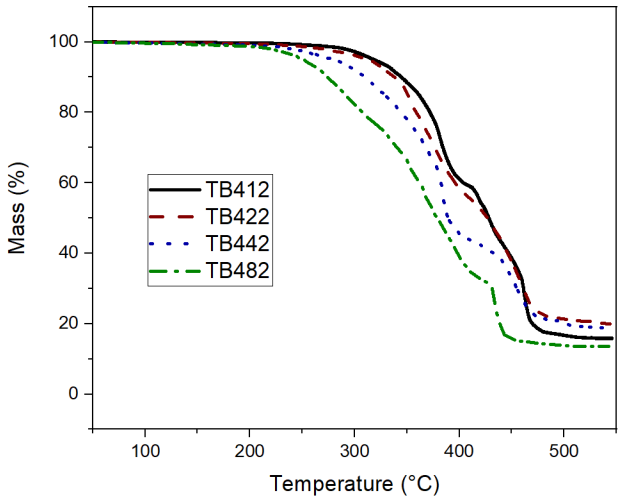

Figure B.S32. Dynamic thermogravimetric analysis scans of TB4X2 series materials. Scans were collected at a 10 °C/min ramp rate under 60 mL/min air flow.

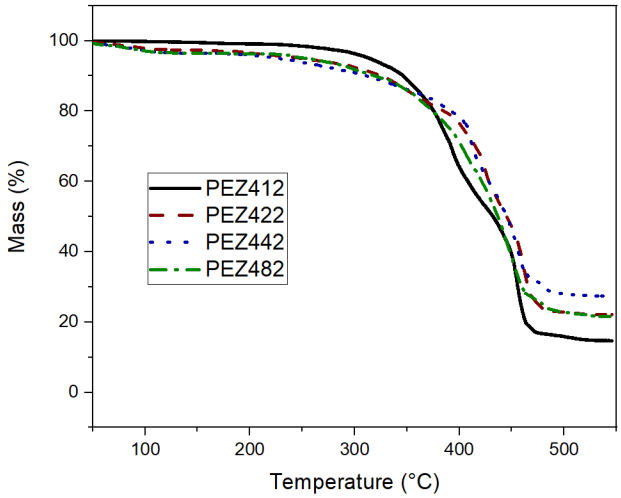

Figure B.S33. Dynamic thermogravimetric analysis scans of PEZ4X2 series materials. Scans were collected at a 10 °C/min ramp rate under 60 mL/min air flow.

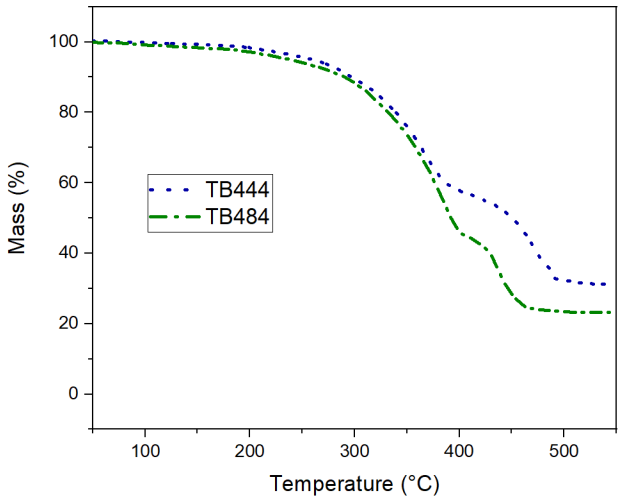

Figure B.S34. Dynamic thermogravimetric analysis scans of TB4X4 series materials. Scans were collected at a 10 °C/min ramp rate under 60 mL/min air flow.

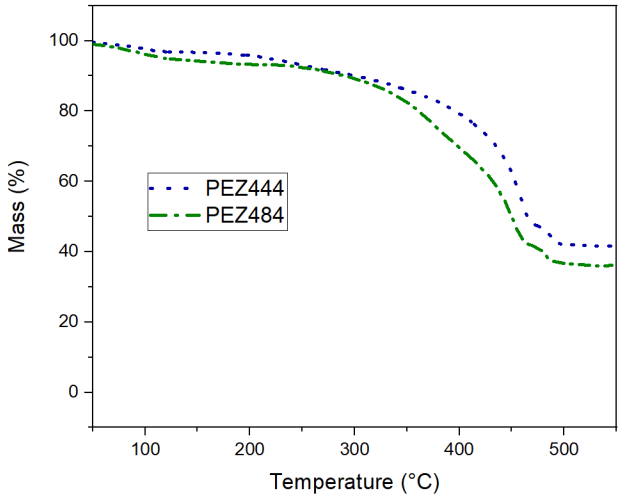

Figure B.S35. Dynamic thermogravimetric analysis scans of PEZ4X4 series materials. Scans were collected at a 10 °C/min ramp rate under 60 mL/min air flow.

Table B.S3. Theoretical and observed residual masses for each TB and PEZ formulation used in the screening process.

Sample	Res. Mass$_{Theo}$ (%)	Res. Mass$_{Obs}$ (%)*	Zeolite Yield (% vs. Theo.)
TB410	0	-1.3	---
TB420	0	0.5	---
TB440	0	0.7	---
TB480	0	0.8	---
PEZ410	0	0.5	---
PEZ420	0	0.5	---
PEZ440	0	0.9	---
PEZ480	0	1.1	---
TB411	16.7	14.6	87
TB421	14.3	12.6	88
TB441	11.1	11.7	105
TB481	7.7	8.3	108
PEZ411	20	14.0	70
PEZ421	20	12.8	64
PEZ441	20	15.1	76
PEZ481	20	12.0	60
TB412†	28.6	15.8	55
TB422	25.0	20.0	80
TB442	20.0	18.8	94
TB482	14.3	13.5	95
PEZ412	33.3	14.8	44
PEZ422	33.3	22.1	66
PEZ442	33.3	26.4	80
PEZ482	33.3	21.6	65

Table B.Continued on Next Page…

Table B.S3 (Cont'd). Theoretical and observed residual masses for each TB and PEZ formulation used in the screening process.

Sample	Res. Mass$_{Theo}$ (%)	Res. Mass$_{Obs}$ (%)*	Zeolite Yield (% vs. Theo.)
TB414†	---	---	---
TB424†	---	---	---
TB444	33.3	31.2	94
TB484	25.0	23.2	93
PEZ414†	---	---	---
PEZ424†	---	---	---
PEZ444	50.0	41.6	83
PEZ484	50.0	36.1	72

* It is assumed that observed residual mass is equivalent to zeolite loading by mass in the material.

† Samples were not processable due to jamming of the compounder at <1:1 PEO:Z13X ratios. Formulation TB412 was recovered from the compounder, but the material exhibited significant heterogeneity. Formulations TB414 and TB424 were not processable whatsoever.

NOTE: The actual value of zeolite loading may be higher in some cases. After solvent etching, it was not possible to fully dry the materials at room temperature, while heating risked collapsing the pore structure. Thus, some etched samples exhibit a mass loss corresponding to the loss of water. Retained water artificially inflates the mass of the sample, correspondingly depressing the measured zeolite loading. For the sake of transparency and rigor, the reported zeolite loading values were ***not*** corrected for excess water retention and are reported exactly as measured.

Characterization of Bulk Materials

This section details supplementary information for the manufacture and characterization of the bulk materials detailed in the main text. Material composition before and after etching was determined by a combination of Fourier transform infrared spectroscopy (FTIR) and thermogravimetric analysis (TGA). Morphology was assessed by scanning electron microscopy (SEM).

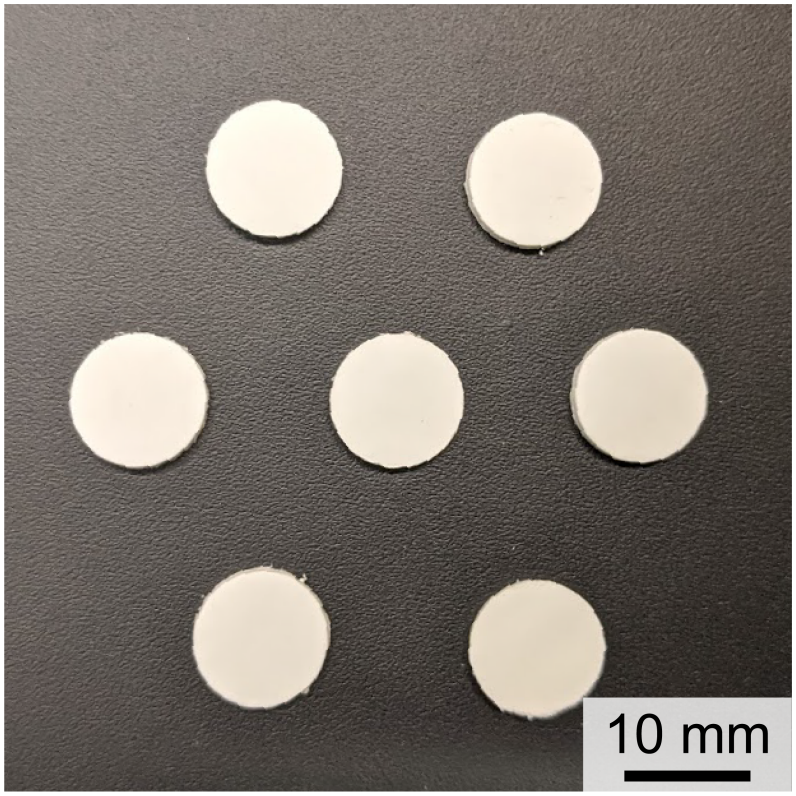

Figure B.S36. Representative optical image of a collection of PEZ444 carriers at higher resolution than presented in the main text. Carriers are highly uniform with a diameter of 11 mm and a thickness of 1.5 mm.

Scanning electron micrographs of bulk materials

The following pages present scanning electron micrographs (SEMs) of ternary blends and etched materials used in the formulation screening section of this manuscript. All micrographs were acquired on an Hitachi SU8230 Field Emission Gun Scanning Electron Microscope at the Characterization Facility Labs at the University of Minnesota. All samples were dried at room temperature under reduced pressure for 24 hr before sample preparation. All samples were sputter coated with 5 nm iridium. Unless otherwise noted, all images were acquired at a 1.0 kV accelerating voltage using both upper and lower detectors for image acquisition. Image contrast of some micrographs has been adjusted for clarity in print; no other modifications (other than cropping to fit) were made.

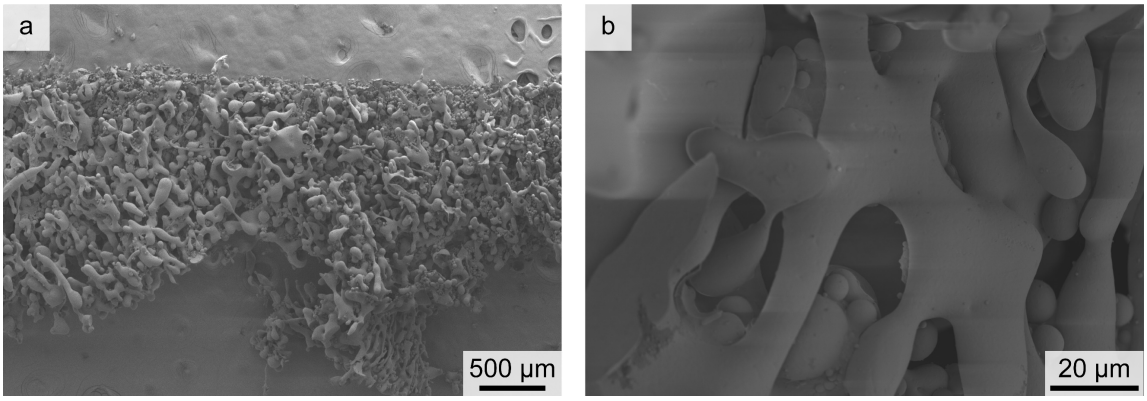

Figure B.S37. Scanning electron micrographs of a PEZ480 carrier disk at 30× (a) and 1,000× (b) magnification. As with the PEZ480 formulation used in the formulation screening study, the carrier disk was not mechanically robust through the freeze facture process.

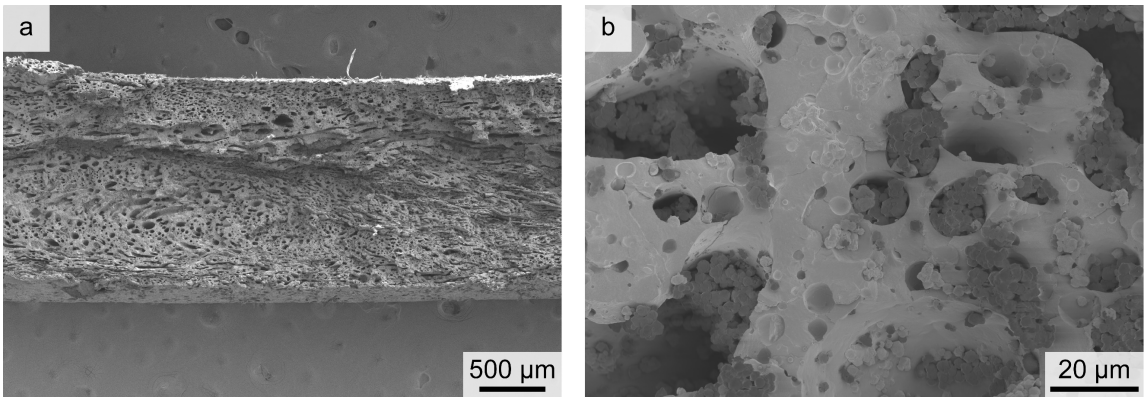

Figure B.S38. Scanning electron micrographs of a PEZ441 carrier disk at 30× (a) and 1,000× (b) magnification. The PEZ441 carrier is mechanically sTable B.through freeze fracture, and the cross section of the material can clearly be seen with the continuous pore structure running throughout the carrier matrix.

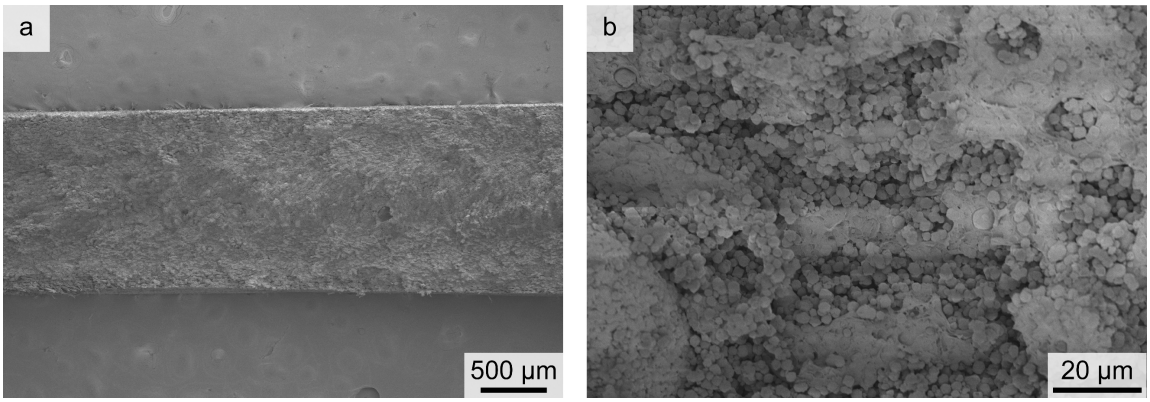

Figure B.S39. Scanning electron micrographs of a PEZ444 carrier disk at 30× (a) and 1,000× (b) magnification. The PEZ444 carrier is mechanically sTable B.through the freeze fracture process, and the cross section of the material can clearly be seen with the continuous pore structure running throughout the carrier matrix and a high degree of entrapped zeolite within the pore network.

ATR-FTIR of bulk materials

The following pages provide FTIR spectra and curves of best fit for the bulk materials prepared as described in the main text. The analytical methods are identical to those described above in the formulation screening section.

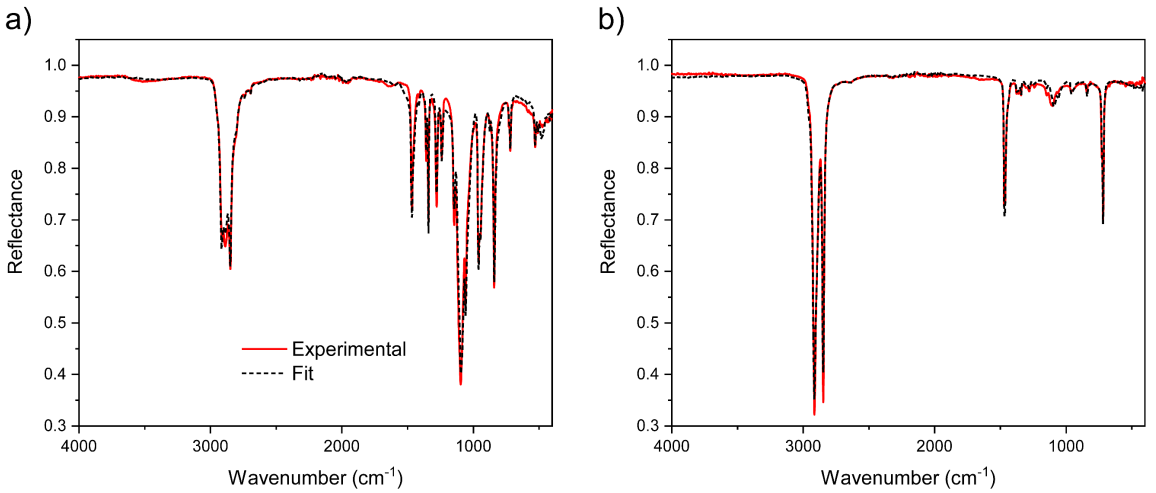

Figure B.S40. Measured ATR FTIR spectra for TB480 (a) and PEZ480 (b) bulk materials and curves of best fit calculated from combinations of standard PE, PEO and Z13X spectra.

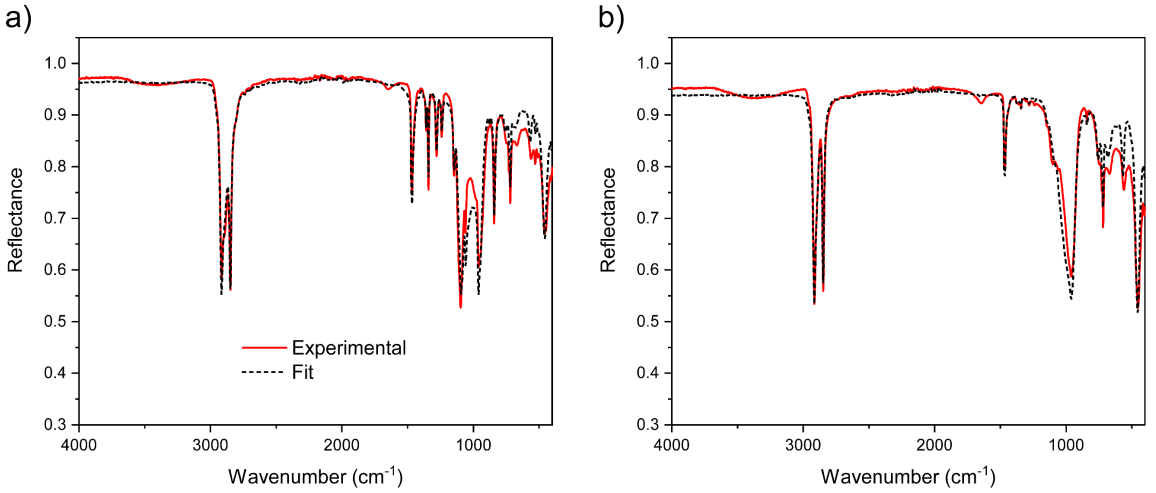

Figure B.S41. Measured ATR FTIR spectra for TB441 (a) and PEZ441 (b) bulk materials and curves of best fit calculated from combinations of standard PE, PEO and Z13X spectra.

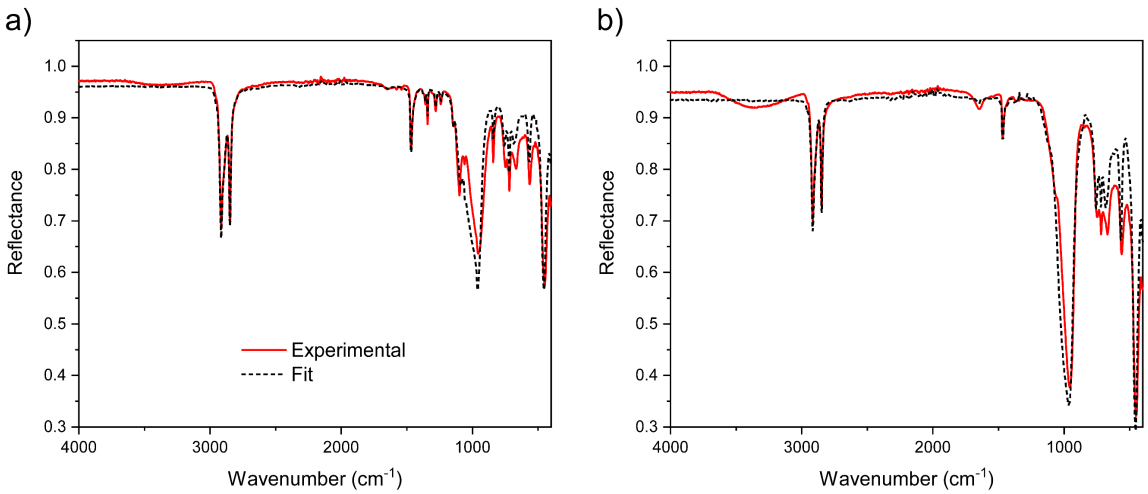

Figure B.S42. Measured ATR FTIR spectra for TB444 (a) and PEZ444 (b) bulk materials and curves of best fit calculated from combinations of standard PE, PEO and Z13X spectra.

Table B.S4. Fitted Spectrum Components and PE:PEO ratios for carrier materials

	Spectral Coefficient			Polymer Fraction (%)	
Sample	f_{PE}	f_{PEO}	f_{PE}	f_{PEO}	f_{PE}
TB480	0.15	0.41	0.02	27.09	72.91
TB441	0.23	0.23	0.19	50.17	49.83
TB444	0.23	0.23	0.19	70.91	29.09
PEZ480	0.46	0.03	0.00	94.75	5.25
PEZ441	0.16	0.06	0.31	91.00	9.00
PEZ444	0.14	0.02	0.66	88.20	11.80

Thermogravimetric analysis of bulk materials

The following pages present thermogravimetric analysis (TGA) traces for each of manufactured bulk materials. Data collection and analytical methods are identical to those described above in the formulation screening section.

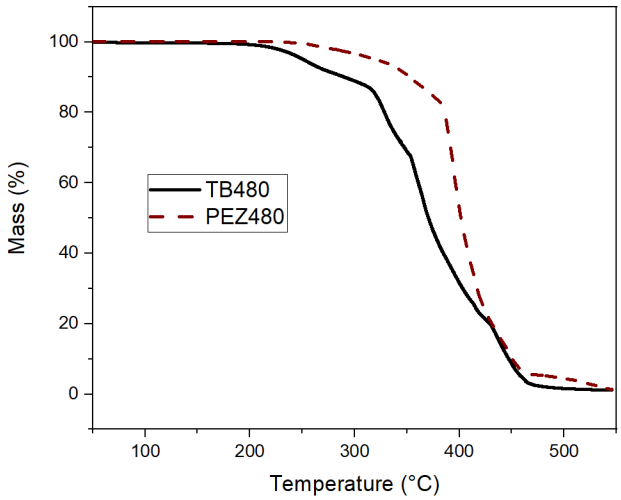

Figure B.S43. Dynamic thermogravimetric analysis scans of TB480 and PEZ480 carrier materials. Scans were collected at a 10 °C/min ramp rate under 60 mL/min air flow.

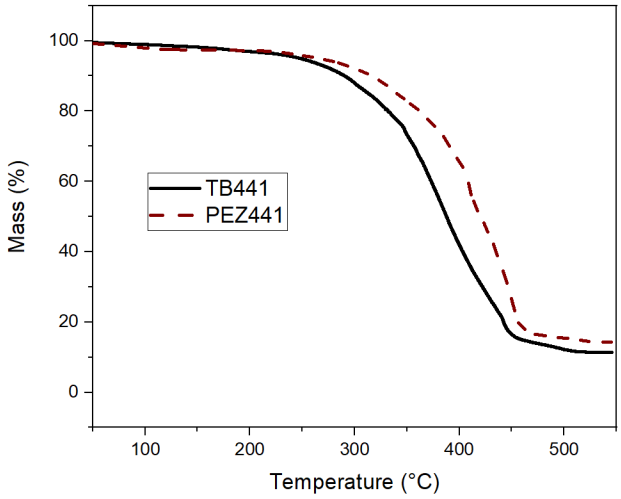

Figure B.S44. Dynamic thermogravimetric analysis scans of TB441 and PEZ441 carrier materials. Scans were collected at a 10 °C/min ramp rate under 60 mL/min air flow.

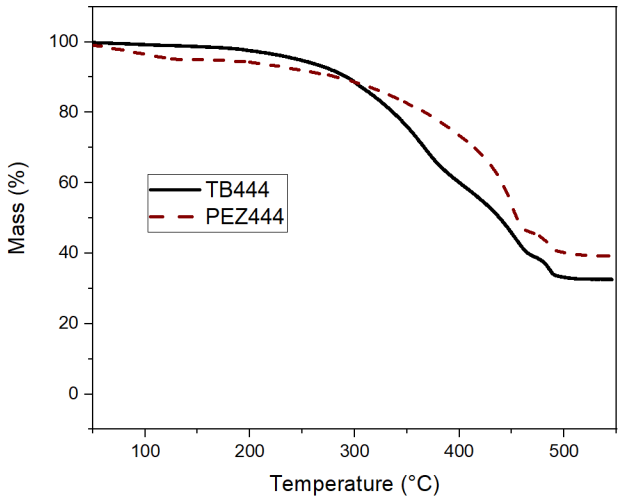

Figure B.S45. Dynamic thermogravimetric analysis scans of TB444 and PEZ444 carrier materials. Scans were collected at a 10 °C/min ramp rate under 60 mL/min air flow.

Table B.S5. Theoretical and observed residual masses for TB and PEZ bulk carrier materials.

Sample	Res. Mass$_{Theo}$ (%)	Res. Mass$_{Obs}$ (%)*	Zeolite Yield (% vs. Theo.)
TB480	0.00	1.2	---
TB441	11.1	11.3	102
TB444	33.3	32.6	98
PEZ480	0.00	1.3	---
PEZ441	20.0	14.3	72
PEZ444	50.0	39.3	79

Ammonium Removal Data

This section details the supplementary data regarding ammonium removal measurements. This includes: data and methods for the determination of ammonium removal by PEZ444 carriers; calculation of the maximum ammonium uptake per PEZ444 carrier based on kinetics experiments; data and methods for the determination of ammonium concentrations in 24 hr uptake experiments by PEZ480, PEZ441, and PEZ444 carriers; SEM-DEX maps and spectra of PEZ444 carriers cross sections before and after ion exchange in ammonium solution and the approximation of sodium ion exchange therefrom; 48 hr ammonium uptake data using PEZ480, PEZ441, and PEZ444 in synthetic wastewater.

Ammonium removal kinetics

The following pages present the UV-Vis spectra used in the determination of total ammonium nitrogen (TAN) concentrations in aqueous solution during ammonium removal kinetics experiments. As described in the main text, a 45 m/L TAN solution was prepared by diluting 153 mg ammonium chloride to a total volume of 1000 mL in deionized water. Glass vials were then charged with 10, 20, or 40 mL of the ammonium chloride solution and a PTFE-coated magnetic stir bar. To each vial was added a single disk of PEZ444, each with a mass of ~125 mg. Aliquots (250 μL) were taken immediately upon mixing and after stirring for 0.5, 1, 2, 3, 6, and 24 hours. Each aliquot was diluted to 10.0 mL total volume with deionized water. A sodium salicylate solution was prepared by dissolving 44.0 g sodium salicylate and 0.028 g sodium nitroprusside in 100 g deionized water; an alkaline citrate solution was prepared by dissolving 1.85 g sodium hydroxide and 10.0 g sodium citrate (tribasic, monohydrate) in 100 g deionized water; and alkaline hypochlorite solution was prepared by gently mixing 90 mL of the alkaline citrate solution and 10 mL of commercial bleach (3%). To each diluted aliquot was added 1.2 mL of the sodium salicylate solution and 2.0 mL of the alkaline hypochlorite solution. The samples were then thoroughly mixed and set in a dark enclosure for 1 hr. After 1 hr, the UV-Vis absorption spectra were measured for each sample.

Each kinetics experiment was conducted in triplicate. The spectra shown in this section represent the average of three experiments for each time point. The concentration of ammonium was determined by comparison of the optical density at 640 nm with the optical density of known standards at the same wavelength. Fresh standards were prepared for each set of experiments, though it was found that the correlation between [TAN] and OD was consistent from day to day.

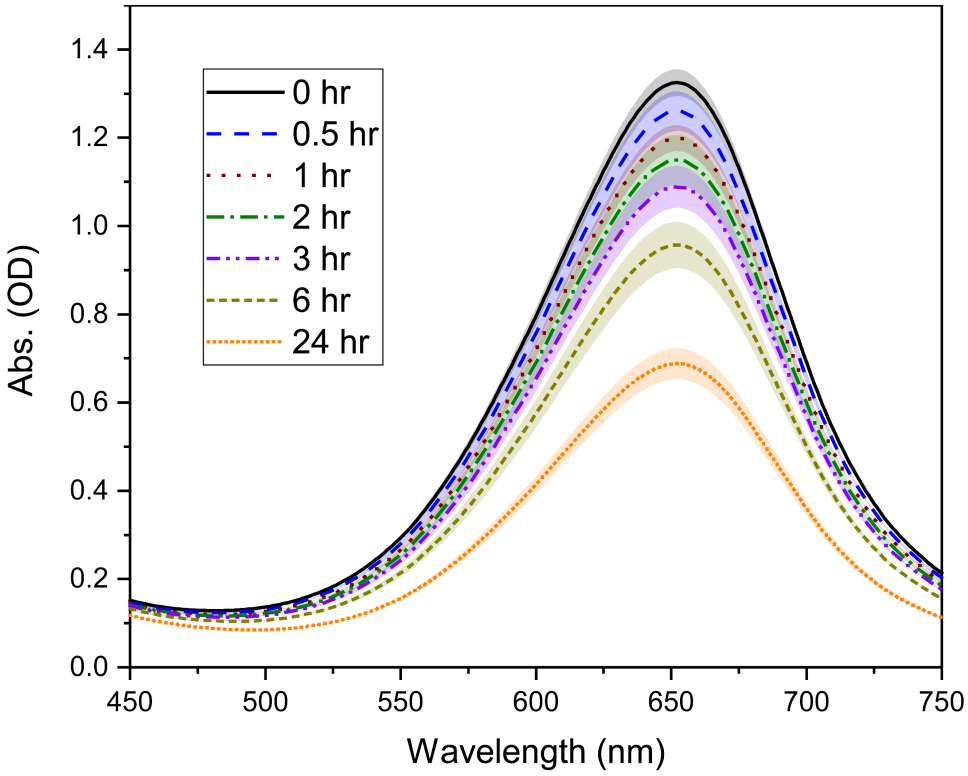

Figure B.S46. UV-Vis spectra used to determine the total ammonium nitrogen (TAN) concentration of aqueous solutions in the presence of PEZ444 carriers at a loading of 25 carriers per liter. Solid and dashed lines represent the average spectrum at a given time point over three separate kinetics experiments. The lighter color bands represent the standard deviation of the three measurements.

Table B.S6. Total Ammonium Nitrogen Concentrations Determined from UV-Vis Spectra in Figure B.S45.

Time (hr)	Absorbance (OD)	$[NH_4^+]$ (mg/L)
0	1.27±0.03	45.5±1.0
0.5	1.21±0.04	41.4±1.5
1	1.15±0.03	39.3±1.0
2	1.11±0.05	37.7±1.9
3	1.05±0.05	35.7±1.6
6	0.92±0.05	31.3±1.8
24	0.66±0.03	22.4±1.2

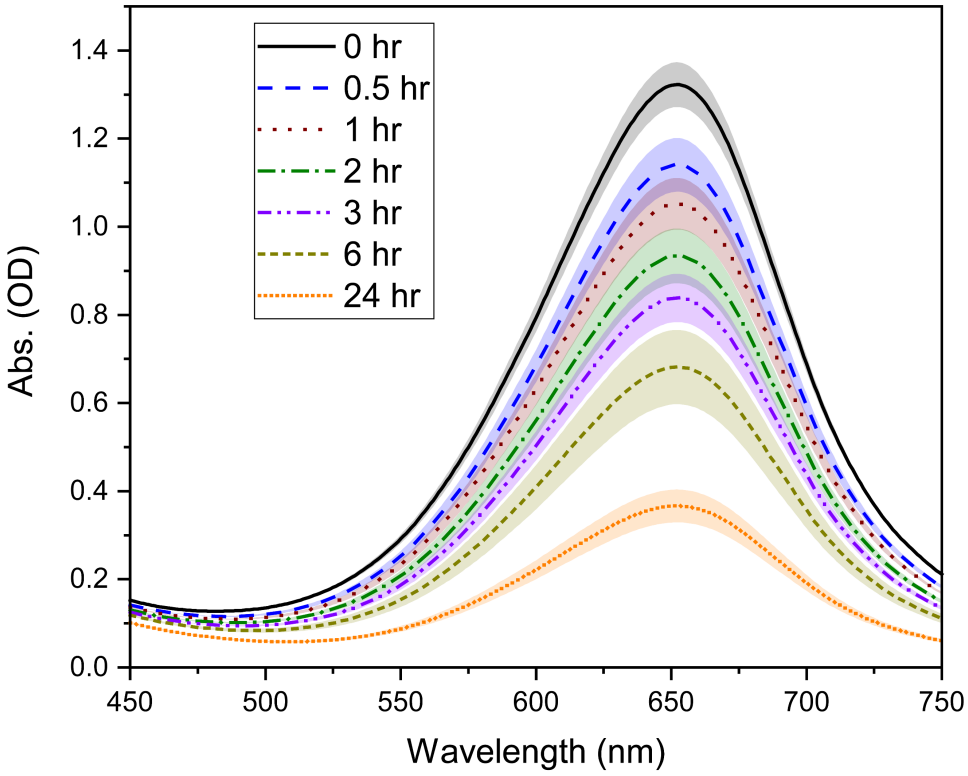

Figure B.S47. UV-Vis spectra used to determine the total ammonium nitrogen (TAN) concentration of aqueous solutions in the presence of PEZ444 carriers at a loading of 50 carriers per liter. Solid and dashed lines represent the average spectrum at a given time point over three separate kinetics experiments. The lighter color bands represent the standard deviation of the three measurements.

Table B.S7. Total Ammonium Nitrogen Concentrations Determined from UV-Vis Spectra in Figure B.S46.

Time (hr)	Absorbance (OD)	$[NH_4^+]$ (mg/L)
0	1.27±0.05	43.4±1.7
0.5	1.10±0.06	37.4±2.0
1	1.01±0.06	34.4±2.0
2	0.90±0.06	30.5±2.1
3	0.81±0.05	27.3±1.8
6	0.66±0.08	22.1±2.8
24	0.36±0.03	11.8±1.1

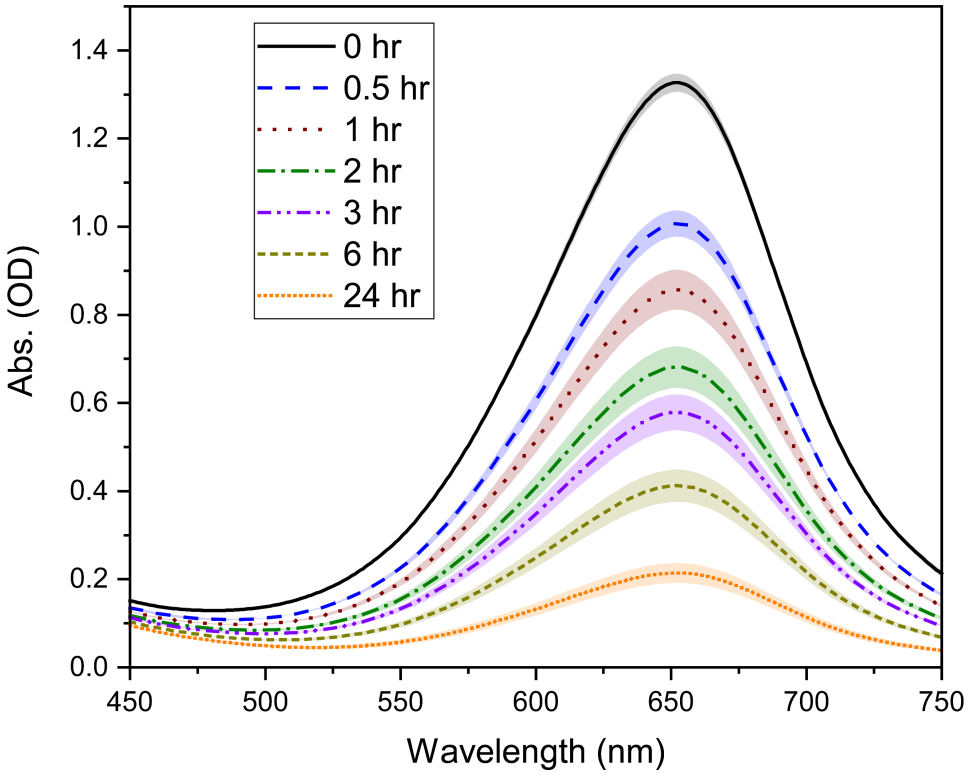

Figure B.S48. UV-Vis spectra used to determine the total ammonium nitrogen (TAN) concentration of aqueous solutions in the presence of PEZ444 carriers at a loading of 100 carriers per liter. Solid and dashed lines represent the average spectrum at a given time point over three separate kinetics experiments. The lighter color bands represent the standard deviation of the three measurements.

Table B.S8. Total Ammonium Nitrogen Concentrations Determined from UV-Vis Spectra in Figure B.S48.

Time (hr)	Absorbance (OD, λ =640 nm)	$[NH_4^+]$ (mg/L)
0	1.28±0.02	43.6±0.7
0.5	0.97±0.03	33.0±1.0
1	0.83±0.04	28.0±1.5
2	0.66±0.05	22.1±1.6
3	0.56±0.04	18.7±1.4
6	0.40±0.04	13.2±1.2
24	0.21±0.02	6.6±0.7

Maximum ammonium uptake via kinetics

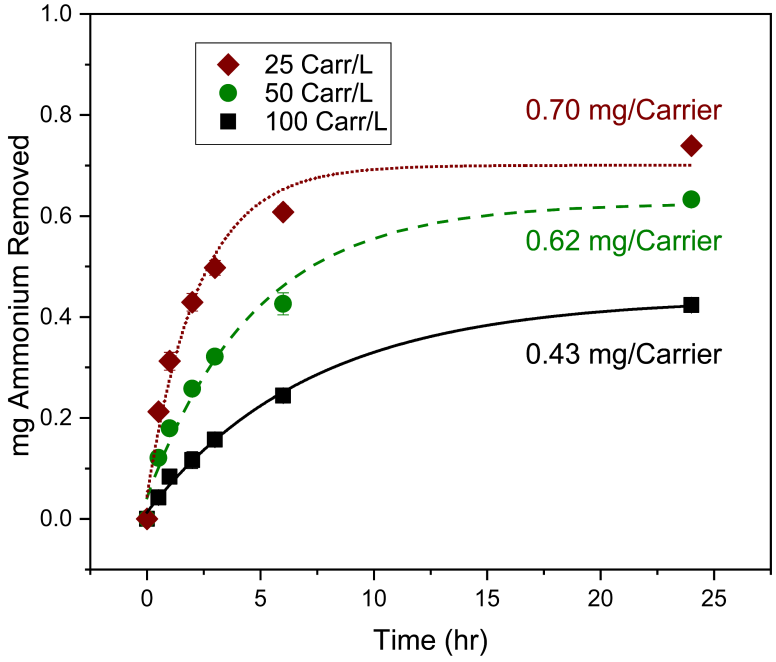

Figure B.S49. Plot of total ammonium uptake by carriers during ammonium removal kinetics experiments. Ammonium removal/uptake is determined from the difference of the initial ammonium concentration and the ammonium concentration at a given time. Maximum ammonium uptake values are determined from a first-order exponential fit to find the ammonium saturation value for a given condition. All values are the average of measurements from three kinetics experiments; error bars are generally eclipsed by data points and represent the standard deviation.

Based on the predicted maximum uptake value of 0.70±0.04 mg NH_4^+ per carrier at the lowest carrier loading conditions, it is possible to estimate the relative degree of sodium ion exchange. Ammonium has a molar mass of 18.039 Da, and sodium has a molar mass of 22.99 Da. Therefore, 0.70±0.04 mg NH_4^+ sequestered by the zeolite corresponds to 0.89±0.05 mg Na released, given a 1:1 stoichiometric ion exchange. The average mass of PEZ444 carriers used in this series of experiments was 129 mg; with a zeolite loading 39% by mass, each carrier comprised, on average, 50 mg Z13X. The empirical formula for Z13X is $Na_7Al_7Si_{17}O_{32}H_{64}$, corresponding to 11.5% Na by mass. Therefore, with an average 50 mg Z13X per carrier, each carrier contains, on average, 5.7 mg sodium. The percentage of sodium exchanged for ammonium is then expressed as:

$$\Delta Na = \frac{Na_{exchanged}}{Na_{carrier}} \times 100\% = \frac{0.89 \pm 0.05\ mg}{5.7\ mg} \times 100\% = 16 \pm 1\%$$

Ammonium removal over 24 hr

The following pages present the UV-Vis spectra used in the determination of total ammonium nitrogen (TAN) concentrations in aqueous solution during 24 hr ammonium removal experiments. As described in the main text, a 45 m/L TAN solution was prepared by diluting 153 mg ammonium chloride to a total volume of 1000 mL in deionized water. Glass vials were then charged with 20 mL of the ammonium chloride solution and a PTFE-coated magnetic stir bar. To three vials were added no carrier; to three vials were added 4-5 disks of PEZ480 for a total mass of 110-125 mg of carrier per vial; to three vials were added a single disk of PEZ441, with an approximate mass of 115 mg of carrier per vial; to three vials were added a single disk of PEZ444, each with a mass of ~125 mg. Aliquots (250 μL) were taken immediately upon mixing and after stirring for 24 hours. Each aliquot was diluted to 10.0 mL total volume with deionized water. An identical workup and analysis procedure was used as described in the ammonium absorption kinetics section. All samples were run in triplicate.

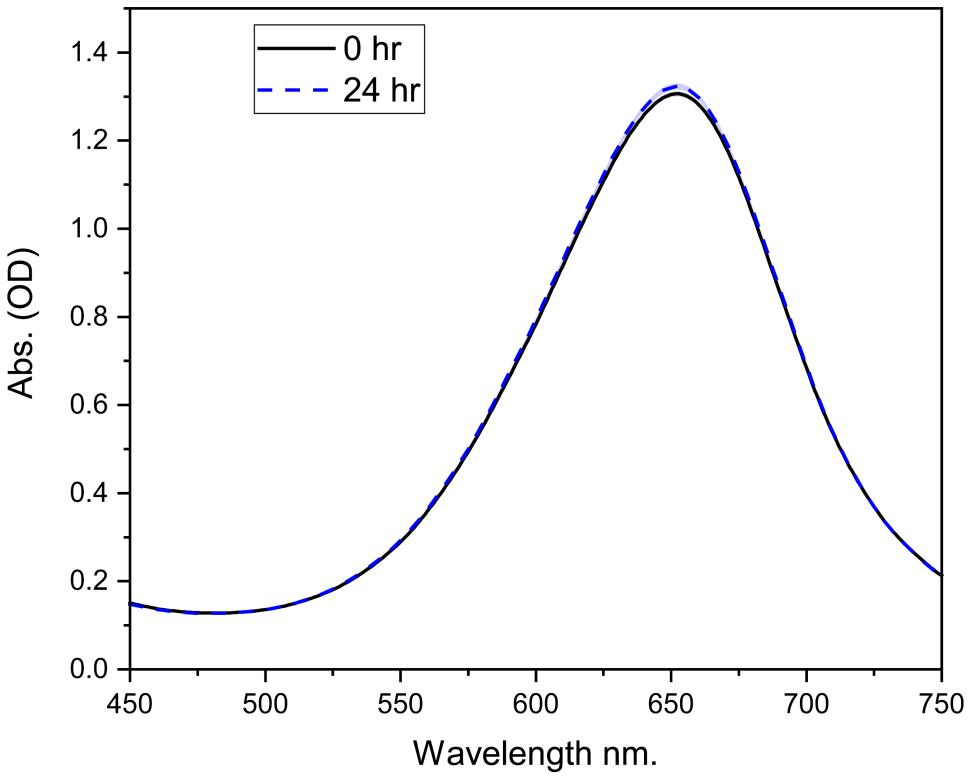

Figure B.S50. UV-Vis spectra used to determine the total ammonium nitrogen (TAN) concentration of aqueous solutions over a 24 hr period in the absence of added carriers. Plotted spectra represent the average of spectra collected from three separate experiments. The lighter colored bands represent the standard deviation of the three measurements. In the absence of carriers, no change in TAN is observable.

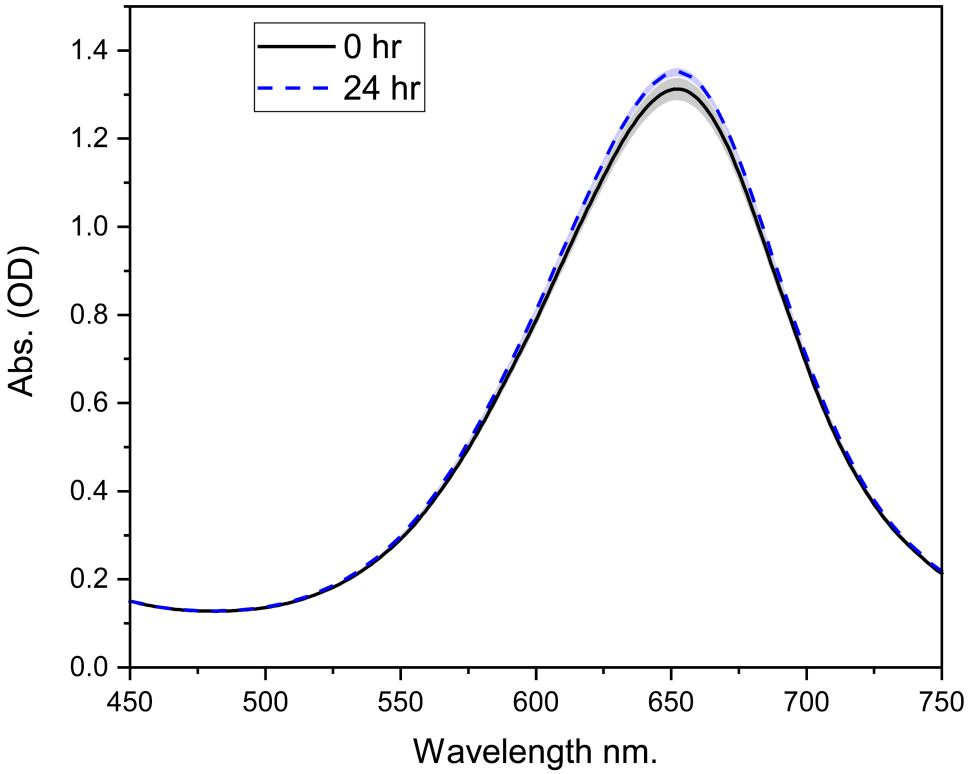

Figure B.S51. UV-Vis spectra used to determine the total ammonium nitrogen (TAN) concentration of aqueous solutions over a 24 hr period in the presence of added PEZ480 carriers. Plotted spectra represent the average of spectra collected from three separate experiments. The lighter colored bands represent the standard deviation of the three measurements. In the presence of the zeolite-free PEZ480 carriers, no change in TAN is observable.

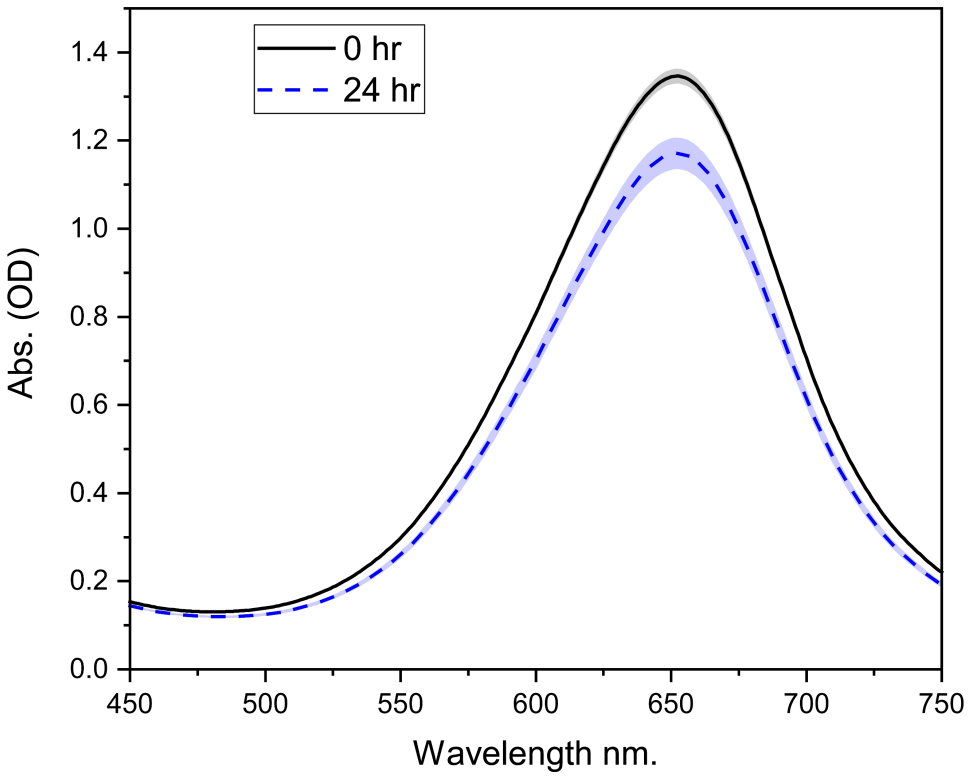

Figure B.S52. UV-Vis spectra used to determine the total ammonium nitrogen (TAN) concentration of aqueous solutions over a 24 hr period in the presence of added PEZ441 carriers. Plotted spectra represent the average of spectra collected from three separate experiments. The lighter colored bands represent the standard deviation of the three measurements. In the presence of low-zeolite loading PEZ441 carriers, a modest decrease in TAN is observed.

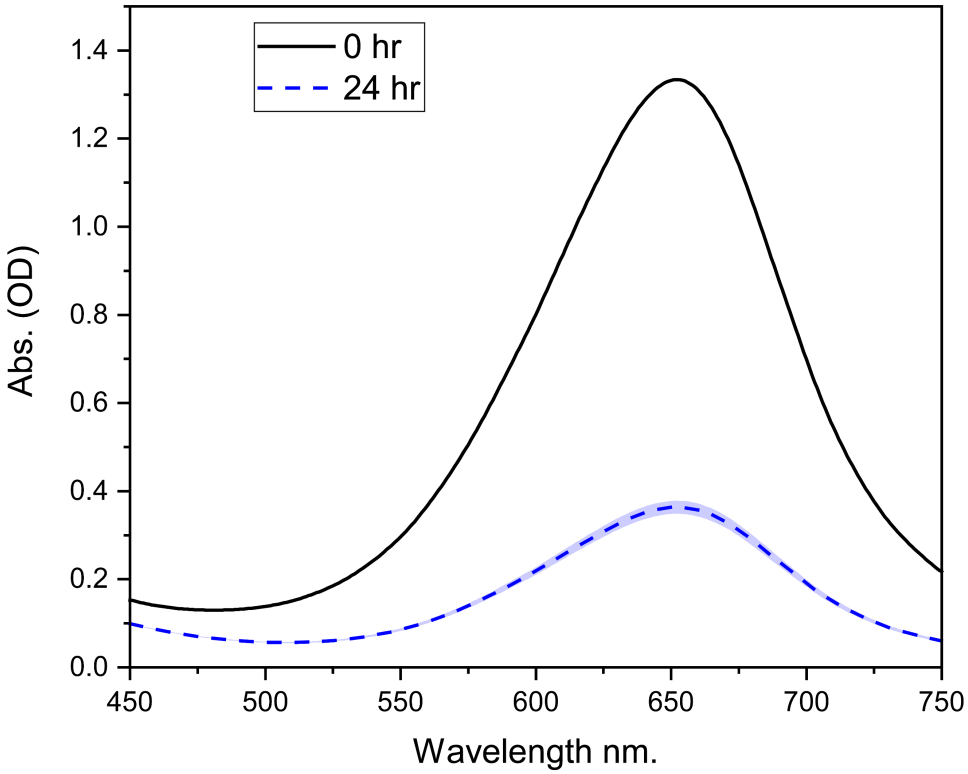

Figure B.S53. UV-Vis spectra used to determine the total ammonium nitrogen (TAN) concentration of aqueous solutions over a 24 hr period in the presence of added PEZ444 carriers. Plotted spectra represent the average of spectra collected from three separate experiments. The lighter colored bands represent the standard deviation of the three measurements. In the presence of high-zeolite loading PEZ444 carriers, a substantial decrease in TAN is observed. Note: error bands for the 0 hr spectra are eclipsed by the average curve.

Table B.S9. Summary of 24 hr Ammonium Absorption Data

Additive	Absorbance, 0 hr (OD, λ = 640 nm)	Absorbance, 24 hr (OD, λ =640 nm)	$[NH_4^+]$, 0 hr (mg/L)	$[NH_4^+]$, 24 hr (mg/L)	$\Delta[NH_4^+]$ (%)
None	1.25±0.01	1.27±0.01	42.9±0.2	43.4±0.2	+1.3±0.7
PEZ480	1.26±0.02	1.30±0.01	43.1±0.8	44.4±0.3	+2.9±2.0
PEZ441	1.30±0.02	1.13±0.03	44.2±0.6	38.4±1.2	-13.1±3.0
PEZ444	1.29±0.00	0.35±0.01	43.8±0.1	11.6±0.5	-73.6±1.1

Energy-dispersive X-ray spectroscopy

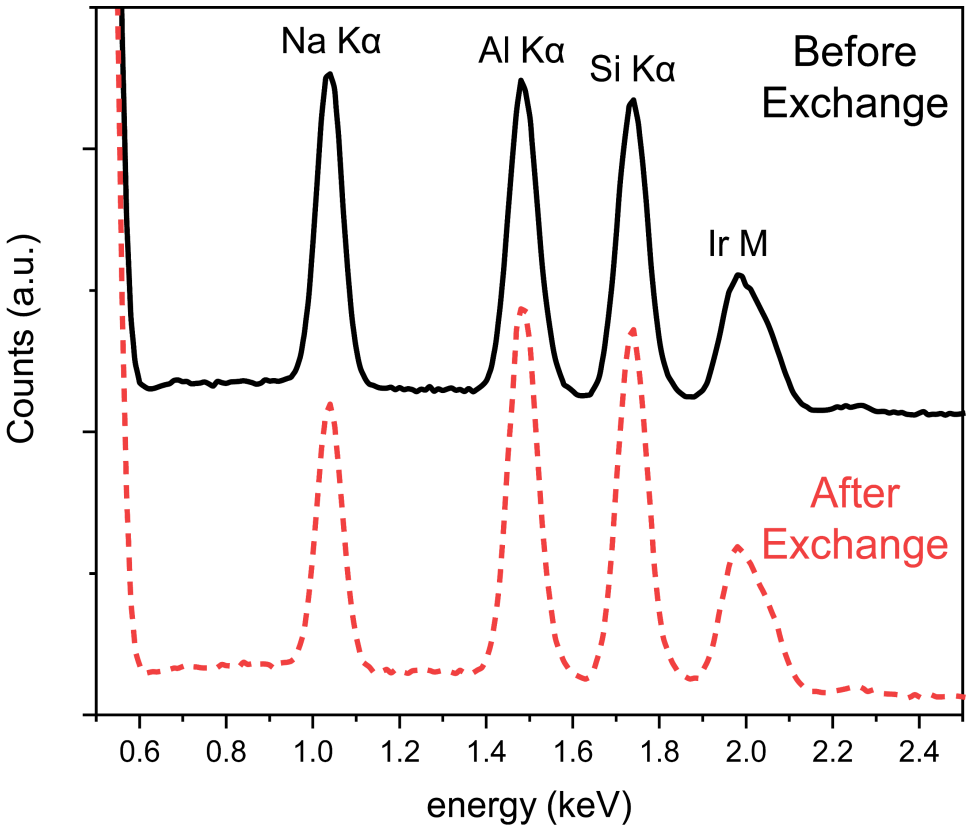

Figure B.S54. Energy-dispersive X-ray spectra of PEZ444 carriers in cross section before (top, black) and after (bottom, red) ion exchange in a 45 mg/L TAN aqueous ammonium chloride solution. The Na Kα peak intensity is attenuated by 25% after ion exchange in relation to both the Al Kα and Si Kα peak intensities.

Table B.S10. EDS Peak Intensities of PEZ444 Cross Section Before and After Ion Exchange

	Before Exchange			After Exchange		
	Na Kα	Al Kα	Si Kα	Na Kα	Al Kα	Si Kα
Peak Center (keV)	1.04	1.48	1.74	1.04	1.48	1.74
Peak Intensity (counts)	12,666	12,435	11,743	10,973	14,340	13,609

Table B.S11. EDS Peak Ratios and Na Kα Attenuation Before and After Ion Exchange

	Before Exchange	After Exchange	Na Kα Attenuation
Na/Al Ratio	1.02	0.77	24.5%
Na/Si Ratio	1.08	0.81	25.0%

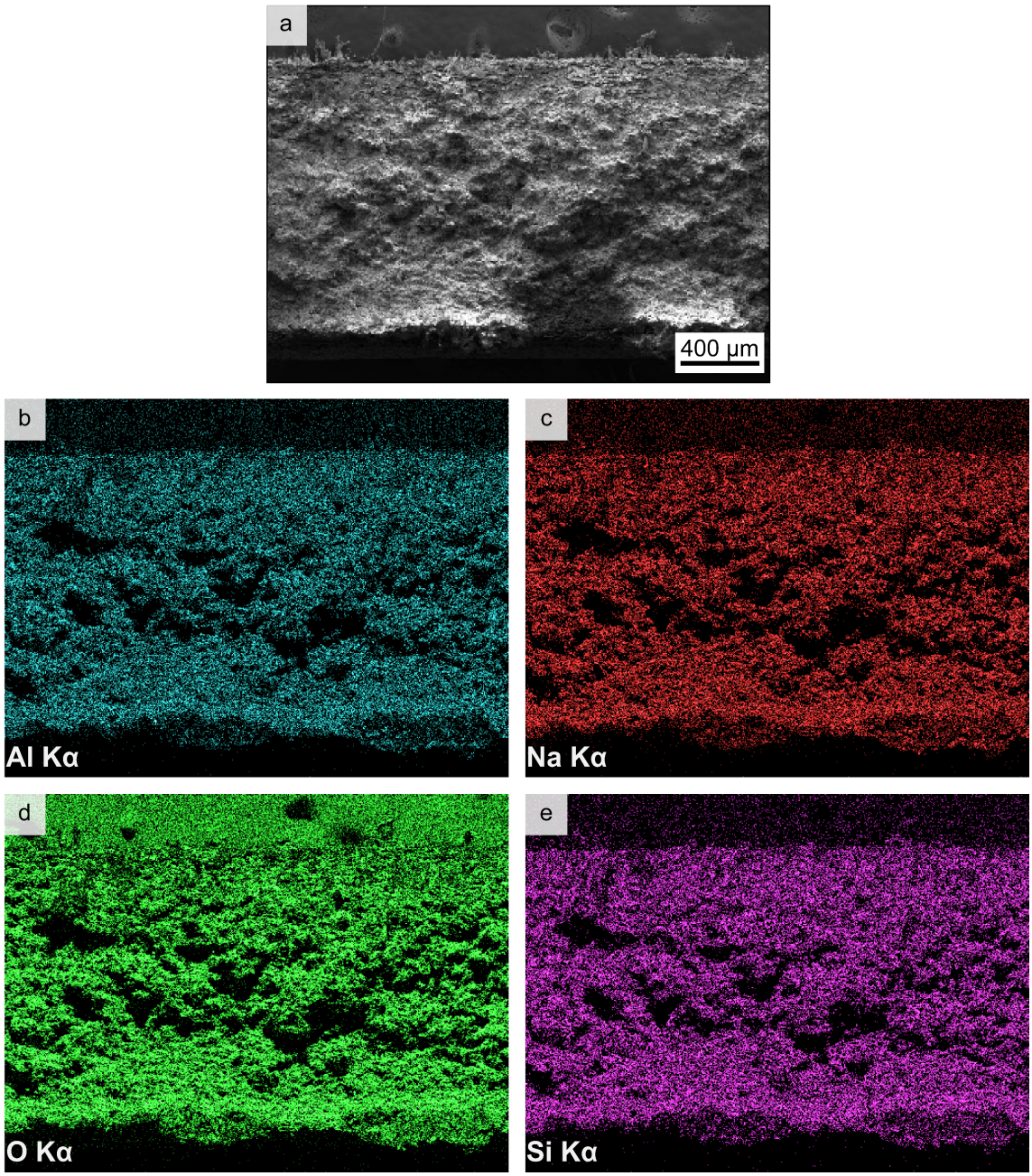

Figure B.S55. Energy-dispersive X-ray spectroscopy image maps of a PEZ444 carrier in cross section before ion exchange. The thickness of the carrier disk is ~1.5 mm, running vertically. A greyscale SEM image of the sample is shown in a. Maps for the Kα signals of aluminum, sodium, oxygen, and silicon are shown in a, b, c, and d, respectively. Significant O Kα intensity was observed in the carbon tape used to adhere the sample.

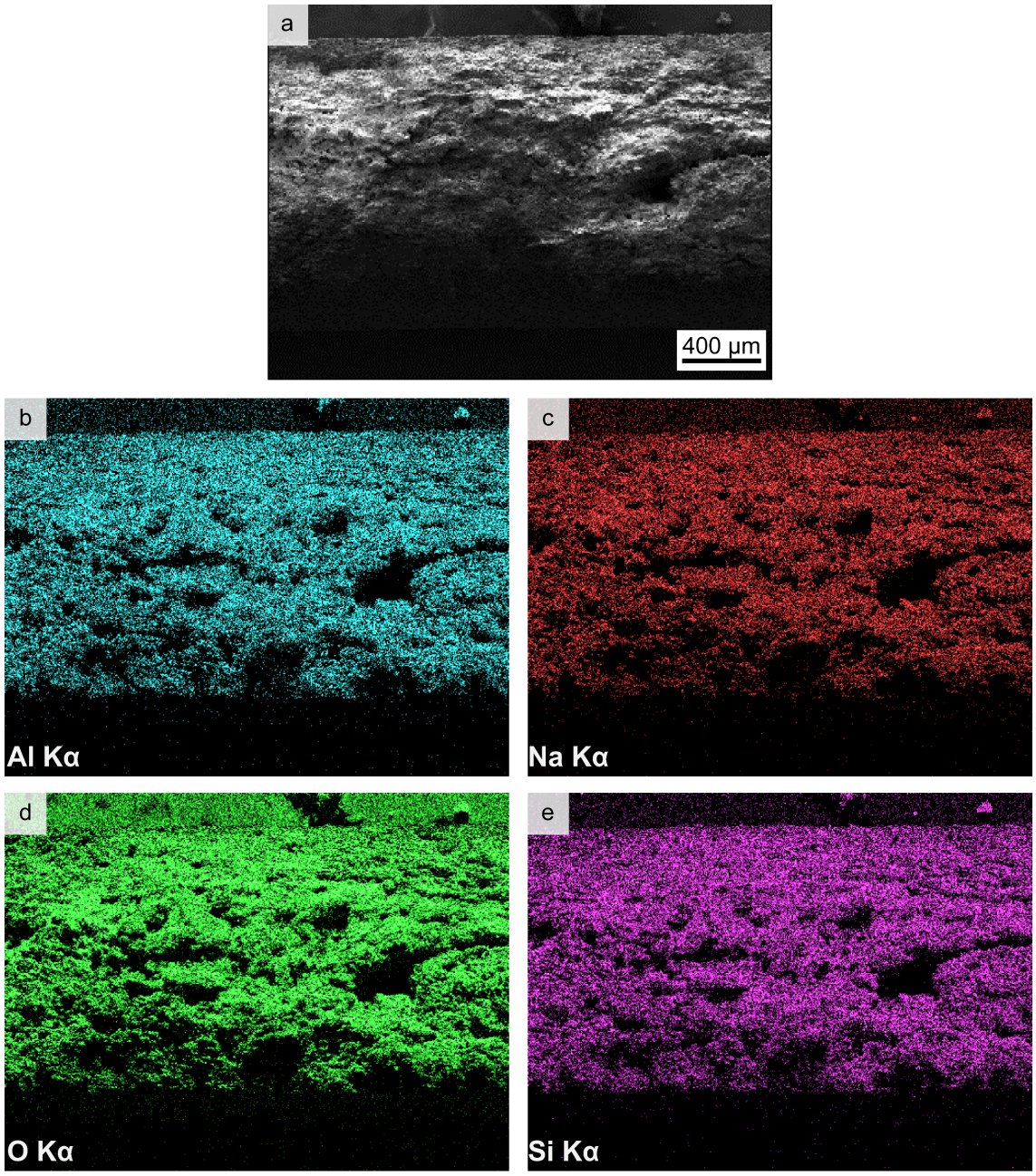

Figure B.S56. Energy-dispersive X-ray spectroscopy image maps of a PEZ444 carrier in cross section after ion exchange. The thickness of the carrier disk is ~1.5 mm, running vertically. A greyscale SEM image of the sample is shown in a. Maps for the Kα signals of aluminum, sodium, oxygen, and silicon are shown in a, b, c, and d, respectively. A significant reduction is Na Kα signal intensity is observable.

Ammonium uptake in synthetic wastewater

Table B.S12. Synthetic wastewater formulation

Additive	Mass (mg)*
NH4Cl	176
Magnesium Phosphate Dibasic Trihydrate	25
Potassium Phosphate Tribasic	20
NaHCO3	275
Sodium acetate	221
Bacteriological peptone	24
Dry meat extract	12
Potato starch	42
Low fat milk powder	50
Glycerine	34

*Additive quantities used to produce 1 L of synthetic wastewater.

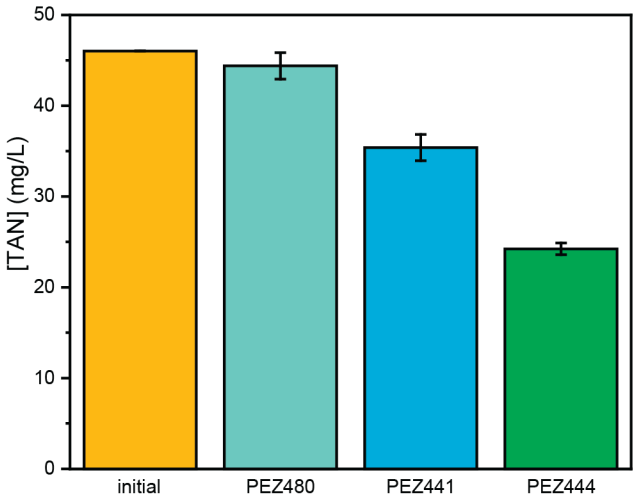

Figure B.S57. Ammonium absorption efficiency of carriers manufactured in this study comparing [$NH4^+$] removal in the presence of one carrier (~100 mg) of PEZ480, PEZ441, and PEZ444 in 10 mL of synthetic wastewater after 48 hours performed in triplicate. Ammonium ion concentrations were measured using an ammonia probe.

Appendix C: Supporting Information for Chapter 2

This Appendix has been published as Supplemental Information in the journal *Environmental toxicology and chemistry* and is cited as:

Huff Chester, A., Gordon, C., Hartmann, H. A., Bartell, S. E., Ansah, E., Yan, T., ... & Schoenfuss, H. L. (2022). Contaminants of Emerging Concern in the Lower Volta River, Ghana, West Africa: The Agriculture, Aquaculture, and Urban Development Nexus. *Environmental toxicology and chemistry*, *41*(2), 369-381.

Table C.S1. Analytes, surrogates (italic) and MRM transitions used for targeted analysis by LC-MS/MS (QqQ).

Compound	Abbreviation	Quantitation Ion				Qualifier Ion				Ion mode	Limit of Detection (ng/L)
		Precursor	Product	Frag (V)	CE (V)	Precursor	Product	Frag (V)	CE (V)		
Sulfonamides											
sulfamethoxazole	SMX	254.1	92.0	110	24	254.1	156.0	110	10	+	0.01
sulfamethoxazole-d4	SMX-d4	258.1	96.1	100	24	258.1	160.0	100	12	+	0.01
sulfamethazine	SMZ	279.1	156.1	120	12	279.1	124.1	120	24	+	0.01
sulfamethazine-d4	SMZ-d4	283.1	186.3	120	12	283.1					0.01
Macrolides											
erythromycin	ERY	734.5	158.1	175	28	734.5	116.1	175	48	+	0.2
erythromycin*H2O	ERY-H2O	716.5	558	160	25	716.5	158.2	160	25	+	0.3
erythromycin-d4	ERY-d4	720.6	162.2	90	25	720.6	562.5	90	25	+	0.2
Fluorquinolones											
ciprofloxacin	CIP	332.1	314.2	135	16	332.1	288.0	135	40	+	0.02
ciprofloxacin-d8	CIP-d8	340.2	322.2	110	20	340.2	296.2	124	20	+	0.02
norfloxcin	NOR	320.1	276.2	135	12	320.1	233.1	135	24	+	0.1
flumequin	FLU	262.1	244.1	115	16	262.1	202.1	115	32	+	0.1
sulfamerazine	SMA	265.1	156	110	15	265.1	108	110	24	+	0.02
sulfamerazine-d4	SMA-d4	269.0	160.1	115	15	269.0	96.1	115	25	+	0.02
Diaminopyrimidines											
trimethoprim	TRI	291.1	123.1	145	24	291.1	261.1	145	24	+	0.05
trimethoprim-d3	TRI-d3	293.9	122.6	145	26	293.9	123.1	145	24	+	0.05
thiabendazole	TBD	202.2	175.2	130	25	202.2	131.2	130	35	+	0.1
thiabendazole-d4	TBD-d4	206.1	179.1	130	25	206.1	135.1	130	35	+	0.1
Other											
DEET	DEET	192.0	119	90	25					+	0.03
DEET-d10	DEET-d10	202.0	119	90	25					+	0.03

Table C.S2. HPLC Parameters

Antibiotic analysis

Solvent A: 0.1% formic acid in water

Solvent B: methanol

Flow rate: 0.300 mL/min

Column Temperature: 30°C

Time (min)	Solvent A	Solvent B
0	80%	20%
3	80%	20%
17	0%	100%
22	0%	100%

Gas temp: 300°C

ESI voltage: +4,000V

PFAS analysis

Solvent A: 0.1% ammonium acetate in water

Solvent B: 0.1% ammonium acetate in 95% methanol

Flow rate: 0.250 mL/min

Column Temperature: 40°C

Time (min)	Solvent A	Solvent B
0	70%	30%
3	70%	30%
5	40%	60%
14	20%	80%
17	0%	100%
22	0%	100%

Gas temp: 300°C

ESI voltage: -4,000V

Untargeted analysis

Solvent A: 0.1% formic acid in water

Solvent B: 0.1% formic acid in methanol

Flow rate: 0.250 mL/min

Column Temperature: 30°C; Reference ions: 121, 922.

Time (min)	Solvent A	Solvent B
0	95%	5%
18	5%	95%
18.5	0%	100%
22	0%	100%

Gas temp: 350°C

ESI voltage: +4,000V

Table C.S3. PFAS MRM transitions

Compound	Abbreviation	MRM Transition (*m*/*z*)		MS Voltages		Limit of Detection (ng/L)
		precursor	product(s)	Fragmentor	CE	
perfluorobutanoic acid	PFBA	213	168.9	50	8	0.33
perfluorpentanoic acid	PFPeA	263	218.9	60	8	0.29
perfluoroheptanoic acid	PFHpA	362.9	319	72	6	0.09
			169	72	12	
perfluorohexanoic acid	PFHxA	313	268.9	70	8	0.64
			119	70	18	
perfluorooctanoic acid	PFOA	413	369	69	4	0.21
			169	69	12	
perfluorononanoic acid	PFNA	463	419	66	4	0.07
			169	66	17	
perfluorodecananoic acid	PFDA	513	469	69	8	0.18
			218.7	100	16	
perfluorohexanesulfonic acid	PFHxS	398.9	99	90	75	0.35
			80	90	41	
perfluorobutanesulfonic acid	PFBS	298.9	98.9	69	32	0.25
			79.9	69	44	
perfluorohexanesulfonic acid	PFOS	498.9	99	100	50	0.15
			80	100	50	
perfluorooctanesulfonamide	FOSA	498	78	69	40	0.44
			47.9	100	100	

Table C.S4. Surrogate recoveries

Surrogate	Percent Recovery*	
	Water	Sediment
sulfamethoxazole-d4	76±11	37±9
sulfamethazine-d4	86±13	49±11
erythromycin-d4	57±20	30±9
ciprofloxacin-d8	23±10	7±8
sulfamerazine-d4	78±11	41±10
trimethoprim-d3	86±3	47±14
thiabendazole-d4	66±9	35±13
DEET-d10	61±9	89±4
[M]PFBA	80±8	n/m
[M3]PFPeA	108±18	n/m
[M]PFHxA	89±33	n/m
[M4]PFHpA	109±20	n/m
[M]PFOA	105±19	n/m
[M]PFNA	99±47	n/m
[M]PFDA	95±22	n/m
[M3]PFBS	100±26	n/m
[M]PFHxS	102±46	n/m
[M]PFOS	106±30	n/m
[M]FOSA	24±17	n/m

*Error is reported in standard deviation (n=18)
n/m = not measured

Table C.S5. qPCR Primers and Annealing Temperatures

Antibiotics	ARG	Mechanism	Primer / Probe sequence (5'- 3')	Annealing Temp. (ºC)	Reference:
tetracycline	tet(D)		F:GGAATATCTCCCGGAAGCGG R:CACATTGGACAGTGCCAGCAG (Aminov et al., 2002)	68	Aminov, R., Chee-Sanford, J., Garrigues, N., Teferedegne, B., Krapac, I., White, B., & Mackie, R. (2002). Development, validation, and application of PCR primers for detection of tetracycline efflux genes of gram-negative bacteria. Applied and environmental microbiology, 68(4), 1786-1793.
	tet(E)		F: GTTATTACGGGAGTTTGTTGG R: AATACAACACCCACACTACGC (Aminov et al., 2002)	61	Aminov, R., Chee-Sanford, J., Garrigues, N., Teferedegne, B., Krapac, I., White, B., & Mackie, R. (2002). Development, validation, and application of PCR primers for detection of tetracycline efflux genes of gram-negative bacteria. Applied and environmental microbiology, 68(4), 1786-1793.
	tet(M)	Ribosomal protection	F: ACAGAAAGCTTATTATATAAC R: TGGCGTGTCTATGATGTTCAC (Aminov, Garrigues-Jeanjean, & Mackie, 2001)	55	Aminov, R., Garrigues-Jeanjean, N., & Mackie, R. (2001). Molecular ecology of tetracycline resistance: development and validation of primers for detection of tetracycline resistance genes encoding ribosomal protection proteins. *Applied and environmental microbiology, 67*(1), 22-32.
	tet(O)	Ribosomal protection	F:ACGGARAGTTTATTGTATACC R: TGGCGTATCTATAATGTTGAC (Aminov, Garrigues-Jeanjean, & Mackie, 2001)	60	Aminov, R., Garrigues-Jeanjean, N., & Mackie, R. (2001). Molecular ecology of tetracycline resistance: development and validation of primers for detection of tetracycline resistance genes encoding ribosomal protection proteins. *Applied and environmental microbiology, 67*(1), 22-32.
	tet(Q)		F: AGAATCTGCTGTTTGCCAGTG R: CGGAGTGTCAATGATATTGCA (Aminov et al., 2001)	63	Aminov, R., Garrigues-Jeanjean, N., & Mackie, R. (2001). Molecular ecology of tetracycline resistance: development and validation of primers for detection of tetracycline resistance genes encoding ribosomal protection proteins. *Applied and environmental microbiology, 67*(1), 22-32.

	tet(X)	Enzymatic modification	F: AGCCTTACCAATGGGTGTAAA R: TTCTTACCTTGGACATCCCG (Ghosh, Ramsden, & LaPara, 2009)	64.5	Ghosh, S., Ramsden, S. J., & LaPara, T. M. (2009). The role of anaerobic digestion in controlling the release of tetracycline resistance genes and class 1 integrons from municipal wastewater treatment plants. *Applied microbiology and biotechnology, 84*(4), 791-796.
Sulfonamides	sulI		F: CGCACCGGAAACATCGCTGCAC R: TGAAGTTCCGCCGCAAGGCTCG (Pei, Kim, Carlson, & Pruden, 2006)	65（use **69.9** from Pruden 2011EST)	Pei, R., Kim, S.-C., Carlson, K. H., & Pruden, A. (2006). Effect of river landscape on the sediment concentrations of antibiotics and corresponding antibiotic resistance genes (ARG). *Water research, 40*(12), 2427-2435. Effect of Various Sludge Digestion Conditions on Sulfonamide, Macrolide, and Tetracycline Resistance Genes and Class I Integrons Yanjun Ma, Christopher A. Wilson, John T. Novak, Rumana Riffat, Sebnem Aynur, Sudhir Murthy, and Amy Pruden Environmental Science & Technology 2011 45 (18), 7855-7861
	sulII		F: TCCGGTGGAGGCCGGTATCTGG R: CGGGAATGCCATCTGCCTTGAG (Pei, Kim, Carlson, & Pruden, 2006)	57.5(use **67.5** from Pruden EST 2011)	Pei, R., Kim, S.-C., Carlson, K. H., & Pruden, A. (2006). Effect of river landscape on the sediment concentrations of antibiotics and corresponding antibiotic resistance genes (ARG). *Water research, 40*(12), 2427-2435. Effect of Various Sludge Digestion Conditions on Sulfonamide, Macrolide, and Tetracycline Resistance Genes and Class I Integrons Yanjun Ma, Christopher A. Wilson, John T. Novak, Rumana Riffat, Sebnem Aynur, Sudhir Murthy, and Amy Pruden Environmental Science & Technology 2011 45 (18), 7855-7861
macrolide antibiotic	erm(B)	rRNA adenine N6-methyltransferases	F:GGTTGCTCTTGCACACTCAAG R:CAGTTGACGATATTCTCGATT G(Koike et al., 2010)	65	Koike, S., Aminov, R. I., Yannarell, A. C., Gans, H. D., Krapac, I. G., Chee-Sanford, J. C., & Mackie, R. I. (2010). Molecular ecology of macrolide–lincosamide–streptogramin B methylases in waste lagoons and subsurface waters associated with swine production. *Microbial ecology, 59*(3), 487-498.

	erm(C)		F: AATCGTGGAATACGGGTTTGC R: CGTCAATTCCTGCATGTTTTAAG G (Koike et al., 2010)	63	Koike, S., Aminov, R. I., Yannarell, A. C., Gans, H. D., Krapac, I. G., Chee-Sanford, J. C., & Mackie, R. I. (2010). Molecular ecology of macrolide–lincosamide–streptogramin B methylases in waste lagoons and subsurface waters associated with swine production. *Microbial ecology, 59*(3), 487-498.
	erm(F)		F: TCTGGGAGGTTCCATTGTCC R: TTCAGGGACAACTTCCAGC (Koike et al., 2010)	65	Koike, S., Aminov, R. I., Yannarell, A. C., Gans, H. D., Krapac, I. G., Chee-Sanford, J. C., & Mackie, R. I. (2010). Molecular ecology of macrolide–lincosamide–streptogramin B methylases in waste lagoons and subsurface waters associated with swine production. *Microbial ecology, 59*(3), 487-498.
beta-lactamase	blaTEM		F:CACTATTCTCAGAATGACTTGGT R: TGCATAATTCTCTTACTGTCATG (Lachmayr, Kerkhof, DiRienzo, Cavanaugh, & Ford, 2009)	60	Lachmayr et al., 2009, "Quantifying nonspecific TEM β-lactamase (blaTEM) genes in a wastewater stream."
	blaCTX-M		F:ATGTGCAGCACCAGTAAAGTGATGGC R:ATCACGCGGATCGCCCGGAAT（Birkett et al., 2007）	58	Birkett et al., 2007, "Real-time TaqMan PCR for rapid detection and typing of genes encoding CTX-M extended-spectrum β-lactamases."
16S rRNA for	341F, 518R		F: 5’-CCT ACG GGA GGC AGC AG-3’ R: 5’-ATT ACC GCG GCT GCT GG-3’	60 °C	Muyzer et al., 19931

Table C.S6-1: Downstream (DS) of Sogakope at river km 31 (Sample A) downstream of aquaculture. Tentatively identified compounds by untargeted analysis. Assignments made if peak height >15000; score >75% isotopic profile, library match. Spiked surrogates denoted by a *. RT= retention time; Rel Area= relative peak area

Assignment	Formula	CAS #	Mass	RT	Score	Rel Area
Phendimetrazine	C12 H17 N O	634-03-7	191.131	14.17	99.19	1.000
Trimethoprim-d3*	C14 H15 D3 N4 O3	1189923-38-3	293.1572	6.549	83.81	0.835
Sulfamethoxazole-d4*	C10 H7 D4 N3 O3 S	1020719-86-1	257.0775	7.825	98.25	0.724
Triethyl phosphate	C6 H15 O4 P	78-40-0	182.0707	11.126	99.81	0.626
6-Hydroxy-4-methylcoumarin	C10 H8 O3	90-33-5	176.0475	14.394	98.45	0.617
Sulfadimidine-d4*	C12 H10 D4 N4 O2 S	1020719-82-7	282.1091	7.102	97.79	0.578
Embelin	C17 H26 O4	550-24-3	294.1833	16.291	99.38	0.574
Thiabendazole-d4*	C10 H3 D4 N3 S	1190007-20-5	205.0609	6.924	47.26	0.527
2-(Benzylmethylamino)ethanol N-oxide	C10 H15 N O2	15831-63-7	181.1104	4.384	99.21	0.511
Phthalic anhydride	C8 H4 O3	85-44-9	148.0162	14.394	99.4	0.504
Sulfamerazine-d4*	C11 H8 D4 N4 O2 S	1020719-84-9	268.0934	5.9	98.17	0.417
DEET-d10*	C12 H7 D10 N O	1215576-01-4	201.1939	14.07	98.46	0.328
Diethyl phthalate	C12 H14 O4	84-66-2	222.0897	14.394	97.95	0.291
DEET / Diethyltoluamide	C12 H17 N O	134-62-3	191.1309	14.109	98.75	0.288
Dibutyl phthalate	C16 H22 O4	84-74-2	278.153	18.435	93.95	0.242
Phthalic anhydride	C8 H4 O3	85-44-9	148.0165	18.435	98.31	0.234
Dibutyl phthalate	C16 H22 O4	84-74-2	278.1526	18.293	95.49	0.200
Terbutaline	C12 H19 N O3	23031-25-6	225.1367	6.103	99.56	0.188
Phthalic anhydride	C8 H4 O3	85-44-9	148.0165	18.297	98.37	0.139
Phenylacrylic acid (Cinnamic acid)	C9 H8 O2	140-10-3	148.0525	16.522	99.54	0.126
O,O-Diethyl phosphate	C4 H11 O4 P	598-02-7	154.0395	11.126	99.7	0.124
Ciprofloxacin-d8*	C17 H10 D8 F N3 O3	1130050-35-9	339.1835	7.481	99.18	0.100
Dodecyldimethylamine oxide	C14 H31 N O	1643-20-5	229.2408	15.781	98.97	0.066
Hydroxyatrazine	C8 H15 N5 O	2163-68-0	197.1278	7.397	87.3	0.052

Embelin	C17 H26 O4	550-24-3	294.1837	15.971	98.13	0.050
Benzyl butyl phthalate	C19 H20 O4	85-68-7	312.1368	18.335	84.24	0.048
Benzophenone	C13 H10 O	119-61-9	182.0736	15.415	98.85	0.037
Atenolol	C14 H22 N2 O3	29122-68-7	266.1635	6.928	98.94	0.037
Atrazine	C8 H14 Cl N5	1912-24-9	215.0943	13.889	90.27	0.033
Glutaraldehyde	C5 H8 O2	111-30-8	100.0523	11.202	87.82	0.027
Dimethyl phthalate	C10 H10 O4	131-11-3	194.058	11.67	85.42	0.022
2-tert-Butyl-4-methoxyphenol	C11 H16 O2	25013-16-5	180.115	13.155	85.19	0.018
Trimethoprim-d3*	C14 H15 D3 N4 O3	1189923-38-3	293.1571	7.921	86.31	0.018
Carboxy Ibuprofen	C13 H16 O4	15935-54-3	236.1049	11.583	83.38	0.017
Tri-(2-chloroisopropyl)phosphate	C9 H18 Cl3 O4 P	13674-84-5	326.0011	15.769	97.52	0.011
Octyl methoxycinnamate	C18 H26 O3	5466-77-3	290.1883	17.636	83.27	0.010
Phthalic anhydride	C8 H4 O3	85-44-9	148.0162	17.982	87.15	0.010
Prohydrojasmon	C15 H26 O3	158474-72-7	254.1884	18.504	85.32	0.009
2,4-Dimethylquinoline	C11 H11 N	1198-37-4	157.0891	5.818	87.67	0.009
Ethyl N-acetyl-N-butyl-β-alaninate	C11 H21 N O3	52304-36-6	215.1522	11.633	82.1	0.008
8-Hydroxychinolin	C9 H7 N O	148-24-3	145.0527	5.848	86.99	0.007
Ethyl 4-hydroxybenzoate	C9 H10 O3	120-47-8	166.0629	16.244	87.07	0.006
Desethylatrazine	C6 H10 Cl N5	6190-65-4	187.0626	9.896	97.76	0.006
Triphenyl phosphate	C18 H15 O4 P	115-86-6	326.0711	17.544	85.38	0.004
Chloramphenicol-d5*	C11 H7 D5 Cl2 N2 O5	202480-68-0	327.0439	9.874	78.64	0.004
Penbutolol	C18 H29 N O2	38363-40-5	291.2199	7.94	85.69	0.004

Table C.S6-2: Downstream (DS) of Sogakope at river km 31 (Sample B) downstream of aquaculture. Tentatively identified compounds by untargeted analysis. Assignments made if peak height >15000; score >75% isotopic profile, library match. Spiked surrogates denoted by a *. RT= retention time; Rel Area= relative peak area

Assignment	Formula	CAS #	Mass	RT	Score	Rel Area
Triethyl phosphate	C6 H15 O4 P	78-40-0	182.0711	11.118	99.22	1.000
Trimethoprim-d3*	C14 H15 D3 N4 O3	1189923-38-3	293.1574	6.541	92.52	0.769
Sulfamethoxazole-d4*	C10 H7 D4 N3 O3 S	1020719-86-1	257.0776	7.812	97.96	0.540
Sulfadimidine-d4*	C12 H10 D4 N4 O2 S	1020719-82-7	282.109	7.091	97.15	0.432
Thiabendazole-d4*	C10 H3 D4 N3 S	1190007-20-5	205.0612	6.914	47.62	0.429
Phthalic anhydride	C8 H4 O3	85-44-9	148.0161	14.384	99.4	0.367
DEET-d10*	C12 H7 D10 N O	1215576-01-4	201.194	14.061	98.23	0.366
DEET / Diethyltoluamide	C12 H17 N O	134-62-3	191.1309	14.105	98.65	0.302
Terbutaline	C12 H19 N O3	23031-25-6	225.1367	6.091	99.57	0.329
Sulfamerazine-d4	C11 H8 D4 N4 O2 S	1020719-84-9	268.0935	5.887	97.85	0.275
O,O-Diethyl phosphate	C4 H11 O4 P	598-02-7	154.0397	11.117	99.65	0.239
Diethyl phthalate	C12 H14 O4	84-66-2	222.0896	14.384	98.33	0.210
Tris(2-butoxyethyl) phosphate	C18 H39 O7 P	78-51-3	398.2437	18.851	98.22	0.163
Dibutyl phthalate	C16 H22 O4	84-74-2	278.1528	18.421	95.11	0.139
Phthalic anhydride	C8 H4 O3	85-44-9	148.0167	18.421	97.39	0.138
Dibutyl phthalate	C16 H22 O4	84-74-2	278.1524	18.279	97.56	0.093
Ciprofloxacin-d8*	C17 H10 D8 F N3 O3	1130050-35-9	339.1838	7.471	99.07	0.088
Dodecyldimethylamine oxide	C14 H31 N O	1643-20-5	229.2408	15.765	99.1	0.072
Phthalic anhydride	C8 H4 O3	85-44-9	148.0163	18.287	99.45	0.069
Atenolol	C14 H22 N2 O3	29122-68-7	266.1636	6.918	98.65	0.045
Hydroxyatrazine	C8 H15 N5 O	2163-68-0	197.1279	7.387	87.5	0.030
Dimethyl phthalate	C10 H10 O4	131-11-3	194.0581	11.66	84.49	0.022
Phenylacrylic acid (Cinnamic acid)	C9 H8 O2	140-10-3	148.0526	11.38	87.45	0.019
Tetradecylamine	C14 H31 N	2016-42-4	213.2458	15.496	86.83	0.014

Trimethoprim-d3*	C14 H15 D3 N4 O3	1189923-38-3	293.1568	7.913	83.07	0.012
Guaifenesin	C10 H14 O4	93-14-1	198.0894	6.637	85.04	0.011
Tri-(2-chloroisopropyl)phosphate	C9 H18 Cl3 O4 P	13674-84-5	326.0011	15.753	97.91	0.010
1-Hexadecylamine	C16 H35 N	143-27-1	241.2771	10.681	87.02	0.008
Phytosphingosine	C18 H39 N O3	554-62-1	317.2934	15.417	85.21	0.008
2,4-Dimethylquinoline	C11 H11 N	1198-37-4	157.0892	5.807	87.8	0.008
1-Hexadecylamine	C16 H35 N	143-27-1	241.2771	15.131	87.03	0.007
Aminophenazone	C13 H17 N3 O	58-15-1	231.1374	5.604	86.82	0.007
Anthraquinone	C14 H8 O2	84-65-1	208.0527	14.346	86.89	0.007
Camphor	C10 H16 O	76-22-2	152.1202	17.337	87.17	0.006
Dodecanoic acid	C12 H24 O2	143-07-7	200.1777	12.56	85.74	0.005
Butylated hydroxyanisole	C11 H16 O2	25013-16-5	180.1149	15.928	86.18	0.005
Cumene hydroperoxide	C9 H12 O2	80-15-9	152.0837	7.318	83.73	0.004
Pentoxifylline	C13 H18 N4 O3	6493-05-6	278.1376	8.303	84.51	0.004
Isomyristic acid	C14 H28 O2	2724-57-4	228.2088	14.996	86.78	0.004
Tributylamine	C12 H27 N	102-82-9	185.2146	9.436	83.92	0.004
17beta-Estradiol (E2)	C18 H24 O2	50-28-2	272.1777	18.553	82.44	0.004
Triphenyl phosphate	C18 H15 O4 P	115-86-6	326.0712	17.53	82.7	0.003
Penbutolol	C18 H29 N O2	38363-40-5	291.2199	7.932	83.24	0.003

Table C.S7-1: Asuture at river km 82 (Sample A) downstream of aquaculture. Tentatively identified compounds by untargeted analysis. Assignments made if peak height >15000; score >75% isotopic profile, library match. Spiked surrogates denoted by a *. RT= retention time; Rel Area= relative peak area

Assignment	Formula	CAS #	Mass	RT	Score	Rel Area
Trimethoprim-d3*	C14 H15 D3 N4 O3	1189923-38-3	293.1575	6.464	68.88	1.000
Sulfamethoxazole-d4*	C10 H7 D4 N3 O3 S	1020719-86-1	257.0776	7.736	97.72	0.931
Sulfadimidine-d4*	C12 H10 D4 N4 O2 S	1020719-82-7	282.1093	7.031	97.69	0.889
Thiabendazole-d4*	C10 H3 D4 N3 S	1190007-20-5	205.0611	6.832	47.6	0.731
Sulfamerazine-d4*	C11 H8 D4 N4 O2 S	1020719-84-9	268.0935	5.843	97.58	0.720
Triethyl phosphate	C6 H15 O4 P	78-40-0	182.071	10.995	99.57	0.646
DEET / Diethyltoluamide	C12 H17 N O	134-62-3	191.1309	14.021	99.15	0.505
DEET-d10*	C12 H7 D10 N O	1215576-01-4	201.1937	13.922	99.53	0.352
Nonivamide	C17 H27 N O3	2444-46-4	293.1993	17.094	99.44	0.187
Ciprofloxacin-d8*	C17 H10 D8 F N3 O3	1130050-35-9	339.1836	7.383	97.73	0.178
O,O-Diethyl phosphate	C4 H11 O4 P	598-02-7	154.0397	10.995	99.84	0.125
Tris(2-butoxyethyl) phosphate	C18 H39 O7 P	78-51-3	398.2438	18.752	98.75	0.119
Terbutaline	C12 H19 N O3	23031-25-6	225.1367	6.047	99.01	0.118
Dibutyl phthalate	C16 H22 O4	84-74-2	278.1527	18.168	93.79	0.073
Embelin	C17 H26 O4	550-24-3	294.1835	15.825	97.79	0.073
Hydroxyatrazine	C8 H15 N5 O	2163-68-0	197.128	7.304	85.83	0.068
Dodecyldimethylamine oxide	C14 H31 N O	1643-20-5	229.2408	15.62	99.37	0.061
Trimethoprim-d3*	C14 H15 D3 N4 O3	1189923-38-3	293.1574	7.824	92.33	0.052
Hymecromone	C10 H8 O3	90-33-5	176.0477	14.245	86.86	0.050
Atenolol	C14 H22 N2 O3	29122-68-7	266.1635	6.861	97.86	0.045
Butylated hydroxyanisole	C11 H16 O2	25013-16-5	180.1153	13.007	99.24	0.045
Phthalic anhydride	C8 H4 O3	85-44-9	148.0166	14.246	97.71	0.041
Atrazine	C8 H14 Cl N5	1912-24-9	215.0941	13.736	95.86	0.019
Benzoic acid	C7 H6 O2	65-85-0	122.0369	16.061	87.72	0.016

Atraton	C9 H17 N5 O	1610-17-9	211.1433	10.204	86.89	0.015
Chloramphenicol-d5*	C11 H7 D5 Cl2 N2 O5	202480-68-0	327.0439	9.754	98.94	0.008
Ecgonine methyl ester	C10 H17 N O3	7143-09-1	199.1208	7.947	86.74	0.005
Triphenyl phosphate	C18 H15 O4 P	115-86-6	326.0713	17.416	84.61	0.004
Penbutolol	C18 H29 N O2	38363-40-5	291.22	7.846	85.31	0.004
Dymanthine	C20 H43 N	124-28-7	297.3397	16.816	83.38	0.002

Table C.S7-2: Asuture at river km 82 (Sample B) downstream of aquaculture. Tentatively identified compounds by untargeted analysis. Assignments made if peak height >15000; score >75% isotopic profile, library match. Spiked surrogates denoted by a *. RT= retention time; Rel Area= relative peak area

Assignment	Formula	CAS #	Mass	RT	Score	Rel Area
DEET / Diethyltoluamide	C12 H17 N O	134-62-3	191.1312	14.171	99.19	1.000
Trimethoprim-d3*	C14 H15 D3 N4 O3	1189923-38-3	293.1575	6.551	80.35	0.877
Sulfamethoxazole-d4*	C10 H7 D4 N3 O3 S	1020719-86-1	257.0775	7.826	98.06	0.760
Tributyltin	C12 H27 Sn	36643-28-4	283.1171	7.104	67.27	0.665
Triethyl phosphate	C6 H15 O4 P	78-40-0	182.071	11.128	99.71	0.656
Thiabendazole-d4*	C10 H3 D4 N3 S	1190007-20-5	205.061	6.927	47.53	0.558
Sulfamerazine-d4*	C11 H8 D4 N4 O2 S	1020719-84-9	268.0935	5.901	98.12	0.447
DEET / Diethyltoluamide	C12 H17 N O	134-62-3	191.1309	14.101	99.10	0.405
DEET-d10	C12 H7 D10 N O	1215576-01-4	201.1939	14.072	98.26	0.359
Nonivamide	C17 H27 N O3	2444-46-4	293.1993	17.223	99.61	0.310
2-(Benzylmethylamino)ethanol N-oxide	C10 H15 N O2	15831-63-7	181.1106	4.38	98.96	0.300
Glutaraldehyde	C5 H8 O2	111-30-8	100.0523	11.206	99.74	0.238
Dibutyl phthalate	C16 H22 O4	84-74-2	278.1527	18.432	95.29	0.205
Tri-(2-chloroisopropyl)phosphate	C9 H18 Cl3 O4 P	13674-84-5	326.0011	15.768	99.3	0.150
Glutaraldehyde	C5 H8 O2	111-30-8	100.0523	11.354	99.79	0.134
O,O-Diethyl phosphate	C4 H11 O4 P	598-02-7	154.0397	11.128	99.63	0.128
Ciprofloxacin-d8*	C17 H10 D8 F N3 O3	1130050-35-9	339.1837	7.482	99.44	0.098
Terbutaline	C12 H19 N O3	23031-25-6	225.1367	6.102	99.7	0.086
Hymecromone	C10 H8 O3	90-33-5	176.0477	14.395	98.31	0.085
Dodecyldimethylamine oxide	C14 H31 N O	1643-20-5	229.2408	15.775	99.09	0.072
Phthalic anhydride	C8 H4 O3	85-44-9	148.0162	14.395	99.52	0.067
Embelin	C17 H26 O4	550-24-3	294.1834	15.967	99.35	0.054
Hydroxyatrazine	C8 H15 N5 O	2163-68-0	197.1279	7.398	86.67	0.048
Atenolol	C14 H22 N2 O3	29122-68-7	266.1633	6.931	99.41	0.045

Phthalic anhydride	C8 H4 O3	85-44-9	148.0161	17.977	87.65	0.040
Diethyl phthalate	C12 H14 O4	84-66-2	222.0897	14.395	98.42	0.039
Butylated hydroxyanisole	C11 H16 O2	25013-16-5	180.1153	13.158	98.35	0.029
Estrone (E1)	C18 H22 O2	53-16-7	270.162	16.8	98.61	0.029
Trimethoprim-d3*	C14 H15 D3 N4 O3	1189923-38-3	293.1572	7.923	86.62	0.018
Benzoic acid	C7 H6 O2	65-85-0	122.0369	16.205	87.75	0.016
Phthalic anhydride	C8 H4 O3	85-44-9	148.0161	16.747	87.62	0.014
Tetradecylamine	C14 H31 N	2016-42-4	213.2458	15.505	87.16	0.014
Desethylatrazine	C6 H10 Cl N5	6190-65-4	187.0628	9.904	90.9	0.009
Coumafuryl	C17 H14 O5	117-52-2	298.0832	7.104	79.59	0.009
Phenylacrylic acid (Cinnamic acid)	C9 H8 O2	140-10-3	148.0525	11.394	87.08	0.009
Oxybenzone	C14 H12 O3	131-57-7	228.079	16.657	86.48	0.007
Dimethyl phthalate	C10 H10 O4	131-11-3	194.0579	11.673	82.43	0.006
Triphenyl phosphate	C18 H15 O4 P	115-86-6	326.0711	17.54	84.87	0.006
8-Hydroxyquinoline	C9 H7 N O	148-24-3	145.0528	5.848	87.83	0.006
Butylated hydroxyanisole	C11 H16 O2	25013-16-5	180.115	15.938	86.88	0.005
Chloramphenicol-d5*	C11 H7 D5 Cl2 N2 O5	202480-68-0	327.0441	9.881	79.87	0.004
Penbutolol	C18 H29 N O2	38363-40-5	291.2199	7.943	82.52	0.004

Table C.S8. Diversity Values

Sample ID	Sample Type	Location	River Mile	Shannon alpha diversity	Faiths phylogenetic diversity	Pielou evenness	Observed OTUs
1Asoil	soil	1	0.45	3.40835727	5.10864239	0.92106818	13
1Awater	water	1	0.45	2.35954763	4.57009874	0.61973409	14
1Bsoil	soil	1	0.45	3.41742016	5.52044627	0.89758382	14
3Asoil	soil	3	5.1	3.94661201	5.53577057	0.92906765	19
3Awater	water	3	5.1	2.25178039	3.60044381	0.75059346	8
3Bsoil	soil	3	5.1	4.15202495	6.27345393	0.94529255	21
3Bwater	water	3	5.1	3.12535464	4.02457067	0.94082549	10
4Asoil	soil	4	6.79	4.2333991	5.97878025	0.92332251	24
4Awater	water	4	6.79	3.61919655	4.61475319	0.83740323	20
4Bsoil	soil	4	6.79	3.75286132	5.78277669	0.91813956	17
4Bwater	water	4	6.79	3.51515078	4.32116928	0.94992786	13
5Asoil	soil	5	16.75	3.8966318	6.33472623	0.9015957	20
5Awater	water	5	16.75	3.41273647	4.43263128	0.89635365	14
5Bsoil	soil	5	16.75	3.90269944	5.05764884	0.90299962	20
5Bwater	water	5	16.75	2.85395403	4.46353727	0.90032226	9
7Asoil	soil	7	17.52	3.79376001	8.72111561	0.89308492	19
7Bsoil	soil	7	17.52	4.2120659	5.62395049	0.94452977	22
7Bwater	water	7	17.52	2.43468072	3.6906995	0.76805625	9
9Asoil	soil	9	29.73	3.5288667	5.05837181	0.95363442	13
9Bsoil	soil	9	29.73	2.52240156	3.31489923	0.89849756	7
9Bwater	water	9	29.73	3.65275394	8.52812536	0.91318849	16
10Asoil	soil	10	33.93	3.80807947	5.52286172	0.93164871	17
10Awater	water	10	33.93	2.76017619	4.38479029	0.87073864	9

10Bsoil	soil	10	33.93	3.45538971	4.10552261	0.93377814	13
10Bwater	water	10	33.93	3.15648031	4.92563267	0.88047791	12
11Asoil	soil	11	36.86	3.68527956	5.36479403	0.92131989	16
11Awater	water	11	36.86	2.13014533	3.31908589	0.61575009	11
11Bsoil	soil	11	36.86	3.27075036	7.95869195	0.8371748	15
11Bwater	water	11	36.86	2.03913879	6.97183019	0.61384194	10
12Asoil	soil	12	39.31	0.72584647	3.45704563	0.28079574	6
12Awater	water	12	39.31	3.77542585	4.71665926	0.90539419	18
12Bsoil	soil	12	39.31	3.28858826	4.08558665	0.9173285	12
12Bwater	water	12	39.31	3.51635834	4.41114032	0.92356988	14
13Asoil	soil	13	48.92	4.05676775	5.92278012	0.95499929	19
13Awater	water	13	48.92	3.5964564	4.57657558	0.92054188	15
13Bsoil	soil	13	48.92	1.54309808	2.97796436	0.97358649	3
13Bwater	water	13	48.92	2.97923833	3.73320978	0.8968401	10
14Asoil	soil	14	54.75	2.93753154	7.50135521	0.88428511	10
14Awater	water	14	54.75	2.69773745	3.09556152	0.96095347	7
14Bsoil	soil	14	54.75	3.8982038	5.63483806	0.97455095	16
14Bwater	water	14	54.75	3.44019988	4.34472342	0.88054677	15
15Asoil	soil	15	59.14	3.79347857	4.75538771	0.90972345	18
15Awater	water	15	59.14	3.1219684	3.33492465	0.93980613	10
15Bsoil	soil	15	59.14	4.17881623	4.48719732	0.93707373	22
15Bwater	water	15	59.14	3.1648197	6.7924531	0.88280413	12
16Asoil	soil	16	60.45	3.14051623	4.90860757	0.82485513	14
16Awater	water	16	60.45	3.57904095	5.01064982	0.94003344	14
16Bsoil	soil	16	60.45	3.33461702	4.62776559	0.90114075	13
16Bwater	water	16	60.45	3.16238746	4.62254381	0.88212567	12
17Asoil	soil	17	69	0.43925589	3.42823566	0.21962795	4

17Awater	water	17	69	3.28931728	3.69959178	0.95082593	11
17Bsoil	soil	17	69	0.38399771	3.58315689	0.19199886	4
17Bwater	water	17	69	3.68152114	4.23759403	0.90068614	17

Table C.S9. P values from the ANOSIM and Mantel Tests

	Mantel Test	**ANOSIM**
	Significance	**Significance**
Sample type		**1.00E-04**
Location		**3.00E-04**
Aquaculture		0.7014
River Mile	**0.0141**	
Clarity	0.7446	
Temp	0.1438	
DO	**0.0148**	
Conductivity	0.0543	
pH	0.0335	
Nitrate	0.0737	
Depth	**0.0494**	
CIP	**0.011**	
ERY	NA	
SMA	0.8543	
SMX	NA	
SMZ	0.5554	
TBD	NA	
TRI	0.0536	
DEET	**0.0046**	

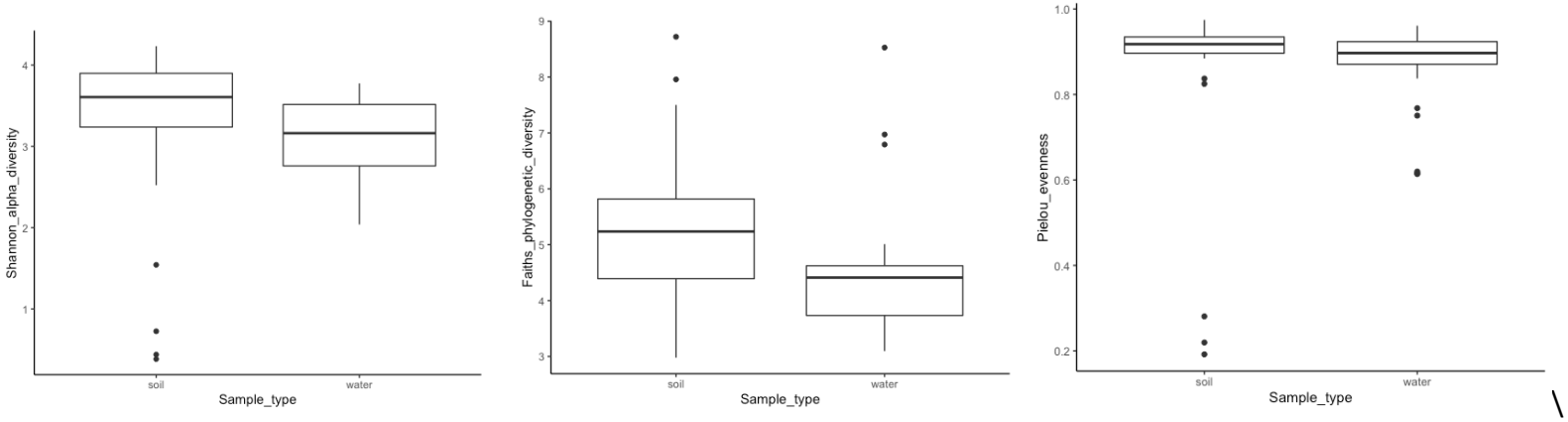

Figure C.S1. Box plots of the Shannon alpha diversity, PD, and evenness indices comparing sediment vs. water samples.

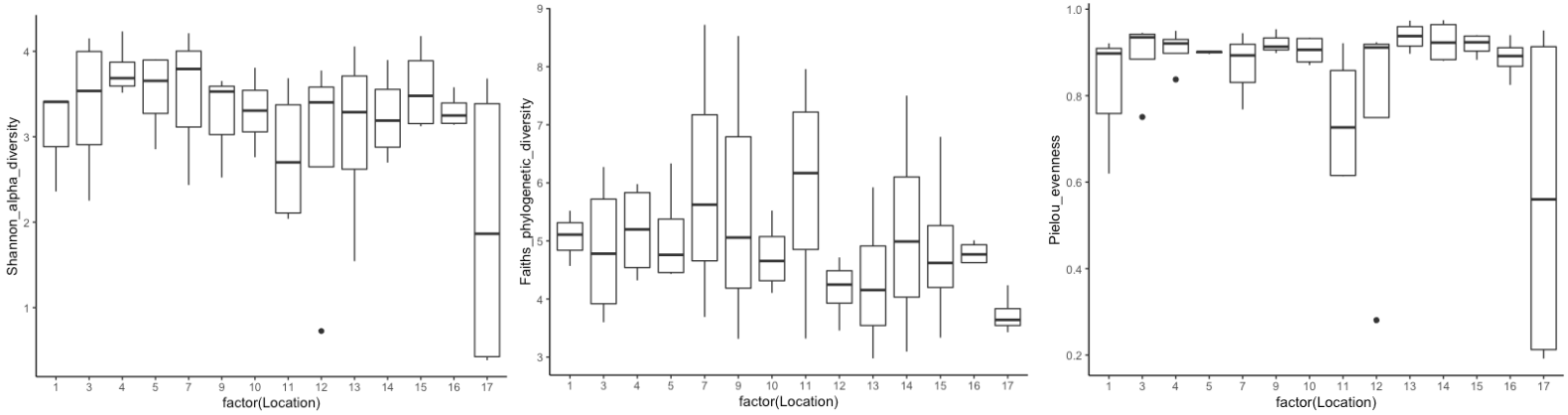

Figure C.S2. Box plots of the Shannon alpha diversity, PD, and evenness indices comparing sample location. The Shannon diversity indices ranged from 0.38 to 4.23 with an average value of 3.17 and the Faiths phylogenetic diversity index (PD) ranged from 2.98 to 8.72 with an average value of 4.93 (Table C.SX). Pielou's evenness index ranged from 0.19 to 0.97 with an average value of 0.85.

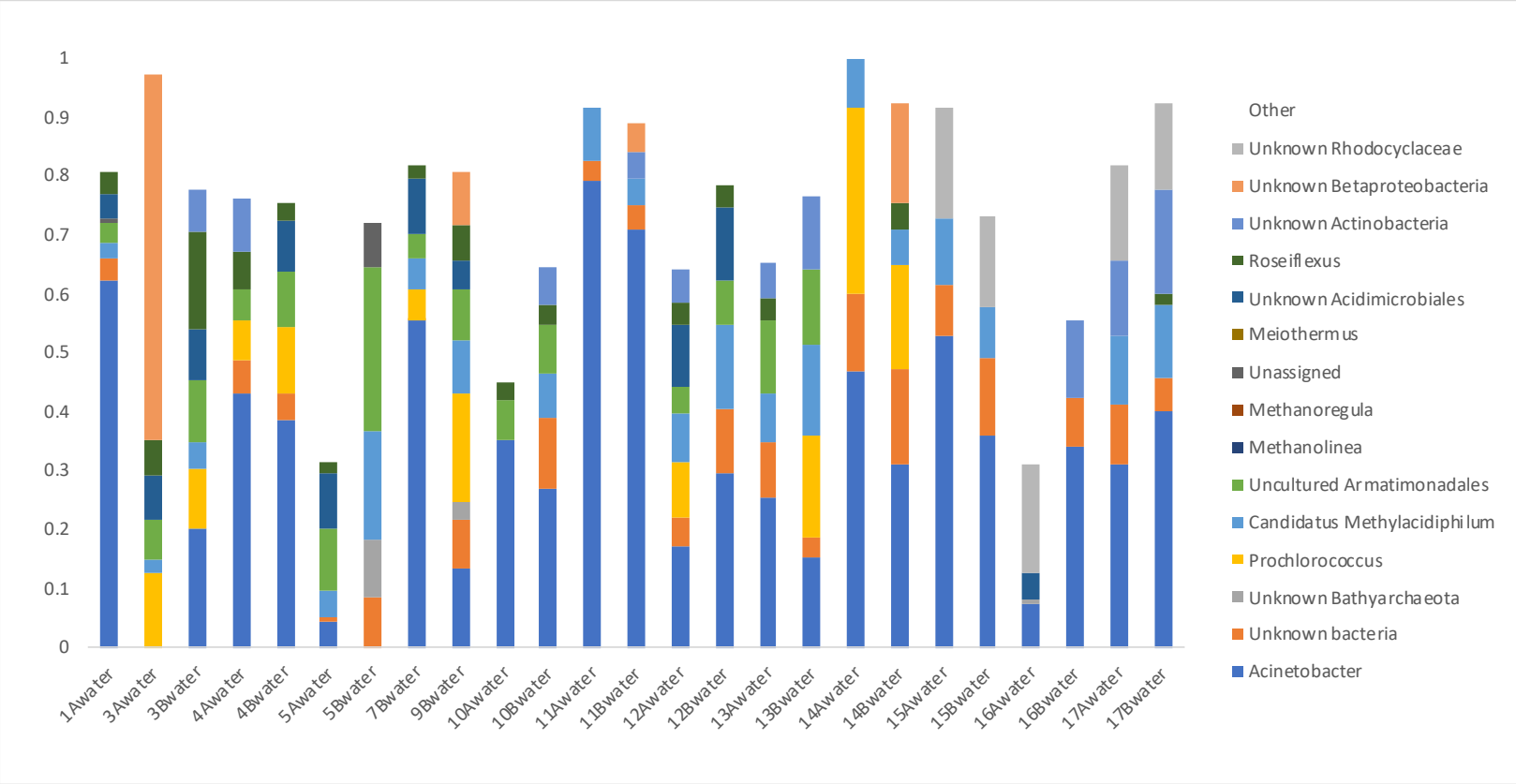

Figure C.S3. Microbial community composition at the genera level for water samples collected at all locations.

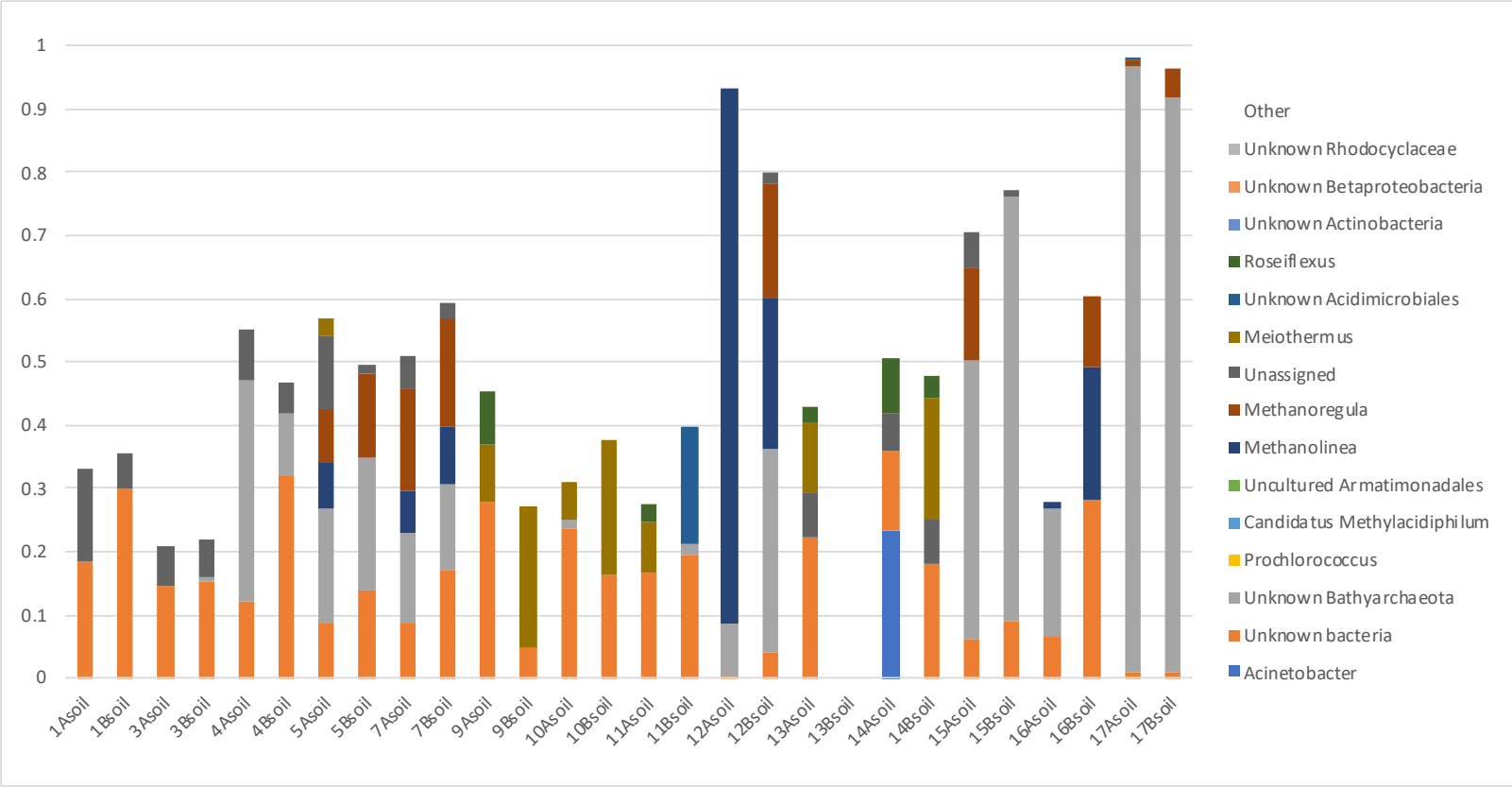

Figure C.S4. Microbial community composition at the genera level for s samples collected at all locations.

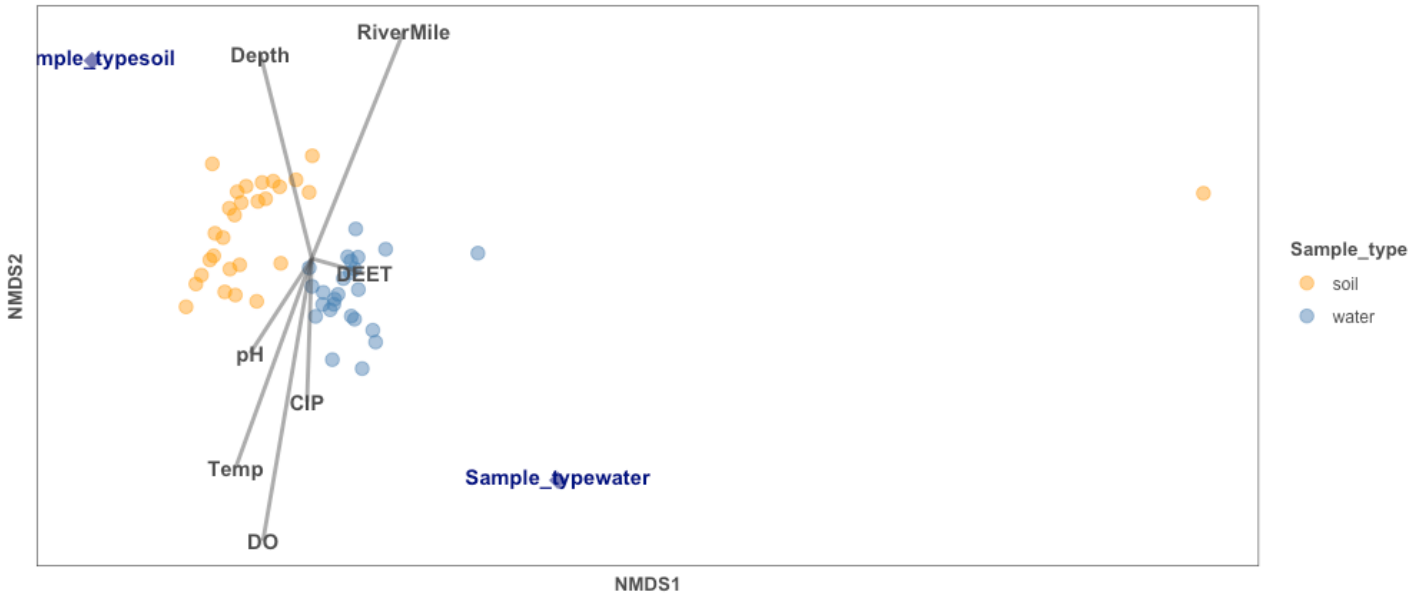

Figure C.S5. NMDS Plot with environmental factors and targeted antibiotic concentration axis including the outlier.

Figure C.S6 NMDS Plots for Individual Environmental Factor or Antibiotics

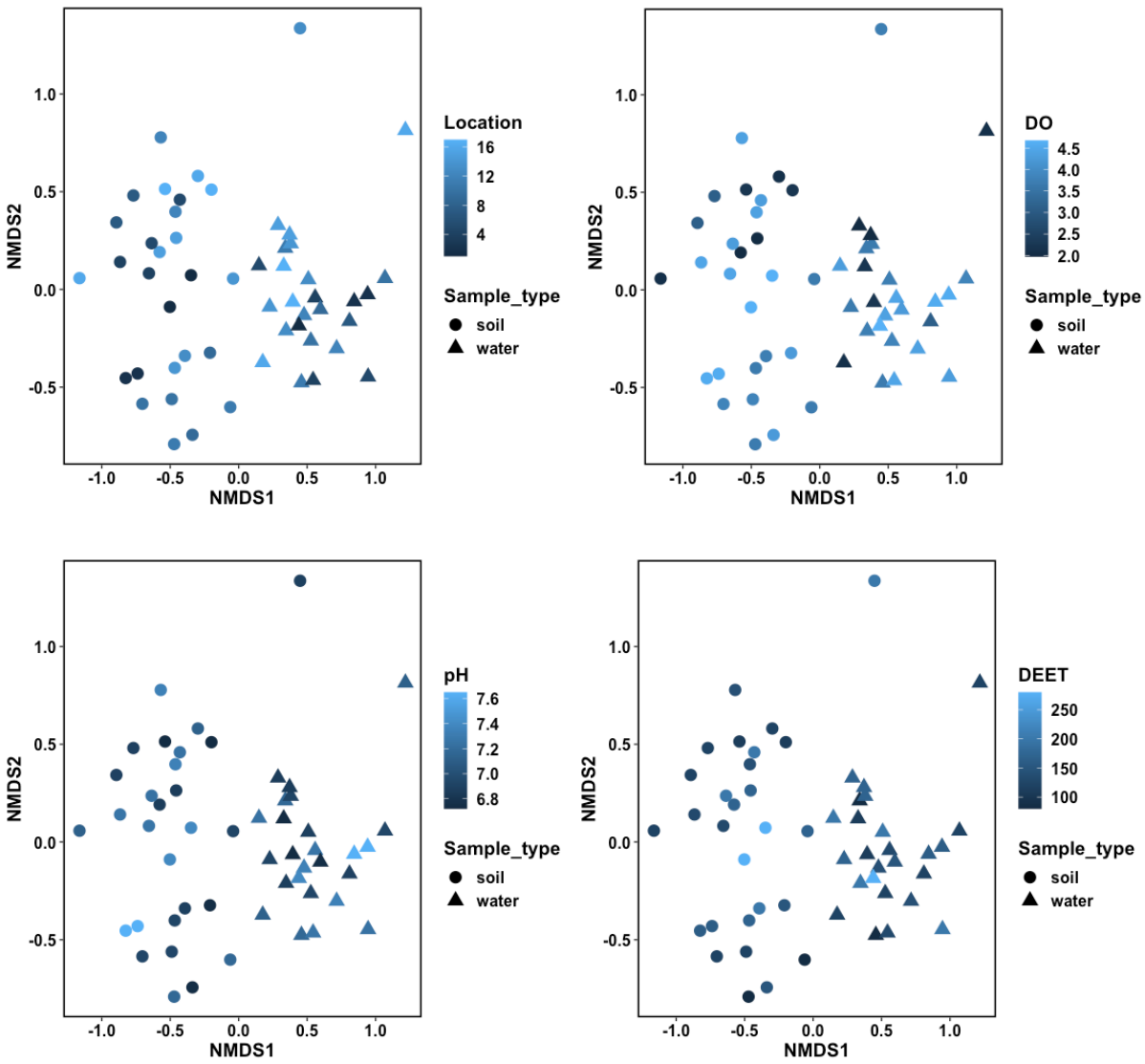
NMDS2
NMDS1
1.0
0.5
0.0
-0.5
-1.0
-0.5
0.0
0.5
1.0
Location
16
12
8
4
Sample_type
soil
water
DO
4.5
4.0
3.5
3.0
2.5
2.0
pH
7.6
7.4
7.2
7.0
6.8
DEET
250
200
150
100

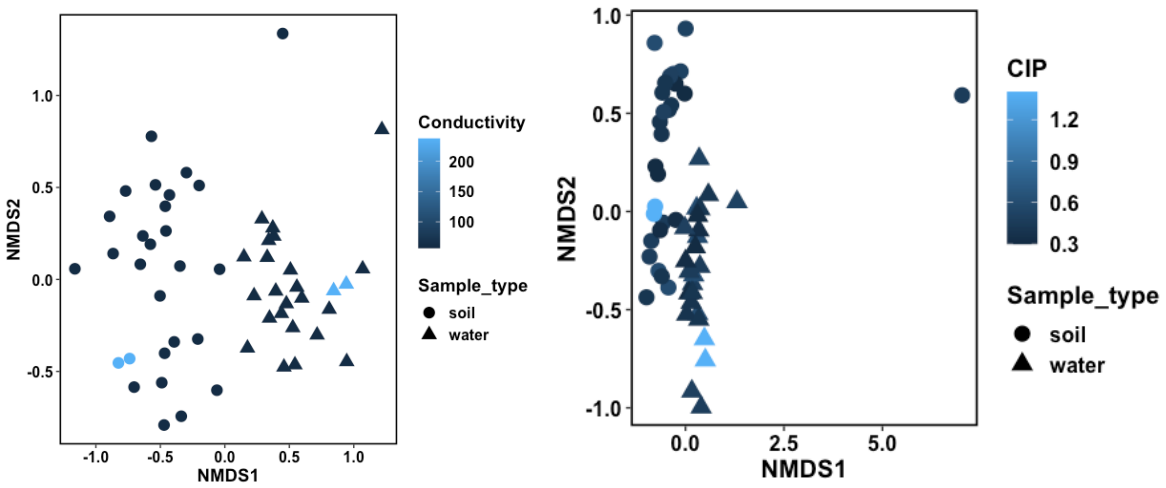
NMDS2
NMDS1
1.0
0.5
0.0
-0.5
-1.0
-0.5
0.0
0.5
1.0
Conductivity
200
150
100
Sample_type
soil
water
NMDS2
NMDS1
1.0
0.5
0.0
-0.5
-1.0
0.0
2.5
5.0
CIP
1.2
0.9
0.6
0.3
Sample_type
soil
water

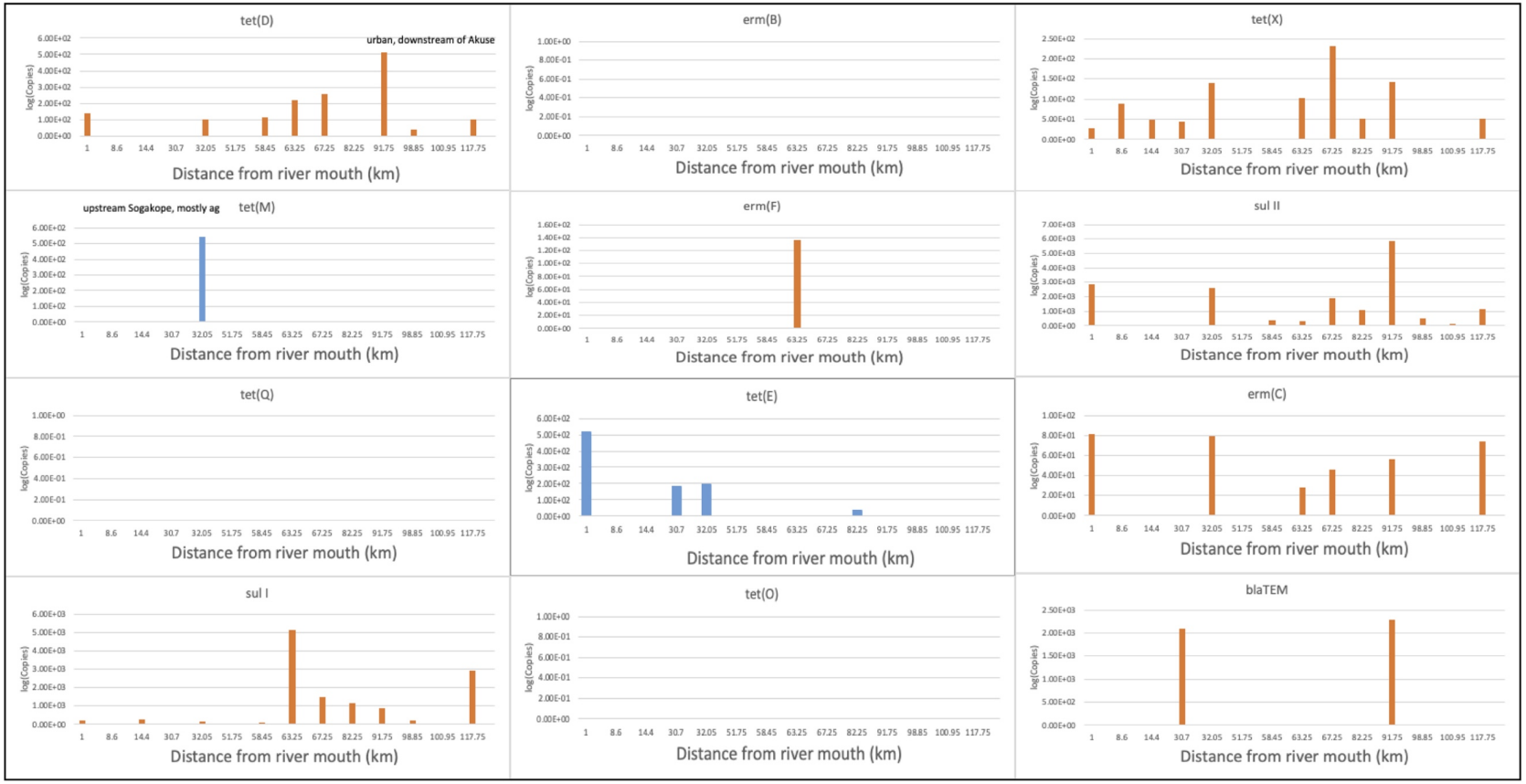

Figure C.S7. Antibiotic resistance genes in water samples. See Table C.1 for site descriptions.

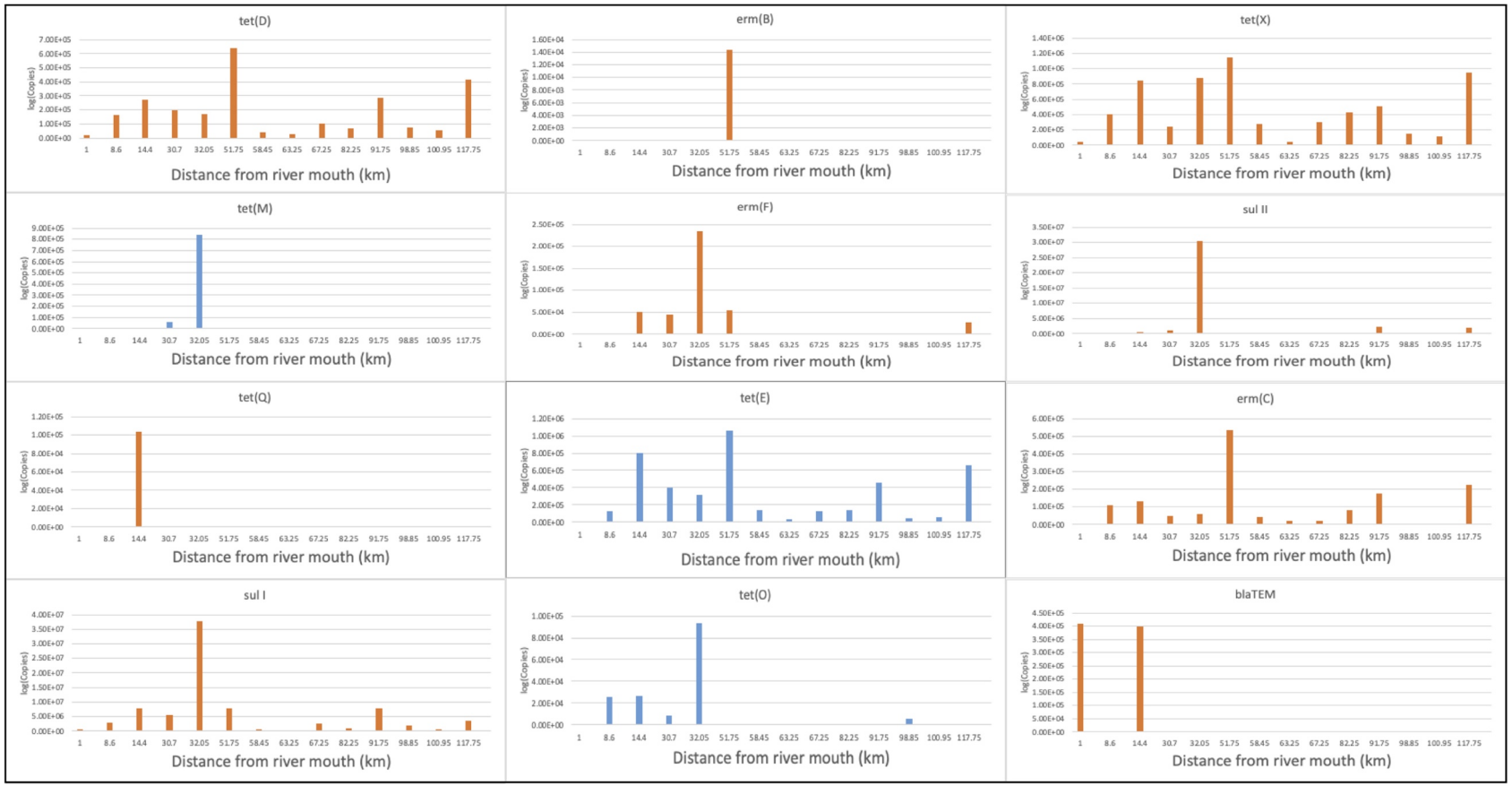

Figure C.S8. Antibiotic resistance genes in sediment samples. See Table C.1 for site descriptions.

Table C.S10: Targeted analysis of Volta River sediments

river km	concentration (ng/g)							
[site #]	CIP	ERY	SMA	SMX	SMZ	TBD	TRI	DEET
118	<5	<25	<12	<2	<2	<20	<2	40±14
101	<5	<25	<12	<2	<2	<20	<2	34±11
99	<5	<25	<12	<2	<2	<20	<2	36
92	<5	<25	<12	<2	<2	<20	<2	67
82	<5	<25	<12	<2	<2	<20	<2	84±6
67	<5	<25	<12	<2	<2	<20	<2	27±14
63	<5	<25	<12	<2	<2	<20	<2	34±18
58	<5	<25	<12	<2	<2	<20	<2	41±8
52	<5	<25	<12	<2	<2	<20	<2	42±27
32	<5	<25	<12	<2	<2	<20	<2	46±10
blank	<5	<25	<12	<2	<2	<20	<2	<5

river km	PBFA	PFPeA	PFHxA	PFHpA	PFOA	PFNA	PFDA	PFBS	PFHxS	PFOS
118	<10	<10	<6	<4	<7	<4	<6	<9	<9	<7
101	<10	<10	<6	<4	<7	<4	<6	<9	<9	<7
99	<10	<10	<6	<4	<7	<4	<6	<9	<9	<7
92	<10	<10	<6	<4	<7	<4	<6	<9	<9	<7
82	<10	<10	<6	<4	<7	<4	<6	<9	<9	<7
67	<10	<10	<6	<4	<7	<4	<6	<9	<9	<7
63	<10	<10	<6	<4	<7	<4	<6	10±0.5	<9	<7
58	<10	<10	<6	<4	7.6±0.3	<4	<6	10±1.4	<9	<7
52	<10	<10	<6	<4	<7	<4	<6	11±0.8	<9	<7
32	<10	<10	<6	<4	<7	4.9±0.5	<6	10±1.4	<9	<7
31	<10	<10	8.2±4-0	<4	<7	5.2±2.8	<6	15±1.4	10±7	<7
14	<10	<10	7.6±7.1	<4	<7	<4	<6	14±3.5	9±2	<7
9	<10	<10	<6	<4	<7	<4	<6	11±11	<9	<7
1	<10	<10	<6	<4	8 ±10	1.2±1.5	0.7±0.8	10±2.3	<9	<7
blank	<10	<10	<6	<4	<7	<4	<6	<9	<9	<7

Appendix D: Supporting Information for Chapter 3

This chapter has been published as Supplemental Information in the journal *Environmental Science & Technologies Letters* and is cited as:

Huff Chester, A. L., Eum, K., Tsapatsis, M., Hillmyer, M. A., & Novak, P. J. (2021). Enhanced Nitrogen Removal and Anammox Bacteria Retention with Zeolite-Coated Membrane in Simulated Mainstream Wastewater. *Environmental Science & Technology Letters*, 8(6), 468-473.

Methods

Membrane Fabrication. The spinning dope suspension composition was (wt %) 38.0% N-Methyl-2-pyrrolidone (NMP), 6.8% polyethersulfone (PES), 54.7% Al_2O_3, and 0.5% polyvnylpyrrolidone (PVP). Spinning conditions are provided in Table D.S1. The raw fibers were sintered at 600 °C for 2 h followed by 6 h sintering at 1600 °C, with a temperature ramping rate of 5 °C/min. Bare alumina fibers approximately 75 mm in length and 1 mm in diameter were dried at 100 °C for several hours.

Table D.S1. Spinning conditions for carbon and alumina raw fibers.

Dope composition (PES/NMP/Al_2O_3/PVP) (wt %)	6.8/38.0/54.7/ 0.5
Dope flow rate (ml/hr)	120
Bore fluid	DI H_2O
Bore fluid flow rate (ml/hr)	80
Air gap (cm)	3
Take up rate (m/min)	*
Operating temperature (K)	RT (~298)
Quench bath temperature (K)	298

*The alumina raw fibers were collected from bottom of the bath instead of using the take-up drum.[1]

Zeolite growth confirmation with SEM-EDS. Scanning Electron Microscopy Energy (SEM) and Dispersive X-ray Spectroscopy (EDS) was performed on a Hitachi SU8230 Field Emission Gun microscope with an attached Thermo Noran System 7 to verify the zeolite layer thickness and type. Samples were secured onto stubs with carbon tape and

sputter coated with 2 μm iridium using a Lecia EM ACE600 sputter coater before imaging.

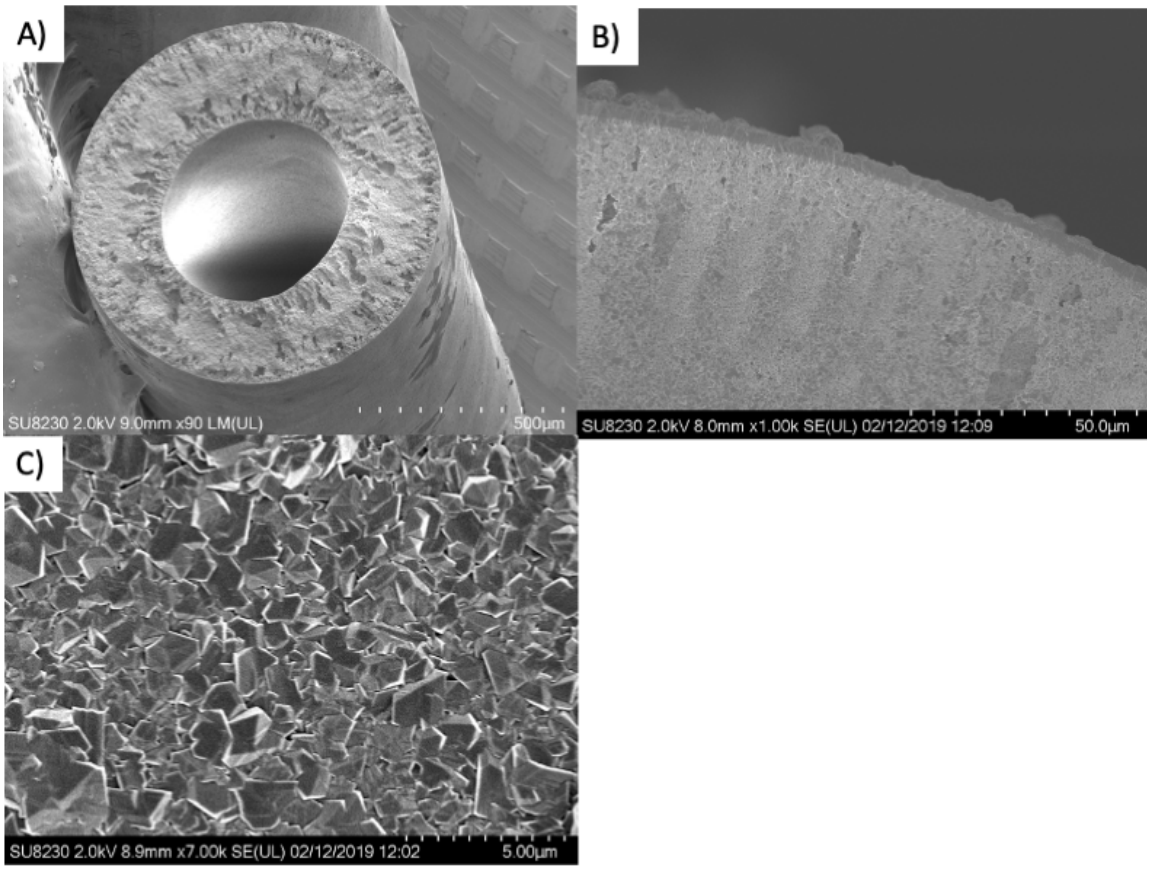

Figure D.S1. SEM image of zeolite-coated membrane. (A) Low magnitude cross section B) high magnitude cross section and C) top-view image of FAU zeolite grown or the outer surface of α-alumina support

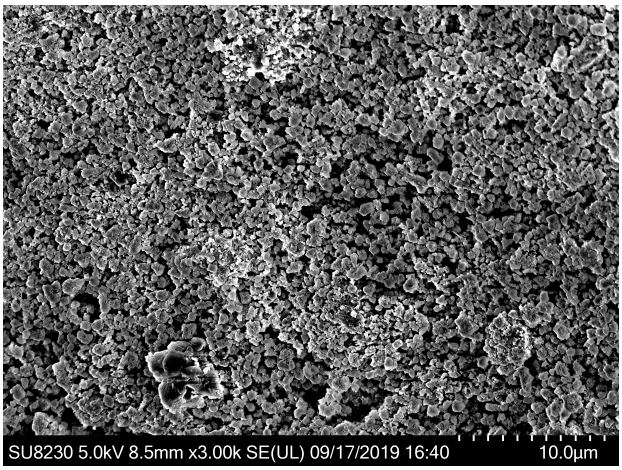

Figure D.S2. SEM image of zeolite particle. Top-view image of FAU particle of the outer surface

Table D.S2. Energy-dispersive X-ray spectroscopy (EDS) mapping of FAU grown hollow fiber.

Index	O		Na		Al		SI	
	Count	Atom %	Count	Atom %	Count	Atom %	Count	Atom %
Point 1	211651	82.05	7599	1.80	56165	6.86	74863	9.28
Point 2	214181	82.19	9041	2.15	54435	6.69	72200	8.96
Point 3	213942	83.65	4524	1.13	47956	6.05	72422	9.16
Average	213258	82.63	7055	1.69	52852	6.53	73162	9.13

Table D.S3. Single-gas permeances through FAU hollow fiber membranes at 25°C

	Bare α-alumina hollow fiber [mol/m^2·pa·s]	FAU layer grown α-alumina hollow fiber, 24 h growth [mol/m^2·pa·s]	FAU layer grown α-alumina hollow fiber, 48 h growth [mol/m^2·pa·s]
N_2	9.24×10^{-6}	4.37×10^{-9}	9.81×10^{-10}
O_2	9.12×10^{-6}	4.18×10^{-9}	9.14×10^{-10}

Biomass Seed and Synthetic Wastewater. Activated sludge for inoculation was collected from the Metropolitan WWTP in St. Paul, MN, concentrated, and preserved as described previously.[30] Anammox sludge was collected from a DEMON sequencing batch reactor operated in the laboratory for four years and initially seeded from Hampton Roads Sanitary District DEMON sludge (York River WWTP, Seaside, VA).[30]

Media for sorption/ammonium removal and reactor experiments.

Table D.S4. Synthetic wastewater components in mg per liter.

	Sorption/ammonium Removal Experiments	Varying zeolite batch experiments	Membrane batch experiment
Urea	75	75	35
Ammonium Chloride	80	80	5
Sodium Nitrite	0	104	49
Sodium Uric Acid	12	12	12
Magnesium Phosphate Dibasic Trihydrate	25	25	25
Potassium Phosphate Tribasic	20	20	20
Bacteriological peptone	12	12	12
Sodium acetate	221	221	221
Dry meat extract	12	12	12
Glycerin	34	34	34
Potato starch	42	42	42
Low fat milk powder	50	50	50
$KHCO_3$*	246	246	
$NaHCO_3$*			275

*$KHCO_3$ was used for sorption/ammonium removal experiments and varying zeolite batch experiment. $NaHCO_3$ was used for the membrane experiment because Na^+ has a lower sorption affinity for faujasite-type zeolite than K^+.

Sorption/ammonium removal experiments. Zeolite particles and zeolite-coated membranes were tested for ammonium removal in synthetic wastewater. Varying masses of particles (0.004 to 0.050 g) or hollow fiber membranes (0.31 to 0.62 g) were added to 5 mL SWW (Table D.S3) with an initial ammonium concentration of 33.3±4.8 mg-N/L and were mixed on a rotator for 24 h. The SWW was filtered (0.45 μm) and the ammonium concentration measured using an ammonium probe. An ammonium removal isotherm was also developed for zeolite-coated and bare alumina membranes in ammonium chloride solution. Batch tests were performed in triplicate. Single membranes were added to 10 mL of ammonium chloride solution with concentrations ranging from 5 to 100 mg-N/L and were mixed on a rotator for 48 hours. Initial and final ammonium concentrations were measured using an ammonium probe. The ammonium removal capacity (q) was calculated using equation (1).

$$q = \frac{(C_i - C_f) \cdot V}{m_{mem}} \quad (1)$$

where C_i is the initial ammonium concentration (mg-N/L), C_f is the final ammonium concentration (mg-N/L), V in the liquid volume (L), and m_{mem} is the mass of the dry membrane (g).

Used, post-experiment zeolite-coated membranes from the biologically active reactors and abiotic reactors were also tested for their ammonia removal to determine if sorption capacity of the zeolite was impacted during the experiment. Since membranes were cut

into thirds for the experiment, three membrane pieces were tested in 10 mL of 23.9±2.29 mg-N/L ammonium chloride solution and were mixed on a rotator for 48 hours. Initial and final ammonium concentrations were measured using an ammonium probe and the ammonia removal of the used membranes were compared to the sorption capacity of the new membranes (Figure D. S5).

Zeolite particle batch experiment. Triplicate reactors (50-mL) contained either zeolite particles (0.05 g, 0.10 g, 0.50 g, or 1.0 g) or 0.50 g of bare alumina particles (control). Sealed reactors contained 25 mL liquid and 25 mL headspace (98% N_2, 2% H_2) and were incubated on a shaker Table D.in an anaerobic glovebag at room temperature (21±2°C) for the duration of the experiment (33 days). All reactors were started with a common well-mixed solution of 500 mL SWW (Table D.S4), 7.5 mL activated sludge, and 2.5 mL anammox sludge.

Liquid (7.5 mL) was removed from the reactors and exchanged with fresh, sterile SWW every three days. The removed liquid was immediately filtered (0.45 μm) and stored frozen (–4°C) until analyzed for ammonium, TN, nitrate, and nitrite. Liquid biomass samples (0.5 mL) were collected at the end of the experiment (Day 33) and stored in lysis buffer at –20°C until DNA was extracted.

Analytical methods. Ammonium was measured *via* an ammonium probe (Orion, Thermo Scientific) for the sorption experiments. Measurements were performed according to the manufacturer's instructions, including the addition of a solution to adjust the ionic

strength. A 5-point standard curve, ranging from 0.1 to 50 mg-N/L (typical R^2 values of 0.99 or higher), was used for quantification. Standards were made gravimetrically with NH_4Cl in ultrapure (MilliQ, Millipore) water.

In reactor experiments, ammonium and TN were measured colorimetrically (Hach) and nitrite and nitrate were measured with an ion chromatograph (Metrohm). The filtered effluent batch reactor samples were analyzed for ammonia and TN using HACH Method 10031 and 10072, respectively. Briefly, the filtered samples were diluted 1:1 with ultrapure water. Nitrite and nitrate concentrations were measured on a Metrohm 930 Compact IC Flex with an A Supp 5 column, 20 uL sample loop, and an eluent carbonate buffer (3.2 mM Na_2CO_3 and 1.0 mM $NaHCO_3$). A 5-point calibration curve ranging from 0.1 mg-N/L to 50 mg-N/L was used to quantify the nitrite and nitrate concentrations in the samples. Standards were made gravimetrically with $NaNO_2$ or $NaNO_3$ in ultrapure water.

Molecular Methods. DNA extractions were performed on the biomass and membrane samples using the FastDNA spin kit (MP Biomedicals) according to the manufacturer's instructions. qPCR of total 16S rRNA genes and several nitrogen cycling genes *(amoA,* Amx*, nxrA, nosZ, nirK, and nirS)* was performed using a thermocycler (Bio-Rad) and the protocols and annealing temperatures described in Table D.S5.[2] Briefly, the qPCR reaction mixtures (15 µl) contained 7.5x EvaGreen Supermix (Bio-Rad Laboratories), 100 nM of each primer, 1x of bovine serum albumin (BSA), and 1 µl 10x or 20x diluted template. The general qPCR cycle was 95 °C initial denaturation for 10 min followed by

40 cycles of 95 °C denaturation for 15 s and 1 min anneal/extension at the specific annealing temperature for each primer set (Table D.S4). A melting curve was completed at the end of each run for quality control and samples were checked for inhibition by a ten-fold serial dilution of template and no inhibition was found.

qPCR methods.

Table D.S5. qPCR primers and annealing temperatures

Target gene	**Primers (forward listed first, reverse listed second)**	**Annealing Temp-erature**	**Source**
16S rRNA for Bacteria	341F 5'-CCT ACG GGA GGC AGC AG-3' 518R 5'-ATT ACC GCG GCT GCT GG-3'	60 °C	Muyzer et al., 1993[3]
16S rRNA for anammox (Amx)	A438F 5'-GTC RGG AGT TAD GAA ATG-3' A684R 5'-ACC AGA AGT TCC ACT CTC-3'	58 °C	Humbert et al., 2012[4]
amoA	*amo*No550D2f 5'- TCA GTA GCY GAC TAC ACM GG-3' *amo*No754r 5'- CTT TAA CAT AGT AGA AAG CGG-3'	56 °C	Harms et al., 2003[5]
nxrA	F1norA 5'- CAG ACC GAC GTG TGC GAA AG-3' R2norA 5'- TCY ACA AGG AAC GGA AGG TC-3'	55 °C	Poly et al., 2008[6]
nirK	nirK2F 5'-GCS MTS ATG GTS CTG CC-3' nirK1040 5'-GCC TCG ATC AGR TTR TGG TT-3'	59 °C	Baker et al., 1998[7] Hallin and Lindgren, 1999[8]
nirS	cd3aF 5'-GTS AAC GTS AAG GAR ACS GG-3' R3cd 5'-GAS TTC GGR TGS GTC TTG A-3'	59 °C	Throbäck et al., 2004[9]

nosZ	nosZ1F 5'-ATG TCG ATC ARC TCV KCR TTY TC-3' nosZ1R 5'-WCS YTG TTC MTC GAC AGC CAG-3'	60 °C	Henry et al., 2006[10]

Results

Membrane Isotherms. The uncoated membranes did not remove ammonium (Figure D. S3). Both Langmuir and Freundlich isotherm curves were fitted to the q values of the zeolite-coated membranes (Figure D. S3), generating the following equations.

$$q_e = \frac{q_{max} \cdot K \cdot C_f}{1 + K \cdot C_f} = \frac{41.56 \cdot 0.000946 \cdot C_f}{1 + 0.000946 \cdot C_f} \text{ (Langmuir)} \quad (2)$$

where q_e is the ammonium removed (mg-N/g), q_{max} is the amount of ammonium per unit mass of zeolite membrane corresponding to complete monolayer coverage (mg-N/g), and K is the Langmuir constant related to binding energy.

$$q_e = k_f \cdot C_f^{\frac{1}{n}} = 0.0465 C_f^{\frac{1}{1.0588}} \text{ (Freundlich)} \quad (3)$$

where k_f and 1/n are constants. The R^2 for the Langmuir and Freundlich curves were 0.9910 and 0.9914, respectively.

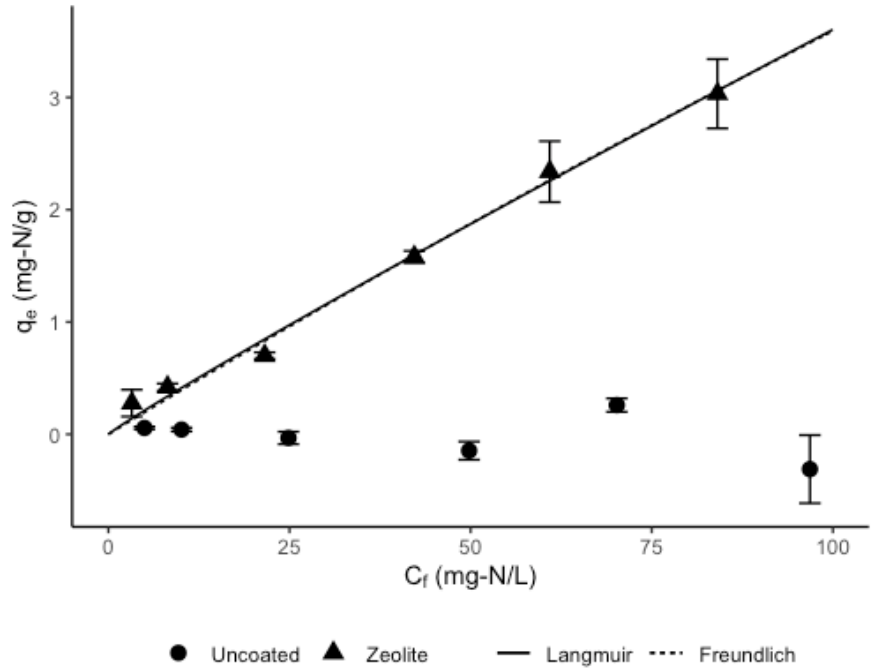

Figure D.S3. Langmuir and Freundlich isotherm curves fit to ammonium removal data for zeolite-coated membranes and uncoated membranes.

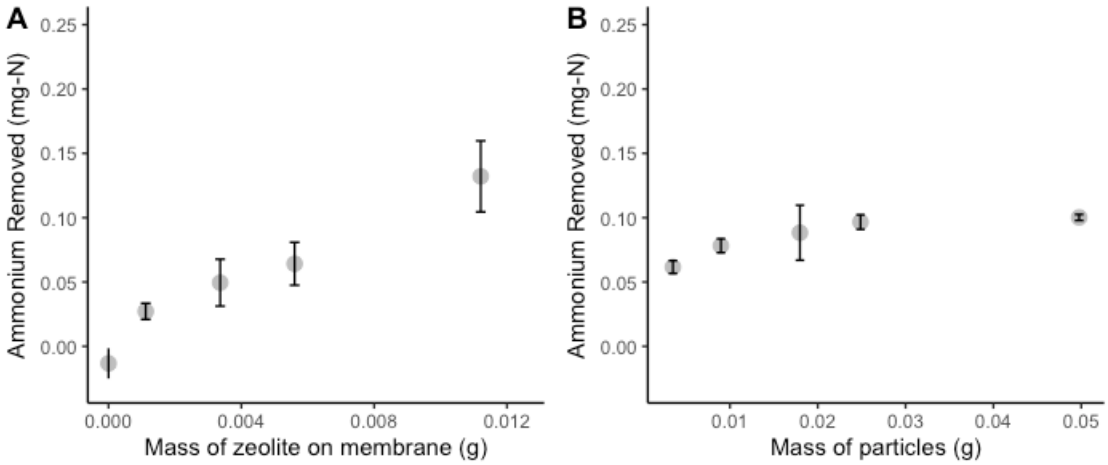

Figure D.S4. Ammonium removal from synthetic wastewater by sorption/ion exchange. A) Removal with zeolite-coated hollow fiber membrane and B) Removal with zeolite particles.

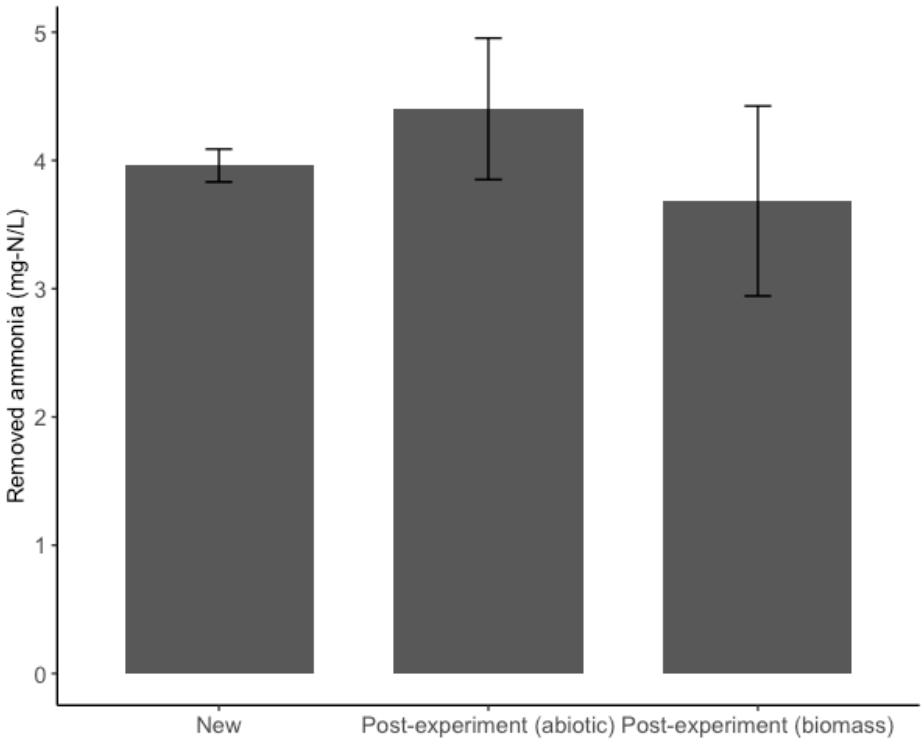

Figure D.S5. Ammonia removed by new and used post-experiment membranes from the biologically active zeolite-coated reactors and the abiotic zeolite-coated reactors.

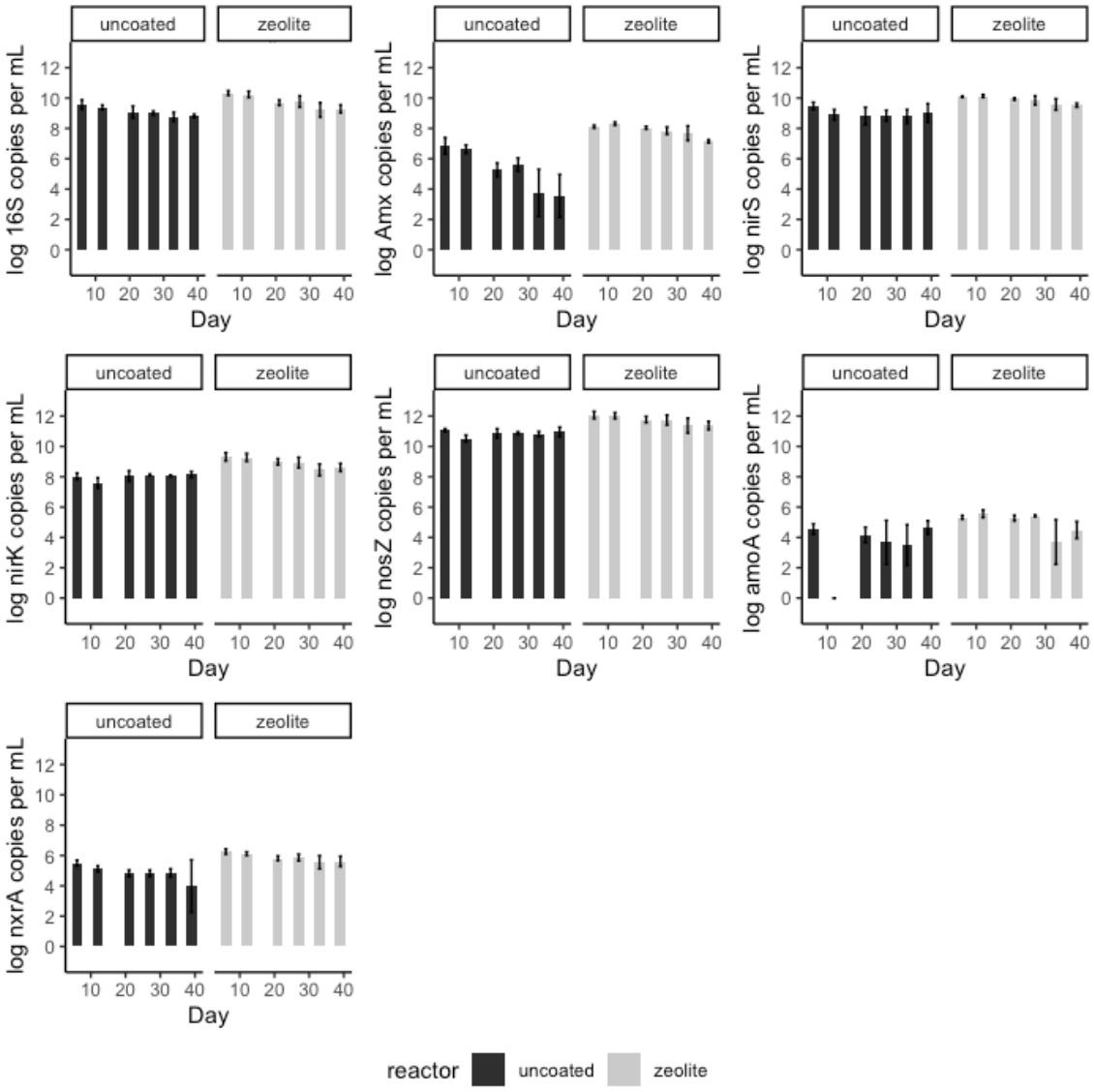

Figure D.S6. qPCR results from the bulk liquid membrane experiments. Log copies of nitrogen cycling genes from bulk biomass samples over time. P values for statistical tests comparing the zeolite-coated membranes to the uncoated control membranes are as follows: *nosZ* P=3.8x10^{-5}, *nirK* P=7.6x10^{-6}, *nirS* P=1.5x10^{-5}, *amoA* P=0.0028, *nxrA* P=7.6x10^{-6}.

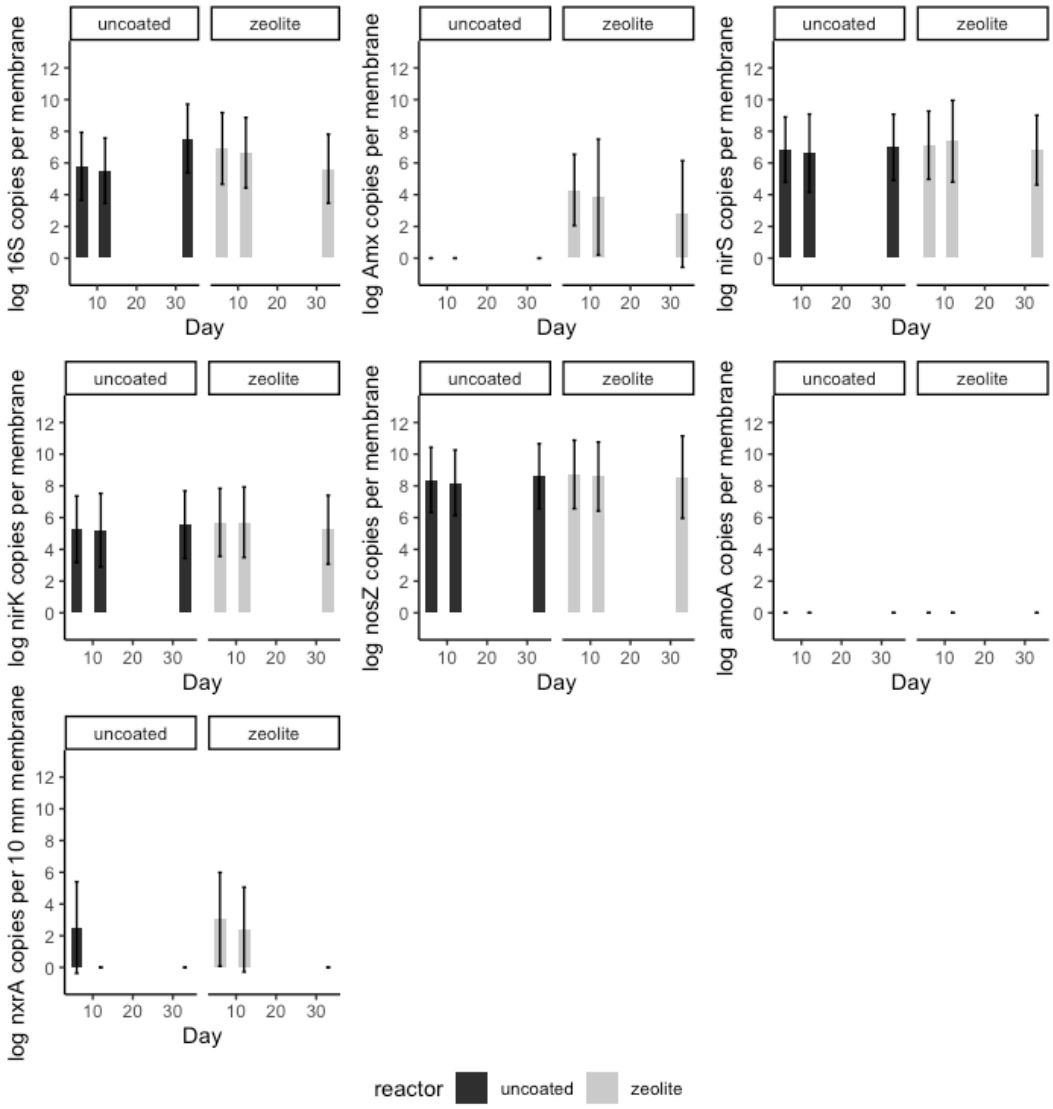

Figure D.S7. qPCR results showing the log of the copies of nitrogen cycling genes from membrane biomass samples. Sampled membrane segments were 10 mm. (16S rRNA P=0.91, Amx P=0.036, *nirS* P=0.20, *nirK* P=0.20, *nosZ* P=0.13, *amoA* P=NA, *nxrA* P=0.18).

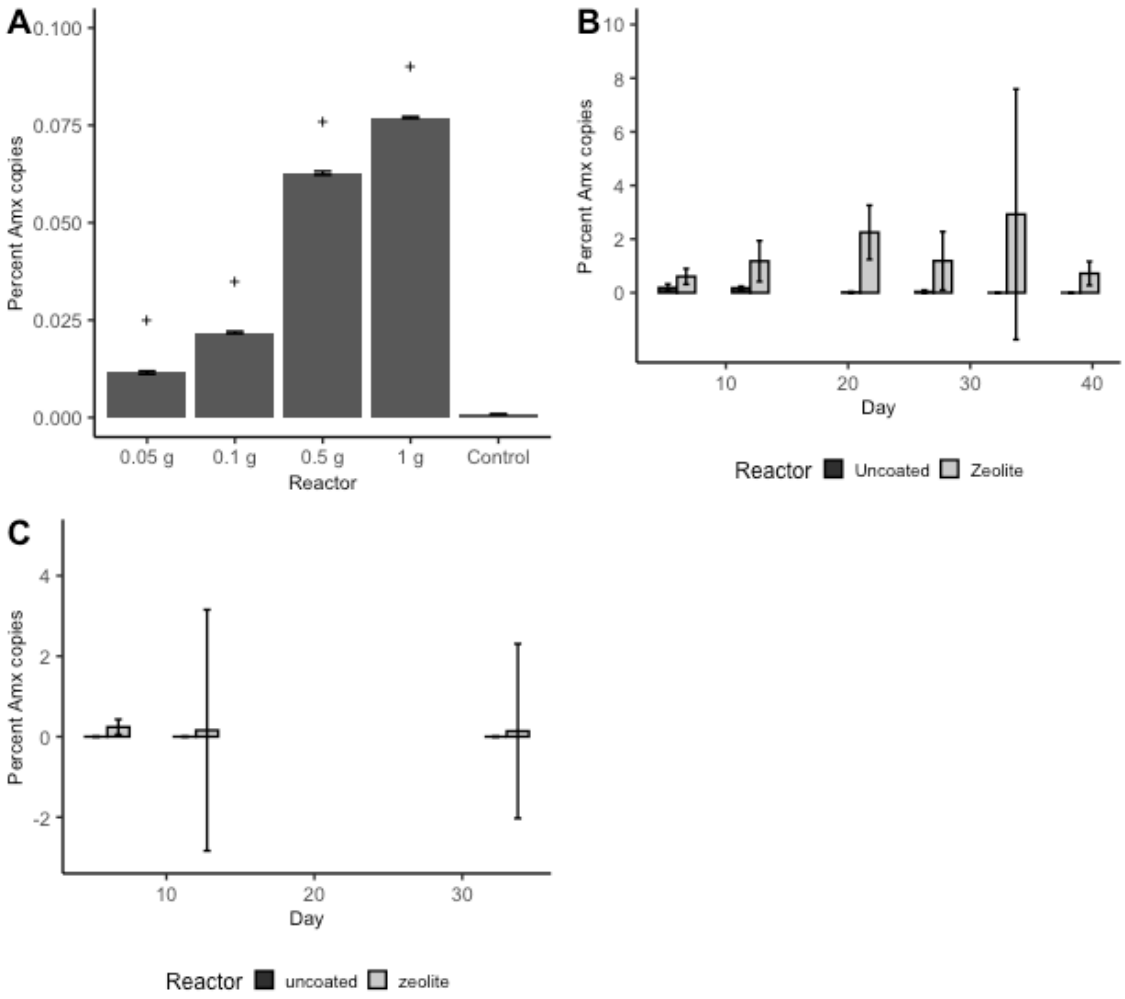

Figure D.S8. qPCR results showing the percent of Amx gene copies divided by 16S rRNA gene copies. A) Bulk liquid biomass samples from zeolite particle reactors. + indicates samples with more gene copies/mL reactor bulk than control samples, with a $P<0.1$. B) Bulk liquid biomass samples from membrane reactors, and C) Membrane biomass samples from membrane reactors. For both B and C, the zeolite-coated membrane reactors had significantly ($P<0.05$) higher percent Amx than uncoated membrane reactors when data was pooled for all of the time points.

Membrane reactor experiment with sodium azide added to abiotic reactors. Degradation of nitrite in the abiotic-zeolite membrane reactors was observed in the first experiment; therefore, the experiment was repeated with sodium azide added to the abiotic reactors to ensure that no biological contamination had occurred and further investigate the possible zeolite-catalyzed abiotic degradation of nitrite. Influent nitrite concentrations were low, so to better analyze the fate of nitrite in the abiotic reactors, the influent nitrite concentrations were increased from 10 mg-N/L to 20 mg-N/L on Day 15 of the 30-day experiment. Once the influent concentration was increased, formation of nitrate was observed in the abiotic reactors, indicating that the zeolite-driven abiotic transformation of nitrite occurred. Removal rates of TIN were much greater in the biologically active reactors, with the zeolite-coated biologically-active membrane reactors having the highest nitrogen removal rates.

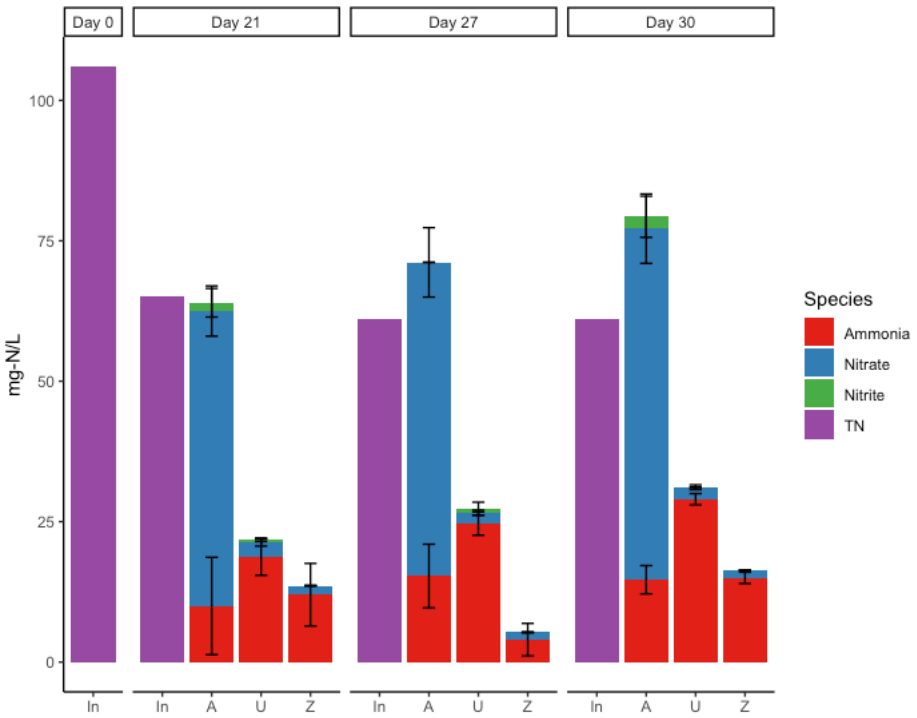

Figure D.S9. Influent and effluent nitrogen concentrations in the experiment to which 10 mM sodium azide was added to the abiotic zeolite-coated membrane treatments. Influent concentrations are TN as mg-N/L and effluent concentrations are ammonia, nitrite, and nitrate, which added together are TIN, as mg-N/L. Error bars show standard deviation for three replicate samples. In = influent, A = abiotic reactors containing zeolite-coated membranes, U = biotic reactors containing uncoated membranes, Z = biotic reactors containing zeolite-coated membranes.

References

(1) Shao, J.; Zhan, Z.; Li, J.; Wang, Z.; Li, K.; Yan, Y. Zeolite NaA Membranes Supported on Alumina Hollow Fibers: Effect of Support Resistances on Pervaporation Performance. *J. Membr. Sci. J.* 2013, *451* (2014), 10–17. https://doi.org/10.1016/j.memsci.2013.09.049.

(2) Temme, H. R.; Novak, P. J. Diverse Dechlorinators and Dechlorination Genes Enriched through Amendment of Chlorinated Natural Organic Matter Fractions. *Environ. Sci. Process. Impacts* 2020, *22* (3), 595–605. https://doi.org/10.1039/c9em00499h.

(3) Muyzer, G.; de Waal, E. C.; Uitterlinden, A. G. Profiling of Complex Microbial Populations by Denaturing Gradient Gel Electrophoresis Analysis of Polymerase Chain Reaction-Amplified Genes Coding for 16S RRNA. *Appl. Envirnomental Microbiol.* 1993, *59* (3), 695–700.
(4) Humbert, S.; Zopfi, J.; Tarnawski, S. E. Abundance of Anammox Bacteria in Different Wetland Soils. *Environ. Microbiol. Rep.* 2012, *4* (5), 484–490. https://doi.org/10.1111/j.1758-2229.2012.00347.x.
(5) Harms, G.; Layton, A. C.; Dionisi, H. M.; Gregory, I. R.; Garrett, V. M.; Hawkins, S. A.; Robinson, K. G.; Sayler, G. S. Real-Time PCR Quantification of Nitrifying Bacteria in a Municipal Wastewater Treatment Plant. *Environ. Sci. Technol.* 2003, *37* (2), 343–351. https://doi.org/10.1021/es0257164.
(6) Poly, F.; Wertz, S.; Brothier, E.; Degrange, V. First Exploration of Nitrobacter Diversity in Soils by a PCR Cloning-Sequencing Approach Targeting Functional Gene NxrA. *FEMS Microbiol. Ecol.* 2008, *63* (1), 132–140. https://doi.org/10.1111/j.1574-6941.2007.00404.x.
(7) Braker, G.; Fesefeldt, A. Development of PCR Primer Systems for Amplification of Nitrite Reductase Genes (NirK and NirS) To Detect Denitrifying Bacteria in Environmental Samples. *Appl. Envirnomental Microbiol.* 1998, *64* (10), 3769–3775.
(8) Hallin, S.; Lindgren, P. PCR Detection of Genes Encoding Nitrite Reductase in Denitrifying Bacteria. *Appl. Environ. Microbiol.* 1999, *65* (4), 1652–1657. https://doi.org/10.1007/BF01644071.
(9) Throbäck, I. N.; Enwall, K.; Jarvis, Å.; Hallin, S. Reassessing PCR Primers Targeting NirS, NirK and NosZ Genes for Community Surveys of Denitrifying Bacteria with DGGE. *FEMS Microbiol. Ecol.* 2004, *49* (3), 401–417. https://doi.org/10.1016/j.femsec.2004.04.011.
(10) Henry, S.; Bru, D.; Stres, B.; Hallet, S.; Philippot, L. Quantitative Detection of the NosZ Gene, Encoding Nitrous Oxide Reductase, and Comparison of the Abundances of 16S RRNA, NarG, NirK, and NosZ Genes in Soils. *Appl. Environ. Microbiol.* 2006, *72* (8), 5181–5189. https://doi.org/10.1128/AEM.00231-06.

Appendix E: Supplemental Information for Chapter 4

Membrane Coating Methods.

Attachment of zeolite procedure using UV (Attachment – UV method). Faujasite zeolite nano particles were made using the following procedure. 1.1 g of $Na_2Al_2SO_4$ (Sigma Aldrich) in 10 mL of water was mixed with 2.4 g of NaOH and 18.1 g of Na_2SiO_3 solution (Sigma Aldrich) were chilled in an ice bath for 30 min. The $Na_2Al_2SO_4$ mixture was added slowly added to Na_2SiO_3. After aging for 24 hours at room temperature, the mixture was freeze dried and then crystalized for 2 days at 50 °C. Solution was centrifuged, washed, and dried to produce a zeolite powder.

PSf membranes were prepared as described by Binahmed et al.[2] Zeolite was attached to the membranes using a similar procedure as described by Kulak et al.[4] Briefly, zeolite was dried for 24 hours at 100 °C using a Schlenk Line (100 millitorr) and treated with 3-aminoproplytriethoxysilane (APTES) (2 mM) (Sigma Aldrich) in toluene for 1 hour at 70 °C under nitrogen. PSf membranes were oxidized with a UV lamp (Spetroline Model EF-160C) for 15 seconds to create carboxylic groups on the membrane surface and treated with [3-(2,3epoxypropoxylpropyl]-trimethoxysilane (GLYMO) (2 mM) (Sigma Aldrich) in iso-octane for 1 hour at room temperature under nitrogen.

The treated zeolite was dried at 70 °C overnight and resuspended in iso-octane and applied to the treated PSf membrane for 1 hour while mixing. Coated membranes were rinsed and sonicated for 20 seconds to remove non-attached particles. Membranes were stored at 4 °C in deionized (DI) water.

Attachment of zeolite procedure using UV and AA (Attachment – AA/UV method). The previous procedure was modified to apply 10% acrylic acid (AA) solution from stock 99% AA (Sigma Aldrich) in MilliQ to the PSf membrane immediately after membrane oxidation with UV exposure for the growth of poly(acrylic acid) and enhance the carboxylic groups on the membrane surface.[3] 10% AA was applied for 5 minutes and immediately rinsed with MilliQ water. A more detailed procedure is described in Wuolo-Journey et al.[3] Procedure continued as described in the attachment procedure using UV.

Attachment of zeolite procedure using EDC-NHS (Attachment – EDC/NHS). Beginning with UV/AA treatment, this procedure then uses 4 mM 1-ethyl-3-(3-dimethylaminopropyl)carbodiimide hydrochloride (EDC) (Sigma Aldrich) and 10 mM N-hydroxysuccinimide (NHS) (Sigma Aldrich), adjusted to pH 5 with 10 mM MES (Sigma Aldrich) supplemented with 0.5 M NaCl. This solution is applied to PSf membrane while mixing at ambient conditions for one hour.[3, 5] Membrane was then rinsed and zeolite applied as described above.

Attachment of zeolite procedure using polydopamine coating (Attachment – PDA). PSf membranes were prepared and stored as described earlier.[2] Dopamine solution was prepared using 4 g of 3,4-dihydroxyphenylalanine (DOPA) (Sigma Aldrich) in 1 L of Trizma buffer (10 mM) (Sigma Aldrich).[2, 8] Once mixed, 50 mg of zeolite, prepared as described above, was added to the solution. The pH was adjusted to 8.5 using 1 M NaOH. Dopamine solution was immediately transferred to the membrane to initiate PDA deposition for 15 minutes while mixing. Membranes were then immediately rinsed thoroughly with MilliQ and stored in MilliQ at 4 °C.

Embedment of zeolite into PSf membranes (Embedment). PSf membranes were prepared as described previously.[2] 50 mg of zeolite nano powder (prepared as described previously) was added directly to the dope solution after solution was stored overnight to remove air bubbles. After the membranes were cast, they were stored in MilliQ at 4 °C until use.

Growth of zeolite on alumina hollow fiber membranes (Growth). Growth of faujasite zeolite on alumina hollow fiber membranes (0.7 mm diameter) is described in previous work.[7] Briefly, raw fibers of 38.0% N-Methyl-2-pyrrolidone (NMP), 6.8% polyethersulfone (PES), 54.7% Al_2O_3, and 05% polyvinylpyrrolidone (PVP) were sintered to make alumina hollow fiber membranes. Zeolite growth on the membrane surface occurred by immersing in a solution of 7.7 M NaOH, colloidal silica (Ludox TM-40, Sigma Alrich), and 0.15 of aluminum for 24 hours at 75 °C. Plain and zeolite-coated membranes were stored dry in sterile containers at ambient conditions until use.

Table E.S1. Synthetic wastewater components in mg per liter for CFTR and ACFTR

	CFTR	ACFTR	
NH_4Cl	133.75	133.75	mg
$NaNO_2$	103.5	0	mg
Magnesium Phosphate Dibasic Trihydrate	25	25	mg
Potassium Phosphate Tribasic	20	20	mg
$NaHCO_3$	275	275	mg
Sodium acetate	221	221	mg
Bacteriological peptone	24	24	mg
Dry meat extract	12	12	mg
Potato starch	42	42	mg

Low fat milk powder	50	50	mg
Glycerine	34	34	mg

Table E.S2. Synthetic wastewater components in mg per liter for MFTR and Bioavailability Test

	MFTR	Bioavailability Test	
NH_4Cl	133.75	0	mg
$NaNO_2$	0	236.4	mg
KH_2PO_4	27.2	27.2	mg
$KHCO_3$	500	500	mg
Trace solution 1	1	1	mL
Trace solution 2	1	1	mL
Mg solution	1	1	mL
Ca solution	1	1	mL

†Trace solutions are detailed in Peterson et al.[22]

References

1. J. Gascon, F. Kapteijn, B. Zornoza, V. Sebastián, C. Casado and J. Coronas, Practical Approach to Zeolitic Membranes and Coatings: State of the Art, Opportunities, Barriers, and Future Perspectives, *Chemistry of Materials*, 2012, **24**, 2829-2844.
2. S. Binahmed, A. Hasane, Z. Wang, A. Mansurov and S. Romero-Vargas Castrillón, Bacterial Adhesion to Ultrafiltration Membranes: Role of Hydrophilicity, Natural Organic Matter, and Cell-Surface Macromolecules, *Environmental Science and Technology*, 2018, **52**, 162-172.
3. K. Wuolo-Journey, S. Binahmed, E. Linna and S. Romero-Vargas Castrillón, Do graphene oxide nanostructured coatings mitigate bacterial adhesion?, *Environmental Science: Nano*, 2019, **6**, 2863-2875.

4. A. Kulak, Y.-J. Lee, Y. S. Park and K. B. Yoon, Orientation-Controlled Monolayer Assembly of Zeolite Crystals on Glass and Mica by Covalent Linkage of Surface-Bound Epoxide and Amine Groups, *Angewandte Chemie*, 2000, **112**, 980-983.
5. H. Croll, A. Soroush, M. E. Pillsbury and S. R.-V. Castrillón, Graphene oxide surface modification of polyamide reverse osmosis membranes for improved N-nitrosodimethylamine (NDMA) removal, *Separation and Purification Technology*, 2019, **210**, 973-980.
6. E. C. Feinberg, A. L. H. Chester, P. J. Novak and M. A. Hillmyer, Porous Polyethylene-Supported Zeolite Carriers for Improved Wastewater Deammonification, *ACS ES&T Engineering*, 2021, **1**, 1104-1112.
7. A. L. Huff Chester, K. Eum, M. Tsapatsis, M. A. Hillmyer and P. J. Novak, Enhanced Nitrogen Removal and Anammox Bacteria Retention with Zeolite-Coated Membrane in Simulated Mainstream Wastewater, *Environmental Science & Technology Letters*, 2021, **8**, 468-473.
8. J. Xue, S. Binahmed, Z. Wang, N. G. Karp, B. L. Stottrup and S. Romero-Vargas Castrillón, Bacterial Adhesion to Graphene Oxide (GO)-Functionalized Interfaces Is Determined by Hydrophobicity and GO Sheet Spatial Orientation, *Environmental Science & Technology Letters*, 2018, **5**, 14-19.